RELATIONSHIP BETWEEN CHEMICAL REACTIVITY AND PHOTOCHROMISM USING 1,2-DITHIENYLETHENE-BASED MOLECULAR SWITCHES

by

Vincent Lemieux
B.Sc. Honours, McGill University 2003

THESIS SUBMITTED IN PARTIAL FULFILLMENT OF
THE REQUIREMENTS FOR THE DEGREE OF

DOCTOR OF PHILOSOPHY

In the
Department of Chemistry

SIMON FRASER UNIVERSITY

Summer 2008

Approval

Name: Vincent Lemieux

Degree: Doctor of Philosophy

Title of Thesis: Relationship Between Chemical Reactivity and Photoactivity Using 1,2-Dithienylethene-Based Molecular Switches

Examining Committee:

Chair — Dr. David J. Vocadlo
Assistant Professor, Department of Chemistry

Dr. Neil R. Branda
Senior Supervisor
Professor, Department of Chemistry

Dr. Ross H. Hill
Supervisor
Professor, Department of Chemistry

Dr. Vance E. Williams
Supervisor
Associate Professor, Department of Chemistry

Dr. Peter D. Wilson
Internal Examiner
Associate Professor, Department of Chemistry

Dr. Michael M. Haley
External Examiner
Professor, Department of Chemistry
University of Oregon

Date Defended/Approved: July 22, 2008

Abstract

Molecular systems with integrated chemical reactivity and photochromic functions are potentially beneficial for the development of novel functional materials. Rationally designed photoresponsive compounds can be used to regulate chemical reactivity using light, and such systems could significantly influence both synthesis and drug delivery by increasing efficiency and decreasing undesired side-reactions or side effects. Chemical reactivity can also be employed to control the photochromic behaviour of photoswitches, providing a locking mechanism and enabling chemical detection through facile monitoring.

Dithienylethene-based molecular switches are particularly well-suited to the development of functional systems with integrated chemical reactivity functions since they can be toggled between two thermally stable and structurally unique isomers when irradiated with light of the appropriate wavelengths. Dithienylethene derivatives exhibit significant differences between their ring-open and ring-closed forms, which can influence their reactivity. Alternatively, multiple strategies permit the regulation of their photochromic properties through chemical reactions or interactions. The research presented in this thesis focuses on the development of novel approaches to integrate photochromism and chemical reactivity.

First, the concept of reactivity-gated photochromism is introduced and demonstrated using a spontaneous and mild chemical reaction. Results show that

non-photoswitchable molecules can be rendered photoactive by creating the dithienylethene architecture using the Diels-Alder cycloaddition.

The use of the dithienylethene architecture as a photocleavable group that combines reactivity-gated photochromism and photogated reactivity is then presented. This approach is based on the Diels-Alder reaction between photostable dienes and dienophiles to generate photoswitchable dithienylethene derivatives. The photoresponsive unit is employed to regulate the reverse cycloaddition, enabling selective and sequential photorelease of the small dienophile auxiliary.

Finally, the Lewis acidity of a boron-containing dithienylethene derivative is photomodulated. Upon exposure to light of the appropriate wavelengths, the isomerisation of the dithienylethene backbone causes a bond rearrangement of the 1,3,2-dioxaborole unit, directly affecting the electron density of the boron centre and changing the Lewis acidity of the atom.

Keywords: Photochromism, reactivity-gated photochromism, photogated reactivity, dithienylethenes, Diels-Alder reaction, photorelease, Lewis acidity.

À Christine, à mes parents, Sylvie et Yvon,

et aux montagnes de la Colombie-Britannique

Acknowledgements

I would like to thank my senior supervisor Neil Branda for his guidance and motivation. In addition, I extend my thanks to the members of my supervisory committee, Vance Williams and Ross Hill, for their helpful advice. Thanks to Philippe Reutenauer for useful discussions concerning the retro-Diels-Alder reaction. Special thanks to Simon Gauthier for his help with the photorelease project presented in *Chapter 3* and to Daniel Spantulescu for his guidance in improving the synthesis of α-hydroxyketones as discussed in *Chapter 4*. I would like to acknowledge Kim K. Baldridge for carrying out calculations concerning the boron project. I am also grateful to the Branda group members, past and present, for sharing their knowledge and experience, especially David Sud who shared his bench with me for 3 years and Chad Warford who shared his fumehood in the last 2 years.

Several technicians and specialists at Simon Fraser University contributed to various extents to my projects: Mei-Keng Yang for elemental analyses; Hongwen Chen and Philip Ferreira for mass spectrometry; Andrew Lewis, Marcy Tracey, and Collin Zhang for NMR services.

Finally, my family and friends have provided invaluable moral support and encouragements; thanks to all of them. I also acknowledge Les Cowboys Fringants, Malajube, Radiohead, The Offspring, Metallica, and all the others who inspired me with their music in the laboratory and during the redaction of this thesis.

Merci Christine, sans toi je n'aurais jamais réussi.

Table of Contents

List of Figures

List of Schemes

List of Equations

List of Tables

List of Abbreviations

>	greater than
δ	chemical shift
Δ	heating
λ	wavelength
λ_{max}	wavelength at the absorption maximum in a given region
µL	microlitre
°C	degree Celsius
AcOH	acetic acid
Anal. Calcd.	analytically calculated
ATP	adenosine triphosphate
B	boron
BF_3OEt_2	boron trifluoride etherate
bd	broad doublet
bm	broad multiplet
bs	broad singlet
C	carbon
C	complex
calc.	calculated
CI	chemical ionisation
cm	centimetre

d	doublet
dd	doublet of doublets
dm	doublet of multiplets
DMF	*N*,*N*-dimethylformamide
DMSO	dimethylsulfoxide
DMSO-d_6	deuterated dimethylsulfoxide
dt	doublet of triplets
DTE	dithienylethene
EA	elemental analysis
EI	electron impact
equiv.	equivalent
Et_2O	diethyl ether
EtOAc	ethyl acetate
exp.	experimental
g	gram
GC	gas chromatography
G	guest
h	hour
H	host
H	proton
H_{het}	heterocyclic proton
$HN(i\text{-}Pr)_2$	diisopropylamine
HOMO	highest occupied molecular orbital

hν	photon energy
Hz	Hertz
J	coupling constant
k	forward reaction rate constant
k’	backward reaction rate constant
K	equilibrium constant
kcal	kilocalorie
LRMS	low-resolution mass spectrometry
LUMO	lowest unoccupied molecular orbital
m	multiplet
M	mole/litre
m.p.	melting point
m/z	mass-to-charge ratio
mA	milliampere
Me	methyl
mg	milligram
MHz	megahertz
min	minute
mL	millilitre
mmol	millimole
MS	mass spectrometry
mol	mole
n-Buli	*n*-butyllithium

NBS	*N*-bromosuccinimide
NEt_3	triethylamine
nm	nanometre
NMR	nuclear magnetic resonance
Ph	phenyl
ppm	part per million
PSS	photostationary state
s	singlet
s	second
st. dev.	standard deviation
T	temperature
t	triplet
t-BuLi	*tert*-butyllithium
*t*BuO	*tert*-butoxy
THF	tetrahydrofuran
TLC	thin layer chromatography
UV	ultraviolet
UV-vis	ultraviolet-visible
vis	visible
W	watt

List of Molecules

Numbered molecules of *Chapter 2*

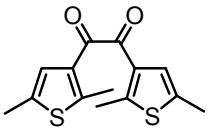

2.1

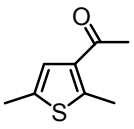

2.2

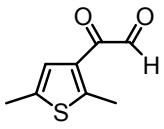

2.3

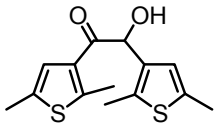

2.4

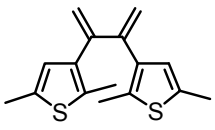

2.5

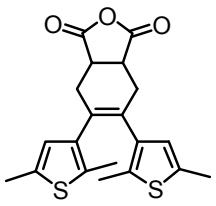

2.6

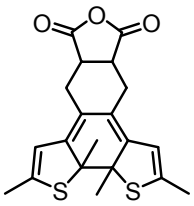

2.7

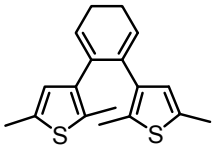

2.8

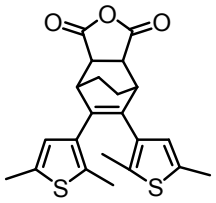

2.9

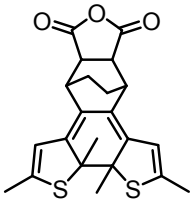

2.10

2.11

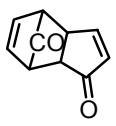

2.12

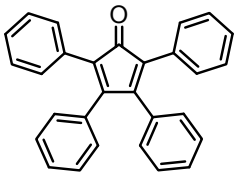

2.13

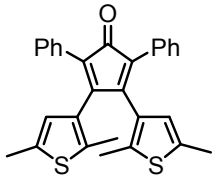

2.14

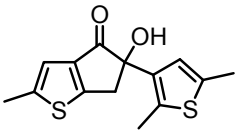

2.15

Numbered molecules of *Chapter 3*

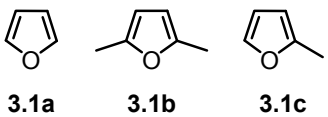

3.1a **3.1b** **3.1c**

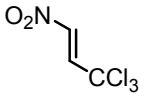

3.2

3.3

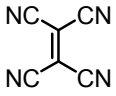

3.4

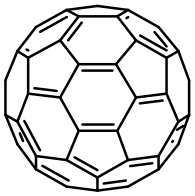

3.5

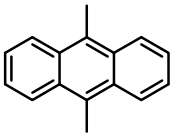

3.6

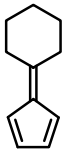

3.7

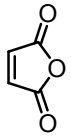

3.8

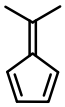

3.9

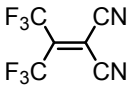

3.10

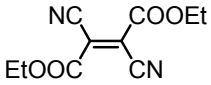

3.11

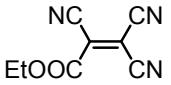

3.12

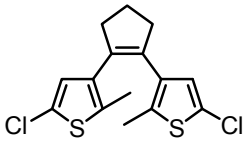

3.13

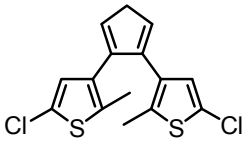

3.14

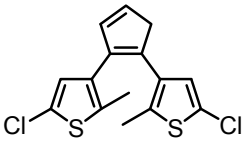

3.15

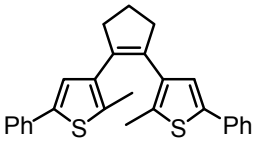

3.13a

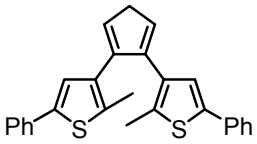

3.14a

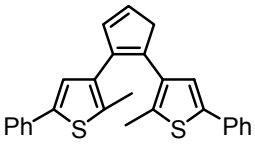

3.15a

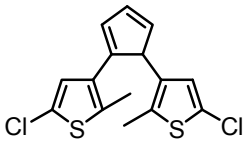

3.16

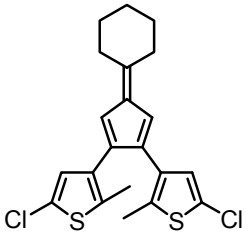

3.17

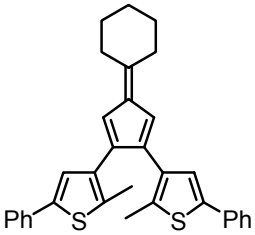

3.18

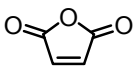

3.19

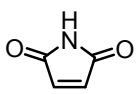

3.20

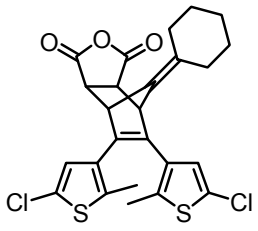

3.21o

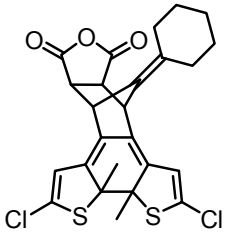

3.21c

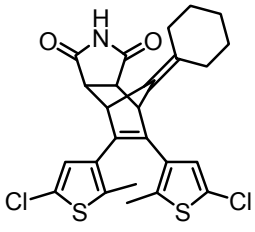

3.22o

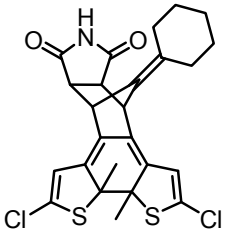

3.22c

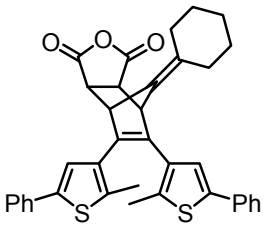

3.23o

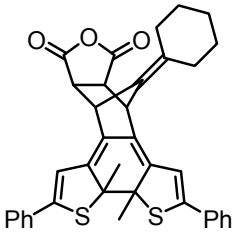

3.23c

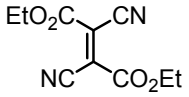

3.24

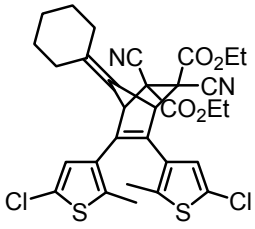

3.25

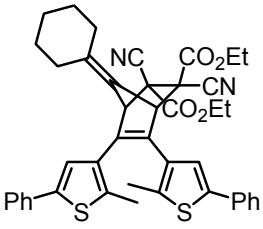

3.26

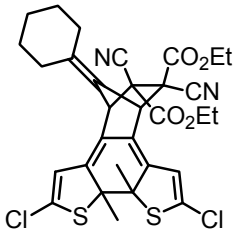

3.27

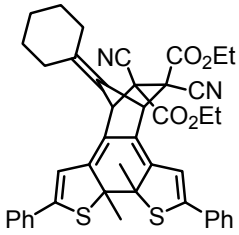

3.28

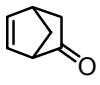

3.29

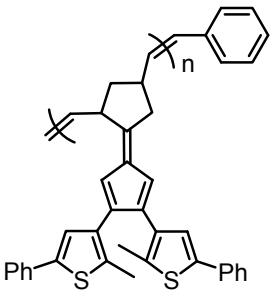

poly(**3.30**)

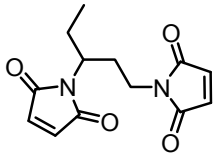

3.31

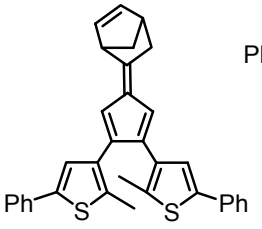

3.30

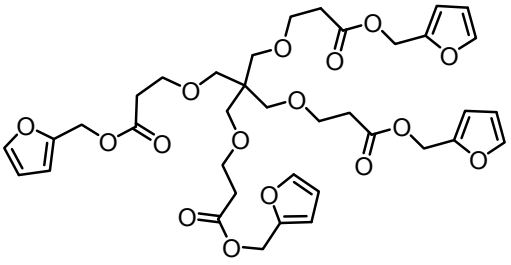

3.32

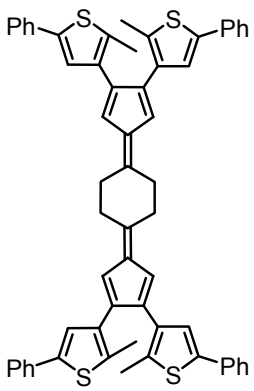

3.33

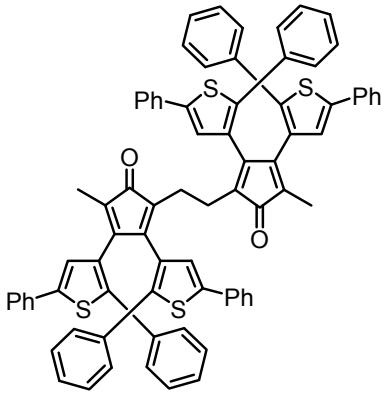

3.34

Numbered molecules of *Chapter 4*

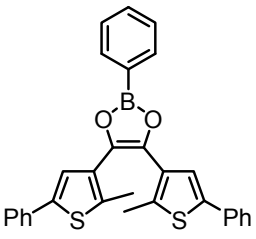

4.1

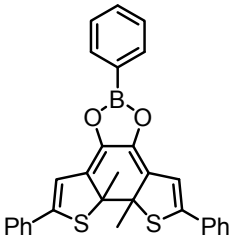

4.2

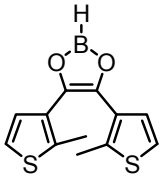

4.1s

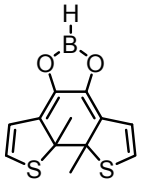

4.2s

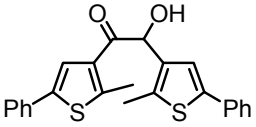

4.3

4.4

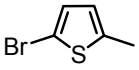

4.5

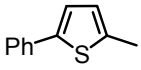

4.6

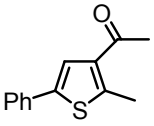

4.7

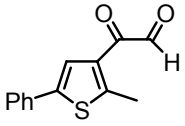

4.8

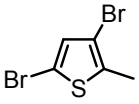

4.9

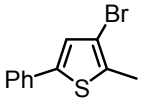

4.10

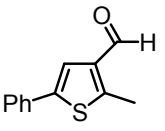

4.11

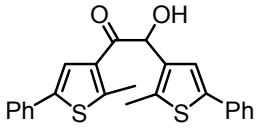

4.12

Chapter 1: Introduction

1.1 Light and chemical reactivity

The relationship between light and chemical reactivity is of key importance to the development of various technologies not only in the field of material sciences, but also in the fields of biological sciences, medicine, and analytical chemistry. Light can provide the activation energy required for a chemical reaction to proceed.[1] It can change the symmetry of a molecule's electronic configuration, enabling otherwise inaccessible reaction paths.[2] Furthermore, if the molecule that is excited by light does not undergo a chemical reaction, the excess energy can be released as thermal or radiation energy, or transferred to another molecule.[1] Thus, light is a powerful tool to activate chemical reactions important to synthetic and physical chemists, and is central to many industrial processes.[3,4] Moreover, light is imperative to photodynamic therapy in the battle against cancer.[5] It offers the precise temporal and spatial control needed to deliver therapeutics,[6,7] agents to initiate biological phenomena,[8] and designer reagents for chemical transformations,[9] as well as for photolithography.[9]

On the other side of the relationship between light and chemical reactivity, a chemical event, such as a reaction or a supramolecular interaction, can offer the necessary transformation to render a molecule photoactive or to inhibit its photoactivity. Subsequent exposure of the substrate to light provides a photochemical output to detect the occurrence of the chemical event. This strategy is the basis of many chemical detection systems.[10-12]

1.2 Photochromism

Photochromism is the reversible light-induced transformation of a chemical species between two forms that have different absorption spectra.[13] Simplistically, it can be described as a reversible colour change upon exposure to light. As shown in Equation 1.2.1, isomers **A** and **B** can reversibly interconvert between the two forms when irradiated with light of appropriate wavelengths. Irradiation of **A** with a light source of photon energy $h\nu_1$ triggers a photoisomerisation reaction producing isomer **B**. In T-type photochromism, isomer B can revert back to **A** either photochemically when exposed to a light source of photon energy $h\nu_2$ or thermally. In P-type photochromism, **B** has an increased thermal stability and reverts back to **A** only photochemically.

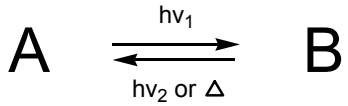

Equation 1.2.1 Exposure of **A** to light of photon energy $h\nu_1$ induces an isomerisation to form **B**. **A** can be regenerated thermally (T-type photochromism) or photochemically using light of photon energy $h\nu_2$ (P-type photochromism).

Photochromic molecules are often termed "switches" or "photoswitches" since they can be toggled between two states using light. They are referred to as "photoresponsive" or "photoactive". Throughout this thesis, the term "photoswitching" is used to describe the action of interconverting a photoswitch from one isomer to the other upon exposure to light.

There are many classes of organic photochromic compounds, the most common being azobenzenes, spiropyrans and spirooxazines, fulgides, and diarylethenes, as shown in Figure 1.2.1.[14-16] The photochromic properties of azobenzenes arise from the *cis*-*trans*

isomerisation of the N=N bond whereas a bond rearrangement between a ring-open and a ring-closed form causes the changes in spiropyrans and spirooxazines.[14-16] These two cases are examples of T-type photochromic molecules, as the reverse reactions are thermally driven. The photochromic properties of fulgides and diarylethenes originate from pericyclic reactions.[14-16] In many cases, these systems show P-type photochromism and do not interconvert between both forms thermally.

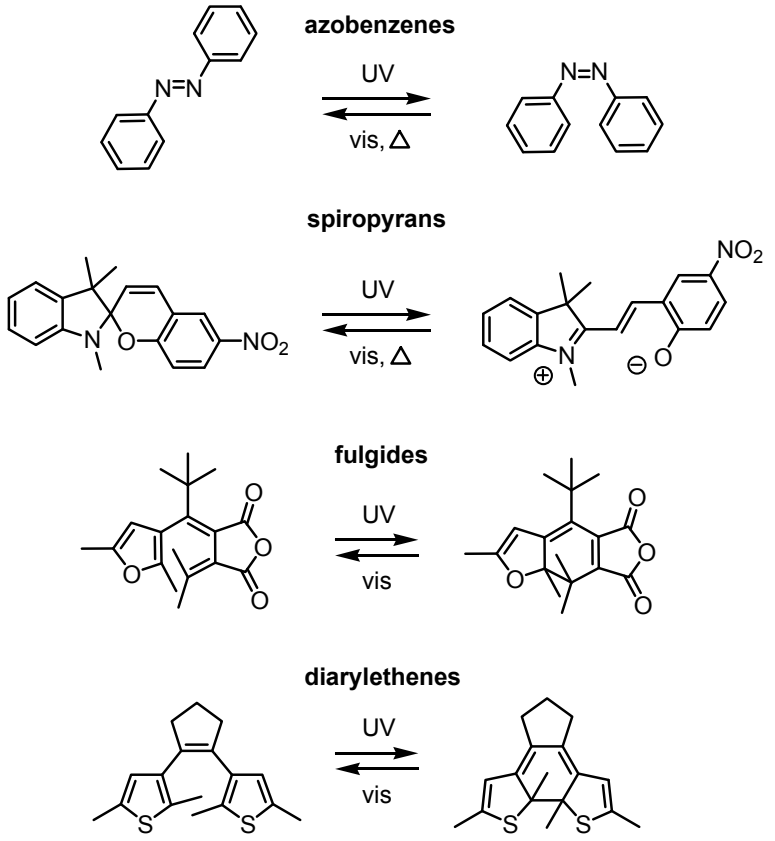

Figure 1.2.1 Selected examples of the four main photochromic groups showing both photoisomers.[14-16]

The integration of photoswitchable units into molecular systems or devices is limited by various factors such as: (1) the thermal reversibility of the photoswitching process at the operating temperature of the system, (2) the formation of side-products

over prolonged exposure to light or over repetitive switching cycles, and (3) the synthetic complexity involved in the preparation of functionalised derivatives of the photoswitches that do not interfere with their photochromic behaviour.[14-16]

In this context, the 1,2-dithienylethene (DTE) architecture offers a promising photoresponsive framework. Most DTE derivatives show P-type photochromism even at elevated temperatures. Their photoswitching is accompanied by large changes in chemical and physical properties and they have good fatigue resistance to light exposure. Most importantly, the DTE framework is tolerant to a wide variety of chemistries and can be tailored with various functionalities.[17-22] The DTE architecture offers a good platform for the integration of photoactivity and chemical reactivity.

1.3 Dithienylethene (DTE) derivatives

1.3.1 General description of DTE derivatives

Molecular switches based on the 1,2-dithienylethene (DTE) architecture,[17-22] illustrated in Equation 1.3.1, undergo reversible ring-closing and ring-opening reactions when irradiated with light of the appropriate wavelengths. The ring-open isomer (**DTE-o**) is usually colourless and contains a 1,3,5-hexatriene functionality (bold in Equation 1.3.1) that undergoes a 6π-electrocyclization reaction when exposed to light in the UV range. The cyclization product (**DTE-c**), referred to as the ring-closed isomer, contains a 1,3-cyclohexadiene moiety (bold in Equation 1.3.1) and is usually coloured due to the formation of an extended π-conjugated path throughout the backbone of the molecule. Irradiation with light in the visible range of the spectrum triggers photochemical ring-opening of **DTE-c**, thus reforming **DTE-o**.

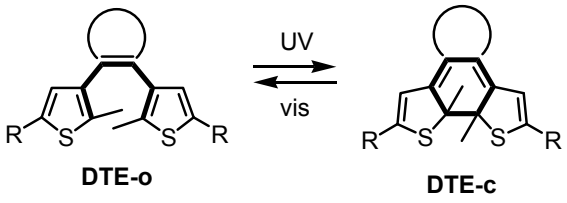

Equation 1.3.1 Dithienylethene (DTE) derivatives can be toggled between the thermally stable ring-open isomer **DTE-o** containing a 1,3,5-hexatriene (bold) and the ring-closed isomer **DTE-c** containing a 1,3-cyclohexadiene (bold) using UV light for the ring-closing reaction and visible light for the ring-opening reaction. The alkene portion of DTE derivatives is usually part of a ring system as represented by the arc.

Generally, the ring-open and the ring-closed isomers are described as being thermally stable because they do not interconvert when kept in the dark, even above room temperature in certain cases.[22] This enhanced thermal stability of DTE derivatives makes them prime candidates for the modulation of chemical reactivity since it enables

spatial and temporal control of the isomerisation, whereas thermally reversible systems do not.

The ethene moiety of most published DTE derivatives is part of a small ring system to prevent its *E-Z* isomerisation, thus increasing the photochromic performances of the switches.[22] In many cases, these derivatives show remarkable photofatigue resistance. For some DTEs, the ring-opening and ring-closing reaction can be triggered more than 10 000 times and each isomer can be exposed to light for long periods before significant loss of performance occurs.[22]

1.3.2 The photochemical ring-closing reaction of DTEs

As illustrated in Scheme 1.3.1, the ring-open isomer can exist in two main conformations: (1) the parallel conformation with the two thiophene rings in mirror symmetry and (2) the anti-parallel conformation with a C_2 axis of symmetry across the molecule.[17,18,22] According to the Woodward-Hoffman rules based on the conservation of orbital symmetry, the 1,3,5-hexatriene framework can undergo a photochemical conrotatory (rotation of the reacting orbitals in the same direction) cyclization or a thermal disrotatory (rotation of the reacting orbitals in the opposite direction) cyclization.[2,23] However, this latter thermal process does not occur due to steric hindrance of the central methyl groups.[23] Thus, due to its orbital configuration, only the anti-parallel conformation of the ring-open DTE is photoactive. Therefore, irradiation produces a mixture of only two enantiomers with the internal methyl groups pointing in opposite directions.

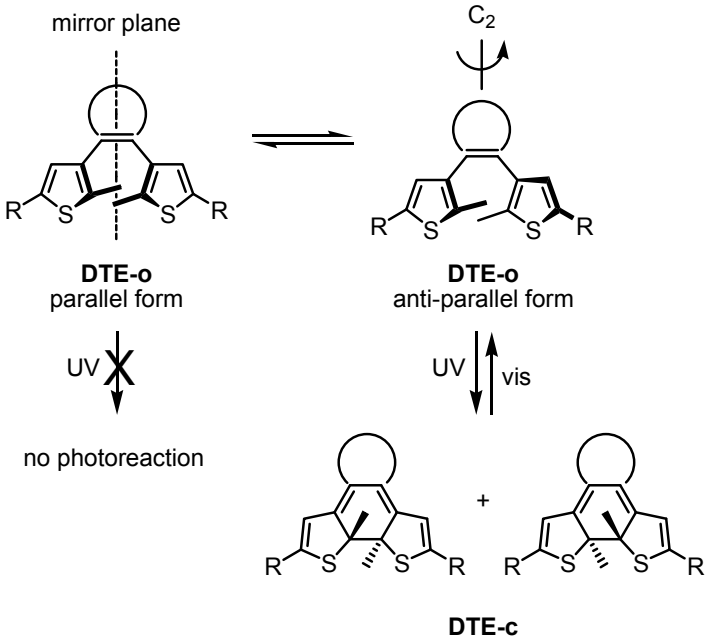

Scheme 1.3.1 As dictated by the Woodward-Hoffman rules,[2] the parallel form of **DTE-o**, which has a mirror plane of symmetry, is not photoactive. The anti-parallel form, which has a C_2 axis of symmetry, can be reversibly ring-closed to form a mixture of two stereoisomers. In this thesis, the stereochemistry of the ring-closed DTEs is always implied but is not represented.

1.3.3 Photostationary state

Exposure of the ring-open isomer to ultra-violet radiation rarely results in complete conversion to the ring-closed isomer.[22] Upon irradiation, a photochemical equilibrium is usually established whereby the ring-closure and ring-opening processes compete. The composition of the system at this moment is termed the photostationary state (PSS).[13] Mathematically, the PSS describes the percentage of the molecular switch that undergoes photoisomerisation at a particular wavelength, as shown in Equation 1.3.2.

$$\text{PSS} = \frac{\#\text{ of isomerised molecules}}{\text{total }\#\text{ of molecules}} \times 100\%$$

Equation 1.3.2 Equation used to calculate photostationary states (PPS) as a percentage.

When performing a photoreaction **A** → **B**, a PSS lower than 100% arises if the light employed can also be absorbed by **B** and triggers the reverse reaction, if the quantum yield of the reverse reaction is larger than zero. In the case of most DTE derivatives, the ring-open and ring-closed isomers both absorb light in the UV region of the spectrum and the ring-closure PSS is rarely 100%. However, the ring-opening reaction is usually quantitative since only the ring-closed form absorbs visible light.[22]

1.3.4 Photochemical side reactions of DTEs

Although some DTE derivatives undergo fatigue-resistant photochromic reactions without any degradation, some cease to be photochromic after a limited number of cycles, even in absence of oxygen.[24,25] The two main isolated by-products of irradiation are illustrated in Scheme 1.3.2. In the presence of oxygen, some derivatives decompose in less than 500 cycles due to the formation of oxidized products as shown in Scheme 1.3.3.[25-27]

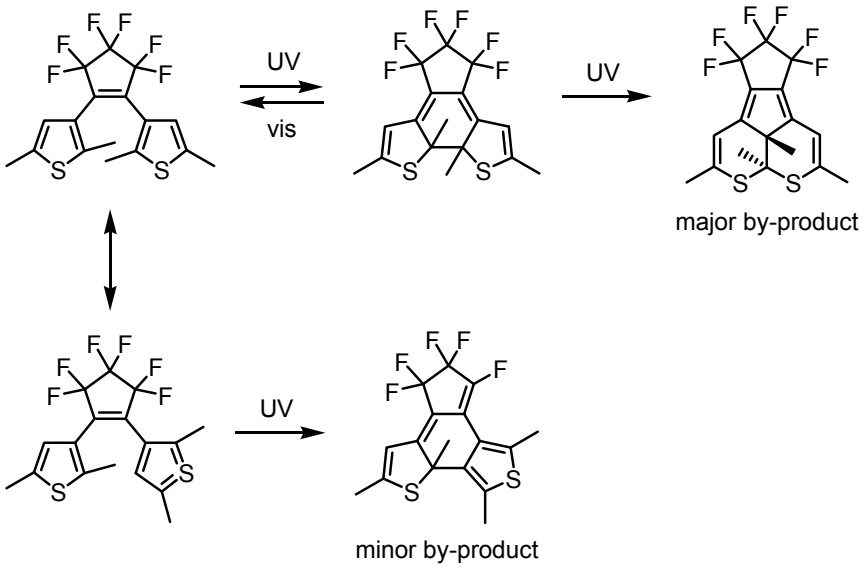

Scheme 1.3.2 Isolated by-products observed upon irradiation of some DTE derivatives.[24]

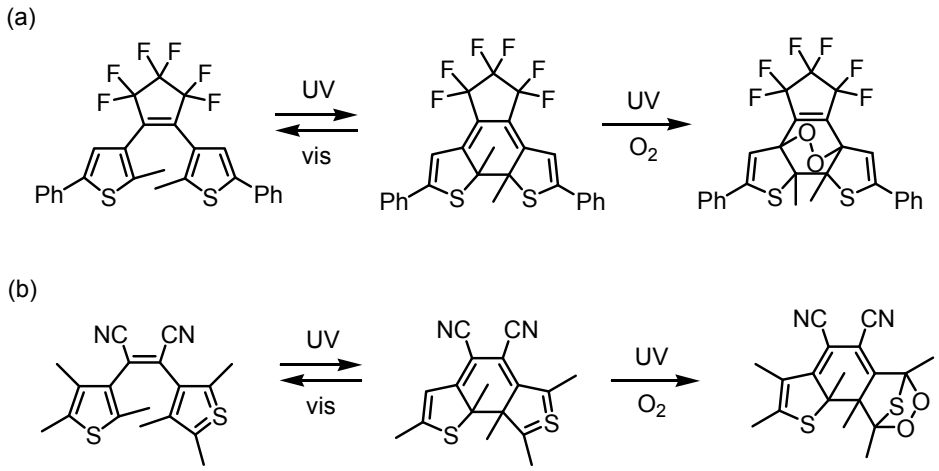

Scheme 1.3.3 Proposed structures of the decomposition products formed through photo-oxidation of (a) the cyclohexadiene moiety in the ring-closed isomer[25] and (b) the thienyl unit after ring-closing in a different configuration.[26,27]

Various strategies can be used to increase the fatigue resistance of DTE photoswitches. (1) Decomposition through photooxidation can be prevented by using deoxygenated solutions[25] or by controlling the oxidation state of the sulphur atoms of the molecules.[28] (2) Decomposition through the formation of the two non-photochromic by-products shown in Scheme 1.3.2 can be avoided by tailoring the 4- and 4'-positions of the thiophene rings with functional groups such as methyl units, or using benzothiophene groups instead of thiophenes.[24,25]

1.3.5 Synthetic versatility of DTE derivatives

As stated in Section 1.2, the DTE framework is tolerant to a wide variety of chemistries and can be easily tailored with various functionalities. This synthetic versatility will be seen through the examples presented in the following section and is attested to in a number of reviews describing DTE derivatives.[17-22] The most common modification sites are highlighted in Figure 1.3.1. Throughout this thesis, the 5- and 5'-

positions and the 2- and 2'-positions of the thienyl groups will be referred to as the "external" and "internal" positions respectively. The cycle bearing the alkene function will be referred to as the "top" or "central" ring.

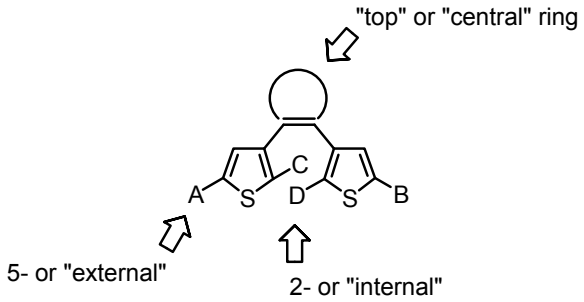

Figure 1.3.1 Functional groups on DTE derivatives can be attached at the "external" positions (5- and 5'-positions) and/or at the "internal" positions (2- and 2'-positions) of the thiophene rings. The "top" or "central" ring can also be modified.

Synthetic tailoring allows the preparation of DTE derivatives in which various functions can be modulated by the photoswitching event. The modifications in bond configuration between the two photoisomers of DTEs result in steric and electronic changes. An appropriate molecular design allows the translation of these changes to other characteristics of a material or molecular system such as its luminescence, electrochemical properties and conductivity, magnetic properties, chirality and optical rotation, dielectric constant, and refractive index.[17-22]

1.3.6 Effects of the ring-closure reaction on DTEs

Upon exposure to light in the UV range, the ring-open isomer undergoes a cyclization reaction causing modifications in the bond configuration of the molecules leading to important geometric (steric) and electronic changes.[17-22]

Geometric (steric) differences between the photoisomers

The ring-open forms of DTEs are relatively flexible; free rotation around the two carbon-carbon bonds connecting the thienyl groups to the central cyclic alkene is possible as illustrated in Scheme 1.3.4. This structural flexibility allows the interconversion between the parallel and anti-parallel conformations and convergence of the functional groups (A and B or C and D) located at the internal (2- and 2'-) or external (5- and 5'-) positions of the thiophene rings. In their ring-closed forms, DTE derivatives are much more rigid due to the presence of a tricyclic structure, and the functional groups on the thiophene rings are forced to diverge. Flexibility can be regenerated using light of visible wavelengths.[17,18,22]

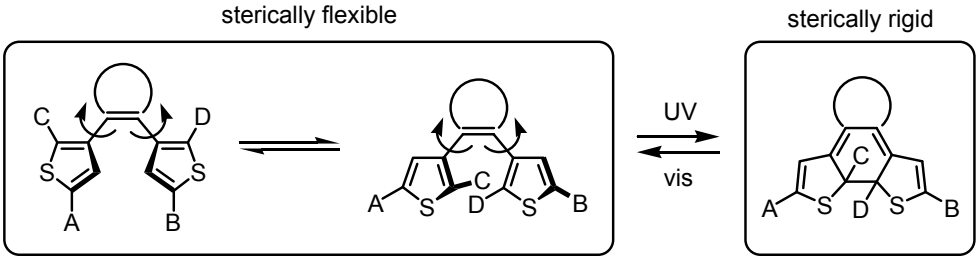

Scheme 1.3.4 Steric changes in DTE derivatives upon photocyclization: The thiophene rings of the ring-open isomer can freely rotate whereas they are locked in the ring-closed isomer forcing the groups A, B, C, and D to diverge from each other. The stereochemistry of the ring-closed isomer is implied.

Electronic differences between the photoisomers

In the ring-open form of DTE derivatives, the two thienyl groups are electronically isolated from one another. Due to steric repulsion at the internal positions, the thiophene rings are not in the same plane and the two π-systems are localised on either ring. Moreover, the pendant groups 'A' and 'B', which are cross-conjugated through the DTE backbone, are electronically insulated from one another, whereas

groups ‘A’ and ‘C’, and ‘B’ and ‘D’ are electronically connected. Upon ring-closure, a linearly π-conjugated pathway is generated through the entire DTE backbone. This extension of the π-system imparts colour to the ring-closed isomer. Moreover, in this state, groups ‘A’ and ‘B’ are electronically connected allowing them to sense each other’s nature. However, the cyclization event generates sp^3 centres between groups ‘A’ and ‘C’, and ‘B’ and ‘D’, insulating them from each other.[17-22]

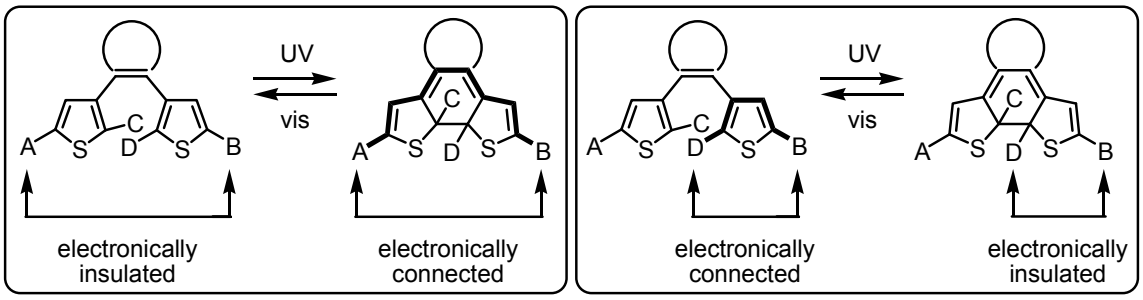

Scheme 1.3.5 Electronic changes in DTE derivatives upon photocyclization: In the ring-open isomer, A and B are electronically insulated and B and D are electronically connected (connection pathway in bold), whereas in the ring-closed isomer, B and D are electronically insulated and A and B are electronically connected (connection pathway in bold). The stereochemistry of the ring-closed isomers is implied.

1.4 Integration of photochromism and chemical reactivity

The first section of this thesis (Section 1.1) describes the importance of the relationship between light and chemical reactivity. Light can be used to control chemical reactions, and chemical events can be used to control photoactivity. When applied to photochromism, this relationship can be very powerful. Not only could chemical events be used to regulate the photochromic behaviour of carefully designed molecules, but photoswitches could also be used to reversibly turn chemical reactions “on” or “off”.

The DTE architecture, described in Section 1.3, offers a very good platform for the development of photoresponsive molecular systems with integrated chemical reactivity capabilities. In this context, several reports show that one can take advantage of the electronic and geometric changes occurring upon isomerisation of DTE derivatives to impart chemical reactivity unique to each form of the photoswitches. Due to the limited amount of work published in this field, Section 1.5 offers a complete literature review of the systems in which photochromism influences reactivity.

Moreover, various strategies are available for the modulation of the photochromic properties of DTE derivatives using chemical events such as changes in supramolecular interactions or the occurrence of chemical reactions. Such events can affect the geometric and electronic configuration of DTEs and can thus modify their photochromic behaviour. It is also possible to disrupt a quenching mechanism preventing photochromism, or to trigger spectral changes. Section 1.6 provides the reader with an extensive review of the examples in which a chemical input influences the photochromic behaviour of DTE derivatives.

In the next two sections, a survey of the reported examples of systems integrating chemical reactivity and the DTE architecture is presented, providing a thorough background regarding the possible strategies for such integration. The reader wishing to proceed immediately to the novel integration strategy described in this thesis may go directly to Section 1.7.

1.5 Modulation of chemical reactivity using DTE derivatives

The relationship between the structure of a molecule and its function is of key importance in chemistry; it is well accepted that the electronic and geometric structures of a compound determine its properties. One of the most dramatic manifestations of this relationship is how a molecule reacts and interacts with others. However, little attention has been given to harnessing the structural and electronic differences between the ring-open and the ring-closed isomers of DTE derivatives to influence chemical reactivity.[29] Nevertheless, this strategy has the potential to advance synthetic methods, photolithography, chemical sensing, and drug delivery. The recent progress in this field is the focus of this section.

1.5.1 Modulation of reactivity using geometric and steric differences in DTEs

In their ring-open state, DTE derivatives are relatively flexible as discussed in Section 1.3.6. This flexibility permits convergence of the functional groups on the thiophene rings and the formation of a binding pocket (Scheme 1.5.1). The photoinduced ring-closing reaction generates a rigid structure and restricts bond rotation, forcing any groups on the heterocycles to diverge away from each other and thus prevents the formation of the intramolecular binding pocket.

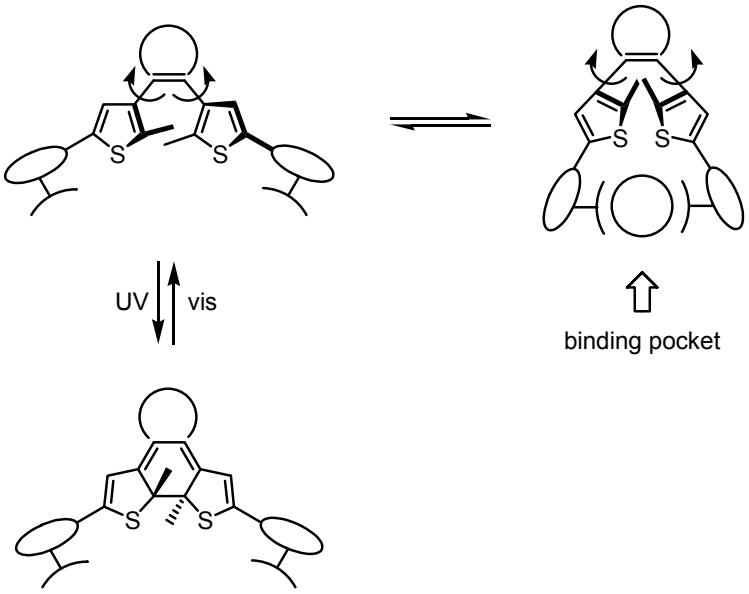

Scheme 1.5.1 Geometric changes in DTE derivatives upon photocyclization allow the reversible formation of a binding pocket present only in the ring-open form of the photoswitches.

Controlling supramolecular events using geometric and steric changes of DTEs

Harvesting these changes in geometry and flexibility between the photoisomers of carefully designed DTE derivatives has allowed the photoregulation of supramolecular interactions between molecular switches and different guests. This approach was first used by Irie and co-workers to create a photoswitchable saccharide receptor.[30] In this example (Figure 1.5.1), the DTE backbone is decorated with boronic acid groups that show good affinity for various sugars. The ring-open form of the photoswitch has greater affinity for glucose compared to the ring-closed form. This observation is attributed to the ability of the two binding sites to freely rotate in the ring-open photoisomer allowing them to face each other like tweezers and to form a 1:1 complex with saccharides. In the ring-closed form, the boronic acid groups are separated from each other and cannot form a 1:1 complex with sugars.

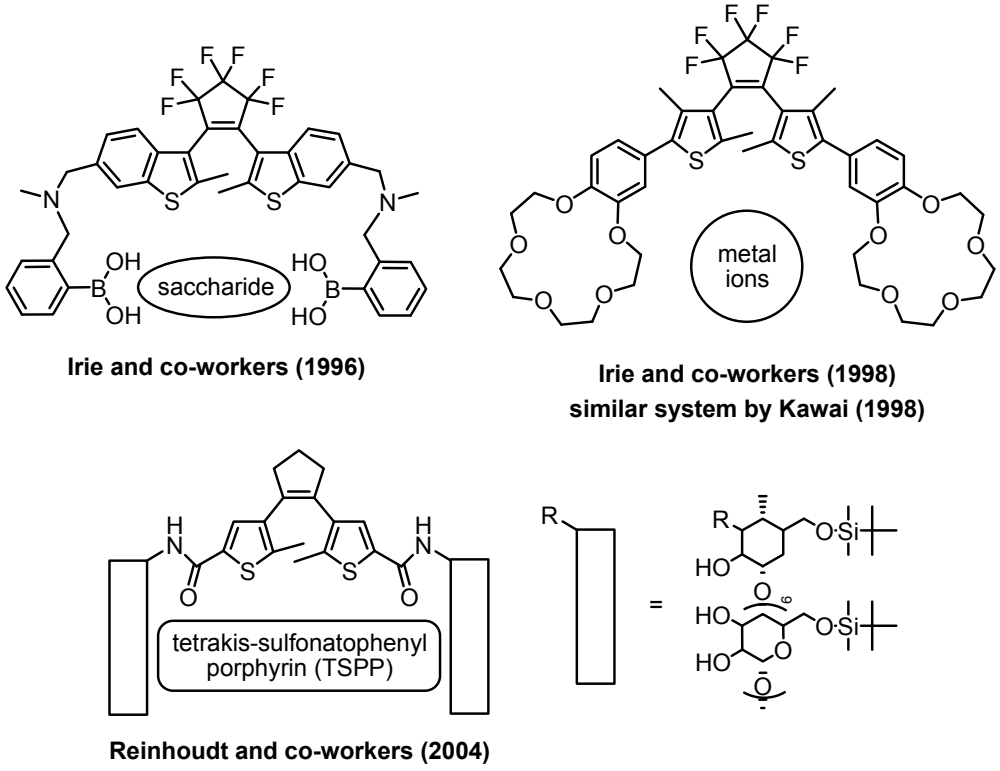

Figure 1.5.1 Examples of photoswitchable hosts for saccharides,[30] ions,[31-34] and a porphyrin.[35]

The same concept has been applied to alkali-metal ion complexation by tailoring the heterocyclic groups on DTE with crown ethers (Figure 1.5.1).[31-34] Active transport of cations such as Na^+, K^+, and Rb^+ between aqueous and organic phases was demonstrated. External control of binding affinities using the geometric difference between both photoisomers of DTEs was also demonstrated with photoswitch-tethered cyclodextrin dimers (Figure 1.5.1).[35] The use of such DTE derivatives allows photocontrolled release and uptake of the *tetrakis*-sulfonatophenyl porphyrin guest.

Photomodulation of catalysis using geometric and steric changes of DTEs

Because of the changes in topology and complexation capabilities occurring after photochemical events, photoswitchable DTEs have great potential for the creation of artificial catalytic systems regulated by light. This approach exploits the thermally

irreversible photochemical ring-closing and ring-opening of catalysts built upon the DTE backbone and harnesses the differences in geometry between the two isomers to regulate metal-catalysed reactions. The first reported photoswitchable catalytic system using the DTE architecture is based on a derivative containing chiral oxazolines at the internal positions of the thiophene rings.[36]

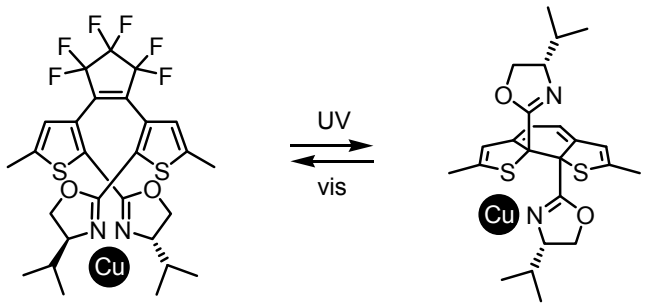

Equation 1.5.1 The bis(oxazoline) DTE photoswitch. The ring-open state provides a chiral environment to perform asymmetric catalysis whereas the ring-closed form does not due to geometric changes.[36]

As shown in Equation 1.5.1, the ring-open state is flexible and forces metal centres, such as copper(I), to reside within a C_2-symmetric chiral environment, commonly used in a wide variety of asymmetric chemical processes involving transition metals.[36] The copper(I)-catalysed cyclopropanation of styrene with ethyl diazoacetate was used as a model reaction to compare the outcome of catalysis using both states of the photoresponsive ligand. The ring-open form of this ligand allows the performance of enantioselective cyclopropanation reactions whereas the ring-closed counterpart does not provide a suitable coordination environment for the metal due to its more rigid architecture and the reactions show insignificant stereoselectivity. This first example of photoregulated catalysis offers interesting prospects for the development of future applications.

1.5.2 Modulation of reactivity using electronic differences in DTEs

In addition to the structural changes induced by the photoreactions of DTE derivatives, the electronic differences between the photoisomers have been extensively studies in the past years.[17-22] It is well known in the photochromism community that the two heterocyclic groups electronically insulated from each other in the ring-open state are placed in electronic communication through photoinduced ring-closure, thus allowing the groups at the external positions on the thienyl groups to sense each other's electronic nature. This approach has been shown to be an effective strategy for the modulation of chemical reactivity in DTE-based photoresponsive systems and is discussed in this section.

Lehn and co-workers have used the change in electronic communication between a phenol and an electron-withdrawing pyridinium group across a DTE backbone to modulate the acidity of the phenol as shown in Scheme 1.5.2.[37] A modified version of this system was recently reported whereby the phenol group is introduced at the internal position of the thiophene bearing a pyridinium ring at the external position.[38] In this example, also shown in Scheme 1.5.2, the phenol group “feels” the electron withdrawing effect of the pyridinium group only in the ring-open state of the switch since the photoinduced ring-closing reaction changes the orbital hybridisation of a carbon between the groups from sp^2 to sp^3, breaking the conjugation in the ring-closed state. Thus, the DTE architecture gives the opportunity to create an “on/off” reactivity switch and to select which form is the “on” state.

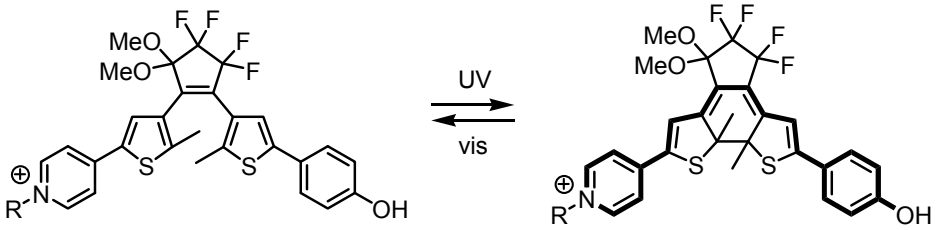

Lehn et al. (1999)

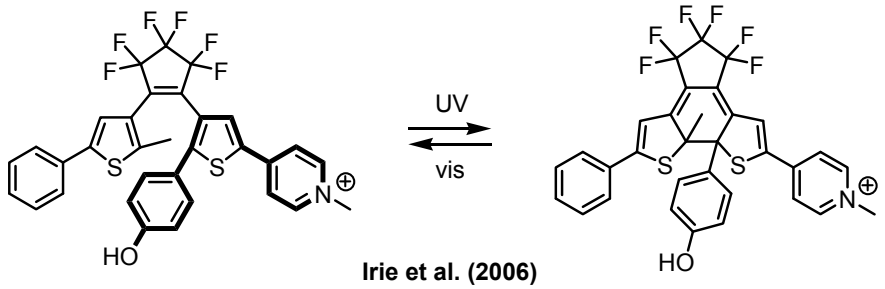

Irie et al. (2006)

Scheme 1.5.2 Photoresponsive DTEs used to photomodulate pK_a. The phenolic groups of these DTEs have different pK_a values in the two photoisomers due to the changes in electronic communication between the phenol unit and the electron-withdrawing pyridinium. The linearly conjugated pathways are highlighted in bold. In Lehn's example,[37] the phenolic group "feels" the electron withdrawing effects of the pyridinium unit only in the ring-closed form, whereas this effect is present only in the ring-open state of Irie's example.[38]

The change in electronic configuration between the two photoisomers of DTE derivatives was also used to photoswitch cation complexation to a monoaza-crown ether-containing DTE as shown in Equation 1.5.2.[39] The external positions of a DTE were substituted with a *p*-phenylaza-15-crown-5 as an ionophore and an aldehyde as a strong electron-withdrawing group. The ring-closed isomer has a binding affinity to calcium that is four orders of magnitude weaker than the ring-open isomer. This lowered binding ability in the ring-closed form is the result of the large decrease in the charge density on the amino group which is the coordinating site for calcium.

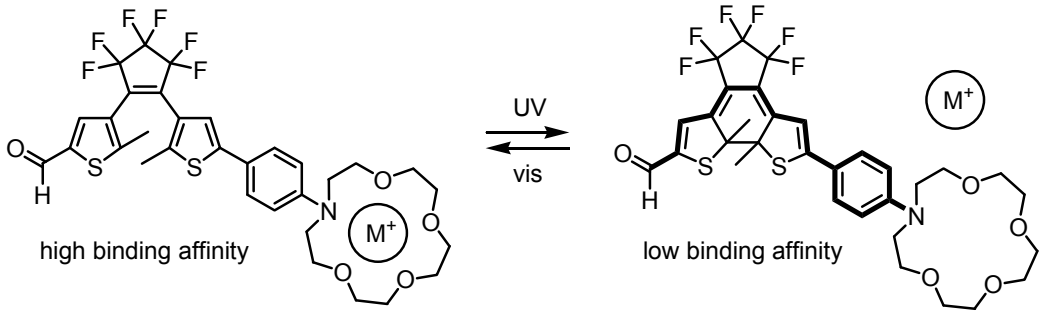

Equation 1.5.2 A DTE derivative using the change in electronic configuration between both photoisomers to affect cation binding.[39] The electron density on the nitrogen atom part of the *p*-phenylaza-15-crown-5 group is reduced in the ring-closed form due the electron-withdrawing effect of the formyl unit. The electronic connection is highlighted in bold.

Pyridine and its derivatives have ubiquitous roles as nucleophilic catalysts in synthesis and biochemical processes.[40,41] Compounds such as *N*,*N*-dimethyl-4-aminopyridine (DMAP) are widely used in coupling reactions.[41] The differences in π-conjugation between the ring-open and the ring-closed isomers of the mono-alkylated *bis*(pyridine) DTE derivative illustrated in Equation 1.5.3 impact the nucleophilicity of the free nitrogen atom.[29,42,43] In the ring-open state, the nucleophilic pyridine does not sense the electron-withdrawing character of the pyridinium group. The ring-closing reaction enables the "free" pyridine to feel the electron-withdrawing pyridinium and reduces its nucleophilic strength. Examination of the alkylation rates of the free pyridines in both photoisomers[43] and of the selective formation of coordination complexes with metalloporphyrins[42] demonstrated the success of this concept. The reaction of an equimolar solution of the ring-open and ring-closed monocations with an excess of 4-bromobenzyl bromide reveals that the ring-open isomer is more reactive and forms its dication product first.[43] Similar results indicating a greater nucleophilicity of the ring-open form are obtained when measuring the stability of complexes between both forms of the photoswitch and a ruthenium-containing porphyrin derivative.[42]

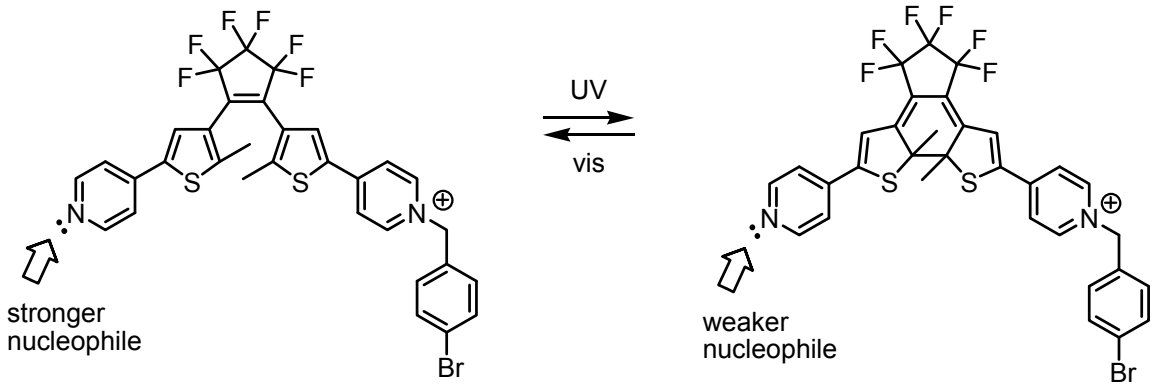

Equation 1.5.3 Reversible photocyclization of this DTE derivative modulates the ability of the pyridine to act as a coordinating ligand.[42] The alkylation rate of the pyridine in both forms of the DTE was also shown to be different.[43]

Based on these results, the mono-alkylated *bis*(pyridine) DTE derivative shown in Equation 1.5.3 is a prime candidate for the photoregulation of chemical processes requiring a nucleophilic catalyst. Preliminary studies have shown that the ring-open form of the molecule is better at catalysing the coupling of dimethylacetylene dicarboxylate (DMAD) to 3-nitrobenzaldehyde.[43]

1.6 Modulation of DTEs photochromism using chemical reactivity

The use of photochromism to control chemical reactivity was discussed in the previous section. The focus of this section is on the opposite approach whereby chemical events are used to control the photochromic properties of DTE derivatives. Termed "reactivity-gated photochromism", this approach describes compounds that do not contain photoisomerisable architectures unless they undergo a spontaneous chemical transformation. This definition can be expended to photochromic systems that are reversibly convertible between photoactive and photoinactive forms using a chemical reaction. This concept was first demonstrated in the work described in *Chapter 2*. Since

then, a few other examples of reactivity-gated photochromism have been reported, while there are several examples of gated photochromism in which one or both forms of the photoswitch are transformed reversibly into photoinactive forms by a gate signal such as electricity, solvation, thermal energy, or chemicals.[13] In order to introduce how chemical reactions can be used to control the photochromic properties of DTEs, this section covers all known examples of reactivity-gated photochromism and chemically-gated photochromism (where chemicals are used to control the photochromic properties of DTEs without inducing a reaction).

1.6.1 Geometric effects on the photochromic properties of DTEs

As discussed in Sections 1.3 and 1.5, the ring-open isomers of DTE derivatives are flexible molecules that can form a parallel and an anti-parallel conformer. The ring-closure photoreaction of DTEs occurs via a conrotatory process, and as dictated by the Woodward-Hoffman rules,[2] can only proceed from the anti-parallel conformation of the photoswitch. The balance between the two conformations therefore limits the maximum quantum yield to 50% if both conformers are present in equal amounts.[22] Modulating the parallel to anti-parallel ratio allows the modification of the photochromic properties of DTE derivatives. This phenomenon can be observed by the introduction of bulky substituents at the internal position of the thienyl groups,[44,45] by the synthesis of DTE derivatives in which one or both thiophene rings are fixed,[46,47] or by the inclusion of the DTE photoswitches in a cyclodextrin cavity.[48-50] It is also possible to use external inputs to reversibly control the spatial conformation of DTEs, and therefore affect their photochromic properties, which is an example of gated photochromism and is discussed in this section.

The first examples of chemically gated photochromism using DTE derivatives are based on the preparation of photoswitches with interlocking arms. The introduction of the appropriate carboxylic acid groups at the external positions of the heterocyclic rings effectively locks the system in the photoinactive parallel conformation in apolar solvents as illustrated in Scheme 1.6.1.[51-53] The addition of hydrogen bond-breaking agents such as ethanol or propylamine disrupts the intramolecular hydrogen-bonds and causes the molecule to freely equilibrate between the parallel and anti-parallel forms, resulting in a significant increase of the ring-closing reaction quantum yield. Thermal energy also offers an effective way to break the hydrogen bonds. When a solution of the compound in decalin is heated above 100 °C, the internal hydrogen bonds are broken and the molecule can isomerise to the anti-parallel form, regaining its photoactivity. Similarly, the introduction of mercaptoalkyl groups to a DTE effectively locks it in the photoinactive parallel conformation by the reversible formation of an intramolecular disulfide linkage upon an oxidation/reduction cycle.[52] Photoactivity can be regained using tri-*n*-butylphosphine as the reducing agent, which disrupts the disulfide bond. This concept is shown in Scheme 1.6.1.

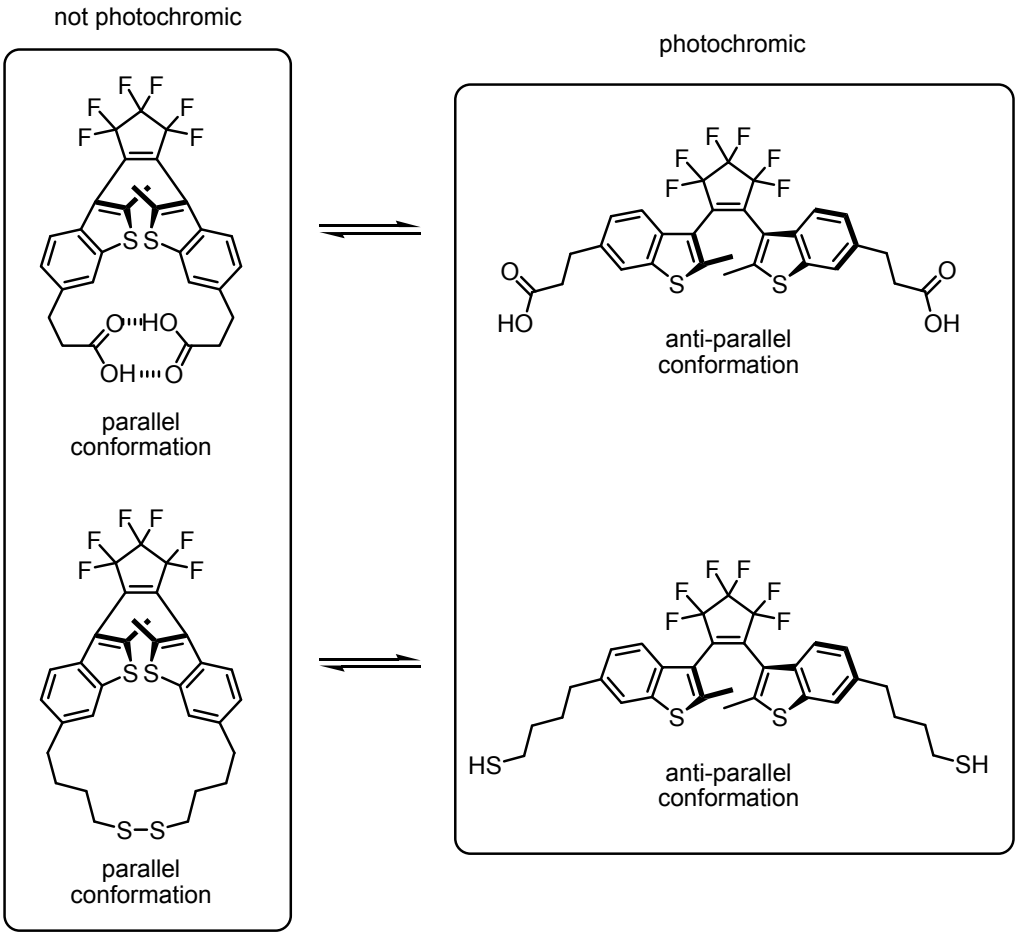

Scheme 1.6.1 The DTE derivatives with intralocking arms shown on the left are locked in the photoinactive parallel conformation. Addition of a hydrogen bonding-breaking agent (top)[51-53] or a reducing agent (bottom)[52] effectively unlocks them, restoring their photochromic behaviour.

Supramolecular interactions of a substrate with a DTE derivative have the potential to affect the spatial orientation of the photoswitch, disrupting or enhancing its photochromic activity. Gated photochromism was observed in many of the systems described in the previous section which focused on modulating the binding affinity of functionalised DTEs towards guests. For example, the addition of glucose to the open isomer of a *bis*(boronic acid) photoswitchable saccharide receptor completely shuts down the possibility to ring-close the system with UV light since the receptor is forced in the photoinactive parallel conformation.[30] A similar gating effect was observed with the ion

tweezers containing two crown ether moieties (Figure 1.5.1).[34] An analogous effect was discovered by Feringa and co-workers who found that copper(I) and acids completely blocks the photochemical ring-closing reactions of DTE analogues in which the thiophene rings are replaced by pyridyl groups (Equation 1.6.1) because of the formation of 1:1 complexes.[54]

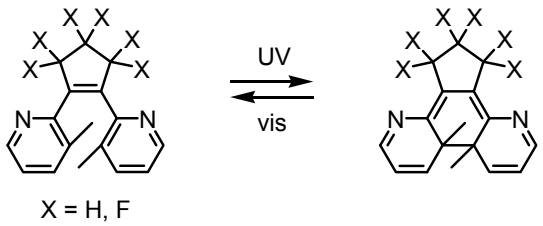

Equation 1.6.1 This dipyridinylethene photoswitch, analogous to DTEs, can be photochemically ring-opened and ring-closed when exposed to light of appropriate energies.[54]

The addition of guest molecules to the ring-open form of DTE derivatives can also improve the photochromic properties of the switches: The presence of Zn^{2+} in a solution of a *bis*(pyridine) DTE derivative was shown to increase the photocyclization quantum yield.[55] Qin and co-workers proposed the formation of a crablike complex formed from two ring-open DTE derivatives and two cations. The photoactive anti-parallel conformer seems to be favoured by the formation of this complex.

Gated photochromism was also observed in an attempt to photoregulate catalysis using a copper(I) metal centre coordinated to a DTE ligand as discussed in Section 1.5.1. The photoinduced ring-closing reaction of the internal *bis*(oxazoline) ligand is inhibited by the addition of Cu(I) in dichloromethane solution.[36] The phenomenon is explained by the fact that the copper is being too tightly bound within the ligand's chelating site to allow photoswitching. The presence of the copper centre prevents the ligand from

undergoing the necessary geometric changes that need to occur during the photoreaction. This problem can be overcome by adding a small amount of acetonitrile, a more competitive coordinating solvent as shown in Scheme 1.6.2. However, the stereoselectivity of the cyclopropanation reaction is affected by this as it partially disrupts the binding of the photoswitchable ligand to the copper centre.

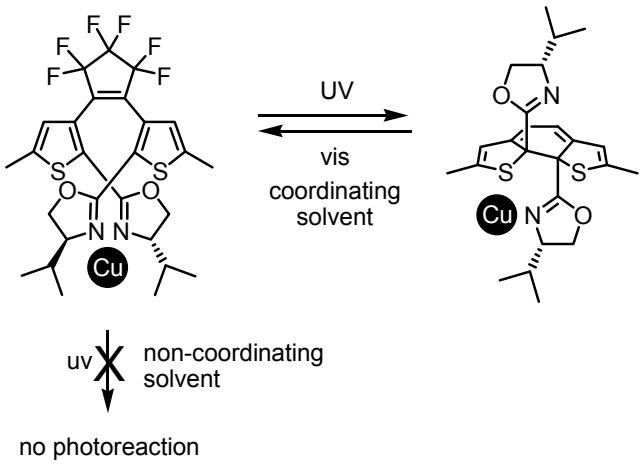

Scheme 1.6.2 Upon the addition of copper(I) to this DTE ligand, the photochemical ring-closing reaction is inhibited. The photoresponsive behaviour of the ligand can be restored by the addition of a competing coordinating solvent.[36]

1.6.2 Electronic effects on the photochromic properties of DTEs

The electronic configuration of a molecule dictates how it interacts and reacts with other compounds. As discussed in Section 1.5, this strategy allows the photocontrol of reactivity using rationally designed DTE derivatives. The same strategy can be used to chemically control the photoactivity of molecular switches. In its ring-open state, a *bis*(phenol) DTE derivative (Scheme 1.6.3) is electrochemically stable and can be ring-closed using light in the UV range.[56,57] In the ring-closed state of the photoswitch, the phenol groups are conjugated to each other and can be easily oxidised to the quinoid form of the molecule. In this form, the electronic structure of the molecule is not suitable for

the ring-opening reaction and the molecule is photoinactive. Hence, the redox chemistry can gate the photochemistry. Reduction to the *bis*(phenol) architecture renders the system photoactive and the photoinduced ring-opening can occur. This system is referred to as a dual-mode photochromic device since the photochemistry is affected by the electrochemistry and *vice versa*.

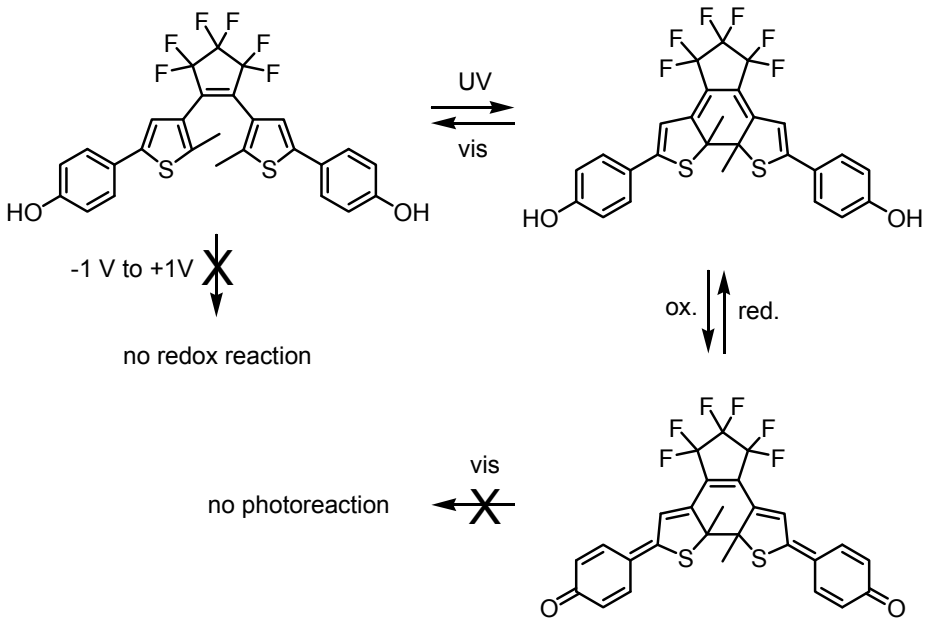

Scheme 1.6.3 An example of dual-mode photochromism.[56,57] The ring-open form of this DTE derivative is not redox active but can be photochemically ring-closed. The ring-closed isomer, which is redox active, can be oxidised to form a photoinactive molecule with a quinoid architecture. Reduction of this locked molecule regenerates the photoactive ring-closed DTE.

The formation of a quinoid-type structure preventing the ring-opening or ring-closing photoreactions was also reported in the two examples where the pK_a of a phenol is affected by the induction effect of a pyridinium group in only one state of the photoswitches (Section 1.5.2).[37,38] For example, at high pH, the phenol group of the DTE derivative described by Irie and co-workers is deprotonated. Since the pyridinium is conjugated to the phenolate in the ring-open isomer, the charge can be delocalised

inducing the formation of a quinoid-type architecture making the molecule photoinactive and locking it in this conformation as depicted in Scheme 1.6.5.[38]

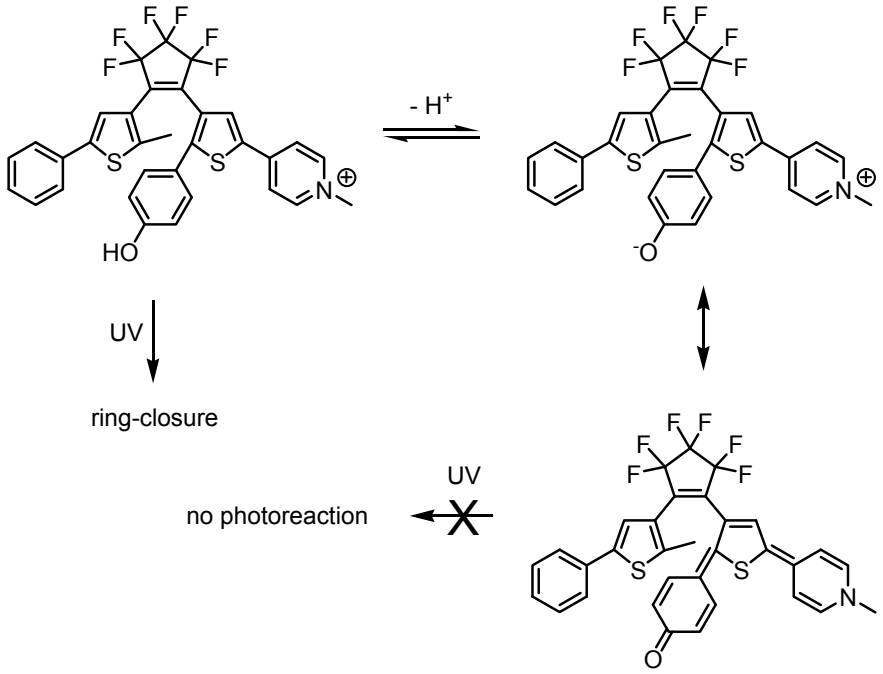

Scheme 1.6.4 Upon deprotonation of the ring-open form of this DTE derivative at high pH, a quinoid structure can be formed preventing the ring-closing reaction.[38] This is an example of acid-base gated photochromism.

Conversely, in the system described by Lehn et al. where the pyridinium group and the phenol unit are attached at the external positions of the thiophene rings, the quinoid form is induced by deprotonation in the ring-closed state.[37] In this case, the photoactivity of the ring-closed photoisomer is reduced upon deprotonation. However, the ring-closing photoreaction is also totally prevented by deprotonation of the ring-open isomer as seen in Scheme 1.6.5. This phenomenon can be explained by a through-space effect whereby an ionic interaction between the phenolate and pyridinium groups locks the molecule in the photoinactive parallel conformation.

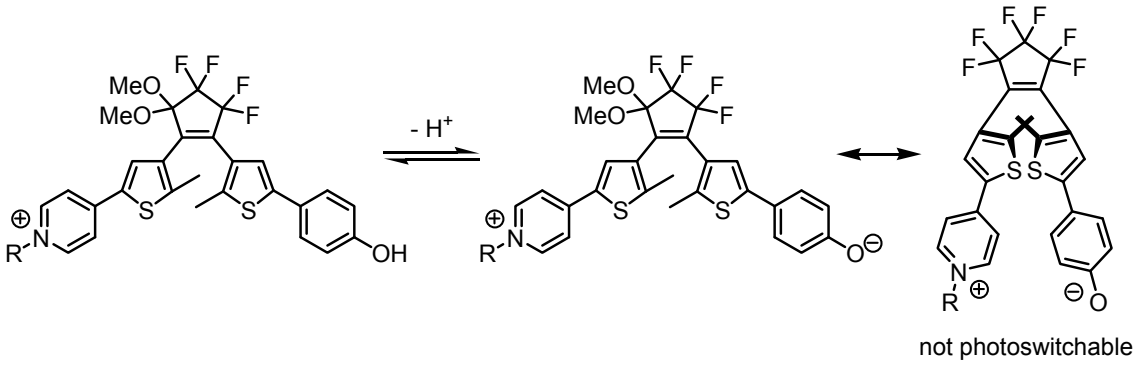

Scheme 1.6.5 An example of through-space acid-base gated photochromism. Upon deprotonation at high pH, the ring-open DTE derivative is locked in the photoinactive parallel conformation.[37]

Recently, Matsuda and co-workers prepared a novel DTE derivative with (4-pyridylethynyl groups directly attached to the 1,3,5-hexatriene moiety (Figure 1.6.1).[58] Upon quaternarisation of the pyridine rings by addition of an acid, the photoreactivity of the system is strongly suppressed and can be recovered by the addition of a base. The electron-withdrawing nature of the pyridinium cations at the photoreactive positions is believed to affect the electronic system of the hexatriene moiety by a through-bond effect shutting down its photoreactivity. A similar gating behaviour had been previously observed by Irie and co-workers whereby the photoactivity of extended π-conjugated DTE derivatives was thermally controlled.[59]

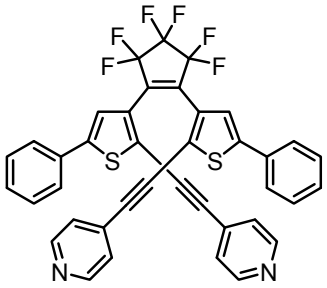

Figure 1.6.1 The photochemical ring-closing reaction of this *bis*-pyridylethynyl DTE derivative is completely inhibited by protonation of the pyridine units. A through-bond effect on the electronic properties of the hexatriene moiety is believed to cause this behaviour.[38]

1.6.3 Quenching effects on the photochromic properties of DTEs

Normally, irradiation of DTE derivatives promotes them to an excited state and eventually results in the ring-closing or ring-opening of the molecules. However, in some systems, other processes efficiently quench the excited states of the molecules.

Recently, Irie and co-workers developed a system in which the excited state of the ring-open form is quenched by an intramolecular proton transfer from a phenol group to a carbonyl group (Scheme 1.6.6).[60] In this form, the molecule is photoinactive. Protection of the phenolic unit by esterification inhibits the proton transfer quenching mechanism and the molecule becomes photoswitchable. When the ring-closed isomer is deprotected by hydrolysis, the phenolic unit is restored; this process does not inhibit the photoinduced ring-opening reaction but rather renders the ring-open form completely photoinactive. This system represents one of the rare examples of reactivity-gated photochromism.

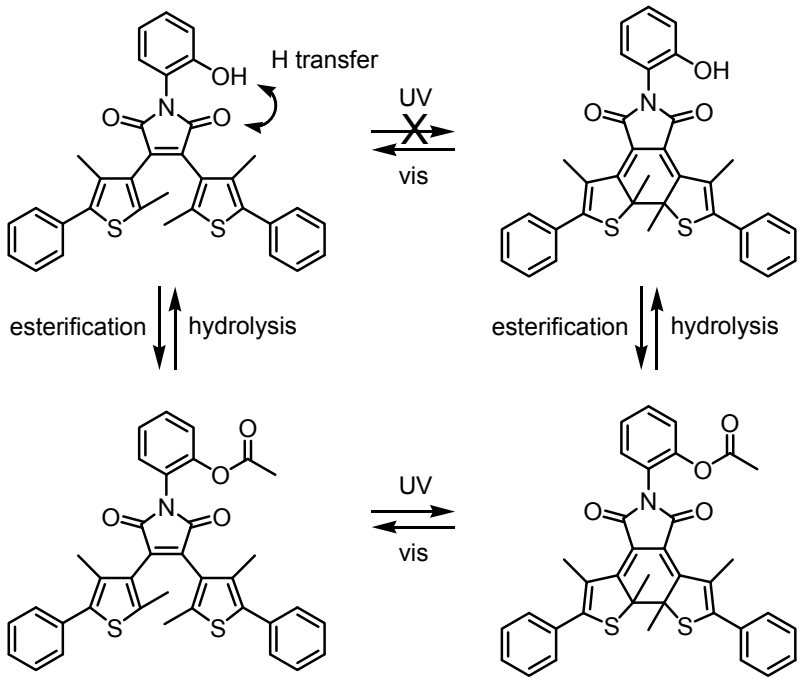

Scheme 1.6.6 An example of reactivity-gated photochromism through esterification/hydrolysis. Prior to estirification of the ring-open isomer of this DTE derivative, the ring-closure reaction is quenched by a proton transfer. The ester-protected DTE is photochromic. The hydrolysed ring-closed isomer can be photochemically ring-opened.[60]

Belser and co-workers have demonstrated another example of reactivity-gated photochromism using a quenching approach.[61] A DTE derivative containing a cyclobutene-1,2-dione skeleton does not exhibit photochromic properties (Scheme 1.6.7). However, when both ketone functions are protected with cyclic acetal groups, photochromism is observed. It is believed that the ring-closing reaction is quenched by the ring-opening of the cyclobutene-1,2-dione unit yielding a 1,2-*bis*ketene moiety as shown in Scheme 1.6.7. When both of the ketone groups are protected, this quenching process cannot occur and the ring-closed form is generated upon irradiation. Deprotection of the ketone units does not inhibit the ring-opening reaction.

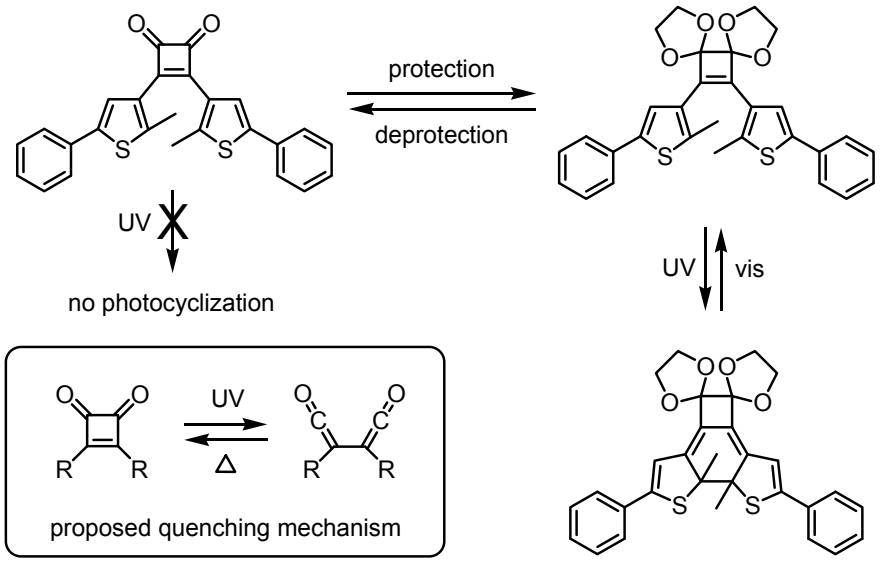

Scheme 1.6.7 An example of reactivity-gated photochromism using this cyclobutene-1,2-dione-containing DTE derivative. The formation of ketene functions upon exposure to light prevents the photochromic process unless the carbonyl groups are protected.[61]

Intramolecular charge transfer states (ICTS) can be used to quench the ring-closure reactions of DTEs. Rationally designed systems offer the possibility to chemically create an ICTS, for instance by introducing pyridinium betaine groups onto the DTE backbone as described by Zang and co-workers (Figure 1.6.2).[62] When deprotonated with a suitable base, zwitterionic pyridinium betaine moieties are formed on the thienyl groups. The dipolar character of betaine is dramatically decreased in the excited state of the molecule through a short-range charge transfer between the aromatic electron donor group and the pyridinium electron accepting group, which quenches the ring-closing mechanism. Protonation of the pyridinium betaine eliminates the charge transfer process and photoswitchability is restored. Due to the energetics of the ICTS, only the ring-open isomer is subjected to this quenching mechanism: the ring-closed form is photoactive.

A similar system was previously described by Irie *et al.* where *N*,*N*-diethyl amino groups at the 5-positions of a *bis*(2-thienyl)perfluocyclopentene suppress the photocyclization reaction (Figure 1.6.2).[63] This is attributed to the contribution of a twisted intramolecular charge transfer (TICT). The addition of trifluoroacetic acid eliminates the electron-donating character of the amino groups and the protonated switch undergoes a normal photocyclization reaction upon UV irradiation.

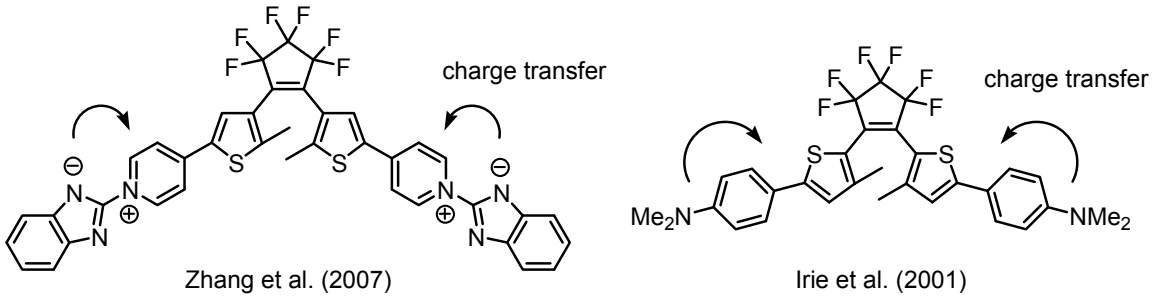

Figure 1.6.2 Photoswitching of these two DTE derivatives is prevented by quenching charge transfers.[62,63] Protonation of the molecules restores their photochromic properties.

It was observed that the addition of a metal-containing porphyrin ring to a dicyanoethylene-thienylethene (DCTE) containing a pyridine group completely inhibits the ring-opening and ring-closing photoreactions through quenching of the excited states whereas the free pyridine-containing DCTE shows normal photochromic behaviour.[29]

1.6.4 Controlling the spectral properties of DTEs

The control of the spectral properties of DTE photoswitches provides another means to affect their photoswitching capabilities. When the absorption spectrum of a molecular switch is shifted outside the irradiation window, the molecule becomes effectively photoinactive. The use of an external signal to modify the wavelength at which a photoreaction can occur has been demonstrated in some examples.

A DTE derivative bearing organoboron groups at the external positions of the thiophene rings can be ring-closed using light in the UV range.[64] The absorption maximum of the ring-closed form is at relatively low energy (655 nm) since the boron moieties are part of the conjugation of the backbone. However, the absorption maximum is shifted to 490 nm upon the addition of a fluoride ion. The Lewis acid-base interaction between the trivalent boron atom and the fluoride ion shortens the conjugation of the backbone since the p-orbital of the boron is no longer available to interact with the DTE backbone, and the system absorbs light of higher energy. This system is discussed in more detail in Section 4.1.4 of *Chapter 4*. A similar behaviour was observed for a mono-substituted DTE system that can interact with fluoride and mercury ions.[65]

More recently, Lewis acid modulation of the spectral properties of a DTE system bearing methylamino groups was accomplished.[66] Absorption and emission properties of an imidazo phenanthroline DTE derivative were also controlled by variation of pH.[67] Moreover, a series of *N*,*N*-donor ligands containing a DTE derivative were shown to display spectral variations caused by the addition of a coordinating metal.[68-70] This is explained by a triplet metal to ligand charge transfer photosensitisation of the ring-closing reaction and a perturbation of the transition state for the ring-opening reaction.

1.6.5 Gating the thermal reversibility of DTEs

DTE derivatives are usually thermally irreversible systems. Terakawa and co-workers have recently reported a DTE system in which the addition of an acid reversibly converts the molecule into a thermally reversible system.[71] This behaviour allows the control of the thermal ring-opening reaction of the molecular switch using light or chemicals.

1.7 Integrating photochromism and chemical reactivity – The strategy developed in this thesis

1.7.1 A novel concept: reactivity-gated photochromism

In the previous section, various approaches towards the modulation of the photochromic properties of DTE derivatives were presented. One of the objectives of this thesis is to present a novel strategy for the regulation of the photochromic properties of DTE derivatives. The conventional approaches include the control of their conformation (parallel versus anti-parallel), the modification of their electronic configuration, the regulation of a competing quenching mechanism, and the alteration of their spectral and thermal properties. However, these methods all have one common point: they use DTE derivatives containing the photoresponsive 1,3,5-hexatriene moiety, and the photochromic properties of the systems are rarely completely inhibited by the external chemical events. Creating or disrupting the DTE architecture on demand offers various advantages that will be discussed throughout this document.

DTE derivatives undergo reversible photocyclization reactions when irradiated with light of the appropriate wavelengths because they possess a 1,3,5-hexatriene substructure. The creation of this architecture by a mild and spontaneous reaction with an external chemical species should be a very efficient way to "gate" the photochromism of a system. Photochromic properties would be gained only after the occurrence of the chemical process, resulting in reactivity-gated photochromism.

The 1,3,5-hexatriene unit of a generic DTE derivative, depicted in Figure 1.7.1, contains two single bonds, two double bonds included in heterocyclic rings, and one double bond within the top ring. This latter linkage can be easier to synthesise using a

simple chemical reaction since it is not part of a functionality with aromatic character. It is therefore targeted for the demonstration of the new reactivity-gated concept.

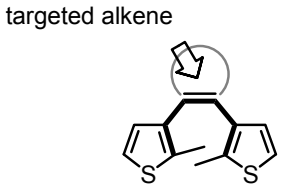

Figure 1.7.1 Targeted bond formation for reactivity-gated photochromism.

Scheme 1.7.1 illustrates the reactivity-gated photochromism concept presented in this thesis. The 1,2-dithienylethane, **DTA**, lacks the required photoresponsive functionality and is thus expected to be photoinactive (not photochromic). The molecule **DTE-o**, generated when **DTA** reacts with an external chemical species, contains the 1,3,5-hexatriene system as part of the photoresponsive DTE architecture. Irradiation with light of appropriate energy should trigger the cyclization reaction and produce **DTE-c**, which could be detected using the numerous output signals available with these derivatives (e.g. absorption, emission, redox properties). The first example of this concept using the Diels-Alder reaction is demonstrated in *Chapter 2*.

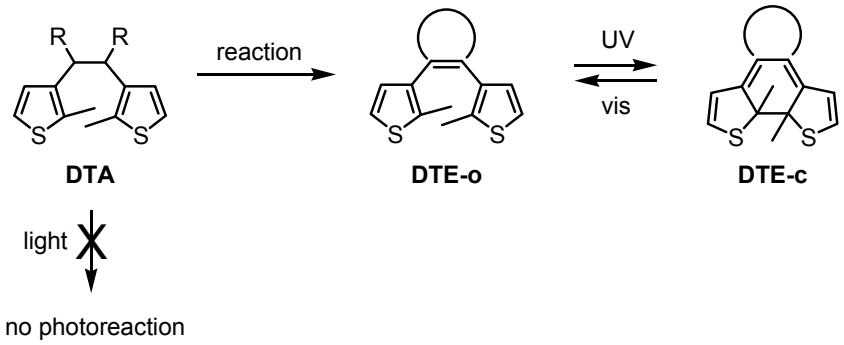

Scheme 1.7.1 The novel approach of reactivity-gated photochromism presented in this thesis: **DTA** lacks a photoresponsive moiety and is thus photoinactive unless it undergoes a chemical reaction generating **DTE-o**, which possesses the required photoresponsive DTE architecture. **DTE-o** should undergo a reversible photochemical ring-closing reaction to form **DTE-c**.

1.7.2 A novel approach for the photoregulation of reactivity using DTEs

A careful analysis of the structures presented in Scheme 1.7.1 reveals another appealing concept. If the reaction forming **DTE-o** from **DTA** is reversible, **DTA** can only be regenerated from **DTE-o** since **DTE-c** lacks the appropriate bond configuration. Thus, photoregulation of chemical reactivity could also be integrated in this system.

A survey of the different strategies previously used for the modulation of chemical reactivity based on the DTE architecture was provided in Section 1.5 of this chapter. The changes in localisation of a π-bond upon photocyclization could offer a novel approach for the regulation of reactivity. The ring-closing photoreaction of DTE derivatives causes a rearrangement of the π-system. As described earlier in this chapter and shown in Equation 1.7.1, the hexatriene unit undergoes a pericyclic reaction to form a cyclohexadiene when irradiated with UV light. The localised central π-bond in the ring-open isomer **DTE-o** becomes delocalised in the ring-closed form **DTE-c**; this rearrangement of π-bonds can be described as the creation and disruption of double bonds in specific locations. In Equation 1.7.1, the circle highlights a localised double bond in

the ring-open isomer **DTE-o**. The same area in the ring-closed isomer **DTE-c** lacks a double bond since it is now delocalised through the backbone of the molecule. The localised double bond can be regenerated by visible light exposure. The integration of this double bond into another reactive functionality would permit the remote control of how this other subunit reacts and interacts with its environment.

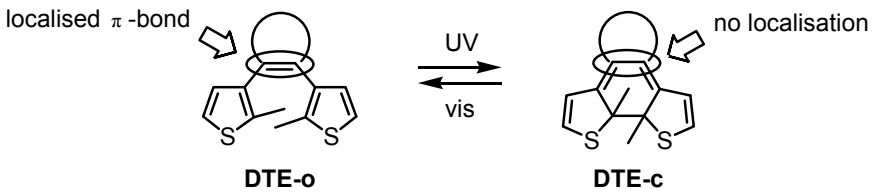

Equation 1.7.1 The ring-closing isomerisation of DTEs is accompanied by the "removal" of the localised π-bond (circled) from the ring-open isomer **DTE-o**. The ring-closed isomer **DTE-c** does not have a localised π-bond in the central position (circled). The localised π-bond can be "created" from the ring-closed isomer upon exposure with visible light, regenerating the ring-open isomer.

The concept of integrating a reactive functional group into the DTE backbone such that it can only exist in one form of the photoswitch was first described using a reversible Diels-Alder reaction and is discussed in detail in *Chapter 3*. The same approach is discussed in *Chapter 4* where the DTE architecture is integrated with a 1,3,2-dioxaborole unit in order to regulate the Lewis acidity of a molecule by light exposure.

The effectiveness of this bond rearrangement strategy has since been demonstrated in an example where the thermal Bergman cyclization is photoregulated using a DTE derivative.[72] In Scheme 1.7.2, the ring-open form of the DTE derivative **DTE-o** contains both a hexatriene and an enediyne group. The thermal Bergman rearrangement can only occur in this form of the molecule. UV light triggers the photocyclization of the hexatriene in **DTE-o** and converts it to its ring-closed counterpart

DTE-c. The photochemical transformation rearranges the π-system and delocalises it along the rigid backbone, hence removing the enediyne architecture necessary for the spontaneous conversion to the diradical and making the ring-closed isomer inactive. Visible light activates the system by triggering the ring-opening reaction, regenerating the enediyne architecture. This concept was demonstrated at 75 °C; a system effective at body temperature could allow photoactivation of chemotherapeutics in order to limit toxic side effects.

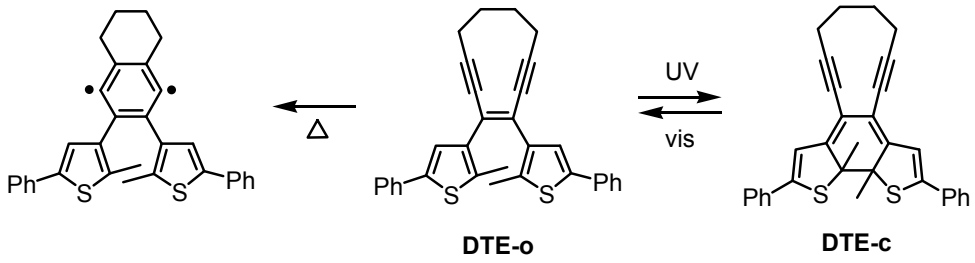

Scheme 1.7.2 Compound **DTE-o** contains an enediyne moiety and can undergo a thermal Bergman cyclization to yield the benzenoid diradical. This reaction can be prevented by taking advantage of the photoisomerisation of **DTE-o** into **DTE-c** which lacks an enediyne moiety. Exposure of **DTE-c** to visible light regenerates **DTE-o** which can undergo the Bergman cyclization.

1.8 Summary

The integration of photochromism and chemical reactivity into molecular systems has the potential to benefit many scientific communities. It can advance synthetic methods and catalysis, allow the regulation of therapeutics and of their deliverance, give control over the initiation of biological phenomena, and be useful for photolithography and in chemical detection applications. In this introductory chapter, the photoswitchable dithienylethene (DTE) architecture was presented as well as its successful integration with chemical reactivity to form systems where light regulates reactivity and where

reactivity regulates photochromism. Finally, the novel approach to integrate photochromism and reactivity developed in this thesis was introduced in the previous section (Section 1.7).

The photochromic properties of DTE derivatives result from the 1,3,5-hexatriene functionality included in their architecture. The generation of this moiety using a mild and spontaneous chemical reaction should provide an effective way to "gate" photochromism. Inversely, the electronic configuration of a functionality dictates its reactivity. The reversible removal and creation of a localised π-bond using the bond reorganisation of DTE derivatives should provide an effective means to "gate" chemical reactivity. The goal of the work presented in this thesis is to apply this novel strategy to molecular systems and to demonstrate its potential for the development of applications.

1.9 Thesis overview

In *Chapter 2*, the first example of reactivity-gated photochromism using the Diels-Alder reaction is presented. The synthesis and properties of a series of dienes (such as compound **1.1** shown in Scheme 1.9.1) are described. These dienes undergo Diels-Alder reactions with various dienophiles to generate photoresponsive molecules containing the DTE substructure such as compound **1.2o**. The development of chemical detection applications is proposed.

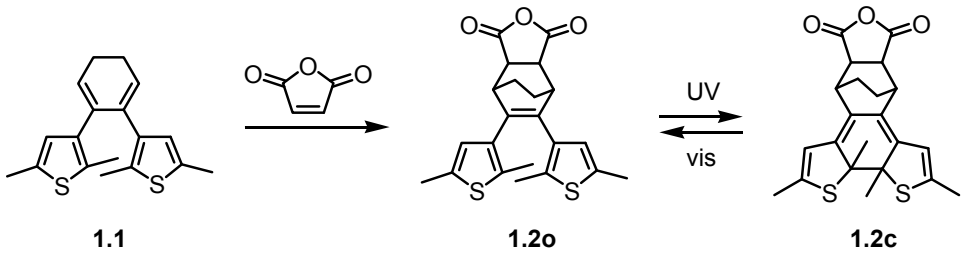

Scheme 1.9.1 A novel approach of reactivity-gated photochromism using the Diels-Alder reaction as presented in *Chapter 2*: Compound **1.1** lacks a photoresponsive moiety and is thus photoinactive unless it undergoes a [4+2] cycloaddition generating compound **1.2o**, which possesses the required photoresponsive DTE architecture. Compound **1.2o** should undergo a reversible photochemical ring-closing reaction to form the ring-closed isomer **1.2c**.

In *Chapter 3*, a novel strategy for the selective and sequential photorelease of a chemical species is presented. The photorelease systems reported represent a versatile approach for chemical species delivery, which is based on combining reactivity-gated photochemistry and photogated reactivity. As shown in Scheme 1.9.2, the Diels-Alder reaction between fulvenes **1.6** or **1.7** and fumarate **1.8** allows the reversible formation of the photoresponsive DTE derivatives **1.4o** or **1.5o**. Upon exposure to UV light, the thermally stable ring-closed photoisomers **1.4c** or **1.5c** are formed and can be isolated.

Further irradiation with light in the visible range triggers the ring-opening reactions and subsequent release of the dienophile **1.8**.

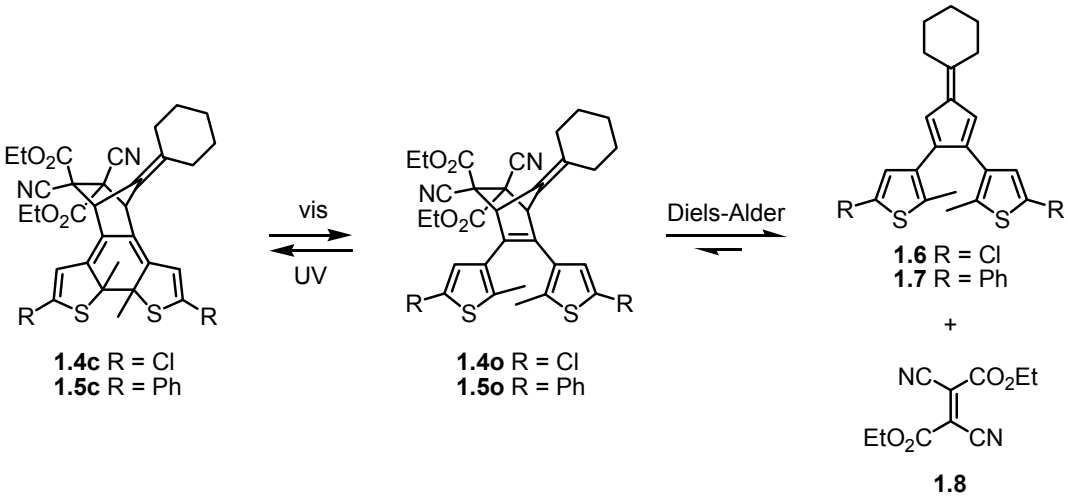

Scheme 1.9.2 Upon exposure of the thermally stable compounds **1.4c** and **1.5c** to visible light, the ring-open isomers **1.4o** and **1.5o** are generated leading to subsequent thermal fragmentations to form the fulvenes **1.6** and **1.7**, and the fumarate **1.8**, through a retro-Diels-Alder reaction. This system is presented in *Chapter 3*.

In *Chapter 4*, an example highlighting how the presence/absence of localised π-systems could be used to photoregulate the Lewis acidity of a boron-containing DTE derivative is discussed. The electronic structure of a 1,3,2-dioxaborole unit is modified by the reversible isomerisation of DTE when exposed to appropriate wavelengths of light. Exposure of the ring-open isomer **1.9o** (Equation 1.9.1) to UV light triggers a pericyclic reaction and yields the ring-closed isomer **1.9c** which shows an increased binding affinity to pyridine. Subsequent exposure to visible light triggers the reverse reaction causing a decrease in the Lewis acidity of the boron-containing DTE derivative the release of pyridine.

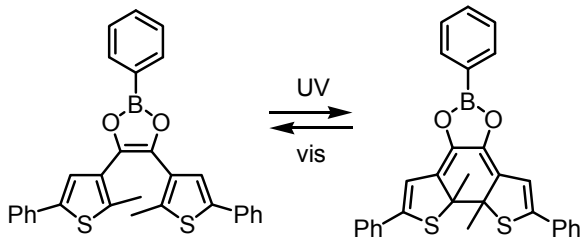

1.9o **1.9c**

Equation 1.9.1 The boron-containing DTE derivative used to modulate the Lewis acidity of the boron centre as described in *Chapter 4*. Compound **1.9o** should undergo a reversible ring-closing reaction when exposed to UV radiation to form photoisomer **1.9c**.

This thesis concludes with a summary of the results presented in each chapter highlighting the success of the new approach towards the integration of chemical reactivity and photochromism.

Chapter 2: Reactivity-Gated Photochromism of 1,2-Dithienylethene Derivatives Using the Diels-Alder Reaction

The research presented in this chapter was published in part as a communication in: V. Lemieux, N. R. Branda, "Reactivity-gated photochromism of 1,2-dithienylethenes for potential use in dosimetry applications", *Org. Lett.* **2005**, *7*(14), 2969-2972. It is also part of a patent application: N. R. Branda, B. Wüstenberg, V. Lemieux, S. Gauthier, M. Adams, "Photochromic and electrochromic compounds and synthesis and use thereof", WO/2006/125317, PCT/CA2006/000862, filed May 25, 2006.

In this chapter, the novel and versatile approach of reactivity-gated photochromism is presented. Using the Diels-Alder cycloaddition reaction, photoinactive dienes are rendered photoswitchable by creating the photoresponsive DTE architecture. Section 2.1 briefly introduces the concept of reactivity-gated photochromism as applied to chemical detection. Section 2.2 proposes the use of the Diels-Alder reaction to demonstrate this concept. Results and discussion are presented in Section 2.3. A brief summary and perspectives are provided in Section 2.4. Finally, Section 2.5 presents the experimental details and synthetic procedures.

2.1 Introduction – Controlling the photochromic properties of DTE derivatives

The thermally irreversible photocyclization reactions of 1,2-dithienylethene (DTE) derivatives are becoming increasingly significant to the materials science community.[17-22] Because the two photoisomers have distinctly different optical and electronic characteristics, compounds containing this 6π-electron backbone have the potential to advance optoelectronic technologies such as optical information processing.[17-22] However, several problems remain, limiting the development of practical applications. For example, most DTE systems lack a mechanism to prevent stored images or memories from being erased when stored under room lighting or after many readout operations. Gated photochromism, which would provide such a mechanism, is therefore strongly desirable but has not yet been achieved adequately.

2.1.1 Gated photochromism

In gated photochromism, an additional external stimulation, such as another photon, an electrical field, a chemical, or heat, must be present before the photochemical events arise.[13] In this way, a non-photochromic molecule is rendered photochromic by an external stimulus.

The reversible transformation of a molecular system between a non-photochromic and a photochromic state through the addition of external chemical species is particularly appealing for the development of chemical detection applications and could provide an efficient means to protect stored information.[51-53] Many strategies have been developed for the regulation of the photochromic behaviour of DTEs through chemical events, as was described in the introductory chapter.

2.1.2 DTE derivatives for chemical detection

A chemical sensor can be defined as "a composite device capable of eliciting a response which quantifies the presence of an analyte".[11] In order to determine the concentration of a chemical species on a real-time basis, the response of a sensor needs to be reversible. Irreversible systems give integrated time-dependent responses (total dose to which it has been exposed over time) and are usually referred to as dosimeters. In this thesis, chemical detection systems that show a reversible response to analytes are referred to as sensors. Systems with an irreversible response are termed dosimeters.

The use of the versatile DTE architecture in sensing and dosimetry applications has not been extensively discussed in the literature. This is surprising since the large variety of properties that are accessible by synthetically tailoring the DTE backbone offers a wide range of useful read-out signals. In addition to changes in colour, the photochemical transformation of DTEs can be accompanied by variations in luminescence, redox potential, conductivity, magnetism, chirality and optical rotation, dielectric constant, and refractive index.[17-22] Hence, an analyte affecting the photochromic behaviour of a carefully designed DTE derivative could be detected using this wide range of read-out signals.

Some reports have described DTEs that may be used for chemical detection, although this application has never been directly addressed. As discussed in the introductory section of this thesis (*Chapter 1*), the concept of gated photochromism has been described in publications illustrating how the complexation to a saccharide[30] or a metal ion,[31-34] the reversible formation of intramolecular hydrogen bonds,[51-53] or the action of a reducing agent[52] can regulate the photochemistry of DTE derivatives. In each

of these cases, the gate input dictates whether the 1,3,5-hexatriene portion of the photoswitch can adopt the appropriate conformation to undergo the conrotatory 6π-electron photocyclization. Generally, the "guest" or "analyte" forces the DTE derivative into a non-photoresponsive conformation, blocking its photochromic properties as illustrated in Scheme 2.1.1. Although this mechanism regulates the behaviour of DTEs, in most cases more effective chemical detection would be achieved if photochromism was activated by the analyte. Moreover, since the binding event between the photoswitch and the guest is reversible, even in the presence of excess guest, the portion of "free" DTE derivative remains photoactive, which may hinder detection of the read out signal.

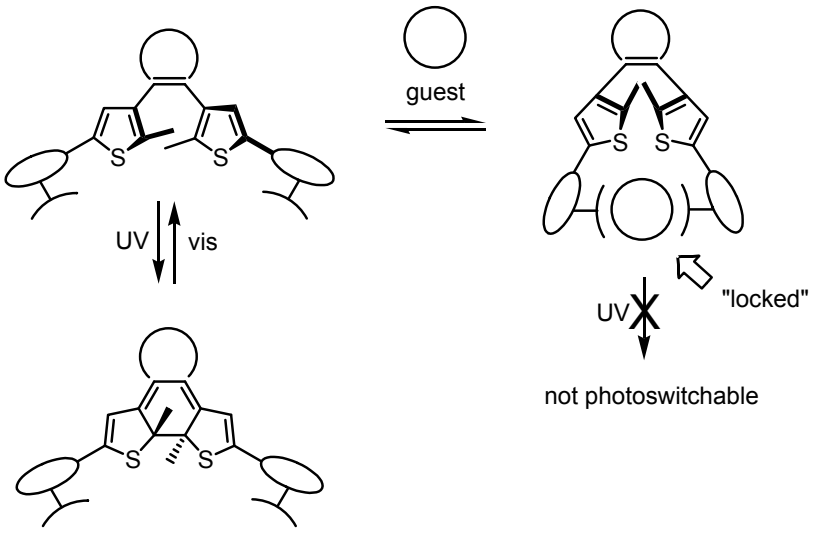

Scheme 2.1.1 Guest detection by blocked photochromism: in the presence of a guest, a DTE derivative is locked in the parallel conformation, thus blocking photochromism.

Regulation of the photochromic properties of DTEs through acid/base interaction has also been discussed in *Chapter 1*. Whether the presence of the acid/base affects the electronic structure of the photoswitch[37,38,58] (Section 1.6.2) or a competing quenching

mechanism[62,63] (Section 1.6.3), pH indicators could be designed using the gated photochromic properties of DTEs.

As discussed in Section 1.6.4 of *Chapter 1*, the addition of fluoride ions to organoboron-based DTE derivatives causes obvious spectral changes to both forms of the molecules.[64,65] This is another promising strategy for the development of chemical detection systems involving gated photochromism and DTE derivatives. However, unless very specific light sources are used, the molecules remain photoactive whether the analyte is present or not, hence the changes in the various properties between the ring-open and ring-closed isomers cannot be used as read-out signals.

Before the publication of the work presented in this chapter, the state of the art in chemically-gated photochromism was based on the use of DTE derivatives containing the photoresponsive 1,3,5-hexatriene moiety. The conventional approaches include the control of their conformation (parallel versus anti-parallel),[30,34,51-53] the modification of their electronic configuration,[37,38,58] the regulation of a competing quenching mechanism,[60-63] and the alteration of their spectral[64-70] and thermal properties.[71]

This chapter describes an innovative approach towards the gated photochromism of DTE derivatives, namely reactivity-gated photochromism. By taking advantage of this concept, which is a novel method to detect specific chemical species on the basis of how they behave in a common organic reaction, the creation and destruction of the DTE architecture is regulated on demand.

2.1.3 Proposed reactivity-gated photochromism concept

DTE derivatives undergo reversible photocyclization reactions when irradiated with light of the appropriate wavelengths because they possess a 1,3,5-hexatriene substructure.[17-22] The creation of this architecture by a mild and spontaneous reaction with an external chemical species would be very efficient way to gate the photochromism of a system, whereby photochromic properties are gained only after the occurrence of the chemical process. The term reactivity-gated photochromism is proposed for this phenomenon that was described in detail in Section 1.7.1.

Scheme 2.1.2 illustrates the concept of reactivity-gated photochromism. The 1,2-dithienylethane **DTA** is not photochromic as it lacks the required photoresponsive DTE subunit. The molecule (**DTE-o**) generated when **DTA** reacts with an external chemical species now contains the 1,3,5-hexatriene system as part of the well-known photoresponsive DTE architecture. Irradiation can then trigger the cyclization reaction and produce **DTE-c**, which can be detected using the numerous output signals available with these derivatives.

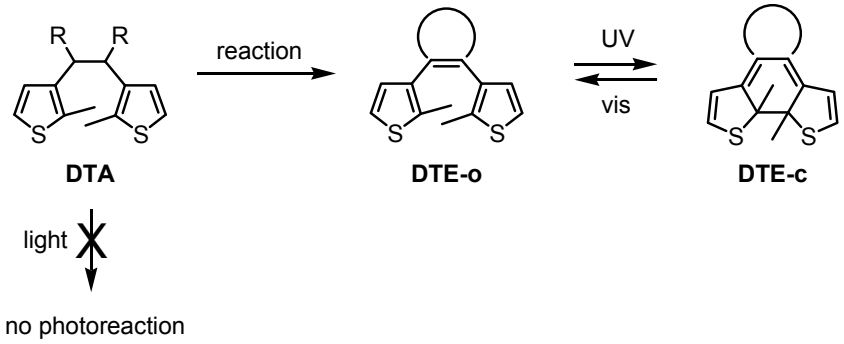

Scheme 2.1.2 Illustration of the concept of reactivity-gated photochromism: **DTA** lacks a photoresponsive moiety and is thus photoinactive unless it undergoes a chemical reaction generating **DTE-o** which possesses the required photoresponsive DTE architecture and can be cycled back and forth between its ring-open isomer **DTE-o** and its ring-closed isomer **DTE-c** using appropriate wavelengths of light.

Various approaches towards reactivity-gated photochromism could be used. Figure 2.1.1 illustrates some of them. The required double bond could be generated by an elimination reaction. In this case, a leaving group (**B**) needs to be present on the molecule. The addition of nucleophile **X**, having affinity for functional group **A**, could induce the elimination of species **B** and the generation of the alkene unit. In this case, the creation of the photochromic unit indicates the reaction between **X** and **A**, and the elimination of **B**. A substitution reaction could have similar results, in which case a photoswitch is generated after the addition of species **X** and elimination of leaving group **B**. Cycloaddition reactions could also be used, and have the advantage of generating no side products.

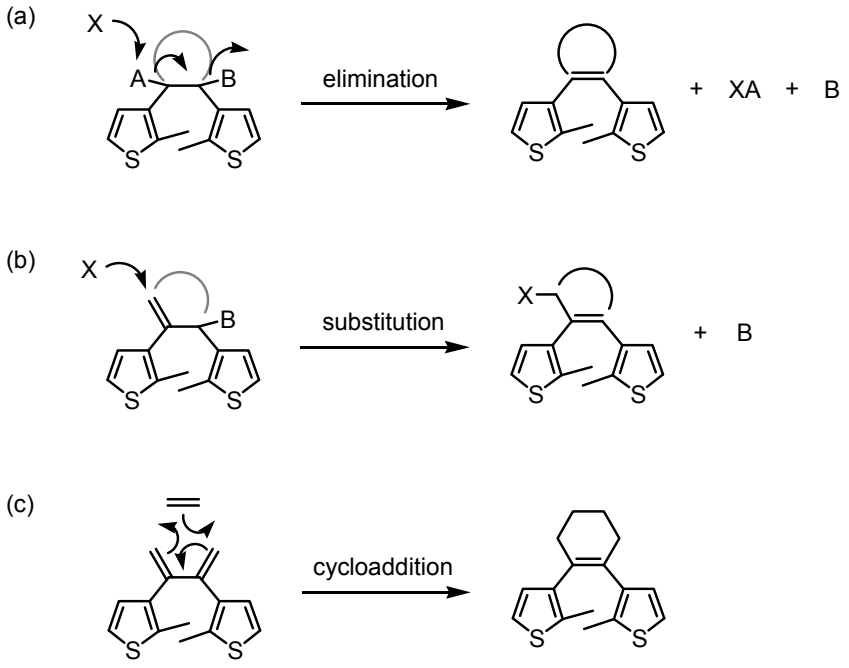

Figure 2.1.1 Possible chemical reactions for reactivity-gated photochromism, in which an external chemical leads to the formation of the photochromic DTE subunit via: (a) elimination, (b) substitution, and (c) cycloaddition.

2.1.4 Proposed reaction requirements for reactivity-gated photochromism

In order to demonstrate the concept of reactivity-gated photochromism, a chemical reaction that is spontaneous under mild conditions must be selected so that it can be used for chemical detection. It should be selective and should not easily undergo any side reactions. An atom efficient reaction has the advantage of generating no side products, thus simplifying the system and its characterisation. For the same reasons non-catalysed reactions are preferable. Finally, it could be advantageous for the reverse reaction to be observable under relatively mild conditions. This reversibility is key to the work presented in *Chapter 3*.

2.2 Proposed approach of reactivity-gated photochromism based on the Diels-Alder reaction

The thermal Diels-Alder cycloaddition usually proceeds under mild conditions with minimal side reactions and with no intermediates or side products.[73,74] Moreover, it requires no reagent or catalyst (in some cases, their use accelerates the reaction) and is also reversible in many systems.[75-77] This last point is an appealing property in dosimetry applications, since it allows for the resetting of the device.[11] Overall, the Diels-Alder cycloaddition should be an ideal reaction to demonstrate the concept of reactivity-gated photochromism.

2.2.1 General concept of reactivity-gated photochromism using the Diels-Alder reaction and the DTE architecture

A system is proposed in which the Diels-Alder cycloaddition gates the photochemistry as shown in Scheme 2.2.1. Compound **I** possesses a butadiene backbone (highlighted in bold) that cannot undergo the targeted pericyclic photoreaction. The

cyclohexene (**DTE-o**) generated when diene **I** reacts with a dienophile now contains the 1,3,5-hexatriene functionality part of the photoresponsive DTE architecture. Irradiation should trigger the cyclization reaction and produce **DTE-c**, which could be detected using the numerous output signals available when using these derivatives (e.g. absorption, emission, redox properties).

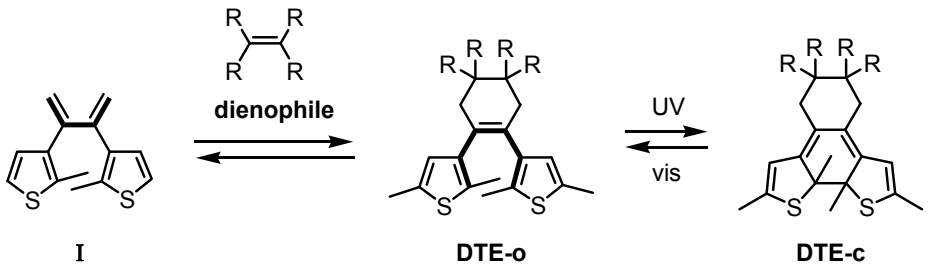

Scheme 2.2.1 Illustration of the proposed approach of reactivity-gated photochromism based on the Diels-Alder reaction: Compound **I** lacks a photoresponsive moiety and is thus photoinactive unless it undergoes a [4+2] cycloaddition generating compound **DTE-o** which possesses the required photoresponsive DTE subunit. Compound **DTE-o** should undergo a reversible photochemical ring-closing reaction to form the ring-closed isomer **DTE-c**.

The reversibility of the thermal [4 + 2] reaction shown in Scheme 2.2.1 is limited to the ring-open form of the photoswitch (**DTE-o**). This implies that the initially targeted dienophile could be liberated and the device reset only after the photoreaction is reversed (**DTE-c** → **DTE-o**). This can be achieved using visible light and should provide an effective mechanism to trap the chemical being targeted and to filter it from the environment. The use of this phenomenon for photorelease applications is the main subject of *Chapter 3*.

Prior to the publication of the work presented in this chapter, the Diels-Alder reaction had been employed only once to generate the DTE architecture. Wang and

co-workers used the Diels-Alder reaction as a synthetic tool to prepare a DTE derivative locked in the anti-parallel conformation as shown in Equation 2.2.1.[46]

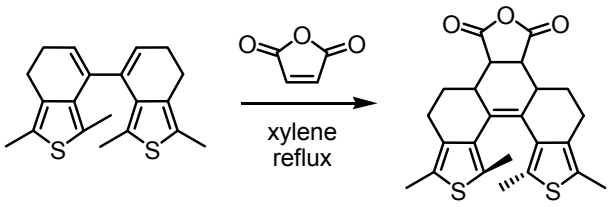

Equation 2.2.1 Previously reported system using the Diels-Alder reaction for the creation of the DTE architecture.[46]

2.2.2 Candidate dienes for reactivity gated-photochromism using the Diels-Alder reaction and the DTE architecture

As shown in Scheme 2.2.1, the diene used in the Diels-Alder reaction must have a very specific architecture in order to generate a product containing the photoresponsive DTE substructure. All potential candidates must possess a 2,3-*bis*(2-methyl-3-thienyl)-1,3-butadiene backbone as illustrated in Figure 2.2.1. This basic architecture offers wide synthetic tunability; modifying the 1,3-butadiene unit should allow control over the Diels-Alder reactivity and tailoring of the thiophene rings should give control over its photochromic properties.

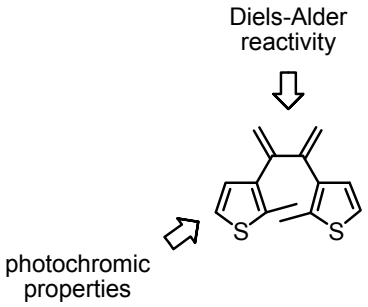

Figure 2.2.1 Basic structural requirements for the dienes. The arrows show the synthetic regions that can be modified in order to affect the Diels-Alder reactivity and photochromic properties of the generated Diels-Alder adducts.

Various dienes meet the structural requirements outlined in this section. Some examples are illustrated in Figure 2.2.2. The butadiene structure represents the simplest diene possible. One of its derivatives is discussed in Section 2.3.2, whereas a cyclohexadiene derivative is covered in Section 2.3.3 and an attempt to prepare a cyclohexadienone derivative is discussed in is Section 2.3.4. Fulvene derivatives are the basis of *Chapter 3* where the preparation of cyclopentadienes is also discussed. Derivatives parent to the furan were also prepared, but are not discussed in this thesis.

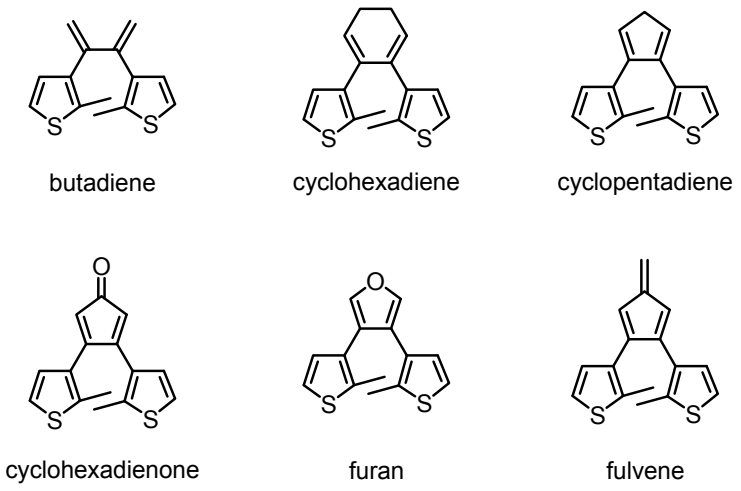

Figure 2.2.2 Examples of functional diene candidates that could be used in reactivity-gated photochromic systems based on the Diels-Alder cycloaddition.

2.3 Results and discussion

2.3.1 General synthetic approach

Synthesis is an important part of the work presented in this thesis. All the dienes presented in *Chapter 2* and *Chapter 3* were previously unknown and the elaboration of synthetic strategies was required. The 1,2-diketone **2.1** illustrated in Scheme 2.3.1 is proposed as a versatile synthetic starting point for many dienes discussed in this thesis.

Moreover, **2.1** has been previously prepared by Irie and co-workers,[78] and Krayushkin and co-workers.[79]

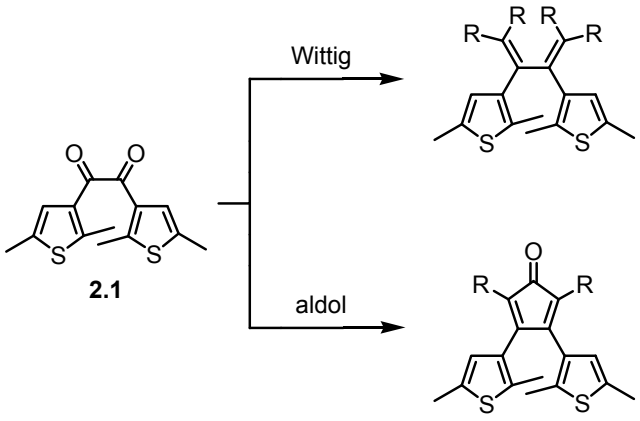

Scheme 2.3.1 The diketone **2.1** is proposed as a versatile starting material for the preparation of functional dienes suitable for Diels-Alder-gated photochromic systems. A double Wittig reaction or a double aldol condensation could result in appropriate dienes.

Compound **2.1** was prepared according to Scheme 2.3.2. Acylation of 2,5-dimethylthiophene with acetic anhydride and $SnCl_4$ in benzene afforded the acetylthiophene **2.2**. Oxidation of this compound with selenium dioxide (SeO_2) in a dioxane/water mixture gave the acetaldehyde **2.3** and subsequent acylation of 2,5-dimethylthiophene with compound **2.3** and $SnCl_4$ in benzene afforded the α-hydroxyketone **2.4**. Oxidation of this compound with copper sulphate in pyridine and water afforded the targeted α-diketone **2.1**.

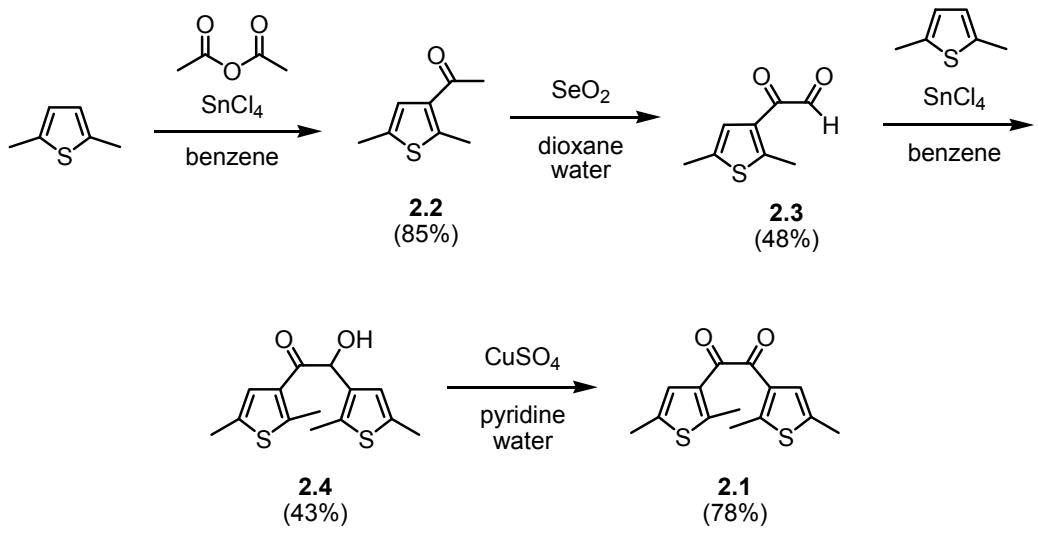

Scheme 2.3.2 Synthesis scheme for the preparation of diketone **2.1**.[78,79]

2.3.2 Derivative based on a butadiene architecture

In order to demonstrate the concept of reactivity-gated photochromism using the Diels-Alder cycloaddition, butadiene **2.5** (Equation 2.3.1) was initially targeted for practical reasons. First, it met the basic architectural requirements shown in Figure 2.2.1 with the simple addition of methyl groups at the external position of the thiophene rings. Secondly, it was anticipated that it could easily prepared through two Wittig condensation reactions between an appropriate ylide and diketone **2.1**.

Synthesis and characterisation of the butadiene derivative

The butadiene **2.5** was obtained from diketone **2.1** by condensing it with the ylide obtained from methyltriphenylphosphonium bromide and *n*-butyllithium (-78 °C in THF) as shown in Equation 2.3.1. The diene product **2.5** can be purified by column chromatography using silica gel and ethyl acetate/hexanes (1:9) as the eluent mixture. As expected, irradiation of **2.5** with light of various wavelengths did not induce a

photochromic response as suggested by the absence of significant changes in colour upon light exposure.

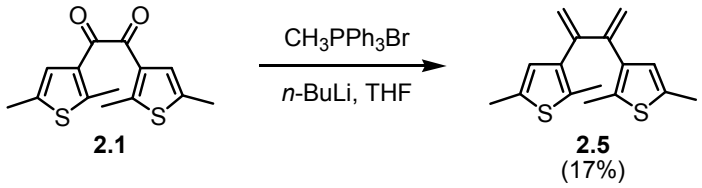

Equation 2.3.1 Synthesis of butadiene **2.5** through two Wittig reactions.

Diels-Alder reactivity of the butadiene derivative

The butadiene **2.5** undergoes a cycloaddition reaction with maleic anhydride to generate the cyclohexene **2.6** as shown by ^{1}H NMR spectroscopy, but only when the reaction mixture is heated to 70 °C in the absence of a solvent. In the presence of a solvent, the cycloaddition reaction between **2.5** and maleic anhydride was not observed. The need for these relatively harsh and limiting conditions is most likely due to the fact that only a small amount of the necessary s-*cis* conformer of **2.5** will exist at any given time (Scheme 2.3.3). From a steric hindrance point of view, the major conformer should clearly be the s-*trans* isomer, which is not appropriately positioned to undergo the [4 + 2] cycloaddition reaction.

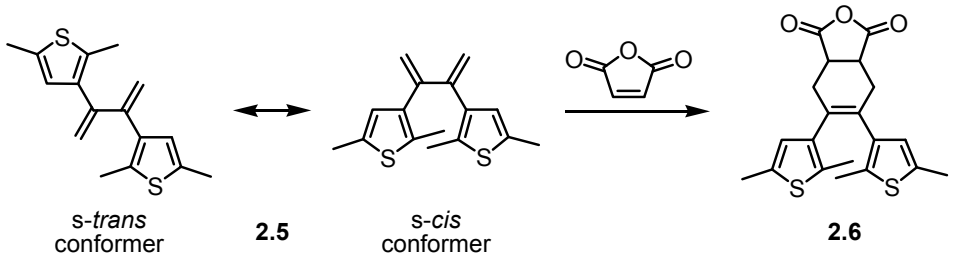

Scheme 2.3.3 Diels-Alder reaction of butadiene **2.5** with maleic anhydride to form the Diels-Alder adduct **2.6**. Only the s-*cis* conformer has the appropriate geometry to react.

Photochromic properties of the Diels-Alder adduct formed from the butadiene derivative

Solutions of the cyclohexene **2.6** produced when the diene **2.5** reacts with maleic anhydride exhibit a colour change from colourless to yellow upon irradiation with UV light (312 nm), which is consistent with the formation of the extended π-conjugated backbone created in the ring-closed isomer **2.7**, as shown in Figure 2.3.1a. The corresponding UV-vis absorption spectra in acetonitrile show trends typically observed for ring-closing reactions of DTE derivatives as illustrated in Figure 2.3.1b. The high-energy bands in the spectra become less intense as a broad band centred at 442 nm appears. Subsequent irradiation of this ring-closed isomer with light of wavelengths greater than 415 nm regenerates the ring-open isomer (Figure 2.3.1c). However, decomposition of the system is apparent even after only one cycle since the original UV-vis spectrum corresponding to the pure ring-open form **2.6** is not fully regenerated. Nevertheless, these results establish that molecule **2.6** is photoactive, demonstrating that the reactivity-gated photochromism was successful obtained in this preliminary example.

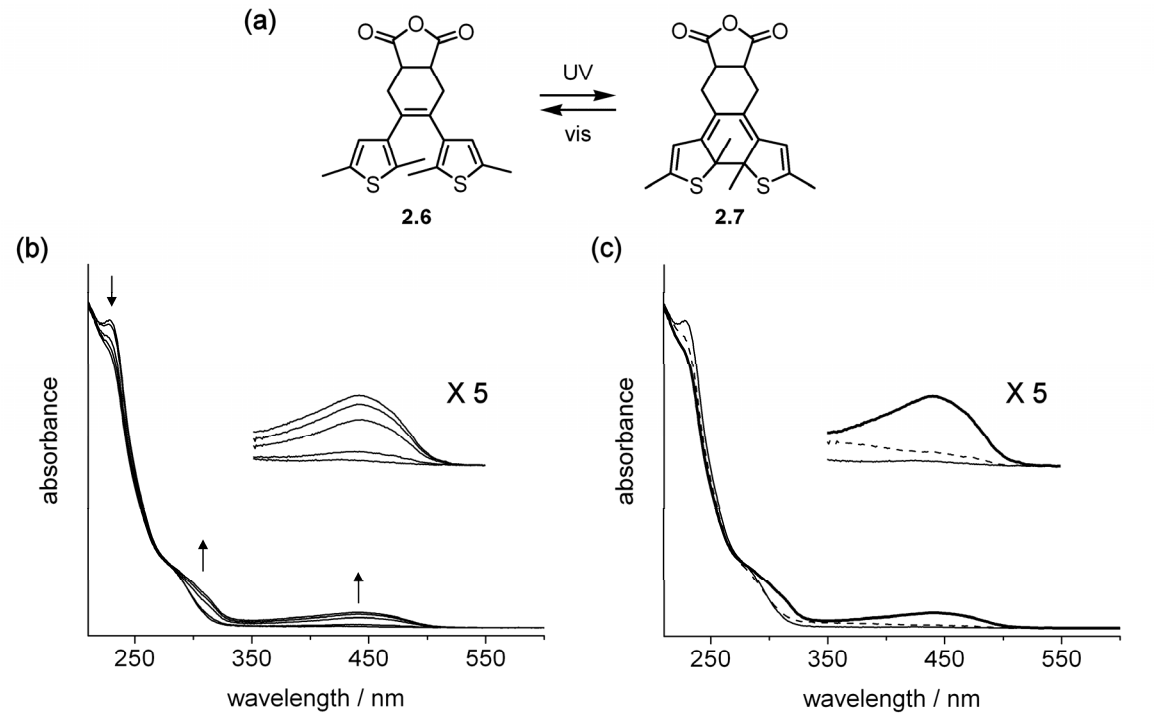

Figure 2.3.1 (a) Reversible photocyclization of the ring-open isomer **2.6** to generate the ring-closed isomer **2.7**. (b) Changes in the UV-vis absorption spectra of an acetonitrile solution (1.0×10^{-5} M) of **2.6** upon irradiation with 312 nm light until no further increase in the absorption band at 442 nm was observed at the PSS. Total irradiation periods are 0, 5, 15, 25, 45 s. (c) UV-vis spectra of **2.6** in acetonitrile before UV irradiation (solid line), at the PSS (bold line) and, after irradiation with light of wavelengths greater than 415 nm for 5 min until no further changes to the spectrum were observed (dashed line). Degradation is clearly taking place since irradiation with visible light does not regenerate the original spectrum of **2.6**.

2.3.3 Derivative based on a cyclohexadiene architecture

The butadiene derivative **2.5**, described in the previous section, was useful to demonstrate the concept of reactivity-gated photochromism with the Diels-Alder reaction. However, the main drawback of this acyclic butadiene is its limited reactivity even with a good dienophile such as maleic anhydride. To solve this problem, an improved system based on the cyclic diene **2.8** (Equation 2.3.2) was developed, which should reduce the rotational freedom in the butadiene fragment and be more suitable for the development of applications in chemical detection.

Synthesis and characterisation of the cyclohexadiene derivative

2,3-*bis*(2',5'-Dimethyl-3'-thienyl)cyclohexadiene **2.8** was synthesised from diketone **2.1** using a procedure that is analogous to the one used to prepare **2.5,** but replacing the 2 molar equivalents of methyltriphenylphosphonium bromide with 1 molar equivalent of 1,4-butane-*bis*(triphenylphosphonium) dibromide. In this case, the *bis*(ylide) was best obtained by using potassium *t*-butoxide as the base (20 °C in dry benzene). The product **2.8** can be purified by column chromatography using silica gel and ethyl acetate/hexanes (1:9) as the eluent mixture. As expected, irradiation of **2.8** with light of various wavelengths did not induce a photochromic response as indicated by the absence of significant colour changes upon exposure to light (Figure 2.3.4 on page 66).

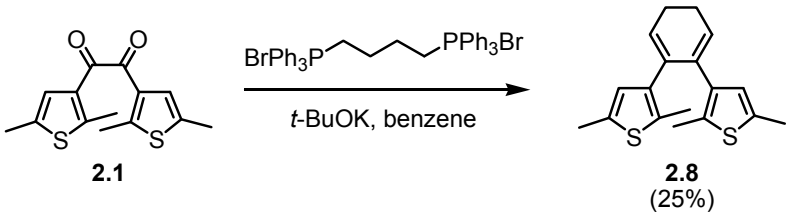

Equation 2.3.2 Preparation of the cyclohexadiene **2.8**.

Diels-Alder reactivity of the cyclohexadiene derivative

When the colourless, photoinert butadiene **2.8** is treated with one equivalent of maleic anhydride in solution (acetone) at 65 °C, it undergoes the [4 + 2] cycloaddition reaction and produces a photochromic compound, **2.9**. Figure 2.3.2 shows the changes in the ^{1}H NMR spectrum of a 1:1 mixture of butadiene **2.8** (8.9 x 10^{-2} M) and maleic anhydride before and after 114h at 65 °C in acetone-d_6. The most pronounced changes come from the formation of a bicyclo[2.2.2]oct-2-ene moiety. Upon the cycloaddition reaction, the signal at 5.90 ppm (peak 'b') attributed to the alkene proton of the

cyclohexadiene moiety of **2.8** broadens and shifts upfield to 3.35 ppm. This signal is characteristic of the "bridgehead" proton of a bicyclic system. Moreover, protons 'C' in compound **2.9** are no longer equivalent and two signals are observed in the spectrum (peaks 'C'). The changes in the NMR signals are consistent with the generation of only one isomer, *endo* or *exo*. However, the stereochemistry of the Diels-Alder adduct was not determined.

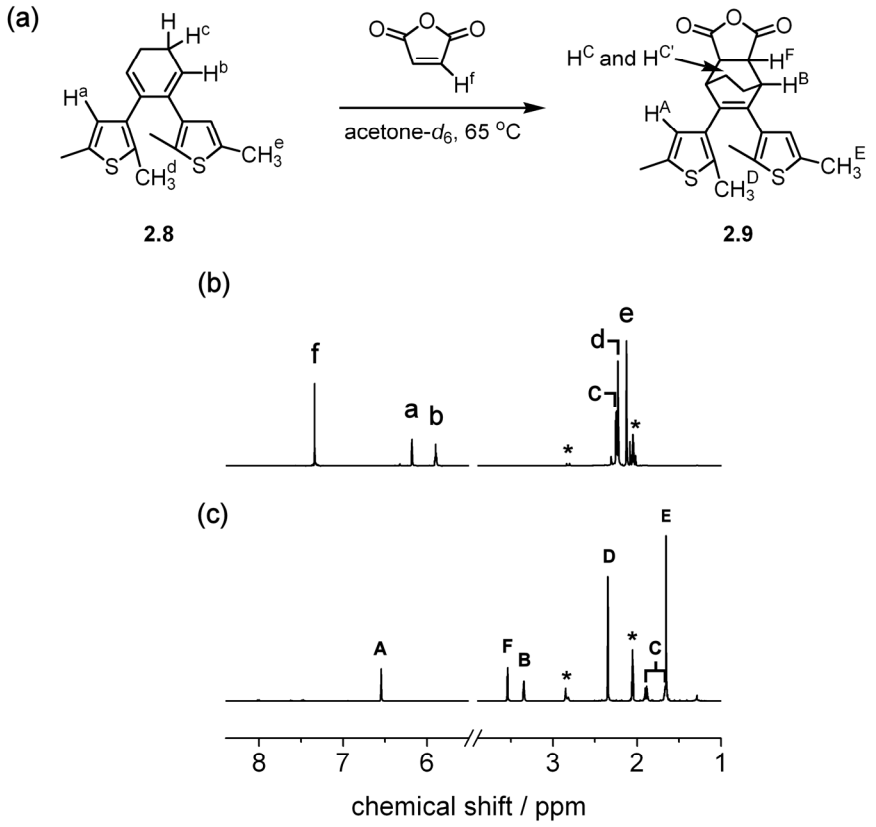

Figure 2.3.2 (a) Reaction of cyclohexadiene **2.8** with maleic anhydride to form the Diels-Alder adduct **2.9**. (b-c) ^{1}H NMR spectra (400 MHz) of a 1:1 mixture of the cyclohexadiene **2.8** (8.9×10^{-2} M) and maleic anhydride in acetone-d_6 (b) before and (c) after 114 hours at 65 °C. Upon heating, a [4 + 2] cycloaddition occurs to form the Diels-Alder adduct **2.9**. Asterisks indicate the signals attributed to the deuterated residual solvent and water.

The reaction was found to proceed at room temperature, albeit over a much longer period than at 65 °C. The reaction is quantitative, and no side products are formed

as measured by ^{1}H NMR spectroscopy. The fact that the Diels-Alder reaction was observed under milder condition with the cyclohexadiene **2.8**, which is reactive in solution, than with the butadiene **2.6**, which is reactive only in the solid state, is consistent with the idea that the reactivity of **2.6** was limited by the presence of the s-*trans* conformer, whereas **2.8** is locked in the productive s-*cis* conformation.

Photochromic properties of the Diels-Alder adduct formed from the cyclohexadiene derivative

When an acetonitrile solution (2.7×10^{-5} M) of the colourless ring-open form (**2.9**) is irradiated with 312 nm light, a broad absorption band centred at 441 nm appears, and the solution turns yellow, which are indications of the occurrence of the ring-closing reaction producing the corresponding ring-closed form **2.10** as shown in Figure 2.3.3a-b. In the absence of visible light, the colour persists, attesting to the thermal stability of the photochromic compound. The photogenerated solutions of **2.10** can be bleached by irradiating them with visible light of wavelengths greater than 415 nm causing the band at 441 nm to decrease, which is indicative that the ring-opening reaction has occurred, regenerating **2.9**. However, decomposition of the system is apparent even after only one cycle since the original UV-vis spectrum corresponding to the pure ring-open form **2.9** is not fully regenerated as seen in Figure 2.3.3c. During these studies, it was also noticed that using 254 nm light produces a greater amount of photocyclization as shown in Figure 2.3.3b. This comes at the expense of stability, however, and more degradation is observed when this higher-energy light is used.

The photochemical interconversion between the ring-open (**2.9**) and ring-closed (**2.10**) isomers of the Diels-Alder adduct was also monitored using ^{1}H NMR

spectroscopy. When a solution of compound **2.9** in chloroform-*d* (1.0 x 10^{-3} M) is exposed to 312 nm light at 22 ^{o}C, a new set of signals appears and is assigned to the ring-closed isomer **2.10**. Figure 2.3.3d-f shows the changes in a selected region of the spectra upon irradiation with UV and visible light.

The signal at 6.45 ppm (peak 'a') is attributed to the thienyl protons on the ring-open isomer **2.9**. Upon irradiation with 312 nm light, two singlets at 5.73 and 5.70 ppm (peaks 'b') appear. These signals are assigned to the corresponding thienyl protons in **2.9** and the upfield shift of these signals can explained by the loss of aromatic character of the thienyl groups upon ring-closure. Two signals are recorded for protons 'b' in the ring-closed isomer compared to one for protons 'a' in the ring-open isomer because the ring-closed form is no longer symmetric. The mole fractions corresponding to the ring-open **2.9** and the ring-closed **2.10** isomers were obtained by integration of the area under the peaks corresponding to signals 'a' and 'b'. With the mole fractions in hand, it is possible to monitor the conversion of **2.9** into **2.10** over time. After 5 minutes of irradiation with 312 nm light, a photostationary state of 31% was reached. Reactivity-gated photochromism was demonstrated in this system since compound **2.9**, obtained under relatively mild conditions from non-photochromic **2.8**, exhibits reversible photocyclization as seen by UV-vis absorption spectroscopy and ^{1}H NMR spectroscopy.

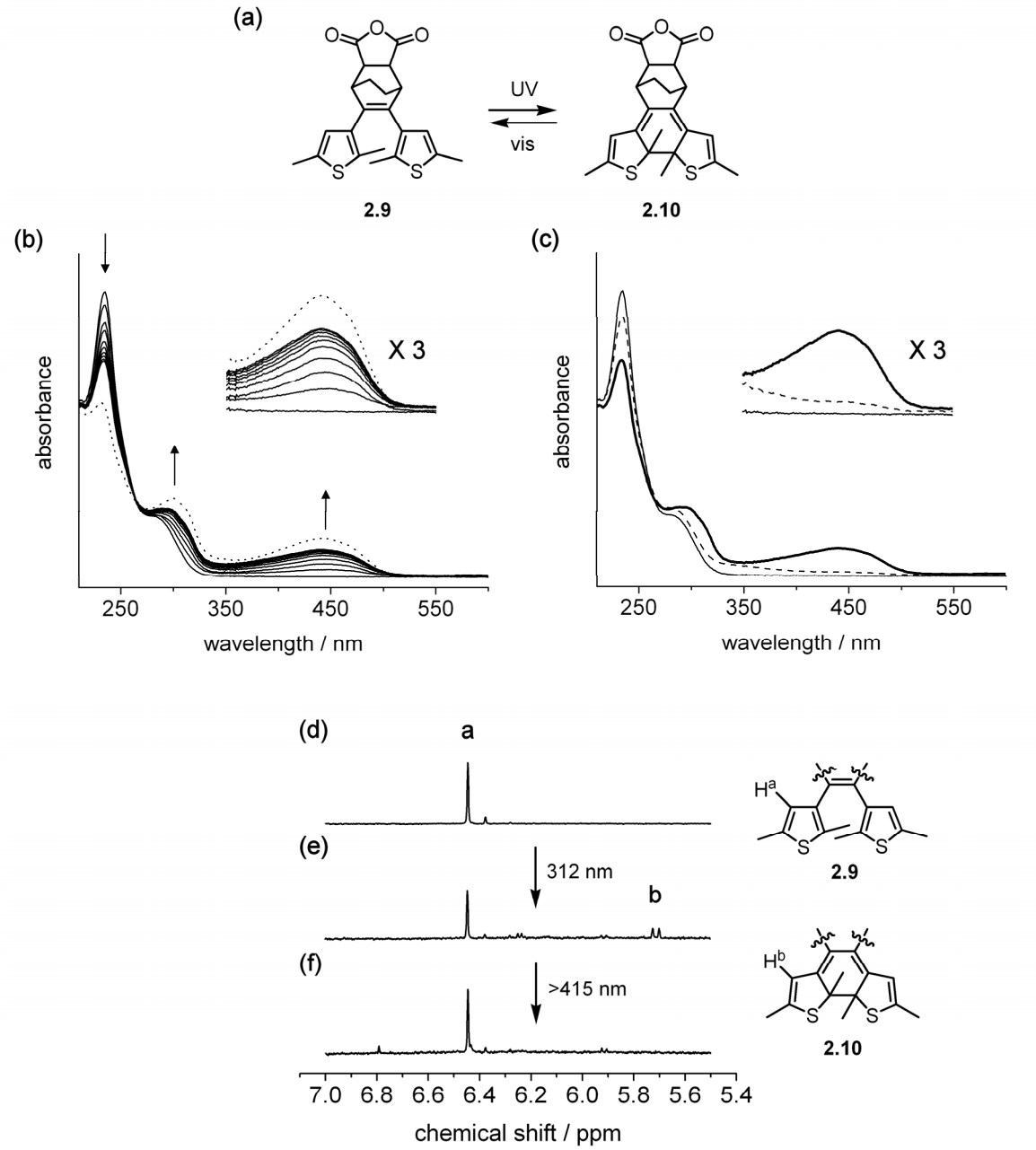

Figure 2.3.3 (a) Reversible photocyclization of the ring-open isomer **2.9** to generate the ring-closed isomer **2.10**. (b) Changes in the UV-vis absorption spectra of an acetonitrile solution (2.7 x 10^{-5} M) of **2.9** irradiated with 312 nm light until there are no further increase in the absorption band at 441 nm. Total irradiation periods are 45 s in 5 s intervals. The dotted line corresponds to the PSS state after irradiation of the same solution with a 254 nm source for 35 s. (c) UV-vis spectra of **2.9** in acetonitrile before 312 nm irradiation (solid line), at the PSS with 312 nm (bold line), and after irradiation with light of wavelengths greater than 415 nm (10 min) until no further changes to the spectrum (dashed line). Degradation is clearly taking place since irradiation with visible light does not regenerate the original **2.9** spectrum. (d-f) Partial ^{1}H NMR (400 MHz, chloroform-*d*) of the ring-open isomer **2.9** (1.0 x 10^{-3} M) (d) before, (e) at the PSS after 5 min irradiation with 312 nm light, and (f) after bleaching with >415 nm light for 10 min.

Visual representation – Advances towards dosimetry applications

Figure 2.3.4 highlights the visible colour changes in the reactivity-gated system. In this demonstration, a small amount of the cyclohexadiene **2.8** (1 mg) was dissolved in pure dimethyl sulfoxide (1 mL) (left spot in the figure) and simultaneously in the same volume of a saturated solution of maleic anhydride in dimethyl sulfoxide (right spot in the figure). Both solutions were kept in the dark overnight. Irradiation with 312 nm light only produced a colour change in the solution containing both **2.8** and the analyte. Irradiation with light of wavelengths greater than 415 nm bleached the sample back to its original colourless state.

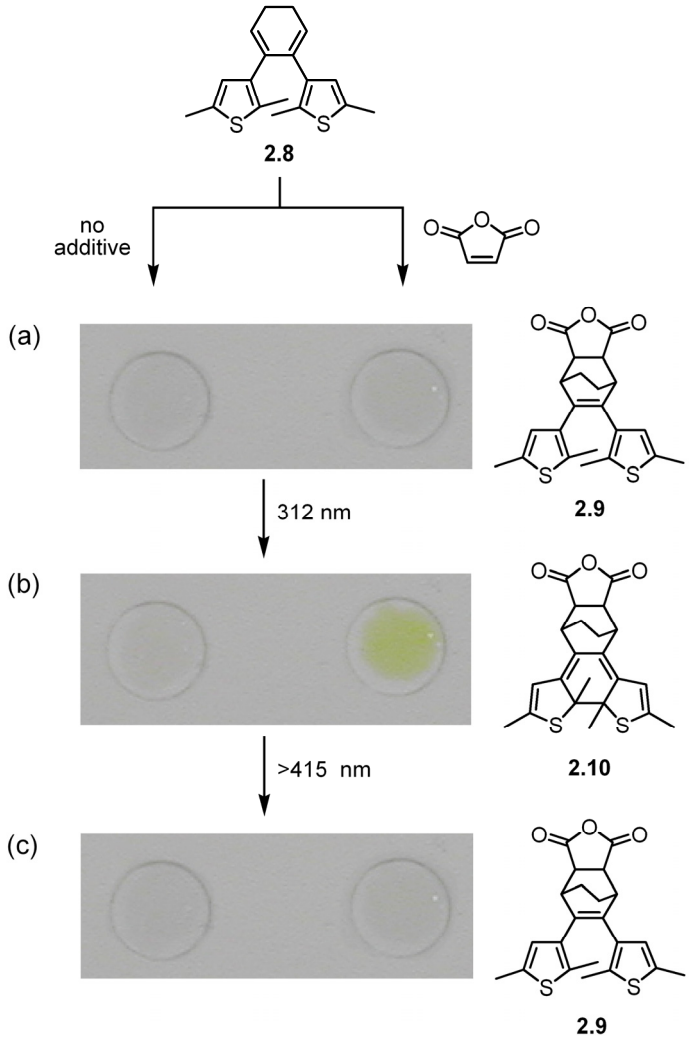

Figure 2.3.4 Visual representation of the concept of reactivity-gated photochromism. (a) (b) Colour change occurring when a DMSO solution of diene **2.8** and excess maleic anhydride is exposed to 312 nm light (right spot); a sample containing only the diene **2.8** (left spot) that has been simultaneously irradiated. (c) The same two spots after bleaching with greater than 415 nm light.

Discussion of the cyclohexadiene-based reactivity-gated photochromic system

These results establish that reactivity-gated photochromism has been successful in this example since the cycloadduct **2.9** undergoes a colour change when irradiated with UV light as it ring-closes to form **2.10**, while the cyclohexadiene **2.8** undergoes no noticeable change in colour when irradiated under identical conditions unless it is

previously treated with a dienophile. Furthermore, the present system shows improved reactivity compared to the acyclic butadiene **2.5**, presented in the previous section, since it reacts under much milder conditions. Preliminary tests of the gated effect observed when exposing cyclohexadiene **2.8** to other dienophiles such as quinones and electron-deficient acetylene derivatives have been successful since photochromic products have been obtained, demonstrating the versatility of this approach.

It is anticipated that further improvements with respect to the amount of the ring-closed isomer in the photostationary state and the colour of this ring-closed form could be achieved by replacing the two methyl groups on the 5-positions of the thiophene heterocycles with groups that are more amenable to photochromic sensing. However, the current synthetic strategy (preparation method of the diketone **2.1** shown in Scheme 2.3.2) hinders the tailoring of compound **2.1** with functional groups, and thus limits possible functionalisation of the DTE backbone. A novel synthetic pathway improving the preparation of compound **2.1** is presented in *Chapter 4*.

Two main concerns arise with the cyclohexadiene **2.8**. First, even though it has an improved reactivity compared to the butadiene **2.5**, this cyclic diene is still not very reactive towards cycloaddition reaction since compound **2.8** does not undergo Diels-Alder addition rapidly at room temperature. Secondly, the retro-Diels-Alder reaction with this type of diene occurs only at very elevated temperature, well above 300 ^{o}C,[75] and was not observed for either the acyclic butadiene **2.5** or the cyclic **2.8** system. Thus, devices based on these molecules could not be reset. Efforts to develop a new system with improved reactivity are described in the following section as well as in *Chapter 3*, which focuses on potentially reversible systems.

2.3.4 Derivative based on a cyclopentadienone architecture

Cyclopentadienone **2.11** is extremely unstable as it dimerises even at very low temperature to form dimer **2.12** (Figure 2.3.5). Its monomeric form has been observed only at -196 °C.[80] In fact, most cyclopentadienone derivatives exist only in their dimeric forms. Only 2,3,4,5-tetraphenylcyclopentadienone (**2.13**) and some of its derivatives exist as monomers, and the dimeric products from 2,5-dimethyl-3,4-diphenyl- and 2,3,5-triphenylcyclopentadienone dissociate readily in solution.[81]

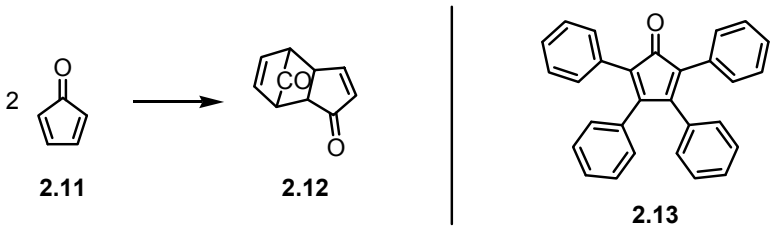

Figure 2.3.5 Dimerisation of cyclopentadienone **2.11**. Compound **2.13**, 2,3,4,5-tetraphenylcyclopentadienone, exits as a monomer.

In an attempt to demonstrate reactivity-gated photochromism at room temperature using the Diels-Alder reaction, the cyclopentadienone **2.14** was targeted. This tetra-substituted analogue of **2.13** should be bulky enough to prevent self-dimerisation, but as observed for compound **2.13**, it should readily undergo cycloadditions with a variety of small dienophiles.

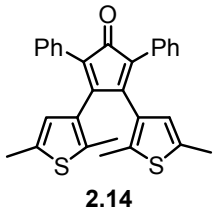

Figure 2.3.6 The targeted cyclopentadienone derivative **2.14**, which was anticipated to have improved Diels-Alder reactivity.

Attempted synthesis of the cyclopentadienone derivative

Cyclopentadienone derivatives, such as 2,3,4,5-tetraphenylcyclopentadienone **2.13**, are usually prepared from the double aldol condensation reaction of an α-diketone, such as benzyl, and an appropriate 1,3-substituted propanone.[82] Hence, the condensation of diketone **2.1** with 1,3-diphenylacetone under basic conditions should allow the preparation of the targeted cyclopentadienone derivative **2.14** as shown in Equation 2.3.3.

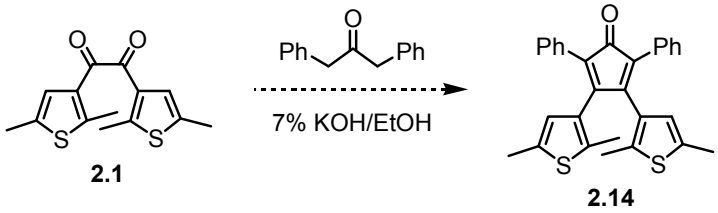

Equation 2.3.3 Proposed synthetic route for the preparation of the cyclopentadienone derivative **2.14**.

The reaction between diketone **2.1** and 1,3-diphenylacetone was monitored by ^{1}H NMR spectroscopy. After one hour, the formation of one main product was apparent. Figure 2.3.7 shows the ^{1}H NMR spectrum of the isolated product in chloroform-*d*. From this spectrum, the formation of cyclopentadienone **2.14** can be ruled out; no signal is observed in the region corresponding to the protons on aromatic phenyl groups. Analysis of this spectrum reveals that the molecule is no longer symmetric since two signals are observed in the thienyl proton region of the spectrum. Moreover, one of the methyl groups seems to have been affected by the reaction and a broad signal is observed at 2.7 ppm, characteristic of a hydroxyl group. It is speculated that under basic conditions, one of the methyl group at the internal position of the thiophene rings is deprotonated. The resulting carbanion could react internally with one of the carbonyl groups to form a 5-membered ring (compound **2.15**) as shown in Figure 2.3.7a. No additional

characterisation was performed on this product since no condensation between the diketone and 1,3-diphenylacetone was observed.

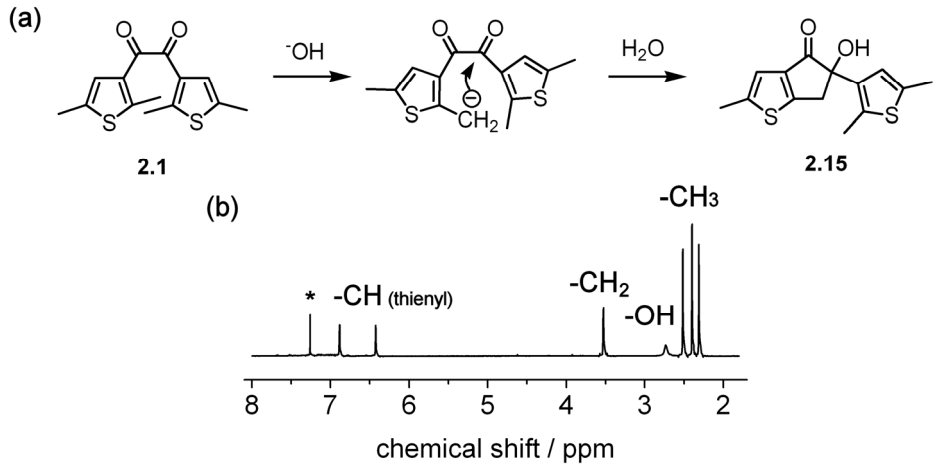

Figure 2.3.7 (a) Proposed reaction occurring when diketone **2.1** is treated with a base. (b) ^{1}H NMR spectra (400 MHz) in chloroform-*d* of the obtained product and proposed alternate mechanism for its formation.

Proposed alternate approach for the preparation of a cyclopentadienone derivative

Assuming the formation of the proposed product **2.15**, the internal methyl group, which is conjugated to a carbonyl group, seems to be fairly acidic and an intramolecular reaction is favoured over the targeted intermolecular condensation. A possible solution to this problem could be to functionalise the internal position of the thiophene rings with less acidic groups such as phenyl rings as shown in Equation 2.3.4. However, DTE derivatives having bulky functional groups at the internal positions are less photoresponsive.[83] Other possibilities include the preparation of the enolate prior to the addition the α-diketone, or the use of a 1,3-diphenylacetone derivative with more acidic α-protons such as 1,3-*bis*(4-nitrophenyl)acetone. These avenues were not pursued since more promising systems were found and investigated, as described in the following chapters.

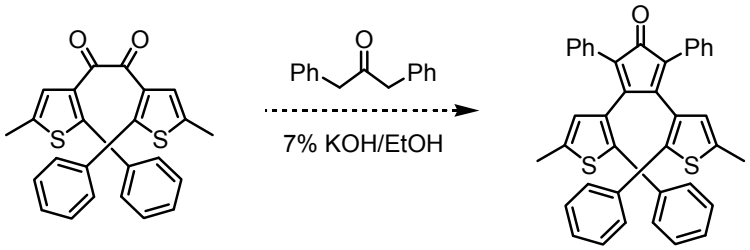

Equation 2.3.4 Proposed diketone with internal phenyl groups for the preparation of a cyclopentadienone derivative.

2.4 Conclusion and perspectives

2.4.1 Summary

The concept of reactivity-gated photochromism was successfully demonstrated. The synthesis of butadiene **2.5** and cyclohexadiene **2.8** was presented. From the synthetically accessible α-diketone **2.1**, a double Wittig condensation affords the desired products. As expected, compounds **2.5** and **2.8** are not photochromic unless they undergo cycloaddition reactions with dienophiles. In presence of maleic anhydride, a dienophile, a Diels-Alder reaction converts the dienes into photoresponsive molecules that possess the well-known photochromic DTE architecture. The photochromic properties of the resulting cycloadducts were assessed. An attempt to prepare cyclopentadienone derivatives such as compound **2.14** was unsuccessful.

2.4.2 Perspectives

This novel example of reactivity-gated photochromism has the potential to significantly impact dosimetry applications and the concept of controlled release of chemical species. The approach could be used to detect and sequester toxic dienophiles such as Lewisite (2-chlorovinyldichloroarsine), a blistering agent similar to mustard gas and a compound that is a powerful respiratory irritant when inhaled (Figure 2.4.1).

Another highly toxic dienophile is the pesticide 1,3-dichloropropene. The DTE derivatives described in this chapter also have the potential to interface with many biologically relevant dienophiles such as those found in the membrane-bound "quinone pool" (bacterial enzyme cofactors such as phylloquinone and menaquinone) and the numerous quinone intermediates in the biosynthesis of antibiotics such as tetracycline.

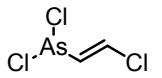

Lewisite

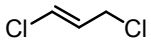

1,3-dichloropropene

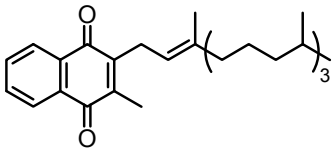

phylloquinone (vitamin K)

Figure 2.4.1 Examples of toxic and biologically relevant dienophiles.

Finally, this approach offers new sites and mechanisms to functionalise further photoresponsive molecular switches based on the DTE scaffold and provides synthetic access to unprecedented and innovative systems.

2.5 Experimental

2.5.1 Materials

All solvents used for synthesis were dried and degassed by passing them through steel columns containing activated alumina under nitrogen using an MBraun solvent purification system. All other solvents were used as received. Solvents for NMR analysis were purchased from Cambridge Isotope Laboratories and used as received. Column chromatography was performed using silica gel 60 (230-400 mesh) from Silicycle Inc. All other reagents and starting materials were purchased from Aldrich.

2.5.2 Instrumentation

^{1}H NMR characterisations were performed on a Bruker AMX 400 instrument working at 400.103 MHz. ^{13}C NMR characterisations were performed on a Bruker AMX 400 instrument working at 100.610 MHz. Chemical shifts (δ) are reported in parts per million (ppm) relative to tetramethylsilane using the residual solvent peak as a reference standard. Coupling constants (J) are reported in Hertz. UV-vis measurements were performed using a Varian Cary 300 Bio spectrophotometer. Microanalysis (C, H, N) were performed at Simon Fraser University by Mr. Mei-Keng Yang on a Carlo Erba EA 1110 CHN Elemental Analyser. Low resolution mass spectrometry measurements were performed at Simon Fraser University by Mr. Philip Ferreira using an HP5985 mass spectrometer with isobutene as the chemical ionization source or a Varian 4000 GC/MS/MS with electron impact operating at 10 mA as the ionization source (EI) or with chemical ionization (CI) using methanol.

2.5.3 Photochemistry

All ring-closing reactions were carried out using the light source from a lamp used for visualising TLC plates at 312 nm (Spectroline E series, 470 W/cm^2). The power of the light source is given based on the specifications supplied by the company when the lamps were purchased. A light detector was not used to measure the intensity during the irradiation experiments. The ring-opening reactions were carried out using the light of a 300-W halogen photo optic source passed through a 415 nm cut-off filter to eliminate higher energy light. The composition of the photostationary state of compound **2.9** was analysed using ^{1}H NMR spectroscopy.

2.5.4 Synthesis

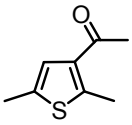

2.2

Synthesis of 3-acetyl-2,5-dimethylthiophene (2.2) - From literature[84]

A solution of $SnCl_4$ (38.31 g, 0.1471 mol) in benzene (20 mL) was added dropwise to a stirred solution of 2,5-dimethylthiophene (15.00 g, 0.1337 mol) and acetic anhydride (15.01 g , 0.1470 mol) in degassed benzene (200 mL). The mixture was stirred overnight at room temperature under nitrogen atmosphere. The reaction mixture was poured onto a mixture of crushed ice (70 g) and concentrated hydrochloric acid (10 mL). The benzene and water layers were separated and the aqueous fraction was extracted with diethyl ether (3 x 50 mL). The organic fractions were combined, washed with water (1 x 50 mL), saturated $NaHCO_3$ solution (3 x 50 mL), and brine (1 x 50 mL), dried with Na_2SO_4, and filtered. The solvent was removed under reduced pressure. The residue was

distilled under reduced pressure to give 3-acetyl-2,5-dimethylthiophene **2.2** (17.54 g, 0.1137 mol, 85%).

^{1}H NMR (chloroform-*d*, 400 MHz): δ 6.95 (s, 1H, H_{het}), 2.62 (s, 3H, CH_3), 2.42 (s, 3H, CH_3), 2.37 (s, 3H, CH_3).

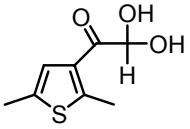

2.3

Synthesis of 2-(2,5-dimethyl-3-thienyl)-2-oxoacetaldehyde (2.3) - From literature[79,85]

3-Acetyl-2,5-dimethylthiophene **2.2** (17.54 g, 0.1137 mol) was added to a solution of selenium dioxide (12.62 g, 0.1137 mol) in dioxane (100 mL) and water (3 mL) at 60 ^{o}C. The stirred solution was heated at reflux for 4 hours. The reaction mixture was filtered at 60 ^{o}C and the solvent was removed under reduced pressure. The residue was dissolved in boiling water, filtered and crystallised to give the glyoxal hydrate **2.3** (10.2 g, 0.0548 mol, 48%).

^{1}H NMR (dimethyl sulfoxide-d_6, 400 MHz): δ 7.27 (s, 1H, H_{het}), 6.51 (d, J = 7.3 Hz, 2H, OH), 5.38 (t, J = 7.3 Hz, 1H, CH) 2.60 (s, 3H, CH_3); 2.37 (s, 3H, CH_3).

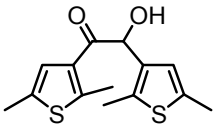

2.4

Synthesis of 1,2-*bis*(2,5-dimethyl-3-thienyl)-2-hydroxy-1-ethanone (2.4) - From literature[79]

A solution of $SnCl_4$ (15.7 g, 60.3 mmol) in benzene (20 mL) was added dropwise to a stirred solution of glyoxal hydrate **2.3** (10.2 g, 54.8 mmol) and 2,5-

dimethylthiophene (6.76 g, 60.3 mmol) in deoxygenated benzene (120 mL). The mixture was stirred overnight at room temperature under nitrogen atmosphere. The reaction mixture was carefully poured into water (70 mL). The benzene and water layers were separated and the aqueous fraction was extracted with diethyl ether (3 x 50 mL). The organic fractions were combined, washed with water (1 x 50 mL), saturated $NaHCO_3$ solution (3 x 50 mL), and brine (1 x 50 mL), dried with $MgSO_4$, and filtered. The solvent was evaporated under reduced pressure. The residue was purified by column chromatography (1:3 ethyl acetate:hexane). The hydroxyketone **2.4** was obtained as a beige solid (6.53 g, 23.5 mmol, 43%).

M.p.: 127-129 ^{o}C; ^{1}H NMR (chloroform-*d*, 400 MHz): δ 6.66 (s, 1H, H_{het}), 6.30 (s, 1H, H_{het}), 5.51 (d, J = 5.9 Hz, 1H, CH_2), 4.41 (d, J = 5.9 Hz, 1H, OH), 2.71 (s, 3H, CH_3); 2.50 (s, 3H, CH_3), 2.32 (s, 3H, CH_3), 2.31 (s, 3H, CH_3); ^{13}C NMR (chloroform-*d*, 100 MHz): δ 194.2, 150.7, 136.7, 135.6, 135.0, 134.4, 131.7, 124.9, 124.2, 70.9, 16.2, 15.1, 15.0, 13.0.

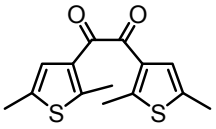

2.1

Synthesis of 1,2-*bis*(2,5-dimethyl-3-thienyl)ethanedione (2.1) - From literature[79]

A solution of hydroxyketone **2.4** (2.00 g, 7.15 mmol) in pyridine (10 mL) and water (10 mL) was added to a solution of $CuSO_4$•$(H_2O)_5$ (16.00 g, 64.35 mmol) in pyridine (20 mL) and water (50 mL). The reaction mixture was stirred and heated to 80 ^{o}C for 2 hours. The solution was cooled to room temperature and the product was extracted with diethyl ether (3 x 30 mL). The extract was washed with a 10%

hydrochloric acid solution (1 x 30 mL), water (1 x 30 mL), dried over $MgSO_4$, filtered, and the solvent was evaporated under reduced pressure. The residue was purified by column chromatography (1:3 EtOAc:hexanes) to yield diketone **2.1** (1.55 g, 5.57 mmol, 78% yield) as a yellow solid.

M.p.: 62.0-64.0 ^{o}C; ^{1}H NMR (chloroform-*d*, 400 MHz): δ 6.90 (s, 2H, H_{het}), 2.72 (s, 6H, CH_3), 2.37 (s, 6H, CH_3); ^{13}C NMR (chloroform-*d*, 100 MHz): δ 189.1, 151.6, 136.1, 131.7, 126.8, 15.9, 14.8.

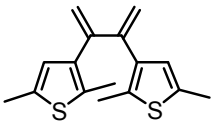

2.5

Synthesis of 2,3-*bis*(2,5-dimethyl-3-thienyl)-1,3-butadiene (2.5) - Adapted from literature[86]

n-Butyllithium (0.64 mL of a 2.5 M solution in hexanes, 1.6 mmol) was added dropwise to a cooled (0 °C) suspension of methyltriphenylphosphonium bromide (0.57 g, 1.6 mmol) in THF (50 mL). After the addition was completed, the ice bath was removed and the reaction mixture was allowed to slowly warm to room temperature, at which point it was stirred for 45 minutes. The resulting yellow solution was cooled to -78 °C and treated dropwise with a solution of diketone **2.1** (0.089 g, 0.32 mmol) in THF (10 mL). The reaction mixture was stirred at -78 °C for 30 minutes, the dry ice/acetone bath was removed and the reaction was allowed to warm to room temperature. After stirring overnight, the reaction was quenched by the addition of water (50 mL) and extracted with ether (3 x 50 mL). The organic extracts were combined, washed with brine (1 x 50 mL), dried over $MgSO_4$ and filtered. The solvent was removed under reduced pressure and the

residue was purified by column chromatography through silica (1:9 EtOAc:hexanes) to yield butadiene **2.5** (0.015g, 0.054 mmol, 17%) as a white solid.

M.p.: 43-44 °C; ^{1}H NMR (chloroform-*d*, 400 MHz): δ 6.52 (s, 2H, CH), 5.13 (d, J = 3.4 Hz, 2H, CH_2), 5.09 (d, J = 3.4 Hz, 2H, CH_2), 2.40 (s, 6H, CH_3), 2.31 (s, 6H, CH_3); ^{13}C NMR (chloroform-*d*, 100 MHz) δ 144.5, 137.7, 135.1, 133.0, 127.9, 118.5, 15.4, 14.1; Anal. Calcd. for $C_{16}H_{18}S_2$: C, 70.02; H, 6.61; Found: 69.74; H 6.41; LRMS (EI): m/z = 274 [M^+].

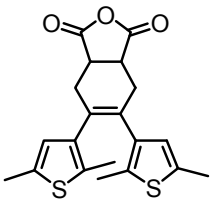

2.6

Synthesis of cyclohexene 2.6

A solid mixture of 2,3-*bis*(2,5-dimethyl-3-thienyl)-1,3-butadiene **2.5** (6.8 mg, 0.025 mmol) and maleic anhydride (4.9 mg, 0.05 mmol) was heated to 70 °C using an oil bath. Upon the complete melting of both solids, a pale pink solid subsequently formed. The cyclohexene product (**2.6**) was purified by column chromatography through silica (1:4 EtOAc:hexanes) as a white solid.

^{1}H NMR (chloroform-*d*, 400 MHz): δ 6.32 (s, 2H, CH), 3.53 (d, J = 2.4 Hz, 2H, CH), 2.96 (d, J = 15.1 Hz, 2H, CH_2), 2.65 (dd, J = 15.1, 2.4 Hz, 2H, CH_2), 2.33 (s, 6H, CH_3), 1.73 (s, 6H, CH_3).

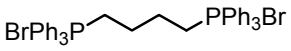

Synthesis of 1,4-butane-*bis*(triphenylphosphonium) dibromide - From literature[87]

A mixture of 1,4-dibromobutane (2.19 g, 10.1 mmol) and triphenylphosphine (5.32 g, 20.3 mmol) in dry DMF (50 mL) was heated under reflux for 14 hours, during which time a white precipitate formed. The solvent was evaporated under reduced pressure. The product was recrystallised from diethyl ether to afford a colourless solid (2.75 g, 3.74 mmol, 37%).

M.p.: >300 °C; ^{1}H NMR (chloroform-*d*, 400 MHz): δ 8.1-7.6 (m, 30H), 4.2-4.0 (m, 4H), 2.2-2.3 (m, 4H).

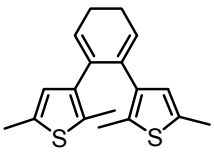

2.8

Synthesis of 3,4-*bis*(2,5-dimethyl-3-thienyl)cyclohexadiene (2.8)

Potassium *t*-butoxide (0.163 g, 1.45 mmol) was added to a suspension of 1,4-butane-*bis*(triphenylphosphonium) dibromide (0.537 g, 0.730 mmol) in benzene (50 mL). The reaction was stirred for 45 minutes at room temperature. The resulting orange solution was heated to reflux and treated dropwise with a solution of 1,2-*bis*(2,5-dimethyl-3-thienyl)ethanedione **2.1** (0.202 g, 0.720 mmol) in benzene (25 mL). The reaction mixture was stirred at reflux for 20 minutes, at which point the heating mantle was removed and the reaction was allowed to cool to room temperature. The reaction was quenched by the addition of water (50 mL) and extracted with diethyl ether (3 x 50 mL). The organic extracts were combined, washed with brine (1 x 50 mL), dried over $MgSO_4$

and filtered. The solvent was removed under reduced pressure and the residue was purified by column chromatography through silica (1:9 EtOAc:hexanes) to yield cyclohexadiene **2.8** (0.055 g, 0.18 mmol, 25%) as a white solid.

M.p.: 55–57 °C; ^{1}H NMR (chloroform-*d*, 400 MHz): δ 6.13 (s, 2H, H_{het}), 5.88 (m, 2H, =CH), 2.26 (m, 10H, CH_3, CH_2), 2.14 (s, 6H, CH_3); ^{13}C NMR (chloroform-*d*, 100 MHz) δ 137.8, 134.4, 133.9, 131.6, 127.4, 126.7, 22.7, 15.1, 14.0; Anal. Calcd. for $C_{18}H_{20}S_2$: C, 71.95; H, 6.71; Found: C, 71.31; H 6.55; LRMS (EI): m/z = 300 [M^+].

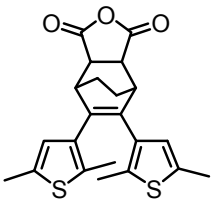

2.9

Synthesis of the bicyclic product 2.9 - Procedure 1

3,4-*bis*(2,5-Dimethyl-3-thienyl)cyclohexadiene **2.8** (5 mg, 0.01 mmol) and maleic anhydride (5 mg, 0.05 mmol) were mixed in a 10 mL round bottom flask. The mixture turned from colourless to yellow within the first few seconds. After standing for 1 h at room temperature, product **2.9** was purified by column chromatography through silica (1:4 EtOAc:hexanes) as a white solid. The efficiency of the reaction was greatly improved when melting both components by heating to 70 °C in an oil bath.

^{1}H NMR (chloroform-*d*, 400 MHz) δ 6.45 (s, 2H, CH), 3.43 (m, 2H, CHC=O), 3.26 (m, 2H, CH), 2.35 (s, 6H, CH_3), 1.65 (s, 6H, CH_3), 1.54 (m, 4H, CH_2). LRMS (EI): m/z = 398 [M^+].

Synthesis of the bicyclic product 2.9 - Procedure 2

3,4-*bis*(2,5-Dimethyl-3-thienyl)cyclohexadiene **2.8** (1 mg, 0.006 mmol) and maleic anhydride (1 mg, 0.01 mmol) were dissolved in acetone-d_6 (1 mL) in an NMR tube and heated at 65 °C in a water bath. The reaction went to completion after 7 days and no side products were observed by ^{1}H NMR spectroscopy.

^{1}H NMR (acetone-d_6, 400 MHz) δ 6.55 (s, 2H, CH), 3.54 (m, 2H, CHC=O), 3.35 (m, 2H, CH), 2.35 (s, 6H, CH_3), 1.89 (dm, J = 7.4 Hz, 2H, CH_2), 1.65 (dm, J = 7.4 Hz, 2H, CH_2), 1.65 (s, 6H, CH_3).

Synthesis of the bicyclic product 2.9 - Procedure 3

3,4-*bis*(2,5-Dimethyl-3-thienyl)cyclohexadiene **2.8** (20.0 mg, 0.07 mmol) and maleic anhydride (6.5 mg, 0.07 mmol) were dissolved in acetone-d_6 (0.75 mL) in an NMR tube and heated at 65 °C in a water bath. The reaction went to completion after 114 hours and no side products were observed by ^{1}H NMR spectroscopy. Thin layer chromatography and ^{13}C NMR spectroscopy showed the presence of trace amounts of impurities. The product was purified by column chromatography through silica (1:4 EtOAc:hexanes).

M.p.: 185 °C (decomposition); ^{1}H NMR (acetone-d_6, 400 MHz) δ 6.55 (s, 2H, CH), 3.54 (m, 2H, CHC=O), 3.35 (m, 2H, CH), 2.35 (s, 6H, CH_3), 1.89 (dm, J = 7.4 Hz, 2H, CH_2), 1.65 (m, 2H, CH_2), 1.65 (s, 6H, CH_3); ^{13}C NMR (acetone-d_6) δ 175.2, 137.8, 137.3, 136.9, 133.9, 127.2, 46.8, 40.7, 25.2, 15.9, 14.8; Anal. Calcd. for $C_{22}H_{22}O_3S_2$: C, 66.30; H, 5.56; Found: C, 66.09; H, 5.60. LRMS (EI): m/z = 398 [M^+].

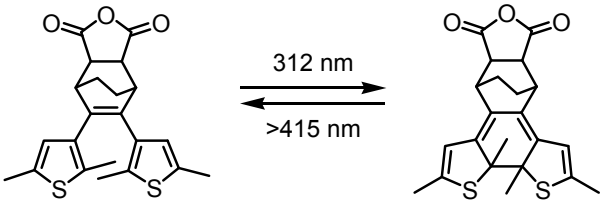

2.9 **2.10**

2.5.5 Characterisation of the photostationary state

A chloroform-*d* solution of **2.9** (1.0 x 10^{-3} M) was irradiated with 312 nm light for 1-minute periods and ^{1}H NMR spectra were obtained after each irradiation. A photostationary state (containing 31% of the ring-closed isomer **2.10**) was reached after a total of 4 minutes of irradiation.

2.10: ^{1}H NMR (chloroform-*d*, 400 MHz): δ 7.72 (s, 1H, H_{het}), 7.50 (s, 1H, H_{het}), 3.23 (m, 1H, CHC=O), 3.22 (m, 1H, CHC=O), 3.12 (m, 1H, CH), 3.11 (m, 1H, CH), 2.08 (s, 6H, CH_3), 1.89 (s, 3H, CH_3), 1.84 (s, 3H, CH_3), 1.54 (m, 4H, CH_2).

2.5.6 Visual representation experiment

Cyclohexadiene **2.8** (1 mg) was added to a saturated solution of maleic anhydride in DMSO (0.5 mL) and a small amount of DMSO was added (~0.5 mL) to dissolve the remaining solid. A solution containing only the cyclohexadiene was also prepared (1 mg in 1 mL). One drop of each solution was deposited on a microscope slide and placed on a heating stage at 35 °C for 30 minutes. After this heating period, the samples were simultaneously irradiated for 30 seconds with 312 nm light. The sample containing maleic anhydride and the cyclohexadiene turned yellow. The other did not. The same behaviour was observed when the solution of maleic anhydride and cyclohexadiene and the control solution were kept at room temperature in the dark for 14 hours before being

irradiated with 312 nm light. Subsequent irradiation with light of wavelengths greater than 415 nm returned the sample to its colourless state. The results are shown in Figure 2.3.4.

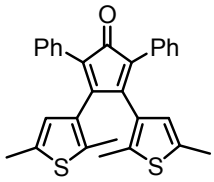

2.14

Attempt to synthesise the cyclohexadienone 2.14 - Procedure 1 - Modified from literature[82]

A solution of potassium hydroxide (0.02 g, 0.36 mmol) in ethanol (5 mL) was added to a refluxing solution of 1,2-*bis*(2,5-dimethyl-3-thienyl)ethanedione **2.1** (0.10 g, 0.36 mmol) and 1,3-diphenylacetone (0.076 g, 0.36 mmol) in ethanol (15 mL). After 30 minutes the reaction was cooled to 0 ^{o}C and the solvent was removed under reduced pressure. The residue was purified by column chromatography through silica (1:3 EtOAc:hexanes). The main fraction was isolated and its structure **2.15** is proposed.

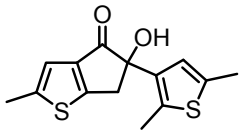

2.15

2.15: ^{1}H NMR (chloroform-*d*, 400 MHz): δ 6.87 (s, 1H, H_{het}), 6.41 (s, 1H, H_{het}), 3.52 (d, J = 3.0 Hz, 2H, CH_2), 3.16 (t, J = 3.0 Hz, 1H), 2.51 (s, 3H, CH_3), 2.39 (3H, s, CH_3), 2.30 (s, 3H, CH_3).

Attempt to synthesise the cyclohexadienone 2.14 - Procedure 2 - Modified from literature[81]

A solution of 1,2-*bis*(2,5-dimethyl-3-thienyl)ethanedione **2.1** (0.08 g, 0.31 mmol) and 1,3-diphenylacetone (0.13 g, 0.62 mmol) in 7% potassium hydroxide/ethanol (40 mL) was heated to reflux. The progress of the reaction was monitored by ^{1}H NMR periodically. The mixture was cooled to room temperature after 24 hours. The residue was purified by column chromatography through silica (1:3 EtOAc:hexanes). The main fraction was isolated and its structure **2.15** is proposed. The residue was purified by column chromatography through silica (1:3 EtOAc:hexanes).

2.15: ^{1}H NMR (chloroform-*d*, 400 MHz): δ 6.87 (s, 1H, H_{het}), 6.41 (s, 1H, H_{het}), 3.52 (d, J = 3.0 Hz, 2H, CH_2), 3.16 (t, J = 3.0 Hz, 1H), 2.51 (s, 3H, CH_3), 2.39 (3H, s, CH_3), 2.30 (s, 3H, CH_3).

Chapter 3: Selective and Sequential Photorelease Using DTE Derivatives

The research presented in this chapter was published in part as a VIP communication in: V. Lemieux, S. Gauthier, N. R. Branda, "Selective and sequential photorelease using molecular switches", *Angew. Chem. Int. Ed.* **2006**, *45*(41), 6820-6824. It is also part of a patent application: N. R. Branda, B. Wüstenberg, V. Lemieux, S. Gauthier, M. Adams, "Photochromic and electrochromic compounds and synthesis and use thereof", WO/2006/125317, PCT/CA2006/000862, filed May 25, 2006. Compound **3.28** was synthesised by Mr. Simon Gauthier following the procedure developed for compound **3.27**; he also participated in some of the studies involving this compound.

This chapter presents a novel and versatile approach, based on molecular photoswitching strategies, for the photorelease of active compounds from their inert "masked" forms. The focus of Section 3.1 is on the currently used photocleavable protecting groups and their limitations. It also covers the use of DTE-based photochromic molecules as photoreleasing moieties. Section 3.2 describes how the integration of chemical reactivity and photochromism through the combination of a reversible Diels-Alder reaction and the DTE scaffold could be used to release small molecules. Section 3.3 introduces two novel functional fulvenes and presents an in-depth discussion of their potential as photoreleasing units. The results presented in this chapter are summarised and placed in perspective in Section 3.4. Experimental details are provided in Section 3.5.

3.1 Introduction to photorelease systems

3.1.1 Photocleavable protective groups

Light is an effective trigger for the release of active chemical and biological species from masked, innocuous forms.[88] It offers the precise temporal and spatial control needed to deliver therapeutics,[6,7,89] agents to initiate biological phenomena,[8] and designer reagents for chemical transformations,[9] as well as for photolithography.[9] There are relatively few classes of molecular structures that can be photochemically cleaved to free a species of interest. Most existing systems are based on the photochemical redox reactions of the 2-nitrobenzyl group, while others are based on 7-nitroindoline, coumarin, hydroxyphenacyl, and benzoin chromophores as shown in Figure 3.1.1 and Figure 3.1.2.[88,90]

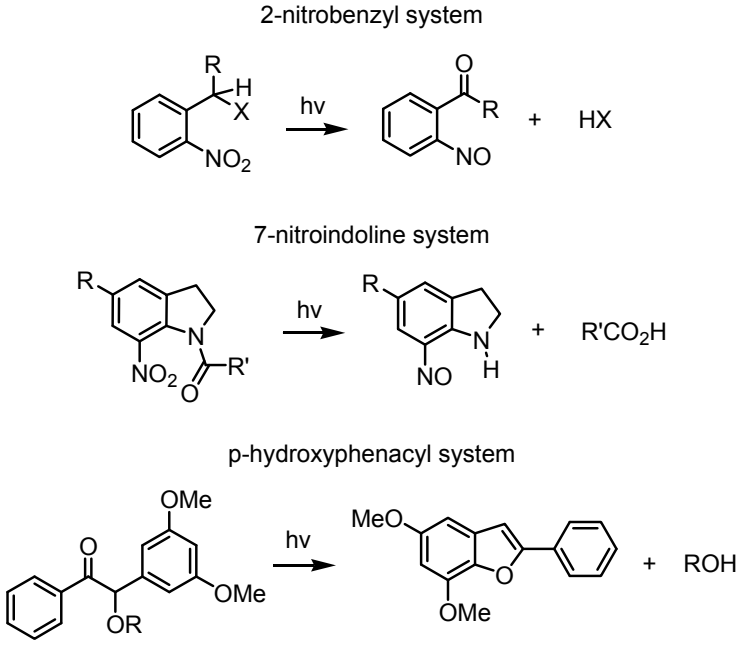

Figure 3.1.1 Examples of previously reported photocleavable protecting groups.[88]

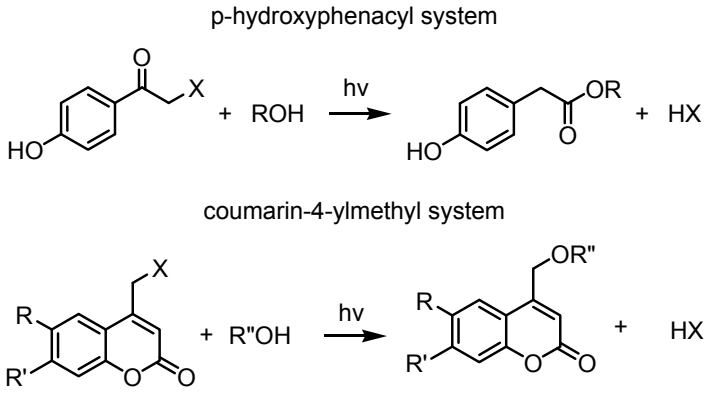

Figure 3.1.2 Examples of previously reported photocleavable protecting groups requiring a nucleophile.[88]

For example, the photolysis of 2-nitrobenzyl offers an efficient means to release ATP from a caged compound as shown in Equation 3.1.1.[91] Although it was preceded by other examples of 2-nitrobenzyl photolysis applied to synthetic organic chemistry, this was the first system applied to a biological problem. In addition to ATP, photocleavable groups have been used to cage various molecules of biological interest such as nucleotides, peptides and proteins.[88]

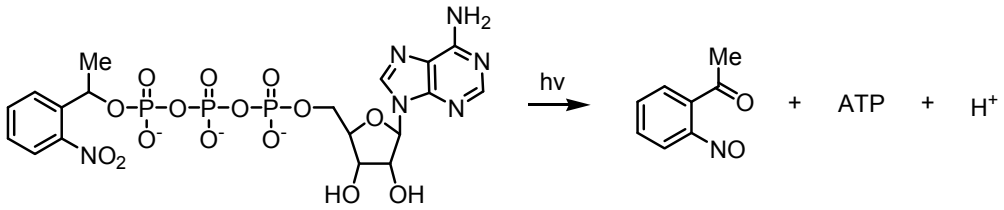

Equation 3.1.1 Light-induced release of ATP from a 2-nitrobenzyl-caged compound.[91]

Widespread use of these systems in practical applications is limited by a number of factors such as the generation of reactive side products, the need for high-energy radiation sources (200-400 nm), which may lead to undesirable side reactions, and most

significantly, the inability to selectively stimulate photocleavable groups in the presence of others due to their absorbing light in the same general spectral range.[8,88,90]

The release mechanisms by which the current photoremovable protecting groups operate require sufficient energy to break a single bond, which explains the requirement for a high-energy light source to trigger the release event.[88] As shown in Scheme 3.1.1, a high-energy photon is required to cleave a proton-carbon bond from the 2-nitrobenzyl group. A thermal rearrangement follows, leading to the release of the molecule of interest (X^-) and the generation of the reactive nitroso side product.

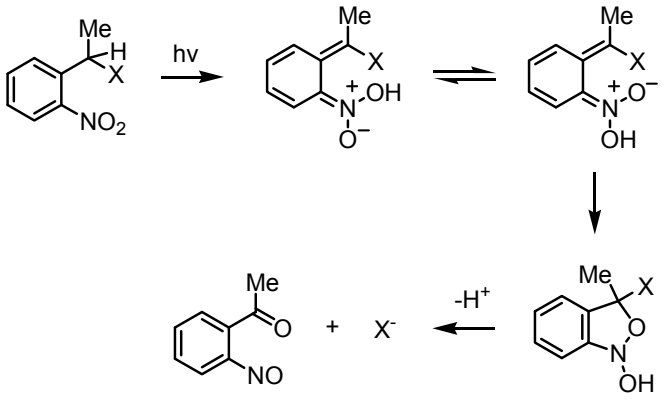

Scheme 3.1.1 Photolysis of generalised nitrobenzyl-caged compounds requiring a high energy photon to break a C-H bond and leading to the release of X^- and the generation of the nitroso by-product.[88]

Most photoremovable protecting groups are designed to absorb light directly.[88] An alternative strategy is to activate photorelease through direct or mediated electron transfer from a photosensitiser[92,93] or tethered chromophore,[94] which allows the use of light in the visible range of the spectrum, thus improving penetration depth in biological tissues and limiting undesired side reactions. However, this requires the introduction of another component in the system and thus complicates the deprotection procedure to a

certain extent.[95] Furthermore, the relatively large amount of sensitiser required to deprotect the system presents an additional obstacle to their practical use.[95]

The selective stimulation of a photocleavable group in the presence of others has also been attempted but is limited by the fact that all photocleavable groups absorb light in the same general spectral UV range.[96,97] Up to now, no simple strategy has been developed to allow efficient and potentially useful selective and sequential release.[88]

3.1.2 Development of a universal photorelease system – Goals of the research presented in this chapter

The goal of the work presented in this chapter is to develop a universal photorelease system by using a common photoresponsive molecular scaffold that (1) can be easily tailored to fine-tune its electronic properties without adversely affecting its performance, (2) strongly absorbs long-wavelength light to minimise cellular damage, (3) generates photoreleased products which absorb at wavelengths that are shifted out of the spectral region triggering the photorelease to minimise side reactions, and (4) is modified using synthetic methods tolerant to a wide range of chemistries. A system that fits this description would offer a means to sequentially release different species by using light of different wavelengths.[8,88,93]

This chapter reports the success in developing a versatile approach to the selective and sequential light-initiated release of an easily functionalised chemical species by using two different thermally bistable dithienylethene (DTE) photoswitches and low-energy visible light of two different wavelengths.

3.1.3 DTE-based photoswitches and photorelease – The state of the art

Photoresponsive compounds containing the dithienylethene backbone are particularly appealing for use in photodelivery applications as described in *Chapter 1*. The optical properties of both photoisomers can be fine-tuned by rationally decorating the two heterocycles on the DTE backbone; an attribute that is central in reports describing the selective ring-opening and ring-closing of multicoloured, multifrequency systems using small molecule DTE derivatives,[98,99] fused trimers[100] and polymers.[101] The good thermal stability of most DTE derivatives is of particular importance to photorelease applications since it can help to avoid premature release of the target compound.

Irie and co-workers described the first example of photorelease using DTE molecular switches in 1998.[31,32] As described in Section 1.5.1, they prepared a photoresponsive ion tweezer that shows high affinity for various metal ions in its ring-open form. Irradiation with UV light triggers the ring-closing reaction and the release of the ion since the molecule no longer has the appropriate geometry to chelate the ion. The drawback of this strategy is the gated-photochromism effect on the ring-open form of the photoswitch caused by the presence of the ion. In this form, the molecule is forced in the photoinactive parallel conformation, greatly limiting the efficiency of the release event. The same tweezer effect was used to photocontrol the release and uptake of a porphyrin guest by dithienylethene-tethered cyclodextrin host dimers.[35]

The changes in electronics between the ring-open and the ring-closed photoisomers of DTE derivatives also offer a means to photocontrol the release of cations such as calcium, sodium and silver. Scheme 3.1.2 shows a system described by Lapouyade and co-workers.[39] In the ring-open form of the photoswitch, the monoaza-

crown ether group shows good affinity to metal ions. However, the binding ability of the photoswitch in the ring-closed isomer decreases due to the electron-withdrawing character of the aldehyde moiety now conjugated to the nitrogen atom of the crown ether group. Irradiation of the ring-open isomer with UV light triggers the ring-closing reaction and thus the release of the metal ion.

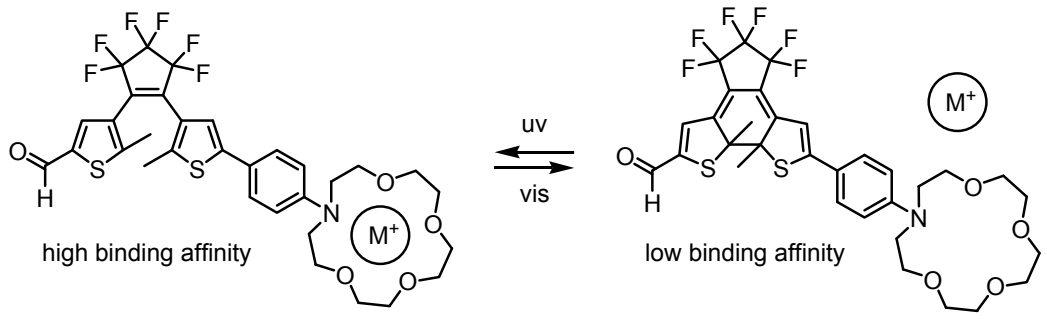

Scheme 3.1.2 Photoswitching of cation complexation using a DTE derivative: in the ring-open state, molecule binds efficiently with a metal ion that can be release by irradiation with UV light, triggering the ring-closing reaction and lowering the affinity of the molecule to M^+.[39]

As shown by these pioneering examples, DTE photoswitches are good candidates for photorelease applications. However, important limitations plague the various strategies previously employed. In many cases, the uptake of the guest molecule renders the complex photoinactive, hindering the release event.[30,34] Moreover, these examples are based on a relative change in the complexation between the two photoisomers.[30,34,39] The release event is favoured in one state of the molecule, but not totally forbidden in the other. Thus, depending on the concentration, release can occur in both forms of the photoswitches. The objective of the project presented in this chapter is to develop a novel approach to control the reactivity of DTE derivative in order to overcome these previously encountered limitations and effectively control the delivery of molecular species.

3.2 Proposed Diels-Alder approach for photorelease applications

3.2.1 Photoregulation of Diels-Alder reactivity – General description of the proposed approach

Chapter 2 described a novel approach for the control of the photochromic properties of DTE derivatives using the concept of reactivity-gated photochromism, which implied that light does not induce a molecular transformation unless it is preceded by a chemical reaction between two or more species, as can be seen in Scheme 3.2.1

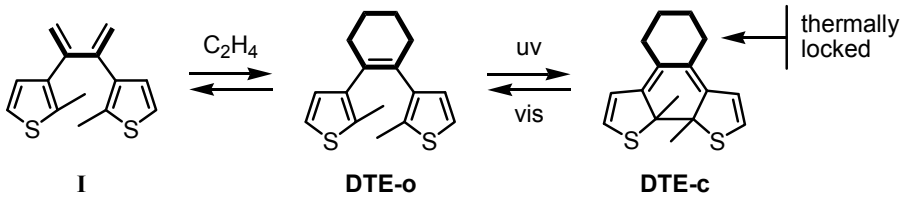

Scheme 3.2.1 Illustration of the proposed approach for photorelease applications based on reactivity-gated photochromism and photogated reactivity using the Diels-Alder reaction: Compound **I** is not photoswitchable unless it reacts with a dienophile to form the photoresponsive **DTE-o**. **DTE-c** lacks the required cyclohexene moiety (bold) required to undergo a retro-Diels-Alder reaction. Upon irradiation with visible wavelengths of light, the ring-opening reaction occurs, generating **DTE-o** which has the required cyclohexene moiety (bold) and could undergo a retro-cycloaddition, releasing the dienophile and **I**, which has a butadiene unit (bold).

In photogated reactivity, which is the opposite approach, light triggers a structural change in the molecule and imparts chemical reactivity unique to each form of the compound. This approach is also illustrated in Scheme 3.2.1, where the reverse Diels-Alder reaction can proceed only from the ring-open form of the compound because **DTE-c** lacks the cyclohexene structure required for the fragmentation reaction. UV light effectively locks the system in its "armed" state, which removes all molecules from the initially established Diels-Alder equilibrium. The ring-closed form can be considered to act as a phototrigger since visible light regenerates the cyclohexene in **DTE-o** and allows

the thermal Diels-Alder equilibrium to be re-established, spontaneously releasing the dienophile. Thus, the photochemistry could gate the thermal Diels-Alder reaction.

Because the release mechanism is thermally driven and independent of the photochemistry, the photochemically active moiety could be tailored to harness a wide range of wavelengths to release the small auxiliary agent, thus offering a relatively universal approach to photorelease technology. The light used to trigger the release reaction is in the visible range, leading to the dual advantages of limiting biological damage and increasing penetration depth in living tissues. Moreover, the light absorbed by the ring-open isomer, the butadiene, and the dienophile should be significantly higher in energy and lie far outside the region used to trigger the photochemistry, thus minimising photochemical side reactions.

Another appealing feature is that the two photoisomers of DTE derivatives display a wide range of properties unique to their structure,[17-22] offering a means to release and report, that is, to quantify the extent and location of discharge by monitoring a readout signal (colour, refractive index, luminescence, or redox chemistry). In a recent account of "release and report", Kutateladze and co-workers are using the change in fluorescence to monitor the release event.[102]

3.2.2 Proposed requirements

Applying the concept of photogated reactivity to the DTE architecture and the Diels-Alder reaction, or more specifically the retro-Diels-Alder reaction, requires the use of a Diels-Alder cycloaddition that is reversible at low temperature, ideally at ambient temperature (around 22 °C). In this thesis, the term reversible is employed to describe the

fact that both starting materials and the Diels-Alder adduct are in equilibrium in solution such that all components can be observed by analytical techniques such as NMR spectroscopy. This implies that a reasonable amount of the photoswitchable Diels-Alder adduct can be formed and locked by irradiation, and the release event from the isolated ring-closed photoisomer can be easily observed. In the case of irreversible Diels-Alder reactions or of Diels-Alder equilibria strongly favouring adduct formation, the release event can be very difficult or impossible to observe. When the retro-Diels-Alder process occurs only at higher temperature, the monitoring of the release event requires heating, complicating the experiment and the instrumentation needed. Moreover, under these conditions the development of *in vivo* or room temperature applications is limited. In the case of a Diels-Alder equilibrium strongly favouring starting materials, only a small amount of the photoswitchable adduct can be formed, diminishing the yield of the process. Lowering the temperature at which the reaction is carried out can increase the yield of the reaction but complicates the experiment and the instrumentation required, and the reaction rate can be slower.

The application of the photogated reactivity concept would be simplified if both the forward and backward Diels-Alder reactions proceed as fast as possible in order to reduce the time needed to perform each experiment or measurement.

Thermodynamic and kinetic considerations

The Diels-Alder reaction, as all chemical processes, is characterised by its reaction profile as shown in Figure 3.2.1. In order to have a reversible Diels-Alder equilibrium at ambient temperature, the absolute value of the reaction free energy needs to be as small as possible so that both the starting materials and the product have similar

energies. If the free energy of the reaction is too negative, the adduct will be favoured too strongly and if the free energy of the reaction is too positive, the adduct will be scarcely formed. In order to have a rapid forward process, the activation energy needs to be as small as possible. In the case of the reverse process, both the activation energy and the reaction free energy need to be minimised. Under these conditions, the Diels-Alder equilibrium should be dynamic.

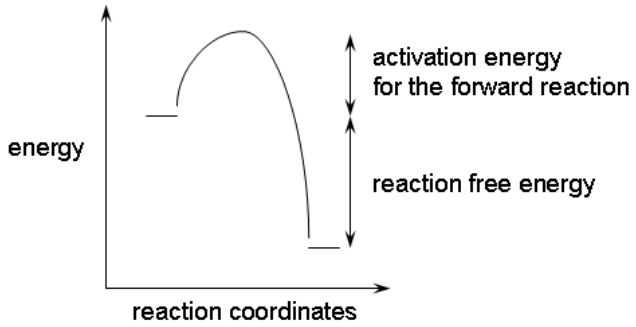

Figure 3.2.1 Energetic reaction profile for the Diels-Alder reaction. The energy of the starting materials lies on the left, and the energy of the products, on the right. The activation energy and reaction free energy are indicated.

3.2.3 Reversible Diels-Alder reactions

Even though an exceptionally large number of studies on the Diels-Alder reaction have been reported, the retro-Diels-Alder process has in contrast received less attention.[76] Nevertheless, it offers great potential for the removal of solubilising groups[103,104] or protecting groups from sensitive dienes and dienophiles.[105,106] For example, self-assembled maleimide monolayers on gold nanoparticles cannot be prepared from the parent maleimide-thiol moiety since maleimide is such a potent scavenger of thiols.[107] However, surface derivation of nanoparticles with furan-protected maleimide followed by a thermally activated retro-Diels-Alder reaction allows the preparation of

maleimide-functionalised surfaces.[107] The Diels-Alder/retro-Diels-Alder process is also very important for the development of novel functional materials such as re-mendable polymers.[108] However, in all of these examples initiation of the cycloreversion requires elevated temperatures.[75]

Empirical observations suggest the following sequence of retro-Diels-Alder activity for dienes: furan, pyrrole > benzene > naphthalene > fulvene > cyclopentadiene > anthracene > butadiene.[75,109,110] However, very few examples of retro-Diels-Alder reactions taking placed at low temperature (below 50 °C) are reported in the literature.[75] Some catalytic enzymes accelerate the rate of the retro-Diels-Alder reaction at ambient temperature[111,112] and chemical activation by forming oxy-anions is effective to promote the fragmentation reaction.[113-115]

The small number of reported Diels-Alder reactions that are reversible at room temperature can perhaps be explained by the difficulty of isolating and characterising the products since by definition they would be unstable at this temperature, being part of an equilibrium. Nevertheless, some examples have been reported (Figure 3.2.2) relying on solution NMR spectroscopy for characterisation. Solutions of furan **3.1a** (or its derivatives **3.1b-c**) and 1,1,1-trichloro-3-nitro-2-propene **3.2** react slowly to form their corresponding Diels-Alder adducts until an equilibrium is reached (81% - 90% of products at room temperature); however, the Diels-Alder adducts degrade to another product.[116] Another example of reversibility at low temperature is the reaction between isocyclopentadiene **3.3** and tetracyanoethylene **3.4**.[117] More recently, Hirsch *et al.* found that the cycloaddition reaction of C_{60} **3.5** and 9,10-dimethylanthracene **3.6** in toluene is

reversible at room temperature.[118] This equilibrium was further characterised by Cross and co-workers.[119]

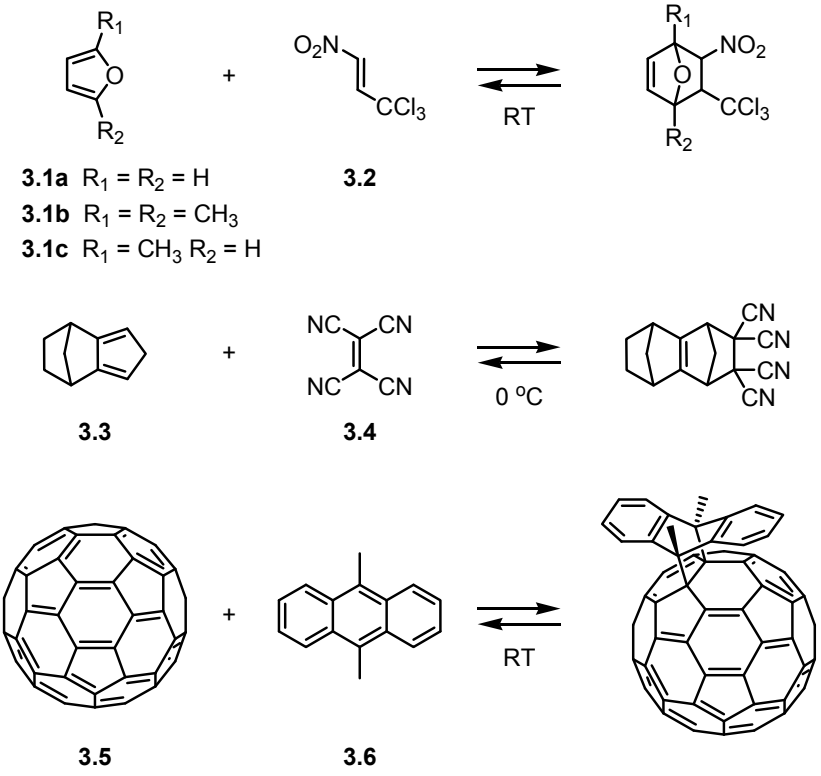

Figure 3.2.2 Examples of previously reported reversible Diels-Alder systems at low temperature.[116-118]

3.2.4 Fulvenes as candidates for reversible Diels-Alder reactions

Fulvenes are very interesting molecules not only because they are very active dienes towards the Diels-Alder reaction, but also because some of their adducts readily dissociate under various conditions.[120-127] As depicted in Figure 3.2.3 fulvene itself, C_6H_6, is an isomer of benzene but with different colour and reactivity. The term *fulvene* comes from the Latin word *fulvus* meaning "dull yellow" or "tawny" and is an accurate description of the colour of the first derivatives prepared by Thiele in 1900.[122,128]

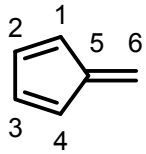

Figure 3.2.3 Fulvene and its numbering scheme.

The capacity of fulvenes to undergo a cycloaddition reaction with maleic anhydride was first observed by Otto Diels and Kurt Alder.[123] Some years after, Kohler and Kable discovered that the adduct of 6,6-pentamethylenefulvene **3.7** and maleic anhydride **3.8** dissociates readily into its components in a variety of solvents, even at low temperature (Scheme 3.2.2).[124] Later on, Alder and Stein called attention to the fact that the reaction of fulvenes with maleic anhydride leads to the formation of two stereoisomers, the *endo* and *exo* adducts.[125] Woodward and Baer observed that the *endo* product formed in greater amount at low temperature, and the proportion of *exo* product increased with temperature.[126] Furthermore, they reported that even cold solutions of the *endo* adduct dissociate, but not those of the *exo* product. This observation led to the general principle of kinetics versus thermodynamics in selectivity.[127]

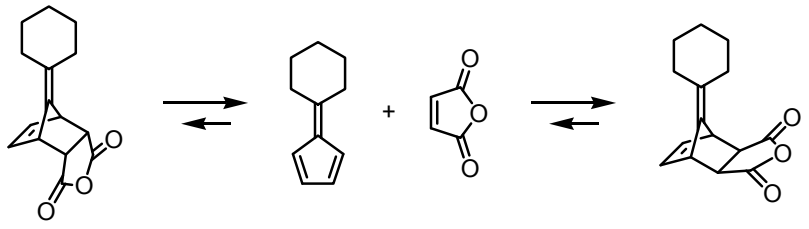

endo **3.7** **3.8** exo

Scheme 3.2.2 Reversible Diels-Alder reaction between pentamethylenefulvene **3.7** and maleic anhydride **3.8**. The *endo* isomer dissociates more readily than the *exo* isomer.[126,127]

Judging from these early studies, fulvenes appear to be good candidates in the search for reversible Diels-Alder equilibria at low temperature. Along this line, Howard and co-workers reported a Diels-Alder reaction reversible at room temperature between 6,6-dimethylfulvene **3.9** and 2,2-*bis*(trifluoromethyl)-1,1-dicyanoethylene **3.10** with an equilibrium constant of 11.2 M^{-1} in toluene-d_8 at 20 °C (Figure 3.2.4). However, the adduct undergoes an irreversible rearrangement in more polar solvents, on contact with silica gel or alumina, and in the solid state.[120]

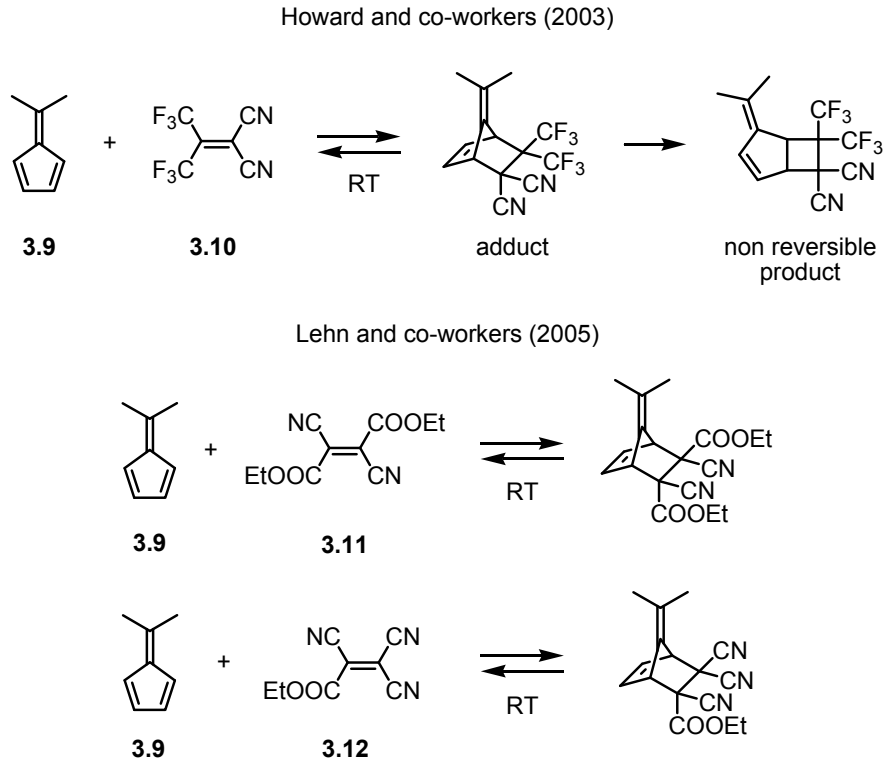

Figure 3.2.4 Examples of previously reported Diels-Alder equilibria involving fulvenes.[120,121]

Lehn and co-workers recently uncovered a series of Diels-Alder reactions that are dynamic between 25 and 50 °C and present efficient kinetics, reaching equilibrium in a matter of 1 minute or less at 25 °C and 100 mM concentration.[121] They found that in

organic media, 6,6'-disubstituted fulvenes such as **3.9** engage in reversible Diels-Alder reactions with two types of cyanoolefincarboxylicesters, dicyano and tricyano compounds, including **3.11** and **3.12**, as shown in Figure 3.2.4. For example, the equilibrium constant for **3.9** and **3.11** is 63 M^{-1} where 33% of the starting materials and 67% of the adduct are observed in chloroform at 100 mM at 25 °C. In the case of compound **3.9** and **3.12**, the equilibrium constant was evaluated to be 581 M^{-1}. Moreover, no side reaction was reported for these systems.

3.2.5 Proposed molecular design

With the aim to develop dienes with high activity towards the Diels-Alder cycloaddition and having the potential to be reversible even at room temperature, fulvene derivatives are good candidates. The fulvene derivative shown in Scheme 3.2.3 should undergo Diels-Alder reactions with various dienophiles to form adducts containing the 1,3,5-hexatriene moiety, making them potentially photochromic. Moreover, in the case of reversible equilibria, the retro-Diels-Alder process could be prevented by locking the compounds in their ring-closed formed.

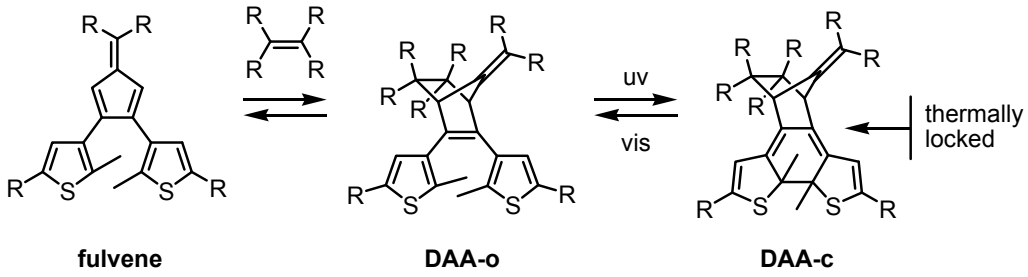

Scheme 3.2.3 The targeted fulvene derivatives and the Diels-Alder concept: The fulvene should not be photoswitchable unless it reacts with a dienophile to form the photoresponsive **DAA-o**. **DAA-c** lacks the required cyclohexene moiety required to undergo a retro-Diels-Alder reaction. Upon irradiation with visible wavelengths of light, the ring-opening reaction occurs, generating **DAA-o** which has the required cyclohexene moiety and could undergo a retro-cycloaddition, releasing the dienophile and the fulvene.

3.3 Results and discussion

3.3.1 Functional fulvenes to generate DTE derivatives

Evolution of the project

As described in *Chapter 2*, one of the objectives of the Diels-Alder project was to develop very active dienes that undergo cycloaddition reactions with various dienophiles at ambient temperature in order to generate the photoactive hexatriene moiety. The butadiene **2.5** and cyclohexadiene **2.8** were used to establish the foundation of the novel reactivity-gated photochromism concept. However, these dienes showed only limited reactivity with good dienophiles such as maleic anhydride.

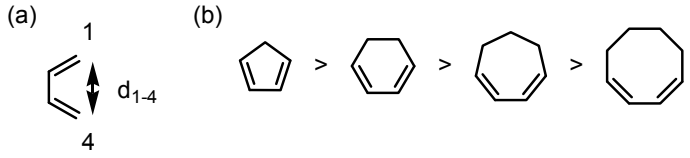

Figure 3.3.1 (a) The distance between atoms 1 and 4 of a diene involved in the Diels-Alder reaction and (b) the trend in reactivity of some conjugated cyclodienes.

A simple improvement on the previously developed system would be to change from a cyclohexadiene to a cyclopentadiene derivative, since the distance between the reacting carbons C_1 and C_4, as shown in Figure 3.3.1, plays an important role in the reactivity of dienes.[74] The better the overlap between the orbitals of the diene and the dienophile, the more reactive is the couple.[74] In this context, cyclopentadiene is more reactive than 1,3-cyclohexadiene which is more reactive than 1,3-cycloheptadiene.[77] Moreover, the self-condensation of cyclopentadiene is a classic example of the Diels-Alder reaction.[129] This process is reversed when the cyclopentadiene dimer is heated to ebullition.[129]

The high activity and potential reversibility of the cyclopentadiene units offers good potential for the development of a new functional diene, hence compound **3.14** was targeted (Equation 3.3.1). Moreover, the cyclopentadiene **3.14** could be prepared from the bromination/elimination reaction of the known photochromic cyclopentene **3.13**.[130,131] However, as shown in Equation 3.3.1, the bromination of **3.13** in dichloromethane or diethyl ether at -40 °C afforded the cyclopentadiene product as mixture of isomers, **3.14** and **3.15,** in a 1:7 ratio. Attempts to separate the isomers were unsuccessful, probably because the compounds are in equilibrium. A [1,5]-hydrogen shift occurring at room temperature could explain the formation of isomer **3.15**. Isomer **3.16** is not observed by ^{1}H NMR spectroscopy. Semi-empirical calculations at the AM1 level show that **3.15** has a heat of formation of 70.4 kcal/mol whereas **3.14** and **3.16** have heats of formation of 71.5 kcal/mol and 75.4 kcal/mol respectively. Hence, **3.15** is more stable by 1.1 kcal/mol compared to **3.14** and by 5 kcal/mol compared to **3.16**, which is in agreement with the experimental results showing that **3.15** is the energetically favoured isomer.

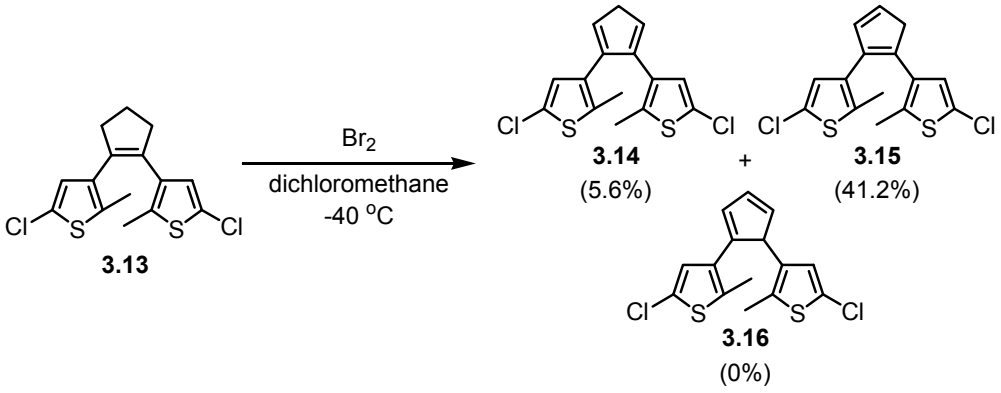

Equation 3.3.1 Attempted synthesis of the cyclopentadienes **3.14** leading to a mixture of isomers **3.14** and **3.15**. Isomer **3.16** was not observed.

Solutions of a mixture of **3.14** and **3.15** become reversibly coloured when irradiated with 312 nm light followed by light of wavelengths greater than 434 nm. This is indicative of the fact that the solution contains a photochromic compound, which is not unexpected considering that the cyclopentadiene **3.15** possesses a 1,3,5-hexatriene moiety. Thus, this mixture of products does not meet the needs of the Diels-Alder project, since one of the compounds is already photochromic and characterisation of the mixture was limited to ^{1}H NMR spectroscopy. A solution to this problem would be to prepare a cyclopentadiene derivative where the diene unit is locked in the desired bond configuration. Fulvene derivatives such as the one depicted in Scheme 3.2.3 could be good candidates for this purpose and might undergo reversible Diels-Alder reactions at low temperature as discussed in Section 3.2.5.

Synthesis of the fulvenes 3.17 and 3.18

Fulvenes can be easily prepared by condensing a cyclopentadiene with a ketone or an aromatic aldehyde in the presence of a base.[122] Traditionally, an alkali metal base in alcohol is used to deprotonate the cyclopentadiene; however, the success of this reaction depends on the reactivity of the carbonyl used and the stability of the fulvene formed. Recently, Ottosson and Chajara proposed an improved pathway for the formation of fulvenes using crystalline sodium cyclopentadienide.[132] However, this synthetic route requires the preparation of the sodium cyclopentadienide, which might lead to complications stemming from the use of more complex cyclopentadiene starting materials such as **3.14** or **3.14a**.

An alternative route towards the preparation of a diverse range of fulvenes was developed by Stone and Little.[133] They showed that pyrrolidine promotes fulvene

formation between cyclopentadiene and carbonyl compounds through the activation of the carbonyl group. This method could be an efficient synthetic route for the preparation of the dithienylfulvenes **3.17** and **3.18** and is depicted in Scheme 3.3.1. First, the cyclopentadiene derivatives **3.14** and **3.15** were prepared from the bromination/elimination reaction of the DTE derivatives **3.13** and **3.13a** in dry and oxygen-free dichloromethane or diethyl ether at -40 °C under inert atmosphere. The use of diethyl ether afforded better isolated yields, as it is more volatile and can be evaporated at lower temperatures. The obtained isomers are thermally unstable and degrade into a non-identified mixture of products when kept at room temperature. A mildly basic work-up removed the excess bromine and the hydrobromic by-product. Purification of the products can be achieved by column chromatography using silica gel under basic conditions, but this step is not necessary. Treatment of the crude cyclopentadiene mixture with pyrrolidine in methanol under inert atmosphere afforded the desired dithienylfulvenes **3.17** and **3.18**. As anticipated, compounds **3.17** and **3.18** show good photostability and their irradiation with UV or visible light does not cause any colour change and results in minimal degradation. Moreover, the purified dithienylfulvenes can be stored indefinitely in their solid states at -20 °C as insignificant decomposition is observed.

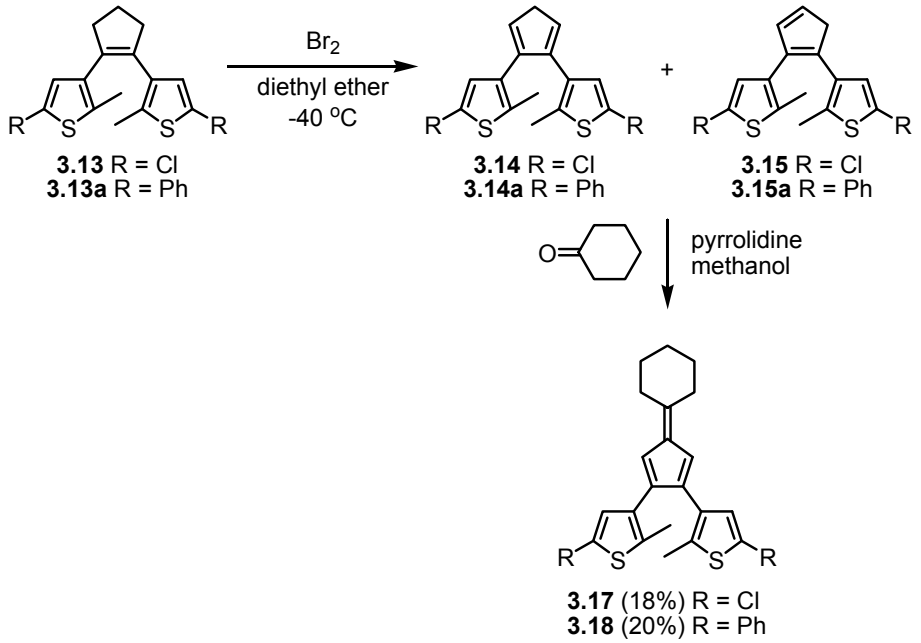

Scheme 3.3.1 Synthesis scheme for the preparation of fulvenes **3.17** and **3.18**.

3.3.2 Thermally stable Diels-Alder adducts of the fulvenes

Diels-Alder reactivity of the *bis*-chlorofulvene 3.17

The chlorinated dithienylfulvene **3.17** was found to readily undergo Diels-Alder reactions when treated with electron-deficient dienophiles such as maleic anhydride **3.19** or maleimide **3.20** to afford the bicyclic products (**3.21o** and **3.22o**) as observed by ^{1}H NMR spectroscopy (Scheme 3.3.2).

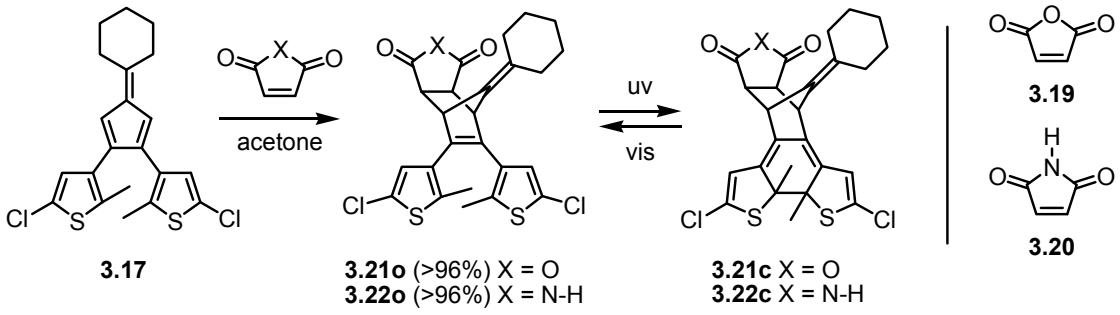

Scheme 3.3.2 Diels-Alder reaction between fulvene **3.17** and maleic anhydride or maleimide.

The reaction between fulvene **3.17** and maleic anhydride **3.19** reaches 96% completion in acetone-d_6 after only 4 hours at 50 °C, which is a major improvement compared to the cyclohexadiene **2.8**. Under these conditions, the *endo* and *exo* isomers are formed in a 1:9 ratio. The region between 3.5 ppm and 4.5 ppm in the ^{1}H NMR spectrum of compound **3.21o** shows two two-proton singlets (Appendices Figure 6.3.9) that can be attributed to protons H_a and H_b of the major isomer and two two-proton doublet of doublets that can be attributed to protons H_a and H_b of the minor isomer (Figure 3.3.2).

Geometry optimisation of both isomers at the AM1 level shows that the torsion angle between protons H_a and H_b for the *exo* product is 74° whereas the angle between the same protons for the *endo* product is only 42°. Hence, larger coupling between H_a and H_b is expected for the *endo* isomer of compound **3.21o**. It can be concluded that the *exo* isomer is the main product of the reaction since the signal of the major product show small couplings (Chapter 6 – Figure 6.3.9).

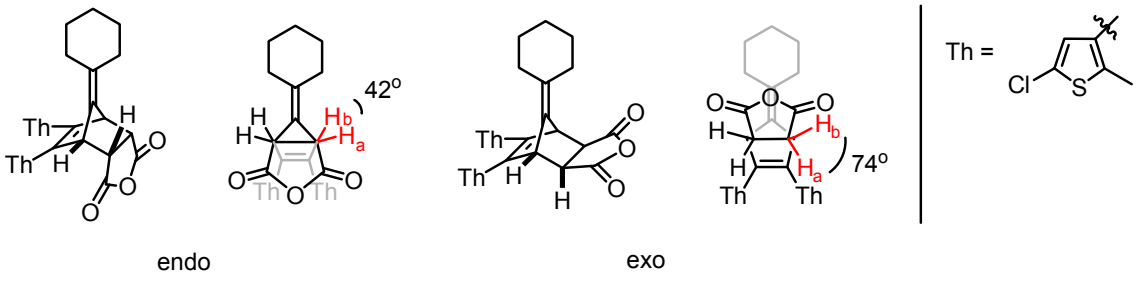

Figure 3.3.2 Torsion angles between proton H_a and H_b in the adduct **3.21o** in the *endo* and *exo* conformations.

The reaction between **3.17** and maleimide **3.20** is much slower; the reaction reaches >96% completion after 100 hours in acetone-d_6 at 45 °C. In this case the *endo*:*exo* ratio was evaluated to be 1:4.

The Diels-Alder adducts **3.21o** and **3.22o** can be isolated by column chromatography and are thermally stable at 22 °C; the retro-cyclization reaction was not observed in either case. However, the retro-Diels-Alder reaction slowly occurs when an acetone-d_6 solution of pure **3.21o** is kept at 50 °C. After 48 hours at this temperature, 10% of fulvene **3.17** and maleic anhydride **3.19** is observed in solution by ^{1}H NMR spectroscopy.

Photochromism of the Diels-Alder adducts 3.21

Irradiating an acetonitrile solution of compound **3.21o** with 312 nm light triggers a change in colour of the solution from colourless to yellow, which is consistent with the occurrence of a photocyclization generating the ring-closed isomer **3.21c** having an extended π-conjugated backbone. The corresponding UV-vis absorption spectra (Figure 3.3.3) show trends typically observed for ring-closing reactions of DTE derivatives. The high-energy bands in the spectra become less intense as a broad band centred at 437 nm appears. At a concentration of 3.5 x 10^{-5} M (in acetonitrile), a photostationary state is reached within 60 seconds. The small changes between the spectra before and after irradiation suggest a low photostationary state relative to other DTE systems, as is common for chloro-functionalised DTE derivatives.[130] The ring-closed isomer is stable at room temperature and the ring-opening reaction is only induced by irradiating the solution with visible light (wavelengths greater than 434 nm). However, decomposition of **3.21** is apparent even after only one cycle since the original UV-vis spectrum

corresponding to the pure ring-open form **3.21o** is not fully regenerated. Due to these limitations, no further studies were pursued with this system.

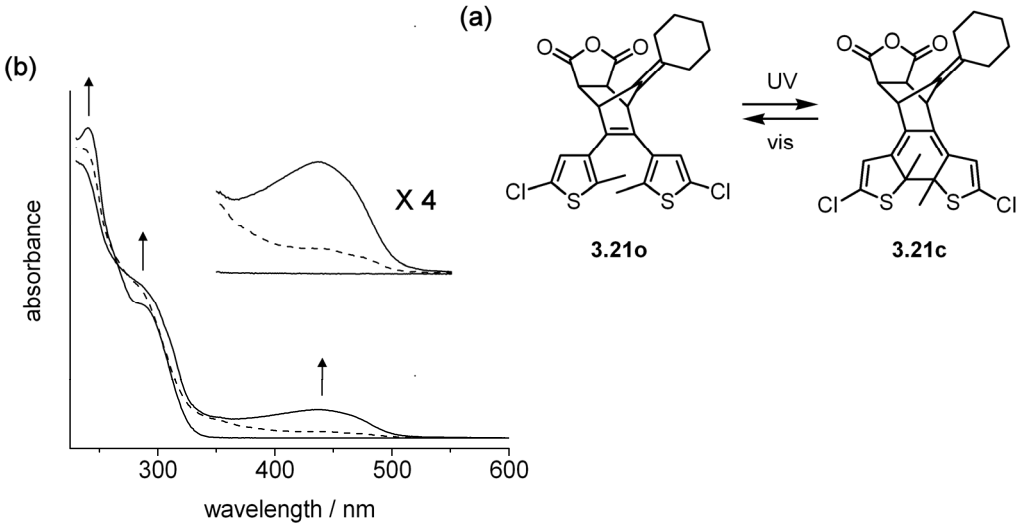

Figure 3.3.3 (a) Reversible photocyclization of the ring-open isomer **3.21o** to generate the ring-closed **3.21c**. (b) Changes in the UV-vis absorption spectrum of an acetonitrile solution of the ring-open form of the Diels-Alder adduct **3.21o** upon irradiation with 312 nm light for 60 s, after which time no increase in the absorption band at 437 nm was observed. The dashed trace corresponds to the spectrum of the solution after irradiation with light of wavelengths greater than 434 nm for 30 min to induce ring-opening. Degradation is clearly taking place since the original spectrum is not fully regenerated.

Diels-Alder reactivity of the *bis*-phenylfulvene 3.18

The *bis*-phenylfulvene **3.18** also readily undergoes Diels-Alder cyclization with maleic anhydride. The reaction was found to reach >96% completion in 47 hours in acetone-d_6 at room temperature (Scheme 3.3.3) when monitored by ^{1}H NMR spectroscopy. The Diels-Alder adduct **3.23o** can be isolated by column chromatography and is thermally stable at 22 °C in acetone-d_6; the retro-cyclization reaction was not observed at this temperature.

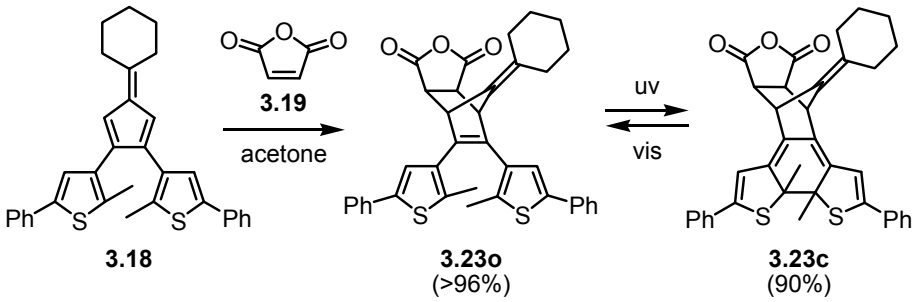

Scheme 3.3.3 Diels-Alder reaction between the *bis*-phenylfulvene **3.18** and maleic anhydride.

Photochromism of the Diels-Alder adducts 3.23

Irradiating an acetonitrile solution of compound **3.23o** with 312 nm light triggers a change in colour of the solution from colourless to pink, which is consistent with the formation of the ring-closed isomer **3.23c** having an extended π-conjugated backbone. The corresponding UV-vis absorption spectra (Figure 3.3.4b) show trends typically observed for ring-closing reactions of dithienylethene. The high-energy bands in the spectra become less intense as a broad band centered at 514 nm appears. As seen by UV-vis spectroscopy at a concentration of 1.7 x 10^{-5} M (in acetonitrile), a photostationary state (PSS) is reached within 15 seconds. As measured by ^{1}H NMR spectroscopy, irradiation of **3.23o** in acetone-d_6 (1 x 10^{-3} M) with 312 nm light affords the formation of 90% of the ring-closed isomer at PSS after 240 seconds. The ring-closed isomer is stable at room temperature. Irradiating the solution with visible light (wavelengths greater than 490 nm) regenerates the original UV-vis and ^{1}H NMR spectra corresponding to **3.23o**, indicating that the ring-opening reaction occurred. However, the photoswitchable adduct **3.23** shows low fatigue resistance to irradiation; after 10 cycles of alternating irradiation with 312 nm light and >490 nm light to toggle the compound

between its ring-open **3.23o** and ring-closed **3.23c** isomers, some degradation is apparent due to the slow decrease of absorbance of the sample as seen in Figure 3.3.4c.

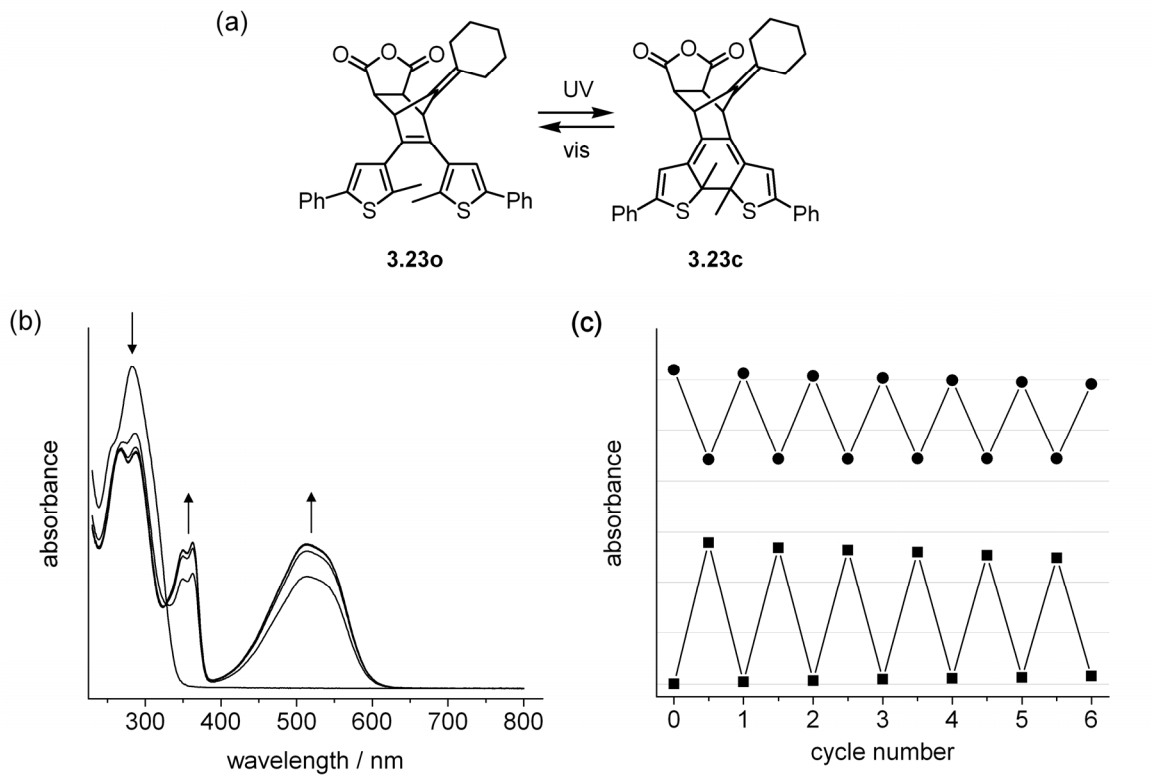

Figure 3.3.4 (a) Reversible photocyclization of the ring-open isomer **3.23o** to generate the ring-closed isomer **3.23c**. (b) Changes in the UV-vis absorption spectra of an acetonitrile solution (1.7×10^{-5} M) of **3.23o** upon irradiation with 312 nm until no further increase in the absorption band at 514 nm was observed at PSS. Total irradiation periods are 0, 5, 10, 15, 20 s. (c) Photochemical cycling study of the same acetonitrile solution of the Diels-Alder adduct between its ring-open form **3.23o** and its ring-closed form **3.23c**. The figure shows the changes in the absorptions at 280 nm (black circles) and 514 nm (black squares) during alternate irradiation at 312 nm for 15 s and at wavelengths greater than 490 nm for 5 min.

As discussed in Section 1.3.4 of the introductory chapter, various strategies could be used to increase the fatigue resistance of DTE derivatives. Decomposition of the photoswitch through oxidation could be prevented by using deoxygenated solutions[25] or by controlling the oxidation state of the sulphur atoms on the molecule.[28] Decomposition of the photoswitch through the formation of the two known non-

photochromic side-products could be prevented by tailoring the 4- and 4'-positions of the thiophene with functional groups, such as methyl units.[24,25] Attempts to improve the photostability of compound **3.23** were not pursued since the main goal of the project, development of a photorelease system, requires the molecule to be switched only once. Moreover, since the fragmentation reaction was not observed with this molecule at ambient temperature, it proved to be unsatisfactory for controlled release purposes, and no further studies were performed.

3.3.3 Thermally unstable Diels-Alder adducts of the fulvenes

The two novel fulvene derivatives presented in the previous section, **3.17** and **3.18**, show increased Diels-Alder reactivity compared to the dienes presented in *Chapter 2*. Although the Diels-Alder products formed using maleic anhydride or maleimide, and fulvenes are photochromic and are good models to characterise the photochemistry of the cycloaddition products, they are not suitable for photorelease applications since their cycloaddition reactions are not significantly reversible at room temperature. As discussed in Section 3.2.4, Lehn and co-workers uncovered a series of dicyanofumarate esters that established equilibrating mixtures of starting materials and products under mild conditions when mixed with various fulvene derivatives in organic media.[121] The use of these dienophiles in combination with the fulvenes **3.17** and **3.18** offers great potential for the development of reversible Diels-Alder equilibria at low temperature, leading to photorelease applications.

Equilibria between the *bis*-chlorofulvene 3.17 and diethyl dicyanofumarate

When a solution of *bis*-chlorofulvene **3.17** in dichloromethane-d_2 (1.8 x 10^{-2} M) was treated with 3.6 equivalents of diethyl dicyanofumarate **3.24** at 22 °C, a reaction was

immediately observed by ^{1}H NMR spectroscopy. As shown in Figure 3.3.5, the aromatic region of the spectrum of the *bis*-chlorofulvene **3.17** prior to the addition of diethyl dicyanofumarate contains a two-proton signal at 6.55 ppm (peak 'a') that can be attributed to the protons at the 4- and 4'-positions of the thienyl groups, and a two-proton singlet further upfield at 6.45 ppm (peak 'b') corresponding to the protons at the 1- and 4-position of the fulvene unit. Reaction of the fulvene **3.17** with diethyl dicyanofumarate **3.24** generates the Diels-Alder adduct **3.25** with two one-proton signals at 6.77 ppm and 7.02 ppm (peaks 'c' and 'd') that correspond to protons on the thienyl groups in **3.25**.

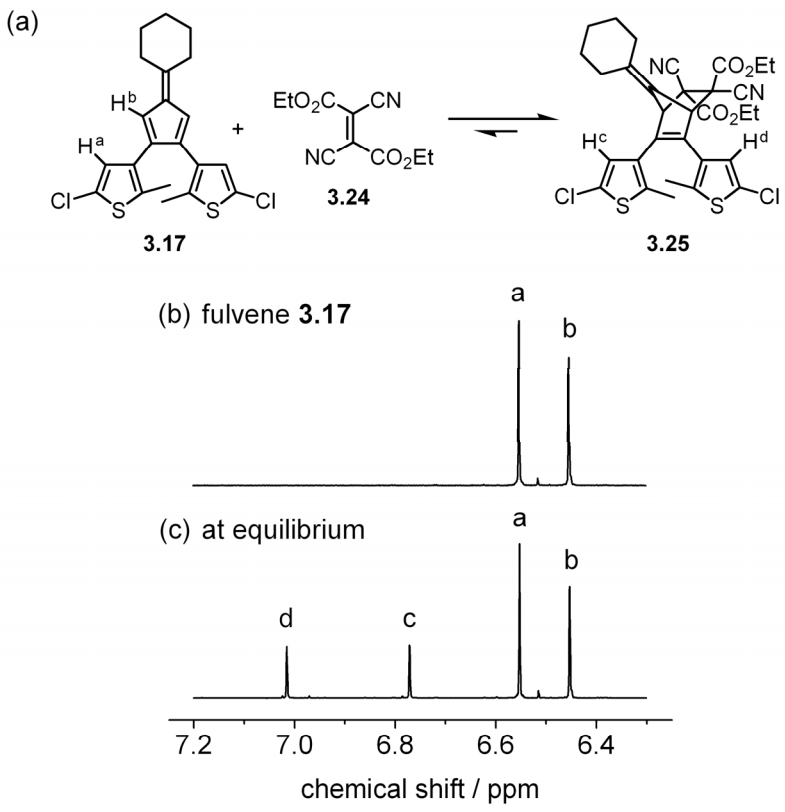

Figure 3.3.5 (a) Diels-Alder equilibrium between fulvene **3.17** and fumarate **3.24**, and adduct **3.25**. (b-c) Partial ^{1}H NMR spectra (500 MHz, dichloromethane-d_2) showing the aromatic region of a solution of the *bis*-chlorofulvene **3.17** (1.8×10^{-2} M) (b) before and (c) after the addition of 3.6 equivalents of diethyl dicyanofumarate **3.24**, once the system reached equilibrium.

The mole fraction of adduct **3.25** was obtained by integrating the areas under the peaks corresponding to signal 'a', 'c', and 'd', as shown in Equation 3.3.2. The value obtained is only an estimate since the T_1 values for the compounds were not determined. This study was carried out in the absence of an internal standard because the ^{1}H NMR spectrum showed no apparent signs of degradation of either the fulvene or the adduct even after 4 hours in solution.

$$\chi_{3.25} = \frac{c + d}{a + c + d}$$

Equation 3.3.2 Equation relating the mole fraction of the adduct **3.25** to the peak integrals 'a', 'c', and 'd'.

With the mole fraction of **3.25** in hand, it was possible to monitor the formation of the Diels-Alder adduct over time as the reaction proceeds and to observe that the mixture reaches equilibrium in approximately 20 minutes. Knowing the extent of the reaction at equilibrium and the initial concentration of the starting materials, it is possible to calculate the equilibrium constant $K_{\mathbf{3.25}}$ for the system using Equation 3.3.3.

$$K_{3.25} = \frac{[\text{adduct}]}{([\text{fulvene}]_o - [\text{adduct}])([\text{fumarate}]_o - [\text{adduct}])}$$

where

$$[\text{adduct}] = [\text{fulvene}]_o \times \chi_{3.25}$$

Equation 3.3.3 Equation relating the equilibrium constant K for the formation of the adduct **3.25** and the concentration of each component in solution, where [adduct] is the concentration of adduct at equilibrium, $[\text{fulvene}]_o$ and $[\text{fumarate}]_o$ are the initial concentration of fulvene **3.17** and fumarate **3.24** and $\chi_{3.25}$ is the mole fraction of adduct **3.25**.

The equilibrium constant $K_{3.25}$ is evaluated to be 13 M^{-1} in dichloromethane-d_2 and 36 M^{-1} in chloroform-*d*. In order to evaluate the effect of the thienyl groups at the 2- and 3-positions of the fulvene, the equilibrium constant of the parent fulvene **3.7** (Scheme 3.2.2) with diethyl dicyanofumarate was measured in chloroform-*d* at 22 °C using the same technique described above. In this case, a value of 72 M^{-1} was obtained.

These results indicate that the thienyl groups diminish the tendency of fulvenes to react with dienophiles. An increase in steric hindrance could explain this variation, as well as delocalisation of the electron density of the fulvene unit due to the presence of thienyl groups, making the compounds less reactive.

Equilibria between the *bis*-phenylfulvene 3.18 and diethyl dicyanofumarate

When a solution of the *bis*-phenylfulvene **3.18** in dichloromethane-d_2 (1.4×10^{-2} M) was treated with 4.2 equivalents of diethyl dicyanofumarate **3.24** at 22 °C, a reaction was immediately observed by ^{1}H NMR spectroscopy. As shown in Figure 3.3.6, the aromatic region of the spectrum of fulvene **3.18** prior to the addition of diethyl dicyanofumarate contains a two-proton signal at 6.92 ppm (peak 'a') that can be attributed to the protons at the 1- and 4-position of the fulvene unit and a two-proton singlet further upfield at 6.66 ppm (peak 'b') corresponding to the protons at the 4- and 4'-position of the thienyl groups. Reaction of the fulvene **3.18** with diethyl dicyanofumarate generated the Diels-Alder adduct **3.26** with two one-proton signals at 7.15 ppm and 7.49 ppm (peaks 'c' and 'd') that correspond to protons on the thienyl groups in **3.26**.

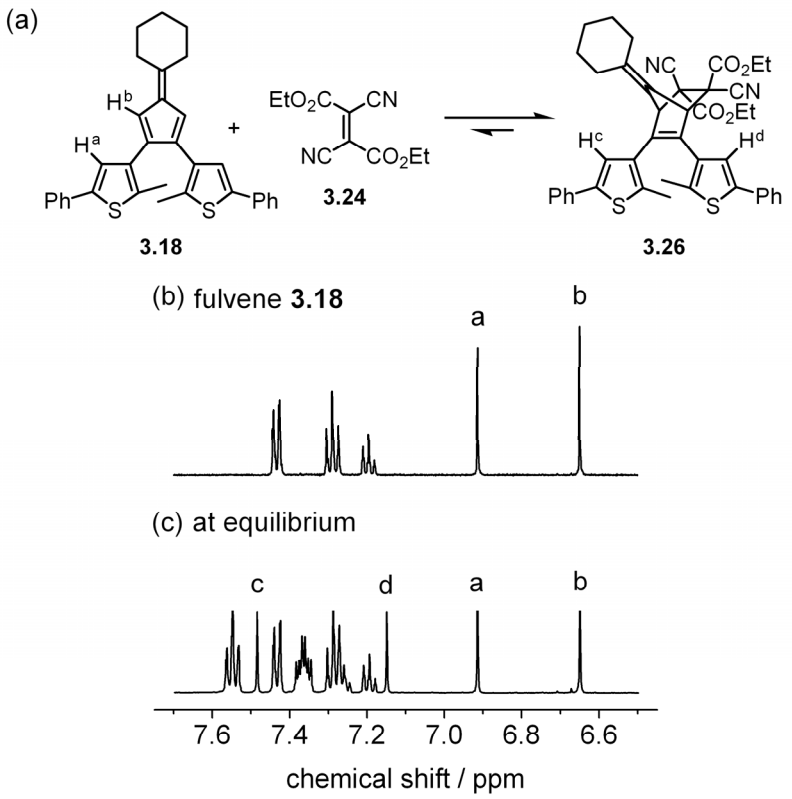

Figure 3.3.6 (a) Diels-Alder equilibrium between fulvene **3.18** and fumarate **3.24**, and adduct **3.26**. (b-c) Partial ^{1}H NMR spectra (500 MHz, dichloromethane-d_2) showing the aromatic region of a solution of the *bis*-phenylfulvene **3.18** (1.4 x 10^{-2} M) in dichloromethane-d_2 (b) before and (c) after the addition of 4.2 equivalents of diethyl dicyanofumarate **3.24**, once the system reached equilibrium.

As described previously, the mole fraction of adduct **3.26** was obtained by integrating the areas under the peaks corresponding to signal 'b', and 'c' and 'd' as shown in Equation 3.3.4. This study was carried out in the absence of an internal standard because the ^{1}H NMR spectrum showed no apparent signs of degradation of either the fulvene or the adduct even after 3.6 hours in solution.

$$\chi_{3.26} = \frac{c + d}{b + c + d}$$

Equation 3.3.4 Equation relating the mole fraction of the adduct **3.26** to the peak integrals 'b', c', and 'd'.

It was then possible to monitor the formation of the Diels-Alder adduct over time as the reaction proceeds and to observed that the mixture was already at equilibrium after 10 minutes. The equilibrium constant $K_{3.26}$ was calculated following the procedure described previously for adduct **3.25**, using Equation 3.3.3, and was found to be 22 M^{-1}. In comparison with the *bis*-chloro system **3.25**, which had an equilibrium constant of 13 M^{-1}, the equilibrium of the *bis*-phenyl system **3.26** favours the Diels-Alder adduct. Calculations at the AM1 level of theory show that the enthalpy of formation of the Diels-Alder adduct **3.26** is -5.5 kcal/mol whereas for the *bis*-chloro system **3.25**, the enthalpy of formation is -5.1 kcal/mol. Hence, as shown experimentally, the *bis*-phenyl adduct **3.26** has increased stability than the *bis*-chloro adduct **3.25**. Moreover, charge analysis on the 1- and 4-positions of the fulvenes, which are involved in the cycloaddition, shows more negative charge for the phenyl system than the chloro one. The fulvene moiety of **3.18** is thus more electron-rich and more reactive than the fulvene moiety of **3.17**.

Isolation of the ring-closed Diels-Alder adducts 3.27 and 3.28 – The concept

Irradiation of solutions containing the fulvenes **3.17** or **3.18**, and fumarate **3.24** with 312 nm light produces compounds that are thermally stable and can be isolated by column chromatography (Scheme 3.3.4). On the basis of ^{1}H NMR spectroscopy, these compounds were identified as the ring-closed forms **3.27** and **3.28**. As long as they are kept in the dark, both **3.27** and **3.28** can be stored with no observable degradation in solution and in the solid state at room temperature. It follows that the reverse cycloaddition reactions to regenerate the fulvenes **3.17** or **3.18** and the fumarate **3.24** can be prevented by locking the structures in their ring-closed, armed forms **3.27** and **3.28**.

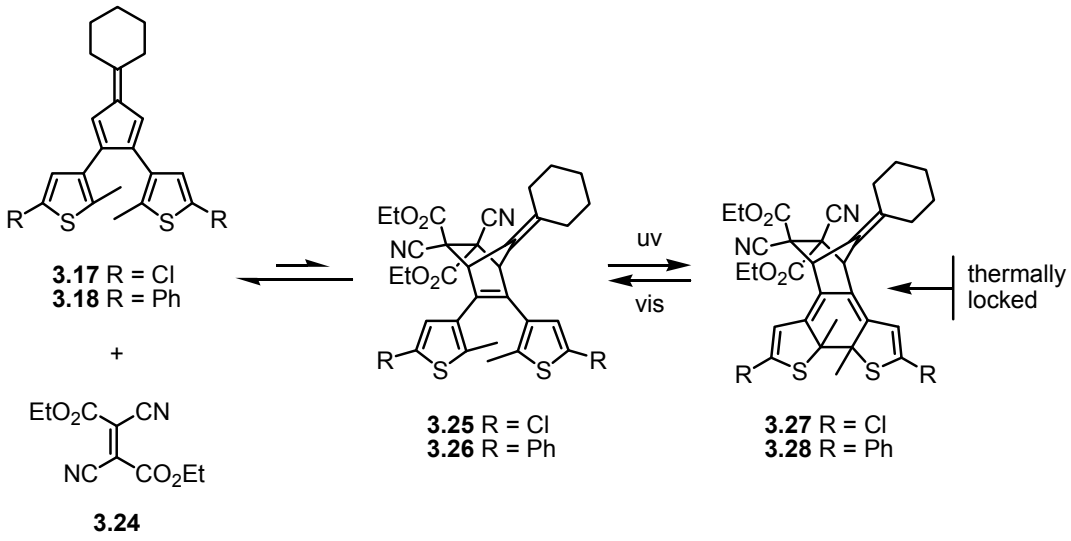

Scheme 3.3.4 Mixture of fulvenes **3.17** or **3.18**, and fumarate **3.24** are in equilibrium with their Diels-Alder adducts **3.25** or **3.26**, which are photoswitchable. The ring-closed Diels-Alder adducts **3.27** and **3.28** can be isolated since they are thermally stable and do not undergo retro-cycloadditions.

Isolation of the *bis*-chloro ring-closed Diels-Alder adducts 3.27

Irradiating an equilibrated dichloromethane-d_2 solution of the *bis*-chlorofulvene **3.17** (1.8×10^{-2} M) and fumarate **3.24** (3.8 equivalents) with 312 nm light triggers a change in colour of the solution from colourless to deep yellow, which is consistent with the formation of the ring-closed adduct **3.27** having an extended π-conjugated. The progress of the photochemical interconversion between the ring-open form **3.25** and the ring-closed form **3.27** of the Diels-Alder adduct was analysed by ^{1}H NMR spectroscopy (Figure 3.3.7). Upon irradiation, a new set of signals corresponding to the two diastereomers of **3.27** (internal methyl groups pointing up and down, or down and up) appear between 6.05 ppm and 6.10 ppm while the peaks corresponding to the ring-open form **3.25** decrease in intensity.

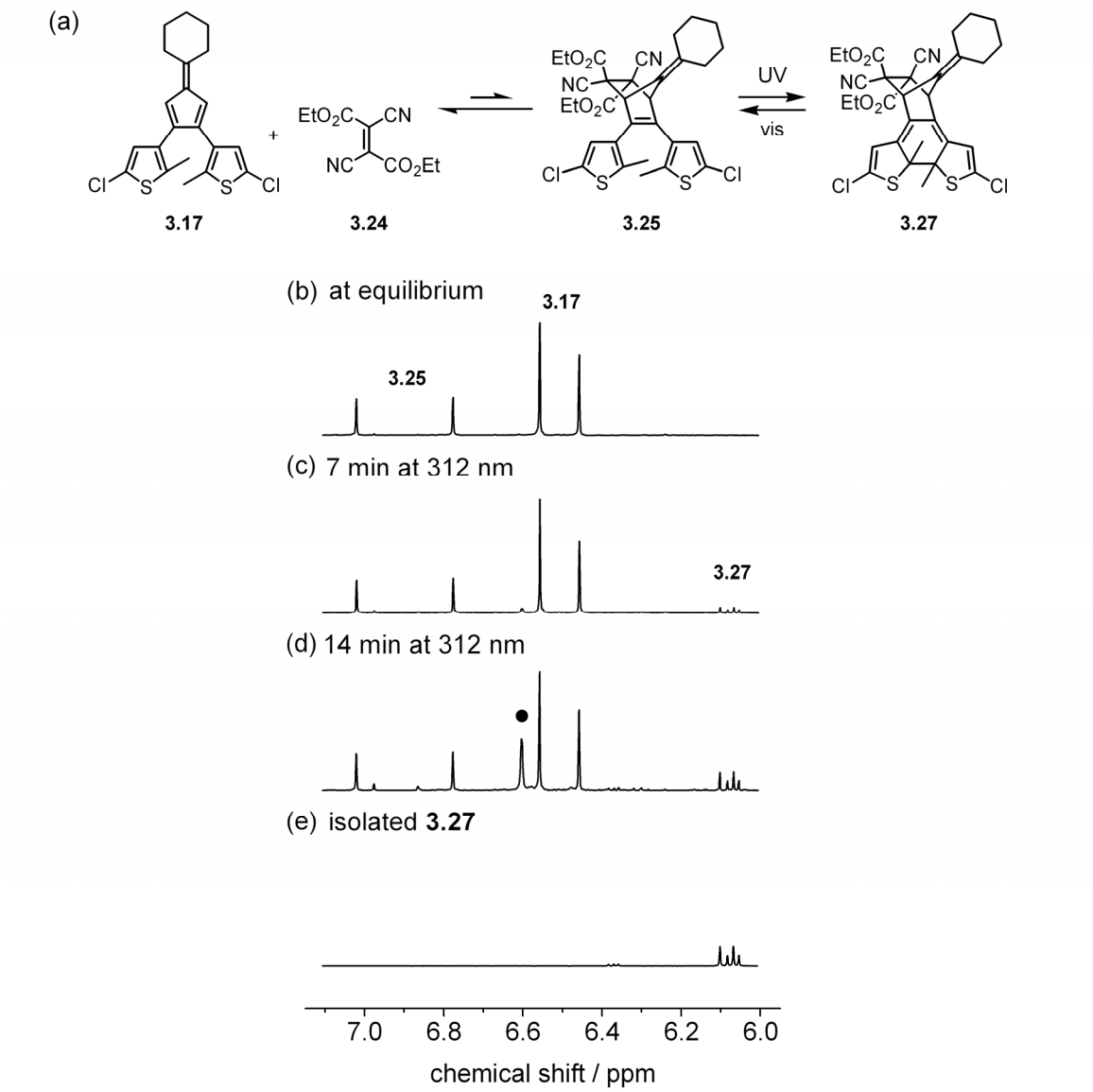

Figure 3.3.7 (a) Diels-Alder equilibrium between fulvene **3.17** and fumarate **3.24**, and adduct **3.25**, and the reversible photocyclization of the ring-open adduct **3.25** to form the ring-closed isomer **3.27**. (b-e) Partial ^{1}H NMR spectra (500 MHz, dichloromethane-d_2) showing the aromatic region of a solution of *bis*-chlorofulvene **3.17** and fumarate **3.24** in dichloromethane-d_2 (b) at equilibrium with the ring-open form **3.25**, after irradiation with 312 nm light for (c) 7 min and (d) 14 min, and (e) after isolation of the ring-closed compound **3.27** by column chromatography. The signal of the side product is identified by a back circle.

Furthermore, the signals corresponding to the *bis*-chlorofulvene **3.17** decrease in intensity, indicating that the Diels-Alder equilibrium is dynamic. As irradiation converts the adduct **3.25** into the ring-closed photoisomer **3.27**, it is removed from the initially

established equilibrium; after each irradiation period, the mixture equilibrates resulting in the formation of more adduct **3.25**. Thus, it is expected that a quantitative amount of ring-closed isomer **3.27** can be prepared using this methodology. However, as shown in Figure 3.3.7c, at least one side product with a signal at 6.60 ppm is formed during the irradiation.

Limited fatigue resistance had also been observed for the adduct **3.21** (Section 3.3.2) formed from the *bis*-chlorofulvene **3.17** and maleic anhydride **3.19**. Degradation can be reduced by limiting the irradiation time to 8 minutes (experimental details are presented in Section 3.5). Column chromatography followed by recrystallisation allows isolation of the ring-closed isomer **3.27**. As long as it is kept in the dark, compound **3.27** can be stored at room temperature with no observable degradation in solution or in the solid state. To prevent the ring-opening reaction during purification and during characterisation, it is necessary to handle the samples in the dark or with properly filtered lighting.

Isolation of the *bis*-phenyl ring-closed Diels-Alder adducts 3.28

Irradiating an equilibrated dichloromethane-d_2 solution of the *bis*-phenylfulvene **3.18** (6.8×10^{-3} M) and three equivalents of fumarate **3.24** with 312 nm light triggers a change in colour of the solution from colourless to deep purple, which is consistent with the formation of the ring-closed adduct **3.28** having extended π-conjugation.

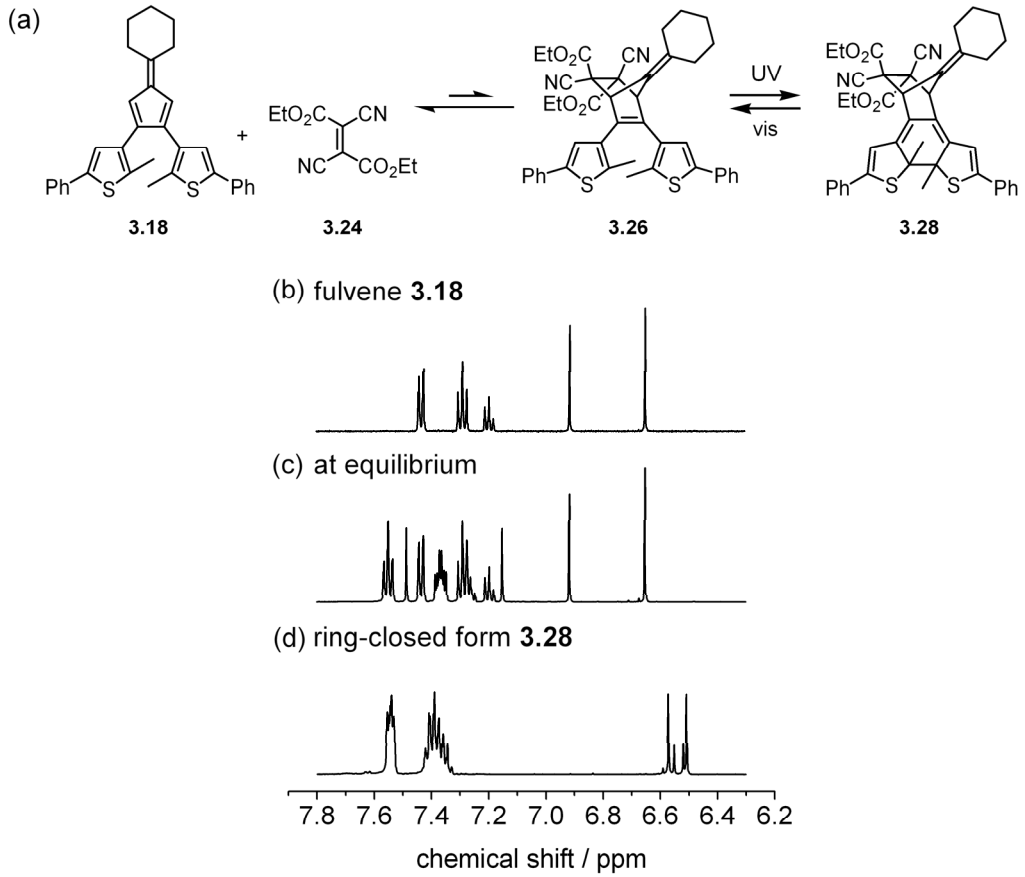

Figure 3.3.8 (a) Diels-Alder equilibrium between fulvene **3.18** and fumarate **3.24**, and adduct **3.26**, and the reversible photocyclization of the ring-open adduct **3.26** to form the ring-closed isomer **3.28**. (b-d) Partial ^{1}H NMR spectra (500 MHz, dichloromethane-d_2) showing the aromatic region of a solution of the *bis*-phenylfulvene **3.18** in dichloromethane-d_2 (b) before and (c) after the addition of 4.2 equivalents of diethyl dicyanofumarate **3.24** at equilibrium, and (d) of a solution of the pure ring-closed form **3.28**.

The progress of the photochemical interconversion between the ring-open form **3.26** and the ring-closed form **3.28** was monitored in the dark by thin layer chromatography. Irradiation was stopped after 15 minutes when the formation of a non-identified side product was apparent. Purification by column chromatography afforded compound **3.28** as a mixture of stereoisomers which were not separated. Figure 3.3.8 shows the partial ^{1}H NMR spectra of the reaction product. In order to avoid ring-

opening of compound **3.28**, the compound must be kept in absolute darkness. This is particularly critical during the purification step to optimise the isolated yield.

3.3.4 Photorelease using ring-closed Diels-Alder adducts

In the previous section, a novel strategy to control the reactivity of chemical species using the DTE architecture was presented. In their ring-open form, compounds **3.25** and **3.26** are at equilibrium with their building blocks as the thermal Diels-Alder and retro-Diels-Alder processes are both possibly allowed. However, after irradiation with ultra-violet light promoting ring-closure of the hexatriene portions of the photoswitches, the thermal retro-reaction cannot occur as the ring-closed photoisomers lack the required bond configuration. As long as they are kept in the dark, both **3.27** and **3.28** can be stored with no observable degradation in solution and in the solid state at room temperature.

It is then expected that irradiation of the solutions with light of the appropriate wavelengths in the visible range could trigger the ring-opening reactions and subsequent release of the dienophile.

Photorelease from the locked *bis*-phenyl adduct 3.28 – Monitored by UV-vis spectroscopy

The effect of exposing the locked compound **3.28** to visible light was monitored using UV-visible absorption spectroscopy. Dichloromethane solutions of the ring-closed *bis*-phenyl compound **3.28** are purple and show an absorption band in the visible region of the spectrum centred at 530 nm as seen in Figure 3.3.9.

Exposure of a dichloromethane solution of **3.28** (3.4×10^{-5} M) with light of wavelengths greater than 490 nm for 10 seconds causes a decrease in the absorption bands centred at 530 nm and 360 nm and an increase in the band at 262 nm and 293 nm

(Figure 3.3.9b-c). When the solution is kept in the dark for 10 minutes and another spectrum is recorded after this relaxation period, an increase in the bands in the ultra-violet portion of the spectrum is observed (Figure 3.3.9b). Hence, a thermally unstable species seems to be formed and to decay over time, presumably it is compound **3.26** which degrades to **3.18** and **3.24**. A subsequent 10 seconds irradiation with visible light of wavelengths greater than 490 nm causes the same decreases and increases in the absorption band recorded earlier and a relaxation time of 10 minutes allows the thermally unstable specie(s) to decay. Subsequent exposures to visible light (>490 nm), for up to 4 minutes, are accompanied by the complete disappearance of the absorption band in the visible region of the spectrum (Figure 3.3.9c). Once equilibrium was reached after the last exposure, the obtained spectrum overlaps very well with the added spectra of fulvene **3.18** and fumarate **3.24** (Figure 3.3.9d).

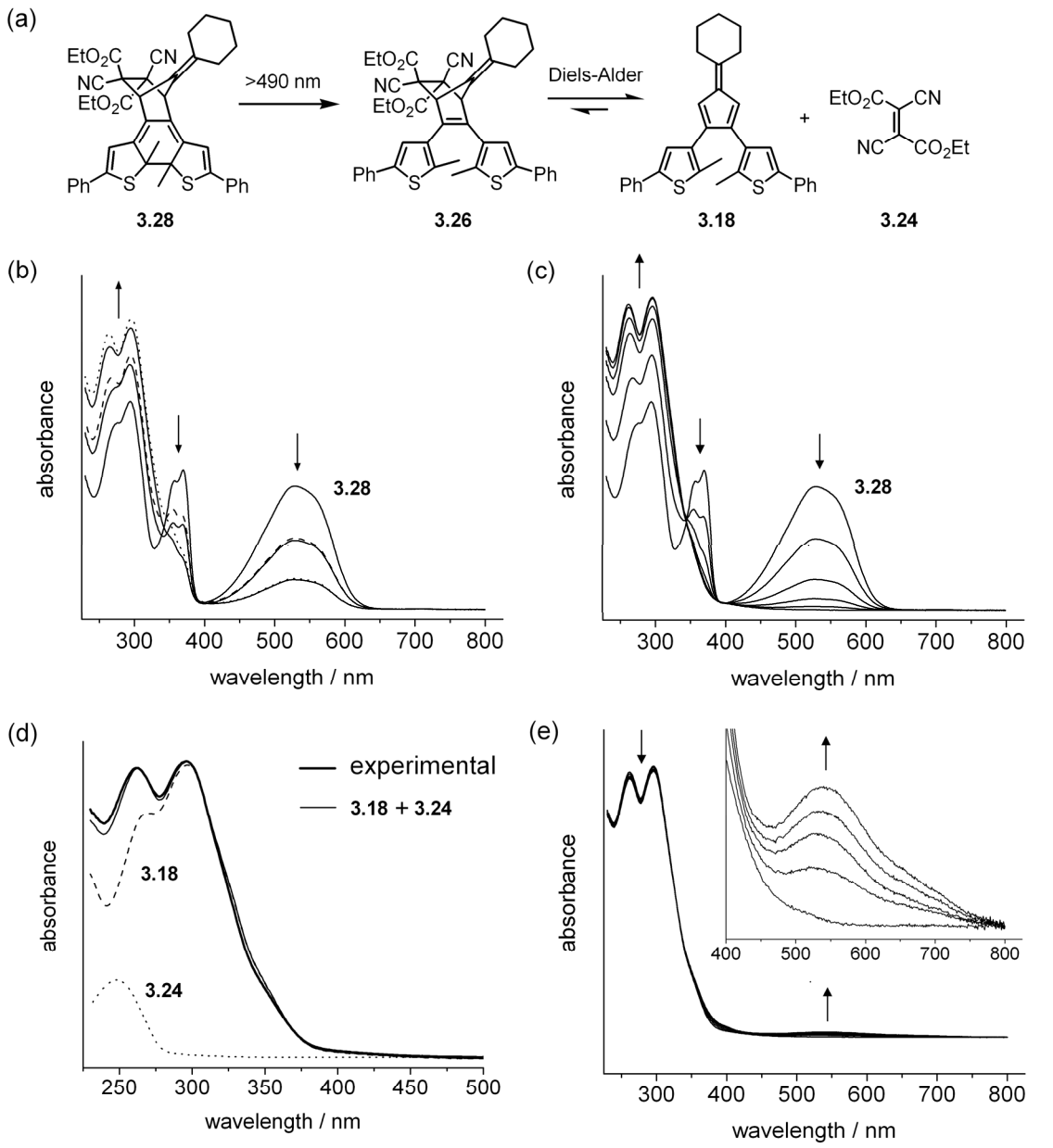

Figure 3.3.9 (a) Light-induced ring-opening reaction of **3.28** into **3.26** and its proposed fragmentation to form **3.18** and **3.24**. (b) Changes in the UV-vis absorption spectra of a dichloromethane solution (3.4 x 10^{-5} M) of **3.28** upon irradiation with light with wavelengths greater than 490 nm for 10 s (solid line), after 10 min in the dark (dashed line), after another 10 s irradiation (solid line), and after another 10 min in the dark (dotted line). (c) Changes in the UV-vis absorption spectra of a dichloromethane solution (3.4 x 10^{-5} M) of **3.28** upon irradiation with light with wavelengths greater than 490 nm for 10, 20, 30, 40 s, and 4 min. Each spectrum is acquired after a 10 min equilibration period in the dark. (d) UV-vis absorption of the fumarate **3.24** (dotted line), the *bis*-phenylfulvene **3.18** (dashed line), the sum of the individual spectra **3.24** + **3.18** (solid line), and the solution used above after irradiation for 4 min with light of wavelengths greater than 490 nm and 10 min in the dark (bold line). (e) Changes in the UV-vis absorption spectrum of the solution after the release experiment upon irradiation with 312 nm light for 5, 10, 15, and 20 s.

From these results, it can be concluded that exposure of **3.28** with visible light triggers the ring-opening reaction forming the ring-open isomer **3.26**, which is thermally unstable and decomposes into its constituents, the fulvene **3.18** and diethyl dicyanofumarate **3.24**, until equilibrium is reached. When the resulting solution is exposed to 312 nm light, a band of very weak intensity centred at 530 nm characteristic of compound **3.28**, appears, which suggests that the ring-open isomer does not fragment quantitatively (Figure 3.3.9e).

Photorelease from the locked *bis*-phenyl adduct 3.28 – Monitored by ^{1}H NMR spectroscopy

As shown in Figure 3.3.10, the aromatic region of the spectrum of the ring-closed isomer **3.28** in dichloromethane-d_2 (1.5 x 10^{-3} M) prior to exposure to visible light contains four one-proton signals between 6.51 ppm and 6.57 ppm that can be attributed to the protons at the 4 and 4'-position of the thienyl groups of both diastereomers. The signals between 7.30 ppm and 7.60 ppm are assigned to the aromatic protons on the phenyl groups and the region between 4.0 ppm and 4.5 ppm contains the signals attributed to the methylene protons on the esters and the bridge-head protons of the norbornene unit.

Exposure of the solution to visible light (>490 nm) generates the fulvene **3.18** with two two-proton signals at 6.66 and 6.92 ppm that correspond to the thienyl and fulvenyl protons respectively, and the fumarate **3.24** with a four-proton quartet centred at 4.47 ppm. Periodic irradiation up to 210 seconds triggers the ring-opening reaction and subsequent quantitative release of the dienophile as shown in Figure 3.3.10b-f.

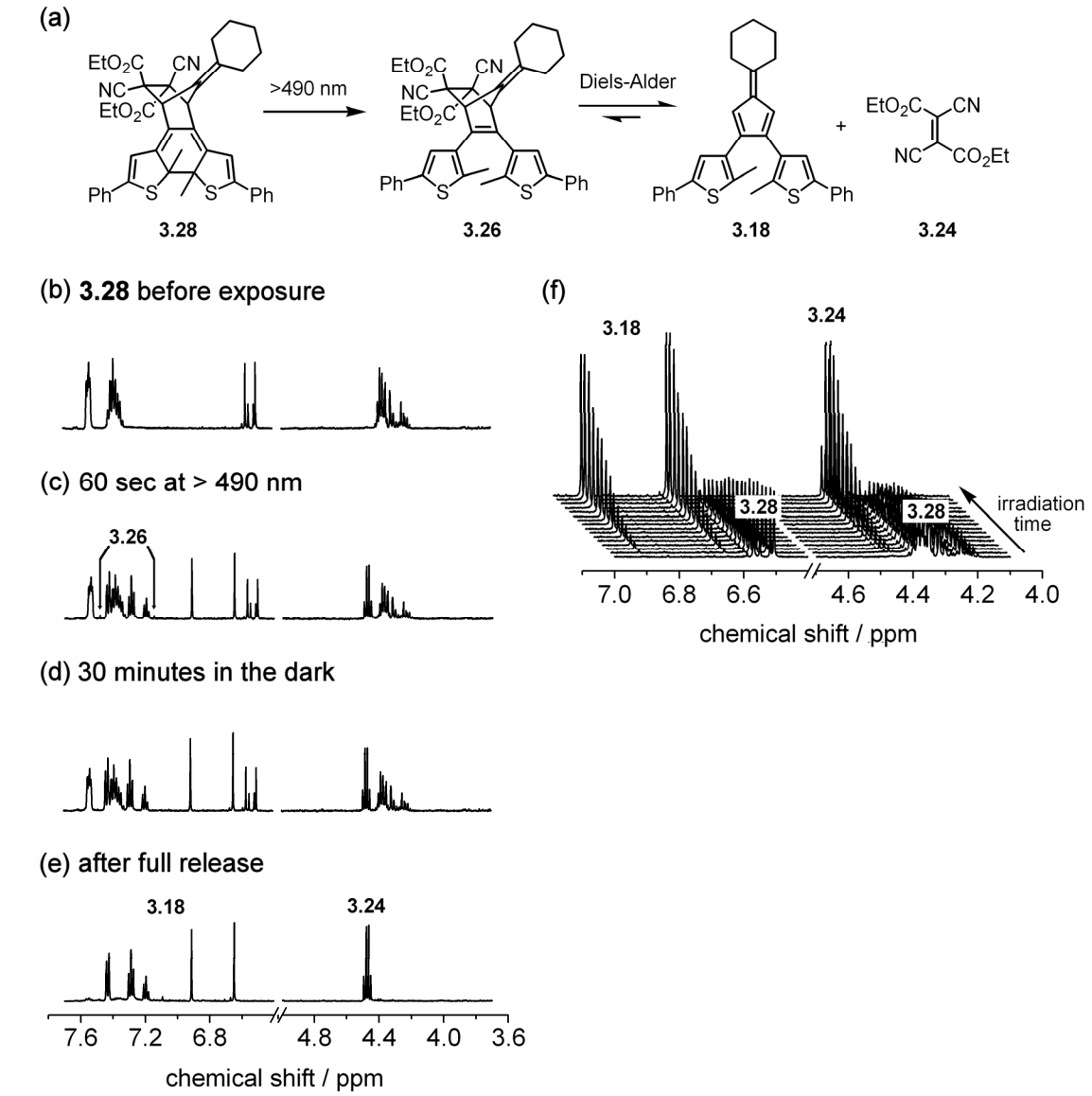

Figure 3.3.10 (a) Light-induced ring-opening reaction of **3.28** into **3.26** and its proposed fragmentation to form **3.18** and **3.24**. (b-f) Partial ^{1}H NMR spectra (500 MHz, dichloromethane-d_2) showing a solution of the ring-closed *bis*-phenyl compound **3.28** in dichloromethane-d_2 (b) before and (c) after 60 s of irradiation with light of wavelengths greater than 490 nm whereby two singlets assigned to the ring-open isomer **3.26** are indicated, (d) after 30 min in the dark (no visible singlets assigned to **3.26**), and (e) after 210 s of irradiation. (f) The spectra after each irradiation period up to 210 s.

Proposed mechanisms of release

So far, it was assumed that compound **3.28** would undergo a photochemical ring-opening reaction followed by a thermal fragmentation reaction when exposed to visible light, as shown in Figure 3.3.11. However, compound **3.28** could also undergo a photochemically allowed cycloreversion involving ten π-electrons. In this case, the fragmentation reaction would occur directly without the formation of the ring-open intermediate.

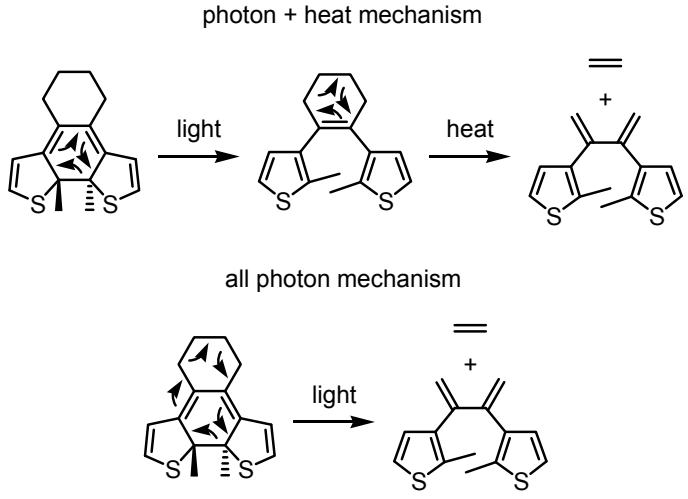

Figure 3.3.11 Proposed release mechanisms, whereby light triggers a ring-opening reaction followed by a thermal retro-cyclization (top), or light triggers a direct retro-cyclization (bottom).

UV-visible spectroscopy studies already showed that a thermally unstable species is formed during exposure to visible light (Figure 3.3.9b). Moreover, a careful analysis of the ^{1}H NMR spectrum after each irradiation period allows the observation of the signal for the thienyl protons of the ring-open isomer **3.26** at 7.16 ppm and 7.56 ppm. After 60 seconds of irradiation, a spectrum was acquired (Figure 3.3.10c) and the sample was subsequently stored in the dark for 30 minutes after which an ^{1}H NMR spectrum showed the disappearance of the signals due to the ring-open isomers (Figure 3.3.10d). These

results support the initially proposed mechanism of photochemical ring-opening followed by thermal fragmentation, but do not entirely rule out the photochemical mechanism.

In order to slow the fragmentation process during the irradiation and the data acquisition period, an ^{1}H NMR experiment was performed at 2 °C. A solution of ring-closed adduct **3.28** was irradiated for 50 seconds with visible light (wavelengths greater than 490 nm) in an ice bath at -10 °C followed by the acquisition at 2 °C of a series of NMR spectra over the next 20 minutes. The solution was irradiated for another 60 seconds a -10 °C followed by another series of acquisitions at 2 °C. As shown in Figure 3.3.12, two one-proton signals at 7.16 ppm and 7.56 ppm assigned to the ring-open isomer **3.26** are formed and slowly disappear over time as the signals attributed to the fulvene **3.18** appear, which corroborates the hypothesis of the photochemical six π-electrons ring-opening process preceding a thermal retro-Diels-Alder reaction. However, even if these results imply that thermal fragmentation is occurring, the direct photochemical fragmentation mechanism cannot be totally dismissed since even at 2 °C, some released product is detected during the first acquisition after irradiation. The absence of fulvene in the moment after irradiation would confirm the proposed two steps mechanism. The use of flash photolysis could provide the answer to this question.

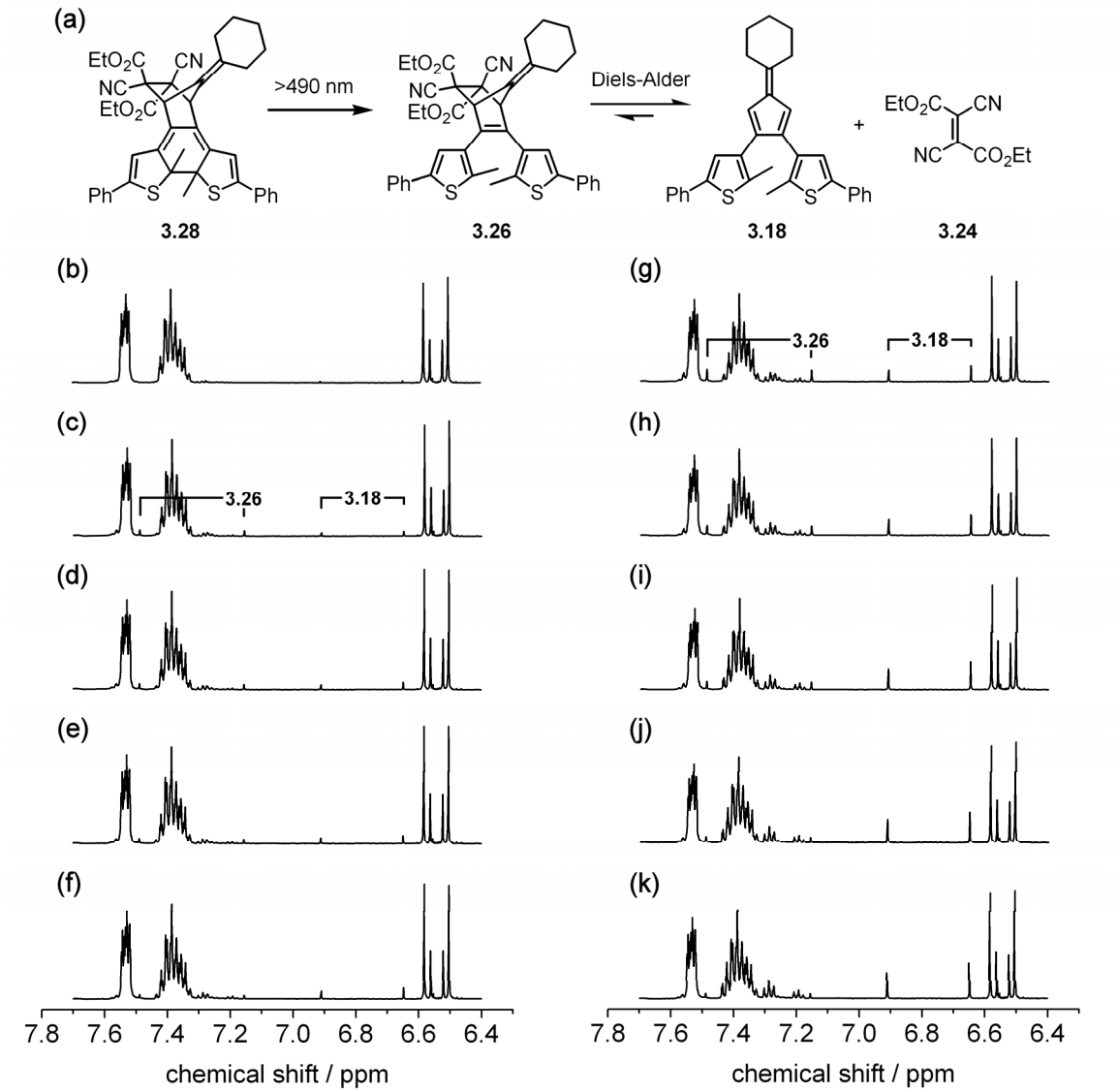

Figure 3.3.12 (a) Light-induced ring-opening reaction of **3.28** into **3.26** and its proposed fragmentation to form **3.18** and **3.24**. (b-k) Partial ^{1}H NMR spectra (500 MHz, dichloromethane-d_2) at 2 °C showing a solution of the ring-closed *bis*-phenyl compound **3.28** in dichloromethane-d_2 (b) before and (c) 3 min, (d) 8 min, (e) 12 min, and (f) 20 min after 50 s of irradiation with light of wavelengths greater than 490 nm at -10 °C, and (g) 2 min, (h) 8 min, (i) 15 min, (j) 25 min, and (k) 33 min after 110 s of irradiation with >490 nm light at -10 °C. At this temperature, the ring-open isomer **3.26** is observed and thermally decomposes into fulvene **3.18** and the fumarate **3.24**.

Photorelease from the locked *bis*-chloro adduct 3.27 – Monitored by UV-vis spectroscopy

Dichloromethane solutions of ring-closed *bis*-chloro adduct **3.27** are yellow and show an absorption band in the visible region of the spectrum centred at 455 nm (Figure 3.3.13). Exposure of a dichloromethane solution of **3.27** (2.5 x 10^{-5} M) to (430 ± 1) nm light using the source of a fluorimeter (details in Section 3.5.3) causes the complete disappearance of the visible band centred at 455 nm and the appearance of two new band in the ultra-violet range of the spectrum at 320 nm and 238 nm after 20 minutes.

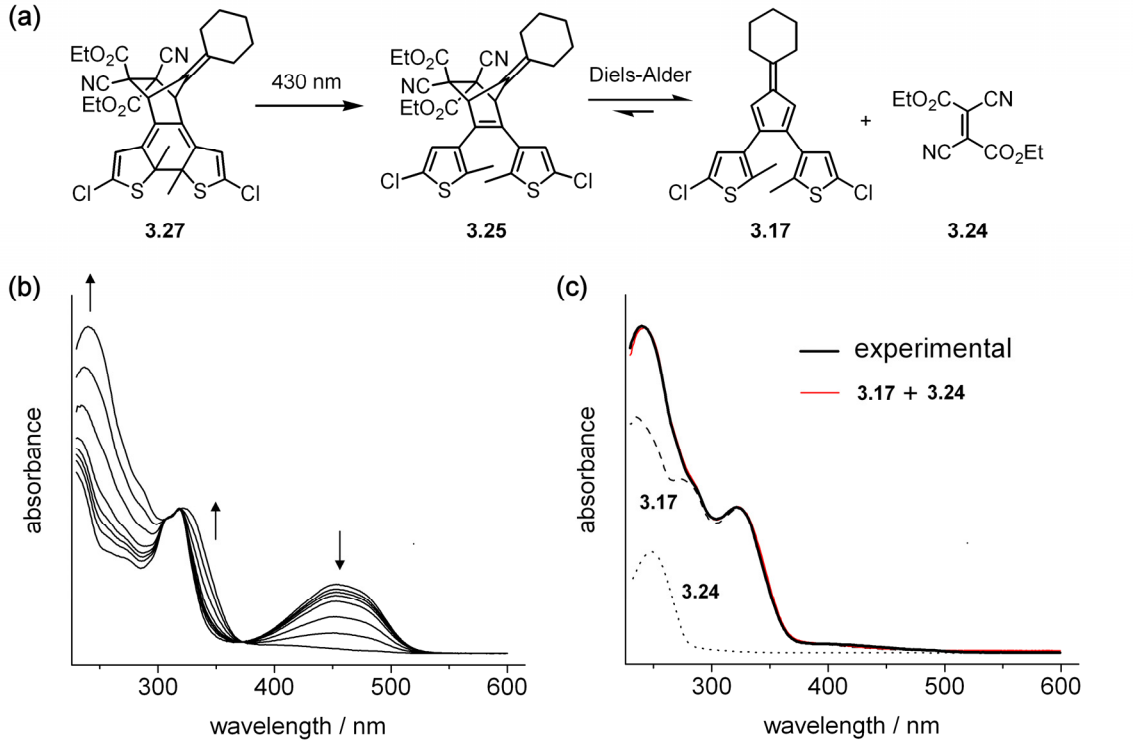

Figure 3.3.13 (a) Light-induced ring-opening reaction of **3.27** into **3.25** and its proposed fragmentation to form **3.17** and **3.24**. (b) Changes in the UV-vis absorption spectra of a dichloromethane solution (2.5 x 10^{-5} M) of **3.27** upon irradiation with 430 nm light for 30, 60, 90, 150, 330, and 630 s, and after 2 minutes irradiation with light of wavelengths greater than 434 nm. Each spectrum was acquired after a 15 min equilibration period in the dark. (c) UV-vis absorption of the fumarate **3.24** (dotted line), the *bis*-chlorofulvene **3.17** (dashed line), the sum of the individual spectra **3.24** + **3.17** (solid line), and of the solution after full bleaching (red line).

As was observed with the *bis*-phenyl compound **3.28**, irradiation of the *bis*-chloro system **3.27** with visible light generates an unstable specie(s) that decomposes thermally. It was apparent that in the case of the *bis*-chlorinated system, the thermal decomposition is much slower than in the case of the *bis*-phenyl system. Waiting periods of 15 minutes in the dark were required for the system to equilibrate after each irradiation. The superposition of the spectrum at equilibrium after complete bleaching with the normalised spectrum of the *bis*-chlorofulvene **3.17** and diethyl dicyanofumarate **3.24** supports the formation of these species (Figure 3.3.13c).

Photorelease from the locked *bis*-chloro adduct 3.27 – Monitored by ^{1}H NMR spectroscopy

As shown in Figure 3.3.14a, the aromatic region of the ring-closed isomer **3.27** in dichloromethane-d_2 (2.5 x 10^{-3} M) prior to exposure to visible light contains four one-proton signals between 6.05 ppm and 6.10 ppm that can be attributed to the protons at the 4 and 4'-position of the thienyl groups of both diastereomers. The small signals between 6.35 ppm and 6.38 ppm are assigned to an unidentified side-product stemming from the photochemical synthesis of **3.27**. The region between 4.0 ppm and 4.4 ppm contains the signals attributed to the methylene protons on the ester groups and the bridge-head proton of the norbornene unit.

Exposure of the solution to visible light of wavelengths greater than 434 nm generates the fulvene **3.17** with two one-proton signals at 6.55 ppm and 6.45 ppm that correspond to the thienyl and fulvenyl protons, respectively, and the fumarate **3.24** with a four-proton quartet centred at 4.47 ppm. Signals corresponding to the ring-open isomer **3.25** at 7.02 ppm and 6.77 ppm are also present after a 6 seconds exposure to visible light (Figure 3.3.14c). The fragmentation of compound **3.25** was monitored over a period of 15

minutes as the intensity of the signals assigned to the ring-open isomer decreased and the fulvene and fumarate signals increased (Figure 3.3.14c-f). Successive visible light exposures up to 60 seconds followed by 15 min equilibration periods allowed the completion of the ring-opening reaction of **3.27** (Figure 3.3.14g-h) and the entire release of the fulvene **3.17** and fumarate **3.24**.

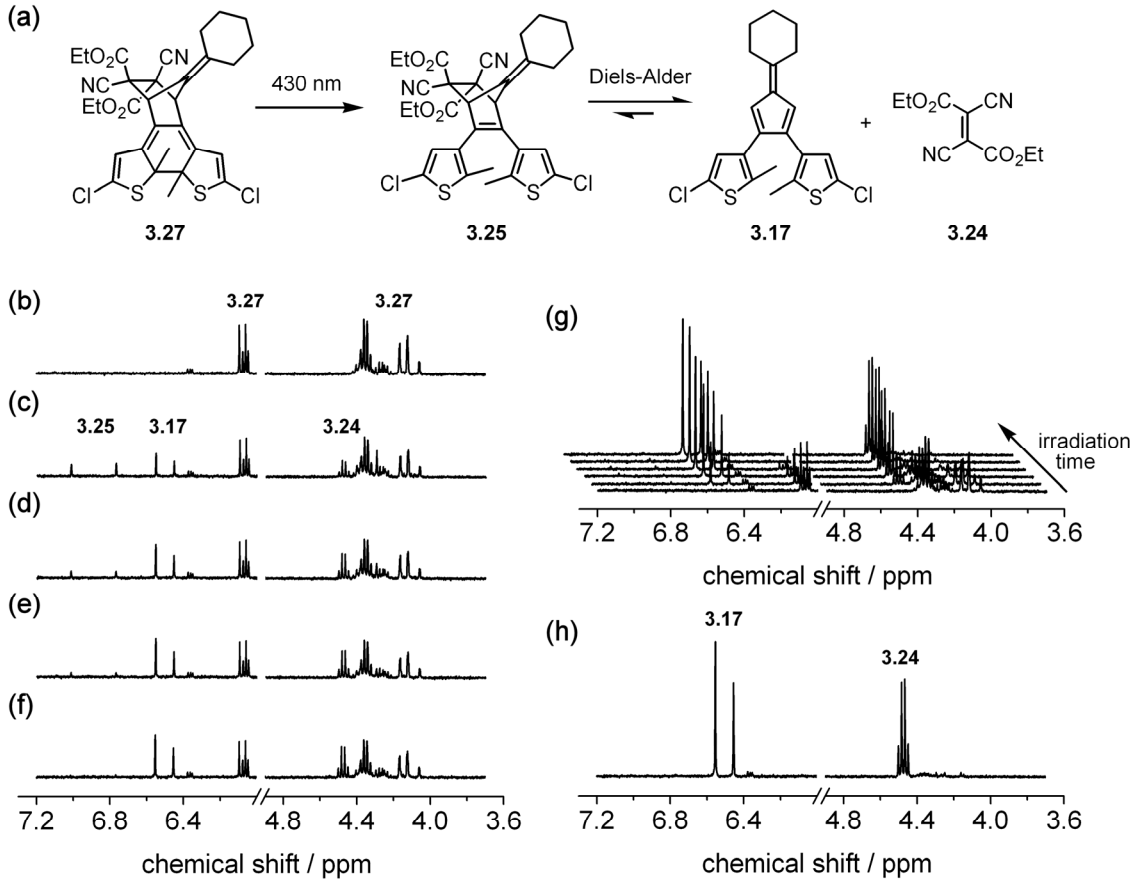

Figure 3.3.14 (a) Light-induced ring-opening reaction of **3.27** into **3.25** and its proposed fragmentation to form **3.17** and **3.24**. (b-h) Partial ^{1}H NMR spectra (500 MHz, dichloromethane-d_2) showing a solution of the ring-closed *bis*-chloro compound **3.27** (dichloromethane-d_2, 2.5 x 10^{-3} M) (b) before and (c) 3 min, (d) 5 min, (e) 10 min, and (f) 15 min after 6 s of irradiation with light of wavelengths greater than 434 nm. (g) Partial spectra showing the solution after 0, 6, 12, 22, 32, and 62 s irradiation with >434 nm light and 15 min in the dark. (h) Partial spectrum of the solution after complete release showing fulvene **3.17** and fumarate **3.24**.

3.3.5 Selective and sequential photorelease ring-closed Diels-Alder adducts

Proposed concept of selective and sequential photorelease

The optical and electronic properties of each photoisomer of DTE derivatives can be fine-tuned by rationally decorating the two heterocycles on the DTE backbone with appropriate substituents.[17-22] The most immediately striking property that can be photoregulated is the colour of the ring-closed form, which is easily adjusted by varying the length of the linearly π-conjugated pathway extending along the molecular backbone.[17-22] Thus, the adduct **3.27** having chlorine groups at the 5-positions of the thienyl rings is yellow, while the adduct **3.28**, which has phenyl groups at the same positions, is pink. Because compounds **3.27** and **3.28** have unique absorption characteristics in their ring-closed states, as shown in Figure 3.3.15, selective and sequential release should be possible by tuning the light source to trigger the ring-opening reaction of only one of the ring-closed compounds.

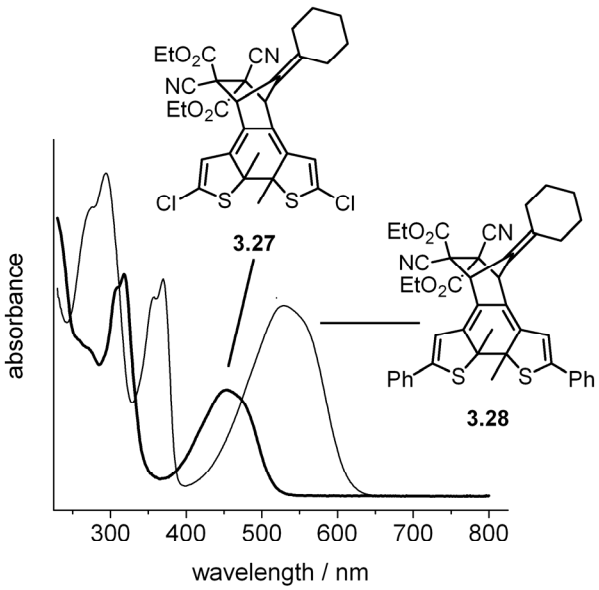

Figure 3.3.15 UV-vis spectra of **3.27** and **3.28** in dichloromethane.

Selective and sequential ring-opening of 3.27 and 3.28 – Monitored by UV-vis spectroscopy

The possibility to selectively trigger the ring-opening reaction of only one of the components, **3.27** or **3.28**, in the presence of the other was initially studied by UV-vis absorption spectroscopy. The bold trace in Figure 3.3.16a shows the UV-vis absorption profile of an equimolar mixture of compounds **3.27** and **3.28** in dichloromethane (1.0×10^{-5} M). The absorption bands centred at 455 nm, characteristic of the *bis*-chloro compound **3.27**, and centred at 360 nm and 530 nm, characteristic of *bis*-phenyl compound **3.28**, are clearly visible.

Irradiation for 10 minutes using the light from the source of a scanning fluorimeter with a 4 nm slit-width centred at 430 nm caused the absorbance band centred at 455 nm due to compound **3.27** to decrease, as seen in Figure 3.3.16a. This is consistent with selective ring-opening of the *bis*-chloro compound **3.27**. Subsequent irradiation of the solution with light of wavelengths greater than 557 nm for 12 minutes using a white light source equipped with a cut-off filter to eliminate higher energy light caused the complete disappearance of the characteristic absorbance of the *bis*-phenyl compound **3.28**, after which only the absorbance band from the residual *bis*-chloro compound **3.27** was observed. This is consistent with ring-opening of the *bis*-phenyl derivative **3.28**. Further irradiation with light of wavelengths greater than 434 nm caused the complete disappearance of the absorption bands in the visible region of the spectrum, indicating that complete ring-opening of the residual component had occurred.

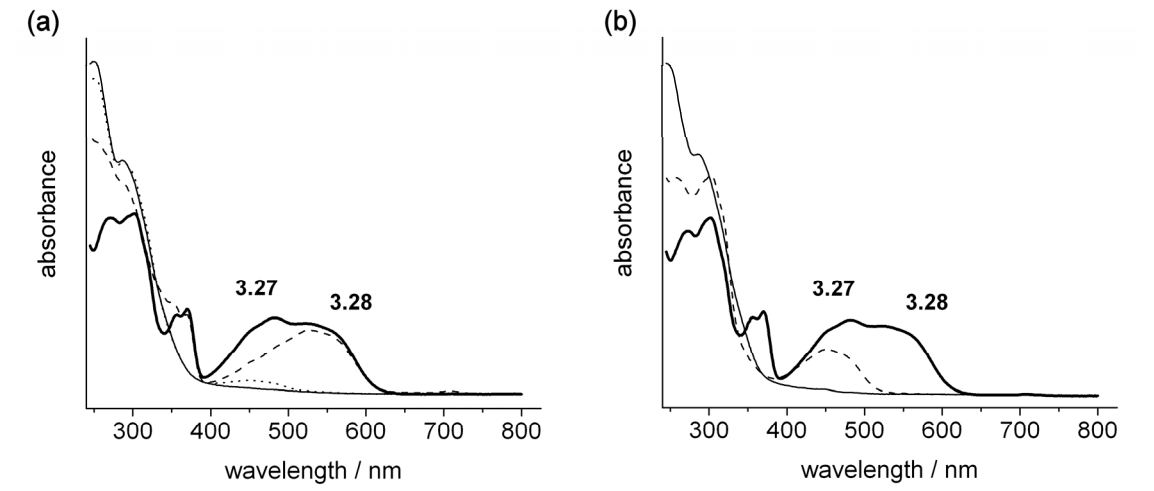

Figure 3.3.16 Selective ring-opening monitored by UV-vis absorption spectroscopy. (a) The *bis*-chloro system **3.27** is ring-opened first. A 1:1 mixture of **3.27** and **3.28** in dichloromethane (1.0 x 10^{-5} M) (bold line) is irradiated with 430 nm light for 10 min (dashed line) and then for 12 min with >557 nm light (dotted line). Finally, the solution is fully bleached using >434 nm light for 4 min (solid line). (b) The *bis*-phenyl system **3.28** is ring-opened first. A 1:1 mixture of **3.27** and **3.28** in dichloromethane (1.0 x 10^{-5} M) (bold line) is irradiated with >557 nm light for 12 min (dashed line) and then for 4 min with >434 nm light (solid line). Equilibration periods in the dark between 5 and 15 min were allowed before each acquisition for (a) and (b).

In the previous experiment, the results suggest that the *bis*-chloro compound **3.27** was ring-opened prior to the *bis*-phenyl derivative **3.28**. In order to demonstrate the versatility of the approach, it was interesting to show that the ring-opening reaction of the *bis*-phenyl compound **3.28** can be triggered first. A portion of the same equimolar stock solution used previously (1.0 x 10^{-5} M of each component in dichloromethane) was irradiated for 12 minutes with visible light of wavelengths greater than 557 nm causing the complete disappearance of the lowest energy band centred at 530 nm attributed to compound **3.28**, indicating the complete ring-opening of the compound. The *bis*-chloro compound **3.27**, which does not absorb >557 nm light, was the only absorbing species left in the visible region. Subsequent irradiation with light of wavelength greater than 434

nm caused complete bleaching of the solution. The results of this experiment are presented in Figure 3.3.16b.

Selective and sequential release of 3.27 and 3.28 – Monitored by ^{1}H NMR spectroscopy

Monitoring of the disappearance of the ring-closed isomers **3.28** and **3.27** is possible using UV-vis absorption spectroscopy. However, this technique does not provide an easy means to observe the formation of the cleaved products since the absorbance bands of fulvenes **3.17** and **3.18**, and fumarate **3.25** overlap in the UV region of the spectrum. As shown for the individual release experiments of **3.27** and **3.28**, ^{1}H NMR spectroscopy is an efficient technique to monitor the decay of the ring-closed isomers and the formation of the released products.

An ^{1}H NMR spectrum of an equimolar solution of **3.27** and **3.28** (1.9×10^{-3} M) in dichloromethane-d_2 was acquired. As shown in Figure 3.3.17a, a selected region of the spectrum contains the four one-proton signals attributed to the protons at the 4 and 4'-position of the thienyl groups of both diastereomers of the ring-closed form of the *bis*-phenyl compound **3.28**, as well as those attributed to the same protons on the *bis*-chloro compound **3.27**. Irradiation for 21 minutes with light of $\lambda = (430 \pm 2)$ nm caused the appearance of two characteristic signals at 6.45 ppm and 6.55 ppm of *bis*-chlorofulvene **3.17** (Figure 3.3.17b), which is indicative of the selective ring-opening reaction of the *bis*-chloro compound **3.27**, leading to the release of fumarate **3.24** and the generation of the *bis*-chloro fulvene **3.17**. Subsequent irradiation with light of wavelengths greater that 557 nm caused the signals attributed to the *bis*-phenyl compound **3.28** to decrease in intensity and caused the appearance of the two one-proton signals at 6.65 ppm and 6.91 ppm attributed to the *bis*-phenyl fulvene **3.18** (Figure 3.3.17c). When this low energy

light is used, no change in the intensity of the signal attributed to the *bis*-chloro system is recorded. Irradiation of the solution with light of wavelengths greater than 434 nm for 3 minutes caused the complete disappearance of the signals attributed to **3.27** and **3.28** (Figure 3.3.17c), indicating that both underwent ring-opening and fragmentation.

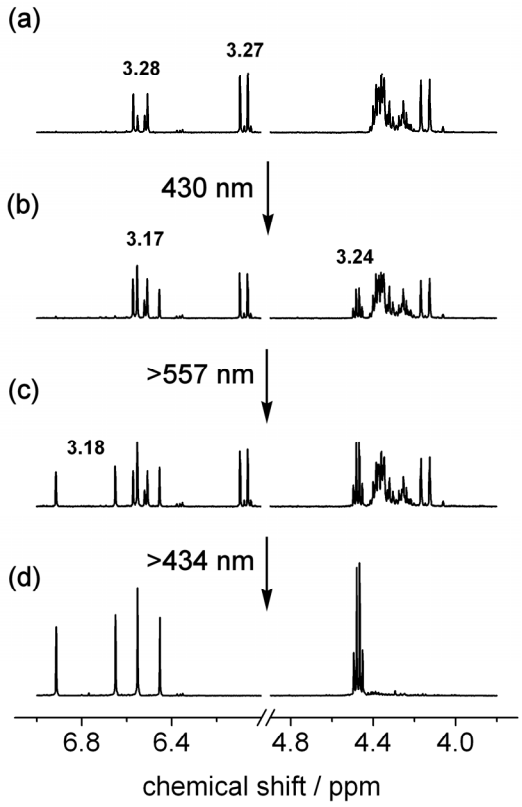

Figure 3.3.17 Selective and sequential release monitored by ^{1}H NMR spectroscopy showing partial spectra (500 MHz, dichloromethane-d_2) of (a) a 1:1 mixture of **3.27** and **3.28**, (b) after irradiating the solution with 430 nm light to partially ring-open compound **3.27**, (c) after irradiating the same sample with light of wavelengths >557 nm to partially ring-open compound **3.28**, and (d) after irradiating the same sample with >434 nm light to fully ring-open both compounds.

3.4 Conclusion and perspectives

3.4.1 General conclusions

In summary, a new approach to deliver chemical species based on combining reactivity-gated photochemistry and photogated reactivity was presented. Adducts containing the photoresponsive DTE architecture were prepared using the reversible Diels-Alder reaction between fulvene derivatives and diethyl dicyanofumarate. Irradiation with light in the UV range effectively prevents the reverse reaction since the ring-closed isomers lack the cyclohexene moiety required for the fragmentation reaction. Exposure of the "locked" compounds to visible light triggers the ring-opening reactions and leads to the release of the dienophile. The use of this low energy light has the dual advantages of limiting biological damage and increasing penetration depth in biological tissues.

The use of the DTE architecture provides an easy means to select the energy of light needed for the release event and thus allows selective and sequential photorelease. In addition, the DTE substructure will facilitate the monitoring of the release events by monitoring a wide range of physical properties, such as the absorbance or emission of light, or electrochemical properties, which are unique to the armed and released systems.

The economical size and chemistry of the fumarate auxiliary implies that it could be modified with various chemical species without significantly interfering with the role of the component of interest, thus offering great potential for practical applications.

3.4.2 Advances towards photodelivery applications

In order to develop practical photodelivery applications, two main requirements are proposed. (1) The system must allow the release of "useful" moieties such as therapeutics. (2) The release must take place from a solid support[134] so that only the molecule of interest is released in order to diminish side effects caused by the photorelease by-product, namely the fulvene.

Tailoring of the fumarate with molecules of interest

The ester moieties of the fumarate unit can be tailored with various functional groups by condensing the appropriate cyano esters in the presence of thionyl chloride.[121,135] A chlorinated version of dicyanofumarate was recently prepared in the Branda group following the procedure outlined in Equation 3.4.1.[136] This versatile molecule could then be post-functionalised to obtain a wide variety of derivatives with components of interest.

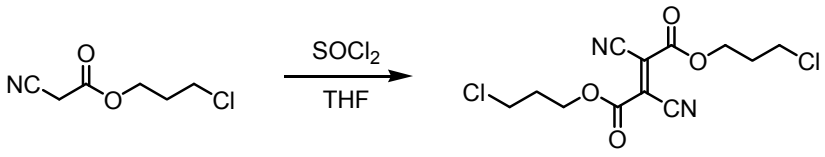

Equation 3.4.1 Preparation of a chlorinated dicyanofumarate.

Another versatile dicyanofumarate intermediate is depicted in Equation 3.4.2. In this case, the allyl moiety could be coupled via olefin metathesis to a variety of biologically relevant molecules such as cyclosporine A, which is a potent immunosuppressant used to reduce the activity of the patient's immune system and therefore reduce the risk of organ rejection after organ transplantations.[137] Olefin

metathesis was recently used to couple cyclosporine A to various resins without affecting the activity of the drug.[138]

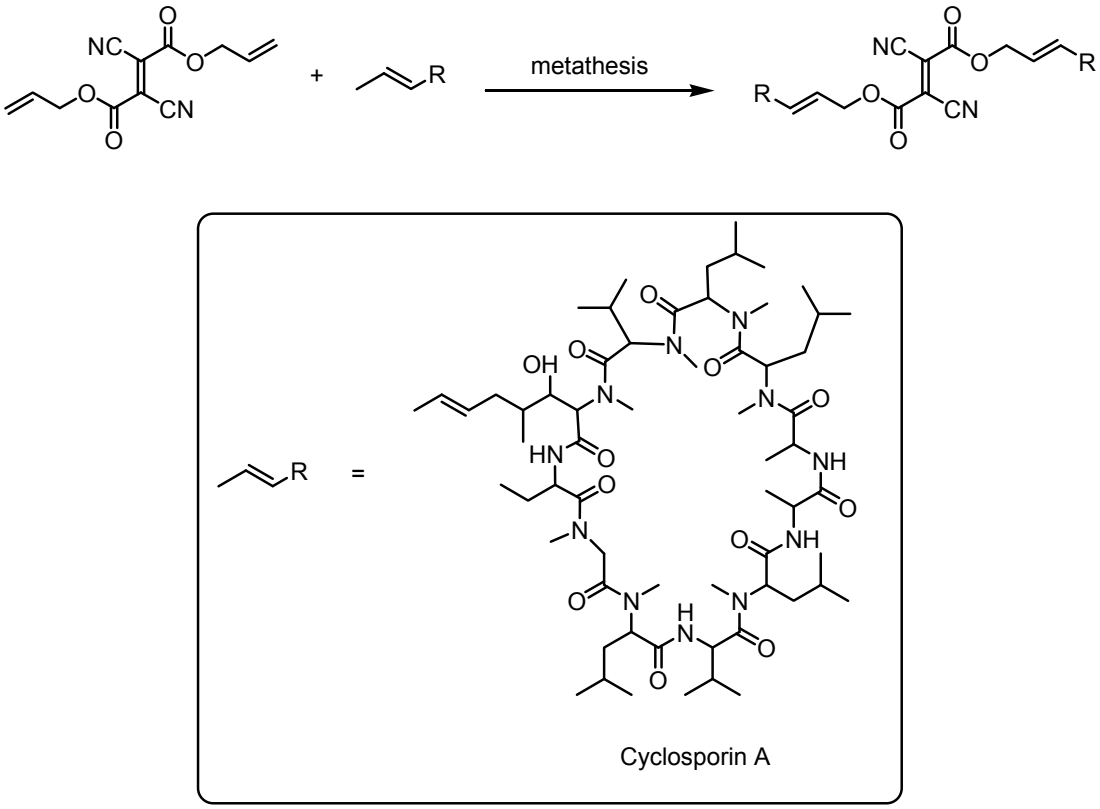

Equation 3.4.2 Proposed synthesis of a dicyanofumarate tethered with cyclosporine A.

In their studies of dynamic Diels-Alder reactions between fulvenes and electron-deficient dienophiles, Lehn and co-workers also reported the use of tricyanoethene derivatives.[121] As illustrated in Figure 3.4.1, such molecules could also be functionalised. However, this class of dienophile is more reactive and establishes Diels-Alder equilibria strongly favouring the adduct formation, limiting their use as photorelease systems.

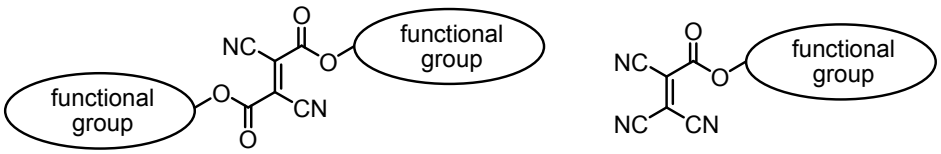

Figure 3.4.1 Functional di- and tricyanoethenes.

Solid support

Two different strategies are envisioned for the development of solid supported fulvenes: (1) direct tethering of the fulvene on the surface of a resin or a particle, or (2) preparation of a monomeric fulvene that can then be polymerised.

The direct attachment of a fulvene unit to a solid support could be achieved in two ways (Figure 3.4.2). Firstly, an appropriately modified fulvene could be coupled to a surface. This strategy implicates the development of a fulvene tolerant to the functionalisation procedure and coupling method, which can be difficult because of the reactivity of fulvenes. However, the formation of a reversible Diels-Alder adduct, which is then locked photochemically, could offer an effective technique to protect the fulvene during its functionalisation. Secondly, the fulvene unit could be synthesised directly on a ketone- or aldehyde-tethered surface using the Stone and Little procedure described in Section 3.3.1.[133] Both methods have the advantage that the supporting material before modification is well characterised. However, characterisation of the fulvene could be more complicated and side reactions could occur during the attachment of the fulvenes on the surface.

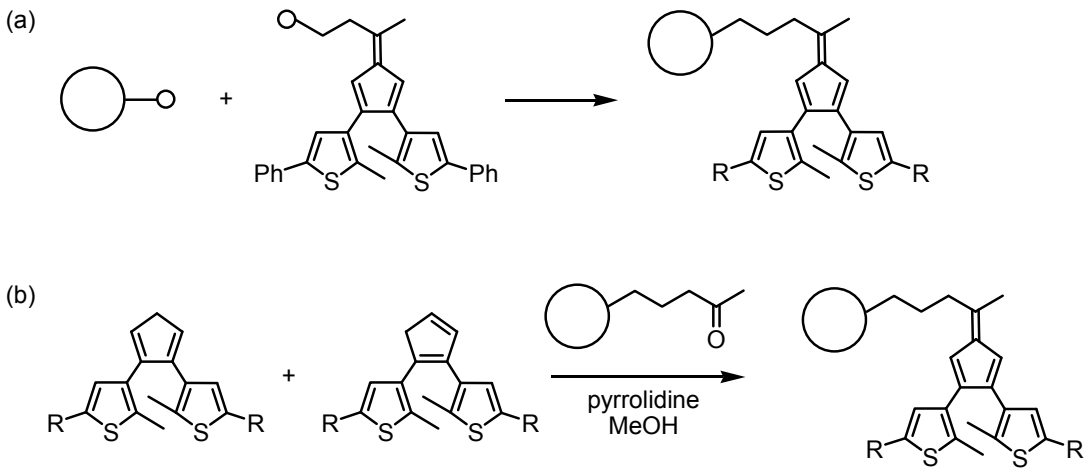

Figure 3.4.2 Two possible methods to functionalise surfaces with fulvene units: (a) direct tethering where the surface and the fulvene have adequate functional groups, or (b) direct synthesis of the fulvene on the surface using the Stone and Little procedure.[133]

Preliminary studies were conducted in order to determine whether Diels-Alder adducts could be photoresponsive on surfaces. Fulvenes **3.17** and **3.18** were dissolved in solutions containing maleimide-functionalised silica gel kindly donated by Silicycle Inc. (Equation 3.4.3). After 1 hour the silica particles were exposed to 312 nm light. The silica that reacted with *bis*-chlorofulvene **3.17** turned yellow and the silica that was exposed to *bis*-phenylfulvene **3.18** turned pink which is indicative that the Diels-Alder reaction occurred effectively and that the bound switches are photochromic.

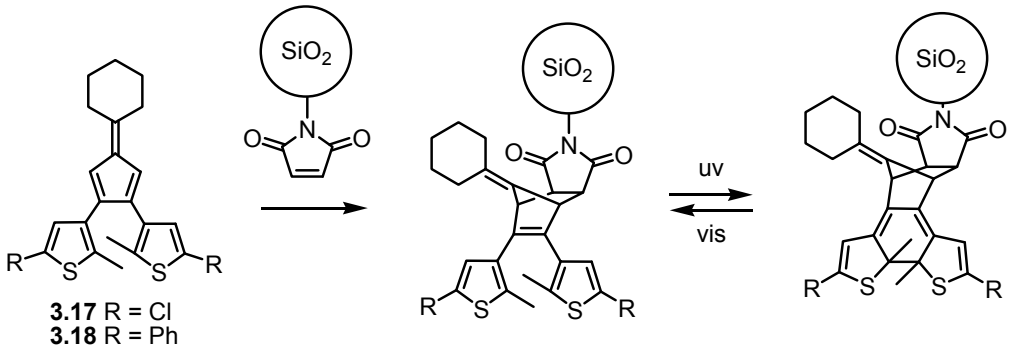

Equation 3.4.3 Reaction of a fulvene with maleimide-functionalised silica.

The second strategy for the preparation of supported fulvenes involves the preparation of fulvene monomers and their polymerisation. This method allows the complete characterisation of the monomer, and a careful selection of the polymerisation reaction could allow the preparation of a material with good structural integrity. Preliminary studies were conducted to demonstrate the validity of this approach.

Fulvene **3.30** was prepared according to the synthetic route outlined in Scheme 3.4.1. The percentage yield (39%) of the coupling reaction between the mixture of cyclopentadienes and ketone **3.29** (prepared using a literature procedure)[139] was greatly improved as compared to the synthesis of fulvene **3.17** and **3.18**. Compound **3.30** combines a fulvene unit and a norbornene group. Norbornene units are commonly used in ring-opening metathesis polymerisation.

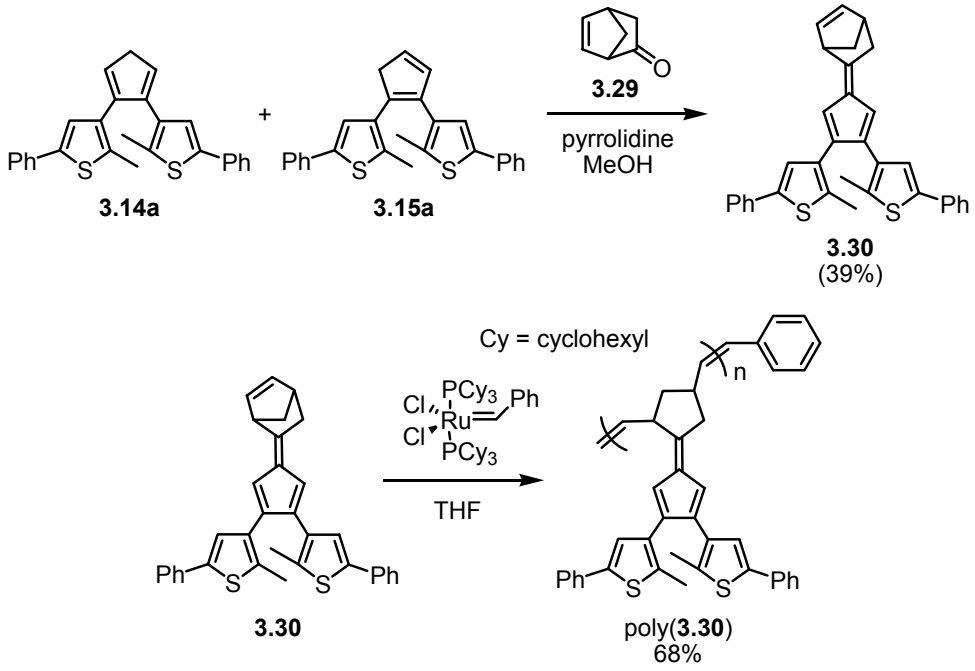

Scheme 3.4.1 Synthesis of monomer **3.30** and its polymerisation via ring-opening metathesis polymerisation.

As shown in Scheme 3.4.1, the addition of the appropriate ruthenium catalyst to solutions of **3.30** yielded polymer poly(**3.30**) where the number of units (n) is between 20 and 30 as determined by gel permeation chromatography. Treatment of poly(**3.30**) with fumarate **3.25** resulted in the formation of a photochromic material. Exposure of the polymers (in solution or in thin films) to 312 nm light induced a colour change from yellow to purple. Subsequent exposure of the polymers to visible light (>434 nm) induced the reverse colour change. The photorelease properties of poly(**3.30**) systems are currently under investigation.

3.4.3 Advances towards novel functional materials (cross-linked polymers)

So far, the systems presented in this chapter were only proposed for controlled release applications, but other uses can be envisioned, notably in the field of polymers. Polymers are very useful materials but have a finite lifetime.[108] Over time, their inherent properties degrade through the accumulation of stress and strain defects. Adhesives provide a means of mending materials at the macroscopic level. However, the cracking of a material starts at the microscopic level. Reversible polymerisation processes enable mending of polymers at the molecular scale and allow full restoration of their original properties, whereas mending at the macroscopic level with adhesives does not restore the original properties of the materials.[108]

The thermal reversibility of the Diels-Alder reaction has been exploited to prepare re-mendable polymers.[108] For example, multifunctional furan- and maleimide-based monomers were used to form highly cross-linked materials (Figure 3.4.3).[140] When a *bis*-maleimide (**3.31**) and a tetra-furan (**3.32**) are allowed to react, a clear solid is

obtained. This material exhibits crack-healing properties when submitted to a heating and cooling cycle after which 83% of the polymer's original strength is recovered.

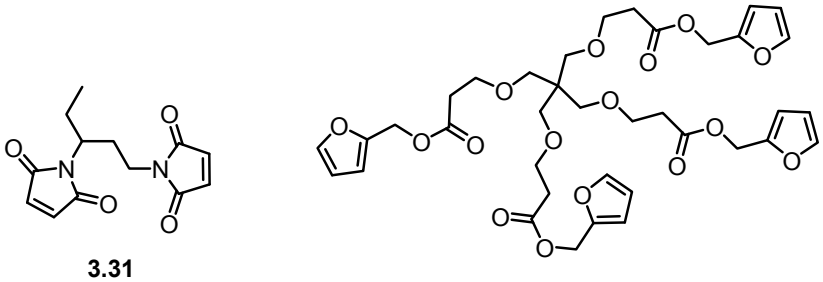

3.31 **3.32**

Figure 3.4.3 Examples of monomers previously used for the preparation of a re-mendable polymeric network.[140]

The main limitation of the previously developed Diels-Alder polymers with re-mendable properties is that they soften when heated since the retro-Diels-Alder reactions occur. This problem could be overcome by integrating functional dienes that become photoswitchable when they undergo cycloadditions. Upon exposure to UV radiation, the cross-links formed by the Diels-Alder adducts could be locked through ring-closure of the DTE moieties, resulting in a thermally stable material. Exposure to visible light would then regenerate the re-mendable properties of the polymeric material.

Scheme 3.4.2 shows a system with potential photoswitchable re-mendable properties using poly(**3.30**) and the *bis*-maleimide **3.31**. This material was prepared by mixing poly(**3.30**) with half an equivalent (compared to the monomers) of compound **3.31** in dichloromethane. Evaporation of the solvent and subsequent heating at 70 °C for 14 hours allowed the formation of a highly insoluble photochromic polymer. Optimisation of the system will be attempted in order to obtain materials with the desired mechanical properties.

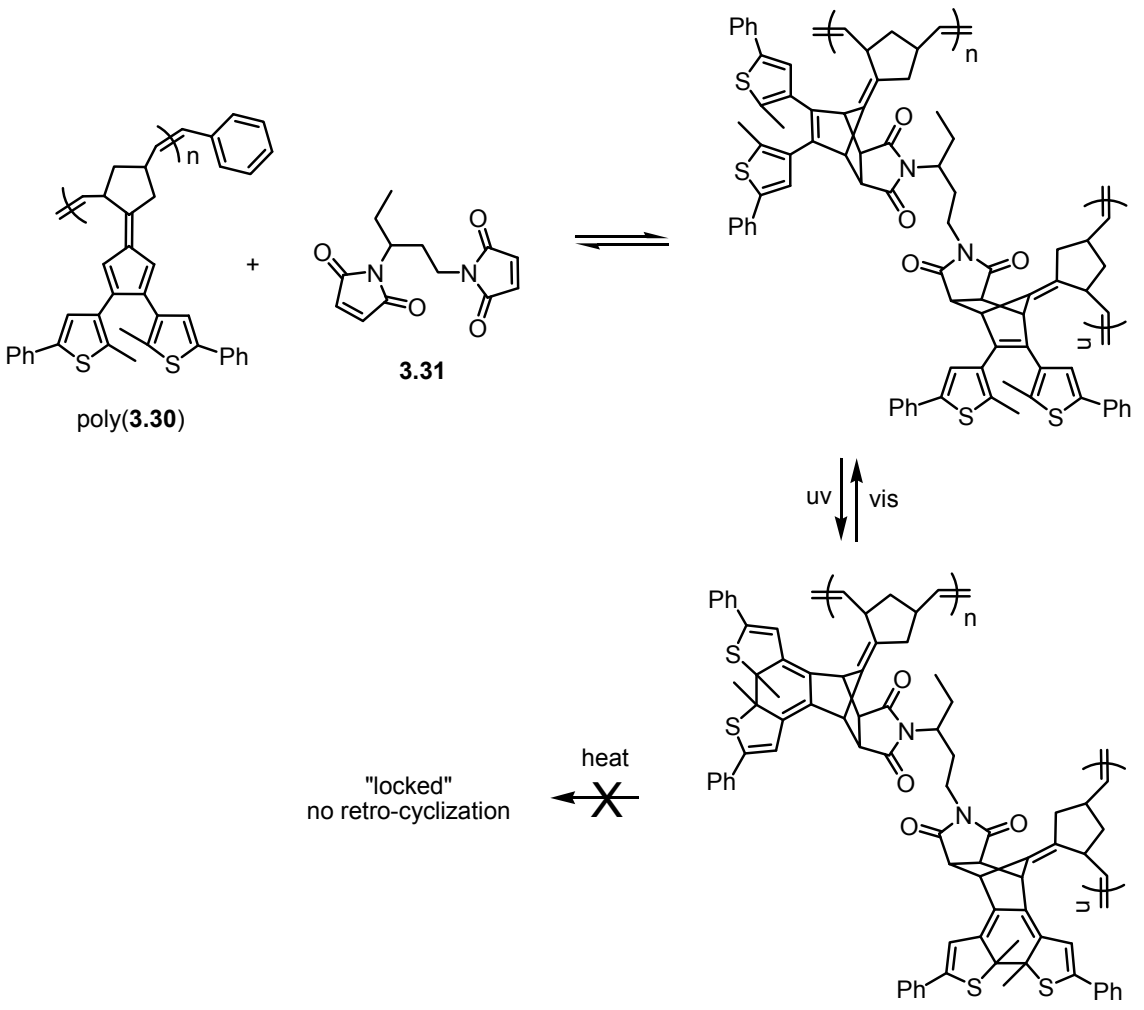

Scheme 3.4.2 Potential "photo-lockable" re-mendable polymer: Poly(**3.30**) could be mixed with a *bis*-maleimide (**3.31**) to form a polymeric network with reversible cross-links. Upon exposure to UV light, the cross-links would be locked since the retro-Diels-Alder reaction would be prevented. Irradiation with visible light would permit the recovery of the re-mendable properties.

Other strategies could be used to create photoswitchable re-mendable materials. For example, the *bis*-fulvene **3.33** (Figure 3.4.4), whose preparation was attempted with promising results, could be used to form cross-linked matrices with the appropriate multifunctional maleimides. Materials with unique properties could also be prepared from the *bis*-cyclohexadienone **3.34**. In this case, self-dimerisation could allow for the formation of re-mendable materials from this single monomer.

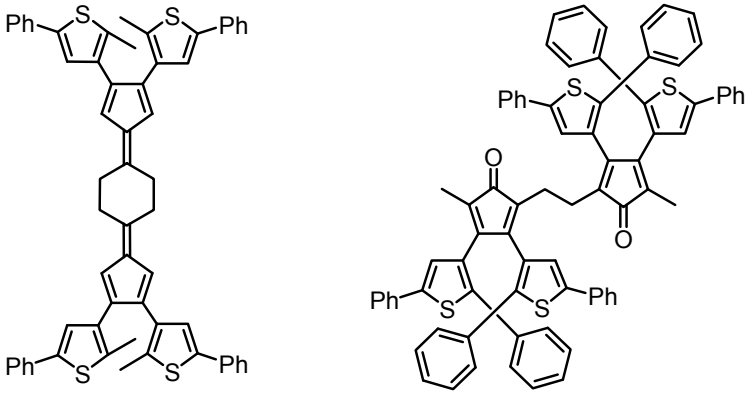

3.33 **3.34**

Figure 3.4.4 *Bis*-diene candidates for Diels-Alder polymerisation. Compound **3.33** contains two fulvene units and compound 3.34 contains two cyclopentadienone groups.

3.5 Experimental

3.5.1 Materials

All solvents used for synthesis and UV–vis absorption spectroscopy measurements were dried and degassed by passing them through steel columns containing activated alumina under nitrogen using an MBraun solvent purification system. Solvents for NMR analysis were purchased from Cambridge Isotope Laboratories and used as received. Column chromatography was performed using silica gel 60 (230-400 mesh) from Silicycle Inc. and solvents purchased from Aldrich that were used as received. All other reagents and starting materials were purchased from Aldrich. 1,2-*bis*(5'-Phenyl-2'-methylthieny-3'-yl) cyclopentene **3.13a**,[130] 1,2-*bis*(5'-chloro-2'-methylthieny-3'-yl)cyclopentene **3.13**,[131] and diethyl dicyanofumarate **3.24**[135] were prepared as described in the literature.

3.5.2 Instrumentation

^{1}H NMR characterisations were performed on a Varian INOVA 500 working at 499.770 MHz. ^{13}C NMR characterisations were performed on a Bruker AMX 400 instrument working at 100.610 MHz. Chemical shifts (δ) are reported in parts per million (ppm) relative to tetramethylsilane using the residual solvent peak as a reference standard. Coupling constants (J) are reported in Hertz. UV-vis absorption spectroscopy was performed using a Varian Cary 300 Bio spectrophotometer. Microanalysis (C, H, N) were performed at Simon Fraser University by Mr. Mei-Keng Yang on a Carlo Erba EA 1110 CHN Elemental Analyser. Low resolution mass spectrometry measurements were performed at Simon Fraser University by Mr. Simon Wong using a Varian 4000

GC/MS/MS with electron impact operating at 10 mA as the ionisation source (EI) or chemical ionisation (CI) using methanol.

3.5.3 Photochemistry

All ring-closing reactions were carried out using the light source from a lamp used for visualising TLC plates at 312 nm (Spectroline E-series, 470 W/cm^2). The ring-opening reactions were carried out using the light of a 300-W halogen photo optic source passed through a 434 nm, 490 nm or 557 nm cut-off filter to eliminate higher energy light. The selective ring-opening reaction of compound **3.27** was carried out using the light source (75 W xenon lamp) from a PTI QM-2000-4 scanning spectrofluorimeter with a 4 nm slit-width centered at 430 nm.

3.5.4 Computational methods

Computational structures and properties of the molecules described in this chapter were carried out using the HyperChem Release 7.1 software that was kindly given to the author, free of charge, as a HyperCube Scholar Award in 2003. Structures were obtained using the semi-empirical AM1 method using a Polak-Ribiere (conjugated gradient) algorithm for geometrical optimisation. After optimisation, the properties were obtained directly from the HyperChem software.

3.5.5 Synthesis

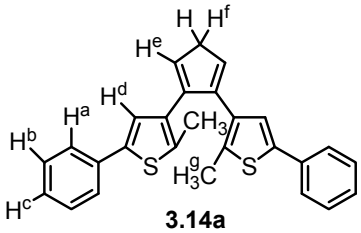

3.14a

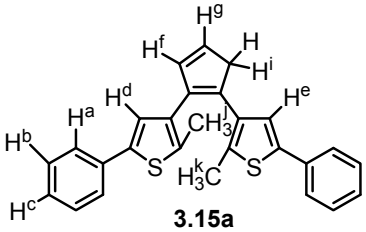

3.15a

Synthesis of cyclopentadiene isomers 3.14a and 3.15a

This compound was synthesised and purified in the dark. A solution of 1,2-*bis*(5'-phenyl-2'-methylthieny-3'-yl)cyclopentene **3.13a** (280 mg, 0.73 mmol) in anhydrous Et_2O (50 mL) was cooled to -40 °C under a nitrogen atmosphere using an acetone/dry ice bath. The solution was then treated with bromine (36 μL, 0.73 mmol) in one portion using a syringe. The cooling bath was removed; the reaction was allowed to warm to room temperature and was stirred for 1 hour. The reaction was quenched with water (10 mL) and stirred for 10 minutes. The aqueous layer was separated and extracted with Et_2O (3 x 50 mL). The combined organic layers were washed with water (10 mL) and brine (10 mL), dried with Na_2SO_4, filtered and evaporated to dryness under reduced pressure. Purification by column chromatography through silica (18:1 hexanes:EtOAc containing 1% Et_3N) afforded a colourless oil containing the isomers **3.14a** and **3.15a** in a 1:4 ratio. Because of the thermal instability of the products, no further characterisation was performed and the yield of the reaction was not evaluated.

(**3.14a**) ^{1}H NMR (chloroform-d_3, 500 MHz): δ 7.42 (H^a, d, J = 7.7 Hz, 4H), 7.29 (H^b, t, J = 7.7 Hz, 4H), 7.21 (H^c, t, J = 7.7 Hz, 2H), 6.87 (H^d, s, 2H), 6.48 (H^e, t, J = 1.5 Hz, 2H), 3.28 (H^f, t, J = 1.5 Hz, 2H), 2.27 (H^g, s, 6H).

(**3.15a**) ^{1}H NMR (chloroform-d_3, 500 MHz): δ 7.50 (H^a, d, J = 7.6 Hz, 4H), 7.33 (H^b, t, J = 7.6 Hz, 4H), 7.22 (H^c, t, J = 7.6 Hz, 2H), 7.09 (H^d, s, 1H), 7.08 (H^e, s, 1H), 6.71 (H^f, dt, J = 5.5, 1.5 Hz, 1H), 6.53 (H^g, dt, J = 5.5, 1.5 Hz, 1H), 3.50 (H^i, t, J = 1.5 Hz, 2H), 2.12 (H^j, s, 3H), 2.03 (H^k, s, 3H).

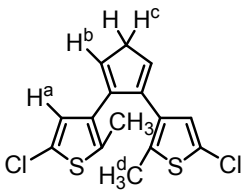

3.14

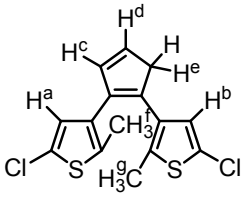

3.15

Synthesis of cyclopentadiene isomers 3.14 and 3.15

This compound was synthesised and purified in the dark. A solution of 1,2-*bis*(5'-chloro-2'-methylthieny-3'-yl)cyclopentene **3.13** (203 mg, 0.61 mmol) in anhydrous Et_2O (25 mL) was cooled to -40 °C under nitrogen atmosphere using an acetone/dry ice bath. The solution was then treated with bromine (31 μL, 0.61 mmol) in one portion using a syringe. The cooling bath was removed; the reaction was allowed to warm to room temperature and was stirred for 1 hour. The reaction was quenched with water (10 mL) and stirred for 10 minutes. The aqueous layer was separated and extracted with Et_2O (3 x 50 mL). The combined organic layers were washed with water (10 mL) and brine (10 mL), dried with $MgSO_4$, filtered and evaporated to dryness under reduced pressure. Purification by column chromatography through silica (19:1 hexanes:EtOAc containing 1% Et_3N) afforded a colourless oil (94 mg, 0.29 mmol, 47 %) containing the isomers **3.14** and **3.15** in a 1:7 ratio. Because of the thermal instability of the products, no further characterisation was performed.

(**3.14**) ^{1}H NMR (chloroform-d_3, 500 MHz): δ 6.41 (H^a, s, 2H), 6.38 (H^b, t, J = 1.8 Hz, 2H), 3.22 (H^c, t, J = 1.8 Hz, 2H), 2.16 (H^d, s, 6H). ^{1}H NMR (acetone-d_6, 500 MHz) δ 6.50 (H^a, t, J = 1.8 Hz, 2H), 6.48 (H^b, s, 2H), 3.28 (H^c, t, J = 1.8 Hz, 2H), 2.20 (H^d, s, 6H).

(**3.15**) ^{1}H NMR (chloroform-d_3, 500 MHz): δ 6.63 (H^a, s, 1H), 6.62 (H^b, s, 1H), 6.57 (H^c, dt, J = 1.5, 5.2 Hz, 1H), 6.48 (H^d, dt, J = 1.5, 5.2 Hz, 1H), 3.36 (H^e, t, J = 1.5 Hz, 2H), 2.02 (H^f, s, 3H), 1.92 (H^g, s, 3H); ^{1}H NMR (acetone-d_6): δ 6.84 (H^a, s, 1H), 6.73 (H^b, s, 1H), 6.65 (H^c, dt, J = 1.5, 5.4 Hz, 1H), 6.55 (H^d, dt, J = 1.5, 5.4 Hz, 1H), 3.47 (H^e, t, J = 1.5 Hz, 2H), 2.06 (H^f, s, 3H), 1.94 (H^f, s, 3H); ^{13}C NMR (acetone-d_6, 100 MHz): δ 139.0, 138.6, 137.1, 136.2, 136.1, 136.0, 135.1, 134.7, 129.8, 129.3, 126.7, 126.4, 47.4, 15.2, 15.1.

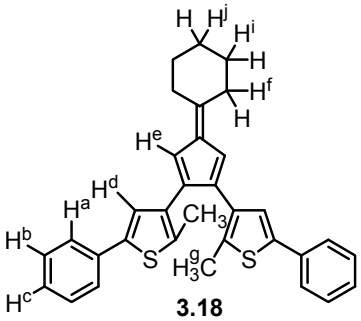

3.18

Synthesis of 2,3-*bis*(2'-phenyl-5'-methylthieny-3'-yl)-6,6-pentamethylenefulvene 3.18 (one-pot procedure)

This compound was synthesised and purified in the dark. A solution of 1,2-*bis*(5'-phenyl-2'-methylthieny-3'-yl)cyclopentene (**3.13a**) (1.00 g, 2.4 mmol) in anhydrous Et_2O (100 mL) was cooled to -40 °C under nitrogen atmosphere using an acetone/dry ice bath. The solution was then treated with bromine (125 μL, 2.4 mmol) in one portion using a syringe. The cooling bath was removed; the reaction was allowed to warm to room temperature and was stirred under nitrogen atmosphere. The reaction was monitored by

TLC (hexanes). After approximately 1 hour all starting materials had been consumed and water (10 mL) was added. The reaction was stirred for 10 minutes, after which the aqueous layer was separated and extracted with Et_2O (3 x 20 mL). The combined organic extracts were washed with water (10 mL) and brine (10 mL), dried with Na_2SO_4, filtered and evaporated to dryness under reduced pressure. The crude product was dissolved in methanol (50 mL) and the solution was deoxygenated by bubbling nitrogen gas through it for 30 min. It was then treated with deoxygenated cyclohexanone (0.50 mL, 4.8 mmol) and deoxygenated pyrrolidine (410 μL, 4.8 mmol). The reaction was stirred at room temperature for 12 hours. The methanol was evaporated *in vacuo* to yield a brown solid. The crude mixture was dissolved in Et_2O (100 mL), washed with water (20 mL) and brine (20 mL), dried over Na_2SO_4, filtered, and evaporated under reduced pressure to yield a brown solid. Purification by column chromatography using silica (hexanes) afforded **3.18** as a yellow solid (242 mg, 0.49 mmol, 20%).

M.p.: 163 °C; ^{1}H NMR (dichloromethane-d_2, 500 MHz): δ 7.46 (H^a, d, J = 7.8 Hz, 4H), 7.30 (H^b, t, J = 7.8 Hz, 4H), 7.20 (H^c, t, J = 7.8 Hz, 2H) 6.93 (H^d, s, 2H), 6.66 (H^e, s, 2H), 2.74 (H^f, m, 4H), 2.32 (H^g, s, 6H), 1.82 (H^i, m, 4H), 1.74 (H^j, m, 2H); ^{13}C NMR (dichloromethane-d_2, 100 MHz): δ 160.5, 141.9, 140.9, 140.1, 137.4, 137.0, 136.4, 130.6, 128.8, 127.4, 127.2, 121.0, 35.5, 30.8, 28.4, 16.1; Anal. Calcd. for $C_{33}H_{30}S_2$: C, 80.77; H, 6.16; Found: C, 80.39; H, 6.35; LRMS (CI) : m/z = 491 (451) [M^++1], 493 (999) [M^++3]; LRMS (EI): m/z = 490 [M^+].

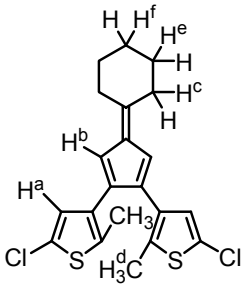

3.17

Synthesis of 2,3-*bis*(2'-chloro-5'-methylthieny-3'-yl)-6,6-pentamethylenefulvene 3.17 (one-pot preparation)

This compound was synthesised and purified in the dark. A solution of 1,2-*bis*(5'-chloro-2'-methylthieny-3'-yl)cyclopentene (**3.13**) (1.00 g, 3.0 mmol) in anhydrous Et_2O (75 ml) was cooled to -40 °C under nitrogen atmosphere using an acetone/dry ice bath. The solution was then treated with bromine (160 μL, 3.0 mmol) in one portion using a syringe. The cooling bath was removed; the reaction was allowed to warm to room temperature and was stirred in the dark under nitrogen atmosphere. The reaction was monitored by TLC (hexanes). After approximately 2 hours, all starting materials had been consumed and water (10 mL) was added to quench any unreacted bromine. The reaction was stirred for 10 minutes, after which the aqueous layer was separated and extracted with Et_2O (3 x 20 mL). The combined organic extracts were washed with water (10 mL), saturated $NaHCO_3$ aqueous solution (10 mL), and brine (10 mL), dried with $MgSO_4$, filtered and evaporated to dryness under reduced pressure. The crude product was dissolved in methanol (50 mL) and the solution was deoxygenated by bubbling nitrogen gas for 30 minutes. It was then treated with deoxygenated cyclohexanone (1.56 mL, 15.2 mmol) and deoxygenated pyrrolidine (1.27 mL, 15.2 mmol). The reaction was stirred at room temperature for 14 hours. The methanol was evaporated *in vacuo* to yield a brown solid. The crude mixture was dissolved in Et_2O (100 mL), washed with water (20 mL)

and brine (20 mL), dried over $MgSO_4$, filtered, and evaporated under reduced pressure to yield a brown solid. Purification by column chromatography using silica (hexanes) afforded **3.17** as a yellow solid (222 mg, 0.54 mmol, 18%).

Mp.: 144–146 °C; ^{1}H NMR (dichloromethane-d_2, 500 MHz): δ 6.57 (H^a, s, 2H), 6.47 (H^b, s, 2H), 2.70 (H^c, m, 4H), 2.21 (H^d, s, 6H), 1.78 (H^e, m, 4H), 1.72 (H^f, m, 2H); ^{13}C NMR (dichloromethane-d_2, 100 MHz): δ 159.6, 138.4, 137.5, 133.5, 133.4, 127.6, 124.2, 119.4, 33.3, 28.6, 26.1, 13.6; Anal. Calcd. for $C_{21}H_{20}Cl_2S_2$: C, 61.91; H, 4.95; Found: C, 61.81; H 5.08; LRMS (EI): m/z = 406 [M^+].

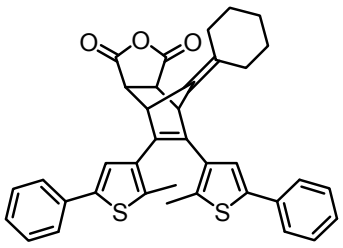

3.23o

Synthesis of bicyclic compound 3.23o

A solution of fulvene **3.18** (3.0 mg, 0.01 mmol) in acetone-d_6 (0.75 mL) was treated with maleic anhydride (**3.19**) (3.0 mg, 0.03 mmol) in one portion in an NMR tube. The reaction was monitored by ^{1}H NMR spectroscopy over 47 hours, after which time the reaction reached > 96% completion. A mixture of *endo*:*exo* isomer (1:9) was obtained. Purification by column chromatography using silica (hexanes:EtOAc 5:1) afforded **3.23o** as its *exo* isomer (non-optimised yield < 50%). Due to the small amount of product obtained, characterisation was limited to ^{1}H NMR and UV-vis absorption spectroscopy.

^{1}H NMR (acetone-d_6, 400 MHz): δ 7.62 (d, J = 7.3 Hz, 4H), 7.43 (s, 2H), 7.39 (t, J = 7.3 Hz, 4H), 7.30 (t, J = 7.3 Hz, 4H), 4.24 (s, 2H), 3.70 (s, 2H), 2.37-2.37 (m, 2H), 2.05-2.02 (m, 2H), 2.02 (s, 6H), 1.7-1.3 (m, 6H).

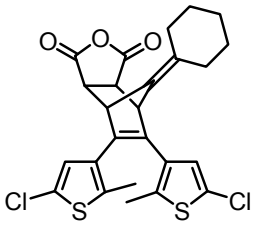

3.21o

Synthesis of bicyclic compound 3.21o

A solution of fulvene **3.17** (12.2 mg, 0.03 mmol) in acetone-d_6 (1.0 mL) was treated with maleic anhydride (**3.19**) (15.0 mg, 0.15 mmol) in one portion in an NMR tube. The NMR tube containing the solution was placed in a water bath at 50 °C. The reaction was monitored by ^{1}H NMR spectroscopy over 4 hours, after which time the reaction reached > 96% completion. Purification by column chromatography using silica (dichloromethane) afforded **3.21o** as a 1:9 mixture of *endo*:*exo* isomers (non-optimised yield < 50%). Due to the small amount of product obtained, characterisation was limited to ^{1}H NMR, ^{13}C NMR, and UV-vis absorption spectroscopy.

3.21o *endo*: ^{1}H NMR (acetone-d_6, 400 MHz): δ 6.94 (s, 2H), 4.12 (s, 2H), 3.62 (s, 2H), 2.33-2.28 (m, 2H)*, 2.00-1.94 (m, 2H)*, 1.96 (s, 6H), 1.65-1.25 (m, 6H)*.

3.21o *exo*: ^{1}H NMR (acetone-d_6, 400 MHz): δ 6.87 (s, 2H), 4.31 (dd, J = 3.1 Hz, 1.7 Hz, 2H), 3.99 (dd, J = 3.1 Hz, 1.7 Hz, 2H), 2.33-2.28 (m, 2H)*, 2.00-1.94 (m, 2H)*, 1.96 (s, 6H), 1.65-1.25 (m, 6H)*.

3.21o mixture: ^{13}C NMR (acetone-d_6, 125 MHz): δ 173.2, 141.8, 137.3, 137.1, 134.3, 128.5, 127.4, 127.0, 53.6, 51.6, 32.1, 29.7, 28.1, 15.4.

* Observed as overlapping peaks of both stereoisomers.

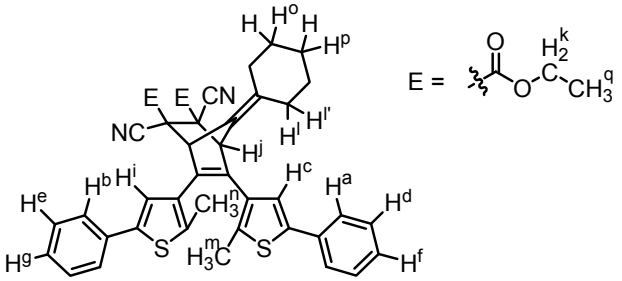

3.26

Synthesis of bicyclic compound 3.26

A solution of fulvene **3.18** (5.0 mg, 0.01 mmol) in dichloromethane-d_2 (0.75 mL) was treated with diethyl dicyanofumarate (**3.24**) (9.4 mg, 0.04 mmol) in one portion in an NMR tube. The reaction was monitored by ^{1}H NMR spectroscopy and reached equilibrium within 20 minutes when 55% of product **3.26** was obtained. The equilibrium constant ($K_{\mathbf{3.26}}$) was evaluated to be 22 M^{-1}. Purification of compound **3.26** was not attempted since it is part of an equilibrium with the starting materials **3.18** and **3.24** at room temperature and is therefore inherently unstable in solution.

^{1}H NMR (dichloromethane-d_2, 500 MHz): δ 7.56 (H^a, d, J = 7.3 Hz, 2H), 7.55 (H^b, d, J = 7.3 Hz, 2H), 7.49 (H^c, s, 1H), 7.36 (H^d and H^e, m, 4H), 7.26 (H^f and H^g, m, 2H), 7.15 (H^i, s, 1H), 4.40-4.00 (H^j and H^k, m, 6H), 2.7-2.6 (H^l, m, 2H), 2.3-2.0 ($H^{l'}$, m, 2H), 1.96 (H^m, s, 3H), 1.90 (H^n, s, 3H), 1.63 (H^o and H^p, m, 6H), 1.14 (H^q, t, J = 7.1 Hz, 6H).

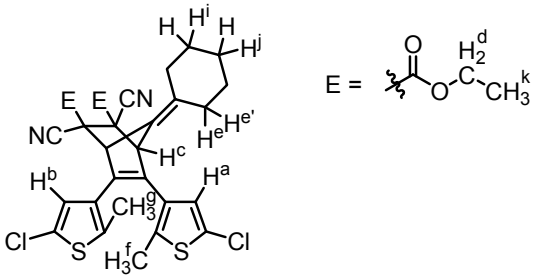

3.25

Synthesis of bicyclic compound 3.25

A solution of fulvene **3.17** (5.5 mg, 0.01 mmol) in dichloromethane-d_2 (0.75 mL) at room temperature was treated with diethyl dicyanofumarate (**3.24**) (11 mg, 0.05 mmol) in one portion in an NMR tube. The reaction was monitored by ^{1}H NMR spectroscopy and reached equilibrium within 20 minutes when 43% of product **3.25** was obtained. The equilibrium constant ($K_{\mathbf{3.25}}$) was calculated to be 13 M^{-1}. Purification of compound **3.25** was not attempted since it is part of an equilibrium with the starting materials **3.17** and **3.25** at room temperature and is therefore inherently unstable in solution.

^{1}H NMR (dichloromethane-d_2, 500 MHz): δ 7.02 (H^a, s, 1H), 6.77 (H^b, s, 1H), 4.30 (H^c, s, 2H), 4.4-4.2 (H^d, m, 2H), 4.1-4.0 (H^d, m, 2H), 2.5-2.0 (H^e, m, 4H), 1.84 (H^f, s, 3H), 1.81 (H^g, s, 3H), 1.7-1.4 (H^i and H^j, m, 6H), 1.42 (H^k, t, J = 7.2 Hz, 3H), 1.23 ($H^{k'}$, t, J = 7.2 Hz, 3H).

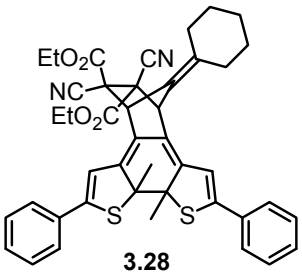

3.28

Synthesis of ring-closed compound 3.28

A solution of the *bis*-phenyl fulvene **3.18** (50 mg, 0.1 mmol) in dichloromethane (15 mL) was treated with diethyl dicyanofumarate (68 mg, 0.3 mmol). The solution was kept in the dark while it was stirred for 15 minutes. The solution was then irradiated with 313 nm light for 15 minutes. Further irradiation resulted in the formation of a significant amount of an uncharacterised side product. The solution was evaporated under vacuum and in the dark to yield a red/purple solid. Purification by column chromatography in the dark using silica (hexanes:EtOAc 18:1) afforded compound **3.28** as a mixture of stereoisomers which were not separated (non-optimised yield <5%). In order to avoid ring-opening of **3.28**, the compound must be kept in absolute darkness. Due to the small amount of product obtained, characterisation was limited to ^{1}H NMR.

Stereoisomer 1 (major): ^{1}H NMR (dichloromethane-d_2, 500 MHz): δ 7.54 (m, 4H)*, 7.39 (m, 6H)*, 6.57 (s, 1H), 6.51 (s, 1H), 4.40-4.20 (m, 6H)*, 2.5-2.1 (m, 6H)*, 2.05 (s, 3H)*, 1.98 (s, 3H)*, 1.7-1.5 (m, 4H), 1.39 (m, 6H)*.

Stereoisomer 2 (minor): ^{1}H NMR (dichloromethane-d_2, 500 MHz): δ 7.54 (m, 4H)*, 7.39 (m, 6H)*, 6.55 (s, 1H), 6.52 (s, 1H), 4.40-4.20 (m, 6H)*, 2.5-2.1 (m, 6H)*, 2.05 (s, 3H)*, 1.98 (s, 3H)*, 1.7-1.5 (m, 4H), 1.39 (m, 6H)*.

* Observed as overlapping peaks of both stereoisomers.

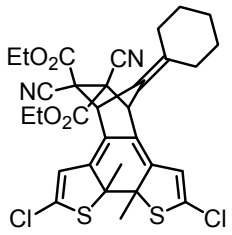

3.27

Synthesis of ring-closed compound 3.27

A solution of the *bis*-chloro fulvene **3.17** (56 mg, 0.1 mmol) in dichloromethane (7.5 mL) was treated with diethyl dicyanofumarate (116 mg, 0.5 mmol). The solution was kept in the dark while it was stirred for 1 hour. The solution was then irradiated with 313 nm light for 8 minutes. Further irradiation resulted in the formation of a significant amount of an uncharacterised side product. The solution was evaporated under vacuum and in the dark to yield a yellow/orange solid. Purification by column chromatography in the dark using silica (hexanes:EtOAc 19:1) afforded compound **3.27** as a mixture of two stereoisomers. Recrystalisation with hexanes afforded a solid enriched with the major stereoisomer and a solute enriched with the minor stereoisomer (non-optimised yield <5%). In order to avoid ring-opening of **3.27**, the compound must be kept in darkness. Due to the small amount of product obtained, characterisation was limited to ^{1}H NMR.

Stereoisomer 1 (major): ^{1}H NMR (dichloromethane-d_2, 500 MHz): δ 6.10 (s, 1H), 6.06 (s, 1H), 4.40-4.20 (m, 4H)*, 4.17 (s, 1H), 4.12 (s, 1H)*, 2.40-2.25 (m, 4H)*, 2.15-2.10 (m, 2H)*, 2.02 (s, 3H)*, 1.94 (s, 3H)*, 1.7-1.5 (m, 4H)*, 1.39 (m, 6H)*.

Stereoisomer 2 (minor): ^{1}H NMR (dichloromethane-d_2, 500 MHz): δ 6.08 (s, 1H), 6.05 (s, 1H), 4.40-4.20 (m, 4H)*, 4.12 (s, 1H)*, 4.06 (s, 1H), 2.40-2.25 (m, 4H)*, 2.15-2.10 (m, 2H)*, 2.02 (s, 3H)*, 1.94 (s, 3H)*, 1.7-1.5 (m, 4H)*, 1.39 (m, 6H)*.

* Observed as overlapping peaks of both stereoisomers.

3.5.6 Photorelease experiments using ring-closed Diels-Alder adducts

Photorelease using ring-closed compound 3.28 monitored by UV-vis spectroscopy

A solution of *bis*-phenyl compound **3.28** (3.4×10^{-5} M) in dichloromethane was prepared and transferred to a quartz cuvette for UV-visible absorption spectroscopy experiments. The sample was periodically exposed to light of wavelengths greater than 490 nm and was kept in the dark for 10 minutes to allow complete decay of the thermally unstable species after each irradiation. Changes in the UV-vis absorption spectra of the solution were monitored by acquiring a spectrum after each irradiation and equilibration periods. The sample was irradiated for a total of 10, 20, 30, 40, and 240 minutes after which the absorption band attributed to compound **3.28** had disappeared completely. Results are shown in Figure 3.3.9.

Photorelease using ring-closed compound 3.28 monitored by ^{1}H NMR spectroscopy

A solution of *bis*-phenyl compound **3.28** (1.5×10^{-3} M) in dichloromethane-d_2 was prepared in a standard boro-silicate NMR tube. The sample was periodically exposed to light of wavelengths greater than 490 nm for up to 60 seconds. The formation of fulvene **3.18** and fumarate **3.24** was monitored by ^{1}H NMR spectroscopy after each irradiation period. Trace amounts of the ring-open isomer **3.26** were also present when the spectra were acquired immediately after the exposure of the sample to light. After a total of 60 seconds of exposure to visible light (>490 nm), the sample was kept in the dark for 30 minutes, after which no observable trace of the ring-open isomer was visible in the spectrum. Periodic irradiation up to 210 seconds triggers the ring-opening reaction and subsequent quantitative release of the dienophile. Results are shown in Figure 3.3.10.

Photorelease using ring-closed compound 3.28 monitored by ^{1}H NMR spectroscopy at 2 °C

A solution of the *bis*-phenyl compound (**3.28**) (1.5 x 10^{-3} M) in dichloromethane-d_2 was prepared in a standard boro-silicate NMR tube. The tube was then placed in a sodium chloride/iced water bath at -10 °C and irradiated with a light source of wavelengths greater than 490 nm for 50 seconds. The sample was transferred into the NMR chamber which was maintained at 2 °C. The thermal fragmentation of the ring-open isomer **3.26** was monitored by acquiring spectra after 3, 8, 12, and 20 minutes. The tube was transferred to the -10 °C bath and exposed to visible light (>490 nm) for another 60 seconds. The decay of the ring-open isomer was monitored at 2 °C by acquiring spectra after 2, 8, 15, 25, and 33 minutes. Results are shown in Figure 3.3.12.

Photorelease using ring-closed compound 3.27 monitored by UV-vis spectroscopy

A solution of *bis*-chloro compound **3.27** (2.5 x 10^{-5} M) in dichloromethane was prepared and transferred to a quartz cuvette for UV-visible absorption spectroscopy experiments. The sample was periodically exposed to the light source from a scanning spectrofluorimeter with a 4 nm slit-width centred at 430 nm after which it was kept in the dark for 15 minutes to allow complete decay of the thermally unstable species. Changes in the UV-vis absorption spectra of the solution were monitored by acquiring a spectrum after each irradiation and equilibration periods. The sample was irradiated for a total of 30, 60, 90, 150, 330, and 630 seconds. The complete ring-opening of compound **3.27** was finally achieved by a 2 minute exposure to light of wavelengths greater than 434 nm. Results are shown in Figure 3.3.13.

Photorelease using ring-closed compound 3.27 monitored by ^{1}H NMR spectroscopy

A solution of *bis*-chloro compound **3.27** (9.0 x 10^4 M) in dichloromethane-d_2 was prepared in a standard boro-silicate NMR tube. The sample was periodically exposed to light of wavelengths greater than 434 nm. The formation for the ring-open isomer **3.25**, fulvene **3.17** and fumarate **3.24** was observed by ^{1}H NMR spectroscopy after each irradiation period. The thermal fragmentation of compound **3.25** resulting in the formation of the fulvene and the fumarate was monitored by acquiring spectra 3, 5, 10, and 15 minutes after each irradiation periods. Quantitative ring-opening was observed after 32 seconds of irradiation. Partial results are shown in Figure 3.3.14.

Selective ring-opening monitored by UV-vis absorption spectroscopy

A solution of *bis*-chloro compound **3.27** (1.0 x 10^{-5} M) and *bis*-phenyl compound **3.28** (1.0 x 10^{-5} M) in dichloromethane was prepared and transferred to a quartz cuvette for UV-visible absorption spectroscopy experiments. The solution was irradiated for 10 minutes using the light from the source of a scanning spectrofluorimeter with a 4 nm slit-width centred at 430 nm to selectively ring-open the *bis*-chloro compound, followed by 12 minutes using light of wavelength greater than 557 nm to selectively ring-open the *bis*-phenyl compound **3.28**, and finally, 4 minutes with light of wavelengths greater than 434 nm to ring-open any residual ring-closed molecules. Spectra were acquired after each irradiation periods. Results are shown in Figure 3.3.16.

Another solution of *bis*-chloro compound **3.27** (1.0 x 10^{-5} M) and *bis*-phenyl compound **3.28** (1.0 x 10^{-5} M) in dichloromethane was prepared and transferred to a quartz cuvette for UV-visible absorption spectroscopy experiments. The solution was irradiated for 12 minutes using light of wavelength greater than 557 nm to selectively

ring-open the *bis*-phenyl compound **3.28**, followed by 4 minutes with light of wavelengths greater than 434 nm to ring-open the *bis*-chloro compound **3.26**. Spectra were acquired after each irradiation periods. In this case, a 15 minutes equilibration period was necessary after the last exposure to light to allow full decay of the thermally unstable species. Results are shown in Figure 3.3.16.

Selective and sequential photorelease monitored by ^{1}H NMR spectroscopy

A solution of *bis*-chloro compound **3.27** (1.9×10^3 M) and *bis*-phenyl compound **3.28** (1.9×10^3 M) in dichloromethane-d_2 was prepared in a standard boro-silicate NMR tube. The solution was irradiated for up to 21 minutes with light of $\lambda = (430 \pm 2)$ nm from the source of a scanning spectrofluorimeter to selectively trigger the ring-opening reaction of the *bis*-chloro compound, after which it was kept in the dark for 15 minutes to allow quantitative release of the fumarate. The sample was then expose to light of wavelengths greater that 557 nm for up to 170 seconds to selectively release the *bis*-phenyl compound. Finally, the solution was irradiated for 3 minutes with light of wavelengths greater than 434 nm to ring-open both systems, and kept in the dark for 15 minutes to allow quantitative release of the fumarate. ^{1}H NMR spectra were acquired after each irradiation and equilibration periods to monitor the process. Results are shown in Figure 3.3.17.

Chapter 4: Photomodulation of Lewis Acidity Using a Boron-Containing Dithienylethene-Based Molecular Switch

The research presented in this chapter was published in part in: V. Lemieux, M. D. Spantulescu, K. K. Baldridge and N. R. Branda, "Modulating the Lewis acidity of boron using a photoswitch", *Angew. Chem. Int. Ed.* **2008**, 47(27), 5034-5037. The synthetic route for the preparation of compound **4.3** was developed in part by Dr. M. D. Spantulescu. Some of the computational results were obtained in collaboration with Professor K.K. Baldridge, as indicated throughout the relevant sections.

4.1 Introduction – Boron compounds as Lewis acids

Tricoordinate organoboron compounds are versatile Lewis acids used as catalysts or reagents for important organic transformations[141] and polymerisation reactions.[142,143] The Lewis acidity of boron also imparts unique properties to new π-electron materials for use in sensing, electron-transport and other materials science applications.[144]

Integrating a stimuli-responsive group to Lewis acidic boron-containing molecules would offer a means to control chemical processes that are catalyzed by these Lewis acids and to modulate the behaviour of functional materials containing them. This integration is the focus of the studies described in this chapter (Sections 4.2 to 4.5). In the present section, the Lewis acid behaviour of trivalent boron compounds is described from a theoretical point of view, various applications of organoboranes (compounds with at least one C-B bond) and other boron-containing Lewis acids are described, an overview

of the diverse techniques used to control their Lewis acid strength is given, and the role of boron within the chemistry of dithienylethene (DTE) derivatives is explored.

4.1.1 Trivalent boron Lewis acids

One key aspect in the chemistry of trivalent boron compounds is their behaviour as Lewis acids. An accurate molecular orbital representation of such molecules should show an orbital capable of acting as an electron pair acceptor. Monoborane (BH_3) is the simplest trivalent boron compound known. Although its existence in the gas phase has been demonstrated, BH_3 is extremely susceptible to attack by nucleophiles and dimerisation occurs in the absence of an external ligand.[145] Construction of the molecular orbital diagram from an atomic orbital basis set allows the visualisation of the reason for this instability or Lewis acidity (Figure 4.1.1).

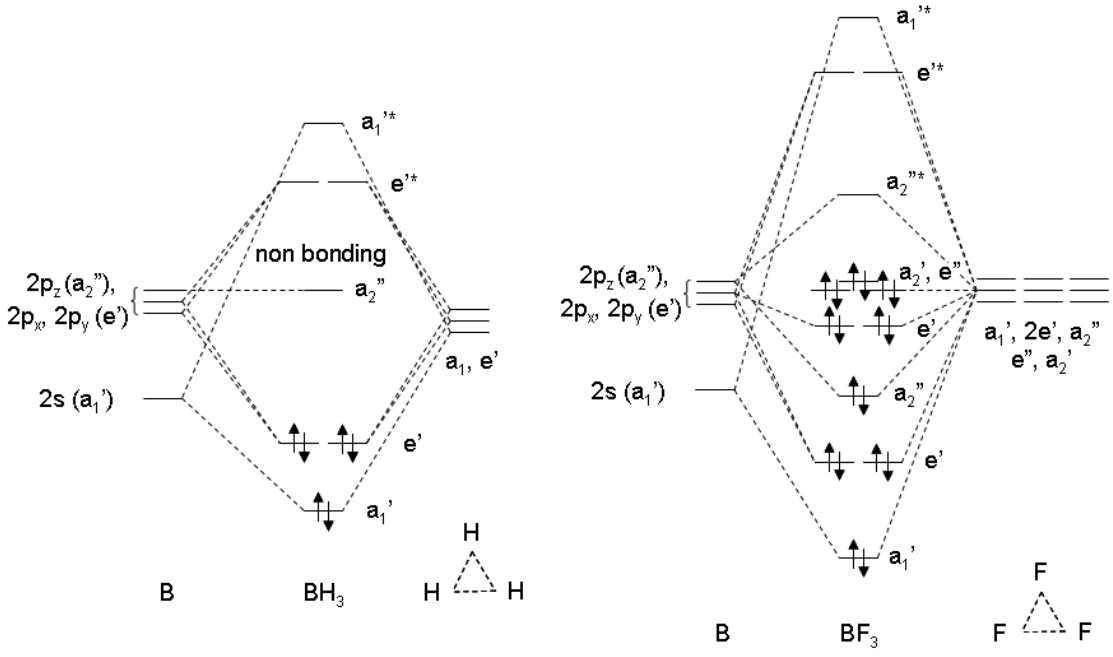

Figure 4.1.1 Molecular orbital diagrams of BH_3 and BF_3. The detailed energy levels of the hydrogen and fluorine atoms are not represented.

The ground state electronic configuration of the boron atom is $1s^2 2s^2 2p^1$. When the valence atomic orbitals of the boron centre (2s, $2p_x$, $2p_y$, $2p_z$) are combined with the three atomic orbitals of the protons with D_{3h} symmetry (a_1' and the doubly degenerate e') to form the molecular orbitals, the non-bonding $2p_z$ orbital on the boron atom remains empty and can accept electrons (Figure 4.1.1). A Lewis base can provide these electrons.

Each compound in the family of boron trihalides, BX_3 (X = F, Cl, Br, I) is monomeric and has a trigonal planar geometry.[146] They all behave as Lewis acids, but their acid strength is significantly less than that of BH_3. The ability of halogen atoms, especially fluorine, to donate lone pair π-electron density into the vacant p-orbital of the boron centre stabilises the molecules and decreases their Lewis acidity.[146] The lowest unoccupied molecular orbital (LUMO) of BX_3 is an empty π-orbital, which has antibonding interactions between the $2p_z$ orbital of the boron and the p_z orbitals of the surrounding halides as shown in Figure 4.1.1. This orbital can act as an electron-pair acceptor in Lewis acid-base interactions. In addition to halides, π-overlap of the vacant p-orbital of boron can occur with other suitable substituents such as nitrogen, oxygen, sulphur, and carbon-based π-systems, each of them affecting the Lewis acidity of the compound to different levels as represented in Figure 4.1.2.[145-148]

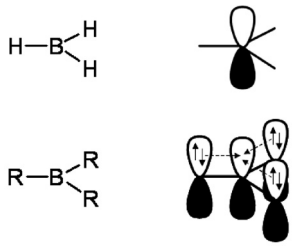

Figure 4.1.2 Diagram comparing the p-orbital of boron in borane with systems where π-overlap of the vacant p-orbital of boron can occur with substituents such as nitrogen, oxygen, sulphur, halogens, and carbon-based π-systems.

Upon coordination with a Lewis base, a trivalent boron compound loses its trigonal planar geometry. Once the vacant p-orbital on the boron accepts a pair of electrons from an external guest, it is no longer non-bonding (or weakly antibonding). A change in geometry occurs in order to accommodate the extra pair of bonding electrons. Thus, the complex undergoes a change from a trigonal planar to a tetrahedral geometry (Equation 4.1.1). This local symmetry modification at the boron centre results in a change in the nuclear shielding experienced by the atom and can be easily detected by ^{11}B NMR spectroscopy.[149]

Equation 4.1.1 Equilibrium between three-coordinate and four-coordinate boron compounds showing the change in geometry upon addition of a ligand (L).

4.1.2 Applications of boron-containing Lewis acids

As discussed in the previous section, trivalent boron compounds have a vacant p-orbital available for π-overlap with suitable substituents or for the formation of Lewis acid-Lewis base complexes. These interactions are crucial to the development of applications using boron-containing compounds, and are currently exploited in many ways:

(1) The overlap between the vacant p-orbital on boron with extended organic π-systems results in interesting linear and non-linear optical properties.[150,151]

(2) Photophysical properties of the boron-containing compounds show distinct changes upon coordination with nucleophiles, a phenomenon that has been widely used in sensor applications.[152,153]

(3) The donor-acceptor interactions between bifunctional organoboranes and bifunctional Lewis bases lead to the formation of reversible assemblies of macromolecular systems.[154]

(4) The donor-acceptor interactions between trivalent organoboron compounds and organic substrates lead to the activation of the organic moieties making three-coordinate boron compounds efficient catalysts and co-catalysts in organic synthesis.[141,148,155] Organoboranes are also commonly used activators for polymerisation reactions.[142,143]

The incorporation of trivalent boron centres in polymers can further improve the properties of these Lewis acidic compounds.[156] In the field of sensor materials, signal amplification effects result from the incorporation of Lewis acidic boron moieties into conjugated polymers.[157] The attachment of Lewis acid catalysts to an inert polymer backbone provides improved stability and recoverability.[158] One can also envision that the interaction between a polymer containing Lewis acidic centres and a polymer containing Lewis basic centres could generate higher order polymer assemblies with self-healing potential.[159,160]

4.1.3 Strategies to control the Lewis acidity of boron centres

The modulation of the Lewis acidity of trivalent boron compounds, especially of organoboranes (compounds containing at least one C-B bond), in order to further improve their performance, has remained a challenge.

The most widely used approach is the modification of the aliphatic or aromatic side groups with electron-withdrawing substituents such as fluorides.[148] For instance, the

Lewis acid strength of $B(C_6F_5)_3$ is much higher than $B(C_6H_5)_3$. It is then not surprising that *tris*(pentafluorophenyl)borane is one of the most widely used boranes. The incorporation of a boron centre into a framework with antiaromatic character[161,162] or into strained cycles or cages,[163,164] also increases its binding strength. Other strategies to affect the Lewis acidic behaviour of boranes include covalently linking positive ions onto boranes[165,166] or the oxidation of ferrocene moieties appended to boron containing compounds.[167]

Another approach used to modify the Lewis acidity of a boron centre is to tether a heteroatom, such as oxygen or nitrogen, in the vicinity of the trivalent centre such that its 2p orbital is filled with the lone pair of the ligand. The resulting tetracoordinate species is not Lewis acidic, but is still in equilibrium with the tricoordinate species. The coordination number of the boron is switched by the addition of an external reagent or solvent leading to changes in electronic properties of the organoboron compound, which can lead to efficient sensors.[168,169]

Organoboranes are efficient initiators for radical polymerisation, but their instability towards oxidation makes them difficult to handle.[170] On the other hand, complexes of boranes and amines are drastically less reactive.[147] The addition of an agent capable of forming a stronger complex with the amine such as an acid, aldehyde, or isocyanate may release the borane, thus activating it. This release is the basis for several commercial adhesive compositions.[170]

The use of light as an external stimulus to change the coordination number or intrinsic Lewis acidity of boranes offers various advantages. For example, the photorelease of trialkylboranes from their complexes with amines has potential for the

coatings industry.[170] In this system, aromatic ketone photoinitiators generate radicals when they react with tertiary amines through an electron transfer process caused by the excited carbonyl triplet state. In this process, ammonium radical cations are formed, disrupting the complexation between boron and nitrogen, thereby releasing the borane and allowing polymerisation activation.[170] However, this system is irreversible; once the system has been exposed to light, it is impossible to "turn off" the process.

Integration of a trivalent boron centre with a molecular switching system with "on" and "off" capability would be beneficial to the development of various new technologies.[171] Lewis acidity could be increased and decreased at will, allowing external control of a chemical process.

Modulation of Lewis acidity using a molecular switch has been reported only once.[171,172] In this report, the Lewis acidity of a catecholborane bearing an azo group was photoswitched based on the change in the coordination number of boron as shown in Scheme 4.1.1. In its *E*-form, the azo group is coordinated to the boron centre, competing with any other Lewis bases. However, irradiation with 360 nm light causes isomerisation of the azo group to its *Z*-form, switching the coordination number of the boron atom from 4 to 3. The change in geometry around the catecholborane induces a marked change in Lewis acidity as indicated by an increase in coordination to pyridine. Irradiation with 431 nm light causes recovery of the *E*-form, which shows small affinity to pyridine due to the coordination of the azo group to the boron centre. These results demonstrated that the complexation ability of a catecholborane can be reversibly changed by photoirradiation.

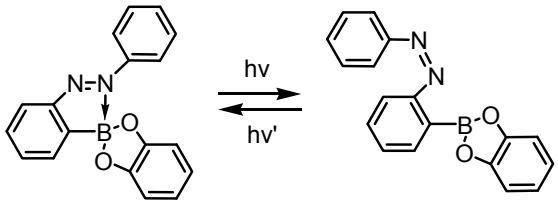

Scheme 4.1.1 Photoswitching of the Lewis acidity of a catecholborane derivative tethered to a photochromic azobenzene moiety. Lewis acidity is lower in **(*E*)-CatB** than in **(*Z*)-CatB** due to the interaction of the boron centre with the nitrogen atom.

However, this approach has several drawbacks, inherent to the use of the azo group as the photoswitchable unit. (1) The photostationary state is small (50 % in the best case) and limits the extent of the changes in acidity. (2) Tuning the wavelength at which the photoisomerisation takes place is not trivial with this system. (3) The rate of photoisomerisation from *E* to *Z* is reduced by the coordination of the photoresponsive unit to the boron centre in the *E*-form. (4) The addition of a stronger Lewis base could displace the azo group in the *E*-form, inhibiting the change in Lewis acidity; the intrinsic Lewis acidity of the boron centre is not affected by the switching event, only its coordination number changes.

4.1.4 Boron and DTE derivatives

The characteristics of the dithienylethene (DTE) architecture[17-22] should make it a promising candidate for the photoregulation of Lewis acidity using a molecular switch. Boron chemistry has always been closely linked to DTE derivatives since their discovery in the late 1980's and early 1990's. The palladium(0) promoted coupling of arylbromides with arylboronic acids permits the preparation of various functional DTE derivatives.[22,130,173]

Boronic acids are useful units for the recognition of sacharrides with important roles in biological systems. As briefly discussed in *Chapter 1*, Irie and co-workers have shown the first example of photochromic saccharide tweezers using a diarylethene functionalised with boronic acid groups as shown in Scheme 4.1.2.[30] In its ring-open form, the flexibility of the photoswitch allows the capture of glucose through the formation of a 1:1 complex in which the two boronic acid groups face each other to bind the sugar. In contrast, in the rigid, ring-closed isomer, the boronic acid groups are separated and cannot form the complex. The lack of photochromic reactivity of the ring-open form of the switch in the presence of glucose also supports the formation of a "tweezer" type 1:1 complex, but is an important drawback limiting reversible modulation of binding affinity.

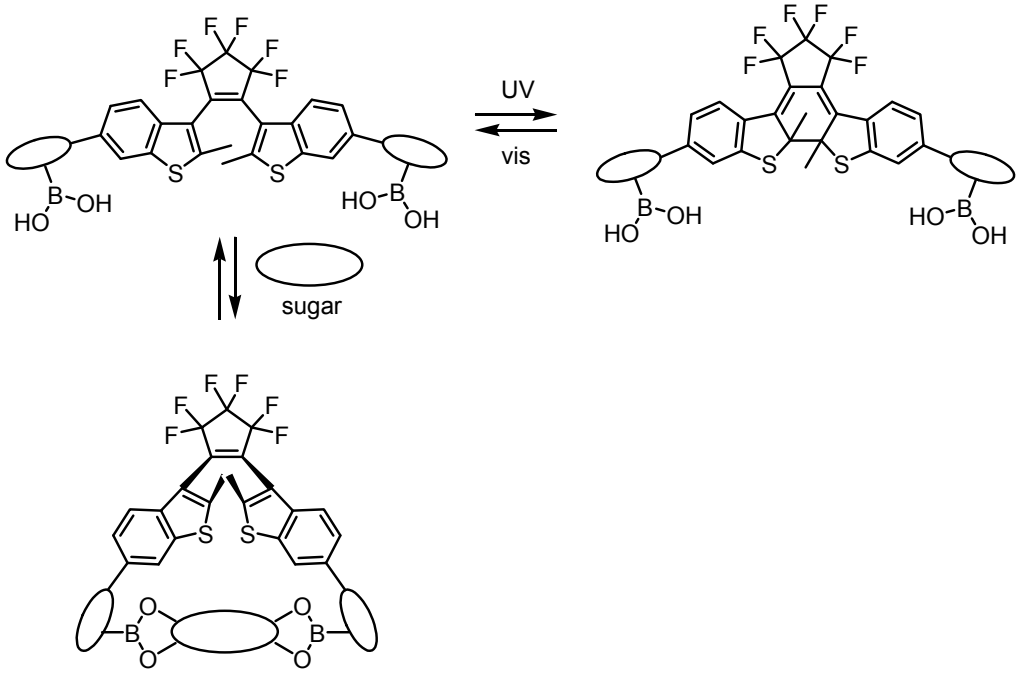

Scheme 4.1.2 Saccharide tweezers based on the DTE architecture. The binding affinity of the ring-open form is larger than that of the ring-closed form due to the capability of the molecule to form a tweezer-like complex.[30]

More recently, Huang and Li have prepared organoboron-based DTE derivatives whose photochromic properties are modulated by fluoride ions as shown in Scheme 4.1.3.[64,65] The molecular design allows the vacant p-orbital on the boron to contribute to the delocalisation of the π-system of the molecular switch. The addition of fluoride anions, a boron-coordinating ligand, disturbs the p-π conjugation between diarylethene and the boron centre, blue-shifting its spectral absorption. The absorption maximum of the photostationary state shifts from 655 nm to 490 nm upon addition of the anion. However, no change in the Lewis acid strength between the two photoisomers of these systems has been reported.[64,65]

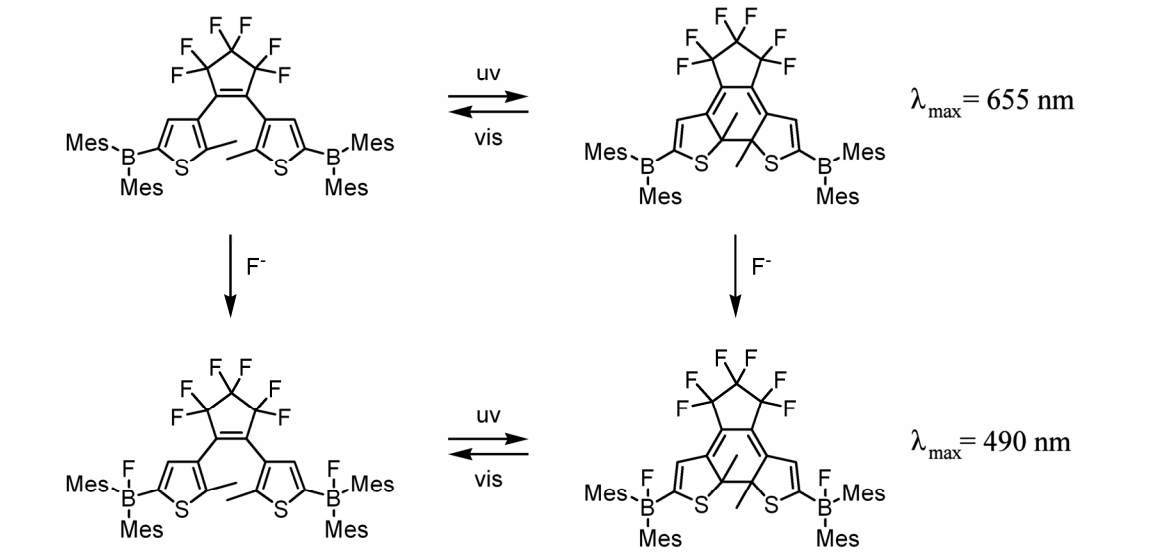

Scheme 4.1.3 Photoswitchable organoboron-based dithienylethene fluoride sensor where Mes = 2,4,6-trimethylbenzene. The spectral properties of both photoisomers are affected by the presence of fluoride.[64]

The objective of the next section of this chapter is to present a novel approach toward the modulation of Lewis acidity using the DTE backbone as the switching unit, potentially affecting the intrinsic Lewis acidity of a boron centre.

4.2 Proposed approach for the modulation of Lewis acidity using a boron-containing DTE derivative

As discussed in *Chapter 1*, there are a scattered few examples describing how the electronic and geometric changes that accompany the photoreactions of the DTE architecture can be used to regulate chemical reactivity and catalysis. However, these systems exhibit only small observable effects, and in most cases, the presence of the reactive substrate significantly reduces the photoactivity of the DTE system. In *Chapter 2* and *Chapter 3*, it was demonstrated that by taking advantage of the photoinduced rearrangement of the π-bond in the central 5-membered ring of the DTE system, more dramatic changes in the reactivity of the photoisomers can be demonstrated. In a well-designed system, the electronic changes localised within the central cyclopentene ring are more significant than the often too subtle electronic and steric differences between the thiophene heterocycles in the ring-open and ring-closed DTE isomers. In this chapter the same concept is applied to the modulation of Lewis acidity.

4.2.1 Description of the approach for the modulation of Lewis acidity using boron-containing DTE derivatives

The central 5-membered ring in compound **DTE-o** (highlighted in bold in Figure 4.2.1) is a 1,3,2-dioxaborole system whose Lewis acidity could be significantly and reversibly modulated using two different wavelengths of light. By analogy with the aromatic imidazoles, oxazoles, and thiazoles, also represented in Figure 4.2.1, the 1,3,2-dioxaborole in this ring-open DTE derivative is a planar, conjugated system of overlapping p-orbitals containing 4n+2 π-electrons.[174] It is therefore expected to have some aromatic character and a low Lewis acidity due to the p-orbital of the boron atom being partially occupied by the delocalised π-electrons.

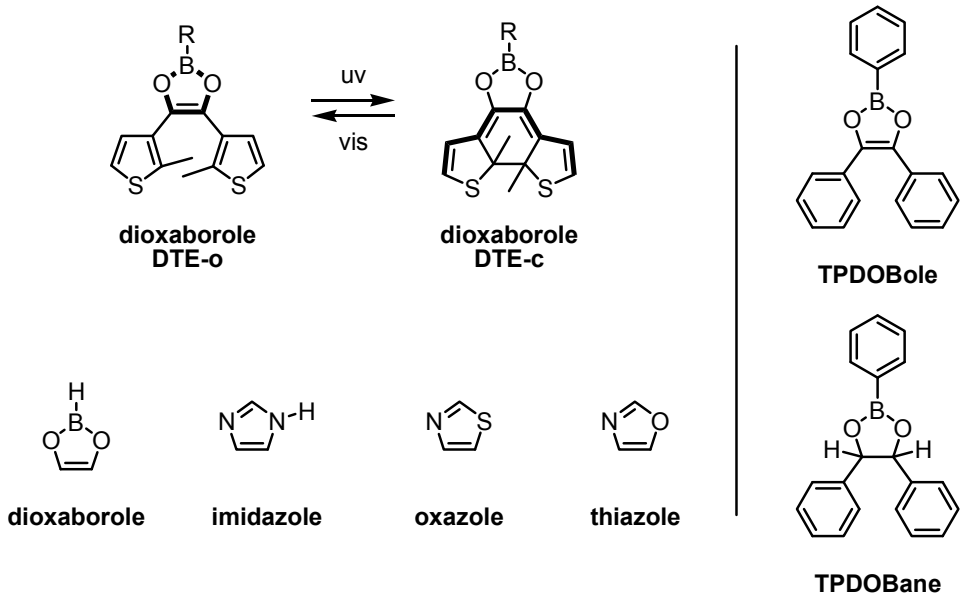

Figure 4.2.1 A photoswitchable 1,3,2-dioxaborole-containing DTE derivative with two analogues (TPDOBole and TPDOBane). The dioxaborole architecture is depicted with other aromatic 5-membered ring heterocycles.

Studies on 2,4,5,-triphenyl-1,3,2-dioxaborole (**TPDOBole**) also suggest that the dioxaborole system might possess some degree of aromatic character.[175,176] This compound exhibits an unusually high resistance towards hydrolysis for an ester of a boronic acid. Moreover, its UV-vis absorption spectrum cannot be explained as merely due to the cis-stilbene portion of the molecule; the absorption spectrum of **TPDOBole** in cyclohexane is red-shifted by 30 nm compared to 2,4,5,-triphenyl-1,3,2-dioxaborolane (**TPDOBane**), which possesses a saturated 5-membered ring, suggesting a strong interaction between the six π-electrons in the 1,3,2-dioxaborole system.[175,176] Additionally, changing the solvent from cyclohexane to ethanol causes a spectral blue-shift of about 30 nm that can be explained as resulting from coordination of the boron centre with the alcohol, thus removing the boron from the π-electron system.[176]

Irradiation with UV light should trigger the cyclization of **DTE-o** to generate **DTE-c**, where the borate group is cross-conjugated with the linear π-backbone of the molecule (highlighted in bold in Figure 4.2.1). This rearrangement of π-electrons should reduce the amount of electron density at the boron centre and turn the Lewis acidity "on". The system could be turned "off" again using visible light to reverse the cyclization reaction and regenerate the aromatic dioxaborole ring system.

4.2.2 Proposed architecture for a boron-containing DTE derivative

In order to demonstrate the previously described concept of photomodulation of Lewis acidity using a DTE derivative, compound **4.1** was targeted (Scheme 4.2.1). Derived from **DTE-o**, compound **4.1** possesses both a boron centre part of the 1,3,2-dioxaborole unit and a 1,3,5-hexatriene functionality. This architecture should allow the reversible modulation of the Lewis acid character of the boron using light of the appropriate wavelengths.

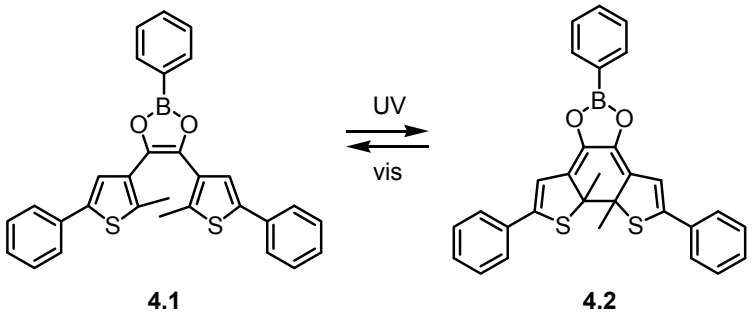

4.1 **4.2**

Scheme 4.2.1 Targeted system incorporating a 1,3,2-dioxaborole moiety in a 1,3,5-hexatriene functionality, and its predicted photochemistry.

The chemical structure of compound **4.1** is relatively simple and it should be straightforward to prepare from the condensation of phenyl boronic acid, which is

commercially available, and the appropriate hydroxyketone. Moreover, the external positions of the thienyl groups are functionalised with phenyl groups, which usually leads to DTE derivatives showing good resistance to damages from irradiation and having high photostationary states.[22] These characteristics make compound **4.1** a good candidate for this project.

4.3 Results and discussion

4.3.1 Computational investigation of the ring-open and ring-closed boron-containing DTE derivatives

In order to qualitatively verify the initial predictions, calculations at the AM1 semi-empirical level of theory were performed for compounds **4.1** and **4.2** using HyperChem Release 7.1 (details are presented in Section 4.5.8). Computational investigations estimated that the ring-open isomer **4.1** is considerably lower in energy than its ring-closed counterpart with an energetic preference of 26.1 kcal/mol. Figure 4.3.1b-c shows a comparison of the lowest unoccupied molecular orbitals (LUMOs) for both photoisomers and reveals that there is orbital density on the boron atom only in isomer **4.2**. This is indicative that there should be a difference in the Lewis acidic nature of the two isomers. Determination of the Mulliken charge of the boron centre for both isomers gives a more positive value for the ring-closed form **4.2** (0.273) than for the ring-open form **4.1** (0.208). The difference in charge density is also apparent when comparing the electrostatic potential map shown in Figure 4.3.1d-e. These results are all indicative of a more Lewis acidic ring-closed isomer.

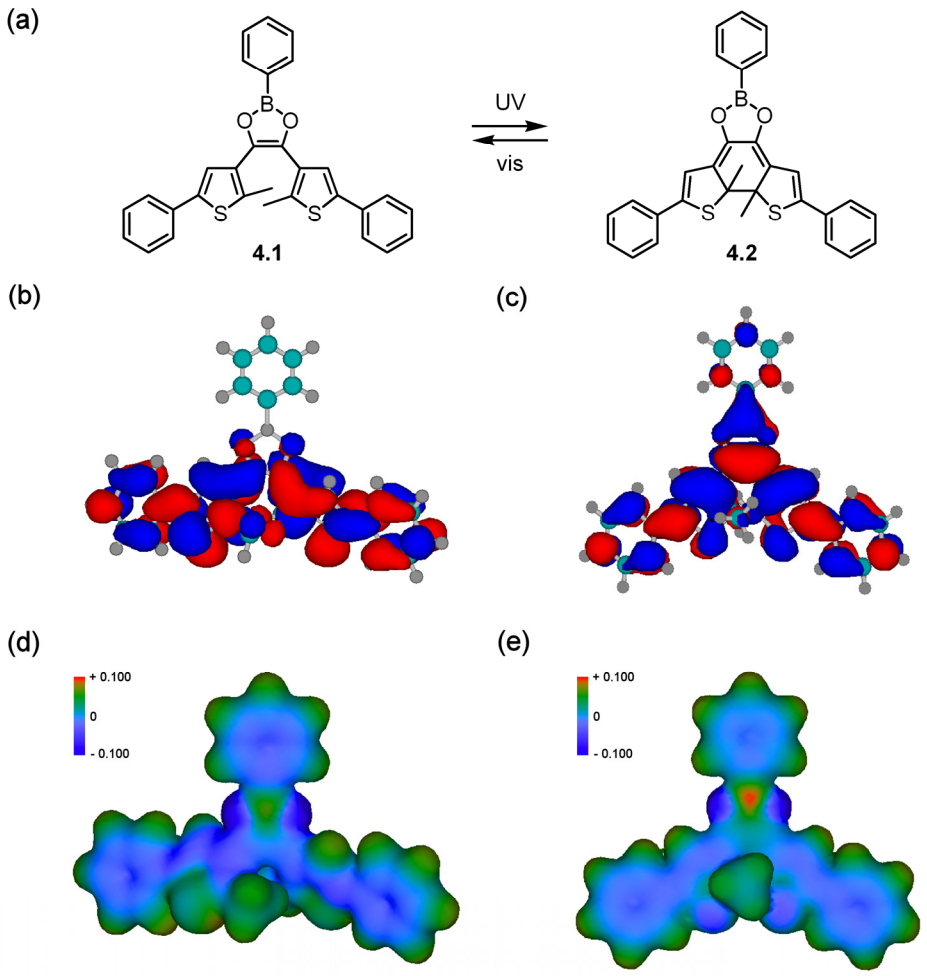

Figure 4.3.1 (a) Expected reversible photocyclization of the ring-open isomer **4.1** to generate the ring-closed isomer **4.2**. (b-e) Computational investigation at the AM1 level of theory for the boron-containing DTE. Orbital density of the LUMO for (b) the ring-open form **4.1** and (c) the ring-closed form **4.2**. Electrostatic potential 3D map for (d) the ring-open form **4.1** and (e) the ring-closed form **4.2** showing a more positive charge at the boron centre for the ring-closed isomer.

In order to have more accurate computational results, calculations were also performed at a higher level of theory in collaboration with Dr. Kim K. Baldridge of the University of Zürich. Computational investigations were first performed on a simplified version of isomers **4.1** and **4.2** (the three phenyl rings were removed). It was estimated that the ring-open form **4.1s** is considerably lower in energy than its ring-closed counterpart **4.2s**, with an energetic preference of 19.0 kcal/mol, calculated at the

M06-2X/DZ(2d,p) level of theory. As anticipated, the molecular orbitals of **4.1s** are part of a conjugated π-orbital system that includes delocalisation within the dioxaborole ring. A comparison of the lowest unoccupied molecular orbitals shows that there is orbital density on the boron atom only in isomer **4.2s**, an initial indication that there should be a difference in the Lewis acidic nature of the two isomers. Other calculated values support the prediction, including the ionisation potentials for **4.1s** and **4.2s**, which are calculated to be 6.90 and 6.03 eV, respectively, the difference in charge distribution on the boron established with a variety of different analyses, and calculations on the reduced forms of the two isomers, which show the preference for ring-open over ring-closed drops to only a few kcal/mol.

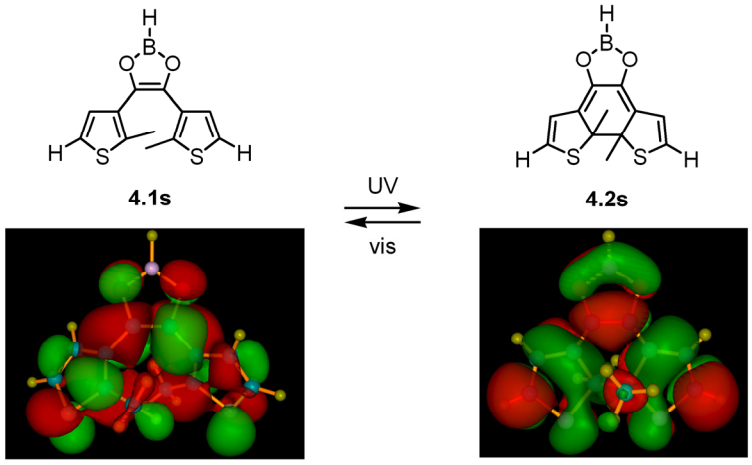

Figure 4.3.2 Computational investigation at the M06-2X/DZ(2d,p) level of theory for the boron-containing DTE. Orbital density of the LUMO for the ring-open form **4.1** and the ring-closed form **4.2**.

Computational structures and properties of the ring-open and ring-closed isomers, **4.1** and **4.2** calculated at the M06-2X/DZ(2d,p) level of theory, are very similar to those already described for the simplified versions, with the former isomer being preferred over

the latter by 18.0 kcal/mol. The molecular orbitals of **4.1** and **4.2** also show similar features to those of the simplified versions. The ionisation potentials of **4.1** and **4.2** are slightly lower, at 5.95 and 4.72 eV, respectively. The reduced forms of compounds **4.1** and **4.2** bring the ring-closed isomer lower in energy than the ring-open form by approximately 5 kcal/mol.

Overall, the computational results are in agreement with the initial prediction of a more Lewis acidic ring-closed photoisomer and suggest that this system is well-designed for the demonstration of photogated reactivity.

4.3.2 Synthesis of the boron-containing DTE derivative

Compound **4.1** was prepared by condensing hydroxyketone **4.3** and phenylboronic acid under azeotropic reflux conditions as illustrated in Scheme 4.3.1.[177]

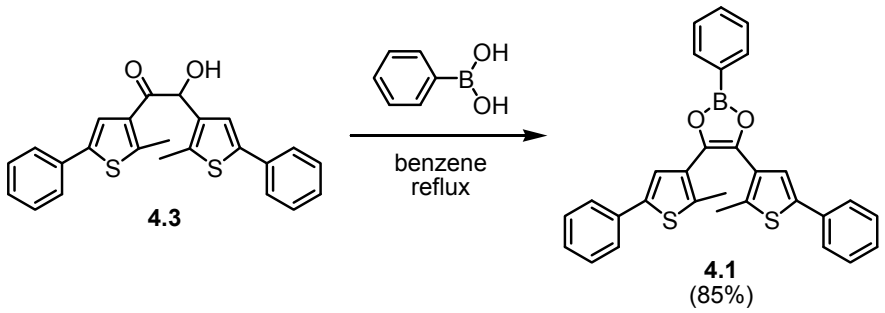

Scheme 4.3.1 Synthesis of the boron-containing DTE derivative **4.1**.

Attempts by previous members of the Branda group to synthesise compound **4.3** using classical benzoin condensation conditions (cyanide ion, water/ethanol) had failed.[178] However, a compound similar to **4.3** has been reported, as discussed in *Chapter 2*, and suggests a route to prepare **4.3** as shown in Scheme 4.3.2.[78,79] Acylation of the known compound 2-methyl-5-phenylthiophene[179] **4.6** with acetic anhydride and

$SnCl_4$ in benzene afforded the acetylthiophene **4.7**. Oxidation of **4.7** with selenium dioxide (SeO_2) gave the acetaldehyde **4.8** in modest yield and subsequent acylation of **4.6** with **4.8** and $SnCl_4$ in benzene afforded hydroxyketone **4.3** with an overall yield of 8%.

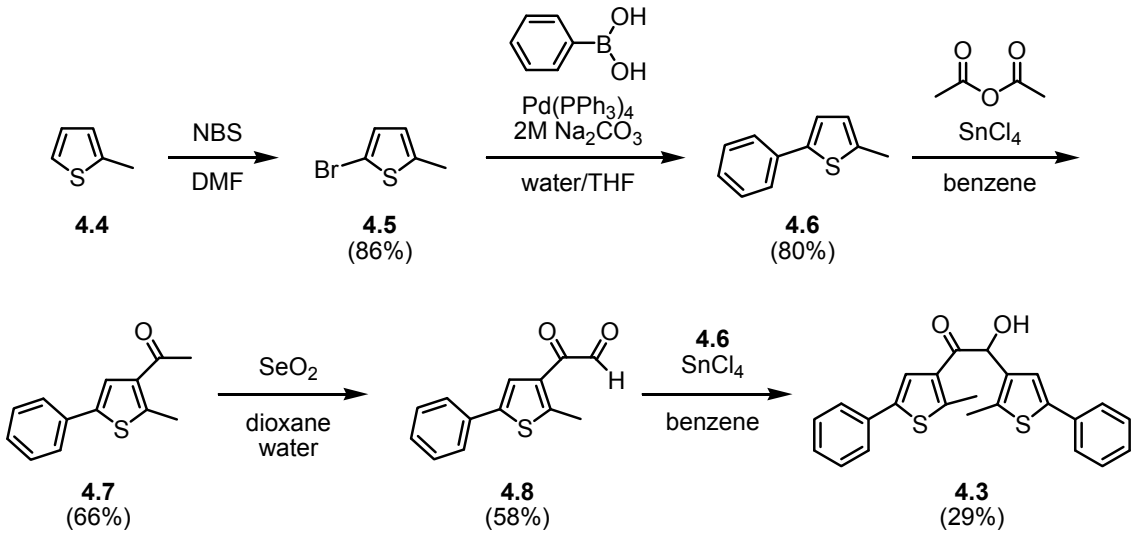

Scheme 4.3.2 Synthesis scheme for the preparation of hydroxyketone **4.3**.

Although this synthetic route allows the preparation of the hydroxyketone **4.3**, the overall yield is low, toxic reagents such as $SnCl_4$ and SeO_2 are required, and compound **4.8** has a very strong and disagreeable odour. To improve the synthesis of **4.3**, a new method was developed, as shown in Scheme 4.3.3. When the known aldehyde[179] **4.11** is treated with 3-benzyl-5-(2-hydroxyethyl)-4-methylthiazolium chloride, the hydroxyketone **4.3** is produced. Although the product is only generated in relatively small amounts, the major compound isolated is the starting aldehyde, which can be resubjected to the reaction conditions. The result is a convenient way to prepare large amounts of compound **4.3** and thus, potentially, the boron-containing derivative **4.1**.

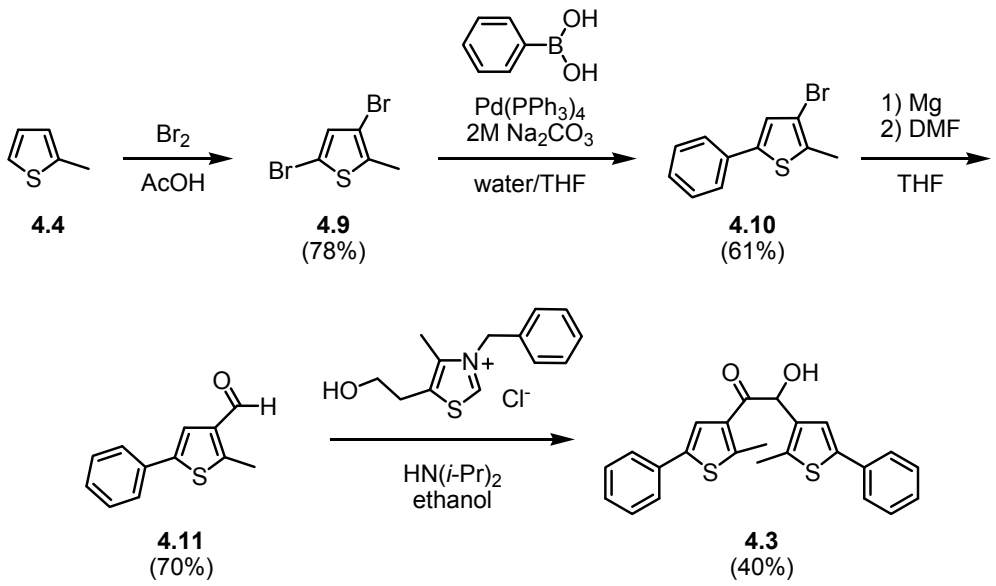

Scheme 4.3.3 Improved synthetic procedure for the preparation of hydroxyketone **4.3**.

As is common with dioxaborole derivatives,[174-177] solutions of **4.1** are easily oxidised in air to yield the diketone version of **4.3** as the deborylation product. In comparison, anhydrous and degassed solutions are highly stable. ^{11}B NMR spectroscopy of **4.1** in benzene-d_6 shows a chemical shift of 31.4 ppm relative to BF_3OEt_2, a result in agreement with a planar tricoordinated boron centre with a vacant p_z orbital.[149] Compound **4.1** was also characterised by means of ^{1}H NMR and ^{13}C NMR, UV-vis spectroscopy, mass spectrometry, and elemental analysis. The results are consistent with the structure shown in Scheme 4.3.1.

4.3.3 Photochromic properties of the boron-containing DTE derivative studied by UV-vis absorption spectroscopy

Irradiating a benzene solution (anhydrous and degassed) of compound **4.1** with 312 nm light causes a change in colour of the solution from colourless to purple, which is consistent with the occurrence of the photocyclization reaction generating the ring-closed

isomer **4.2** having an extended π-conjugated backbone. It was immediately observed that the ring-closed photoisomer **4.2** is significantly more sensitive to oxidation than its ring-open counterpart. All irradiation studies were performed in anhydrous and oxygen-free atmosphere. The corresponding UV-vis absorption spectra show trends typically observed for ring-closing reactions of dithienylethene derivatives as shown in Figure 4.3.3b.

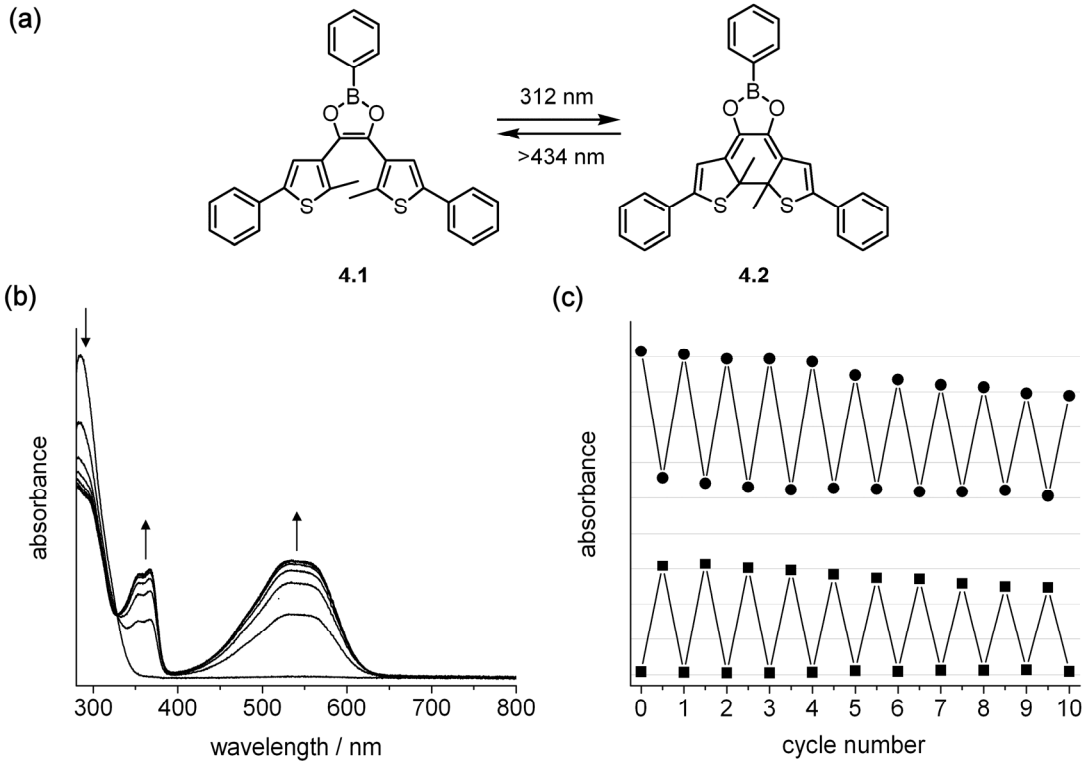

Figure 4.3.3 (a) Reversible photocyclization of the ring-open isomer **4.1** generating the ring-closed isomer **4.2**. (b) Changes in the UV-vis absorption spectra of a dichloromethane solution (3.3×10^{-5} M) of **4.1** upon irradiation with 312 nm light until no further increase in the absorption band at 535 nm was observed at PSS. Total irradiation periods are 0, 2, 4, 6, 8, 10, 12, and 14 s. (c) Photochemical cycling study of a dichloromethane solution (2.5×10^{-5} M) of the boron-containing DTE derivative between its ring-open form **4.1** and its ring-closed form **4.2**. The figure shows the changes in the absorptions at 285 nm (black circles) and 535 nm (black squares) during alternate irradiation at 312 nm for 16 s and at wavelengths greater than 434 nm for 30 s.

The high-energy bands in the spectra become less intense as a broad band centred at 535 nm appears. At a concentration of 3.3 x 10^{-5} M (in benzene-d_6), a photostationary state was reached within 12 seconds. The ring-closed isomer is stable at room temperature and irradiating the solution of compound **4.2** with visible light of wavelengths greater than 434 nm regenerates the original UV-vis spectrum corresponding to compound **4.1** indicative of the occurrence of the ring-opening reaction. However, alternate irradiation with 312 nm light and with light of wavelengths greater than 434 nm for 10 cycles reveals signs of degradation as the intensity of the bands assigned to the ring-open isomer **4.1** and the ring-closed isomer **4.2** decrease after each successive irradiation (Figure 4.3.3c). Two main causes could explain this phenomenon: (1) compound **4.1** and **4.2** form side products when irradiated as described in Section 1.3.4,[24-28] or (2) residual oxygen reacts with **4.1** and **4.2** causing deborylation of the compounds.[177]

4.3.4 Photochromic properties of the boron-containing DTE derivative studied by ^{1}H NMR spectroscopy

The photochemical reaction of the boron-containing DTE derivative was also monitored using ^{1}H NMR spectroscopy. When a solution of compound **4.1** in dichloromethane-d_2 (5.0 x 10^{-3} M) was exposed to 312 nm light at 22 °C, a new set of signals assigned to the ring-closed isomer (**4.2**), appears as shown in Figure 4.3.4b-c. The mole fractions of ring-open **4.1** and ring-closed **4.2** isomers were obtained by integrating the peaks corresponding to signals ‘a’ and ‘j’. These studies were carried out in the absence of an internal standard because the ^{1}H NMR spectra showed very little signs of degradation. Using the mole fractions, it is possible to monitor the conversion of **4.1** in

4.2 over time. After 65 minutes of irradiation with 312 nm light, a photostationary state of 81% was reached as shown in Figure 4.3.4d.

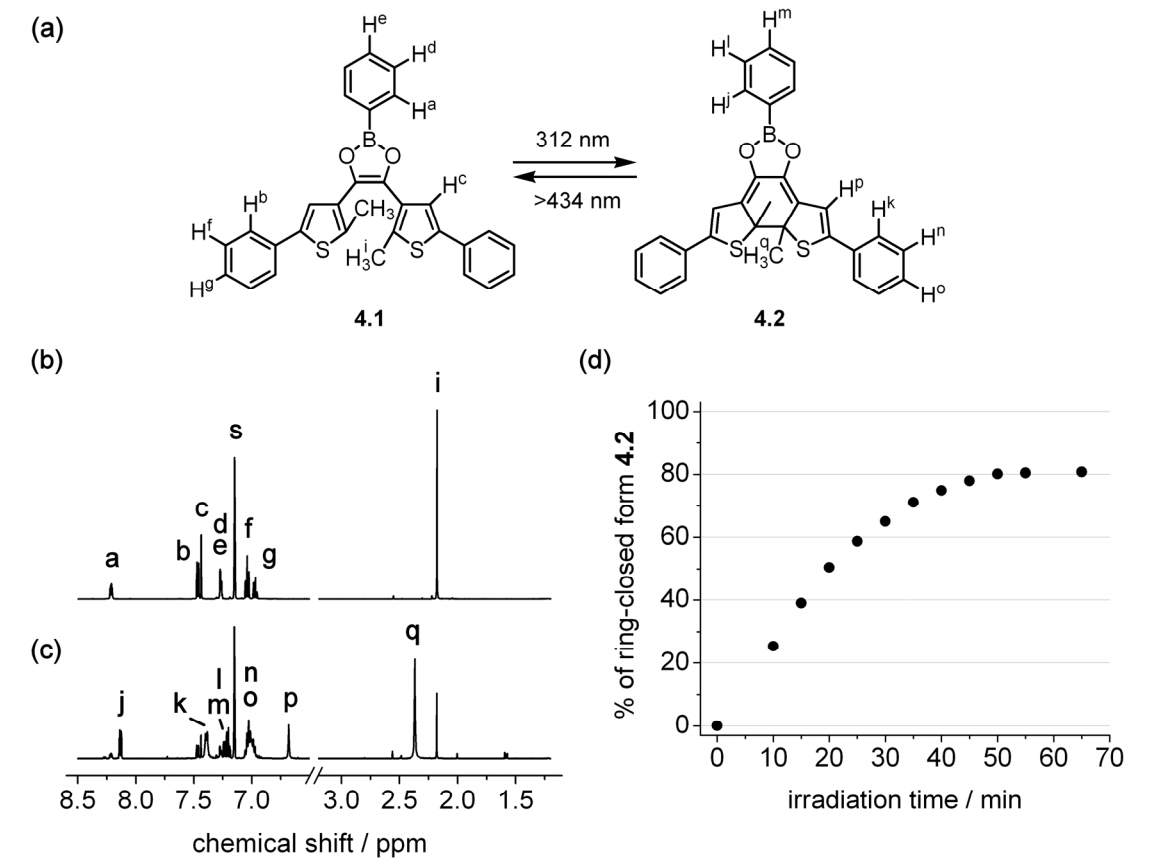

Figure 4.3.4 (a) Reversible photocyclization of the ring-open isomer **4.1** generating the ring-closed isomer **4.2**. (b-c) ^{1}H NMR spectra (500 MHz) of a benzene-d_6 solution (5.0 x 10^{-3} M) of the ring-open isomer **4.1** (b) before irradiation and (c) after irradiation with 312 nm light for 65 min to produce the ring-closed isomer **4.2** at the PSS. Peaks labelled 'a'-'i' are assigned to **4.1**, peaks 'j'-'q' to **4.2**, and peak 's' to the residual solvent. (d) Percent conversion of **4.1** into **4.2** as a function of the irradiation time with 312 nm light.

The first experimental evidence supporting the hypothesis set forth in Section 4.2.1 of this chapter is provided by comparing the peaks observed in the ^{1}H NMR spectra corresponding to the phenyl-ring protons directly adjacent to the boron atom (H^a and H^j in Figure 4.3.4) in isomers **4.1** and **4.2**. The upfield shift (~ 0.1 ppm) observed for these peaks upon ring-closure (Figure 4.3.4b-c) is in agreement with a loss in aromatic

character of the dioxaborole unit as **4.1** is converted to **4.2**. This shift can be expected for protons that were originally lying within the combined deshielding regions of two ring systems having aromatic character (the benzene and the dioxaborole in compound **4.1**) but now feel the effect of only one (the benzene in compound **4.2**). Moreover, the signals attributed to the ring-closed isomer **4.2** are relatively broad (Figure 4.3.4c). This peak broadening might be the result of an interaction with the solvent, an impurity, or other **4.2** molecules through self-association. Additional experimental evidence supporting a more Lewis acidic **4.2** compared to **4.1** is its instability towards oxidation; a better Lewis acid is more susceptible to interactions with molecular oxygen leading to its oxidation.

Another ^{1}H NMR experiment was conducted to study the degradation of the system. As shown in Figure 4.3.5, a selected region of the ^{1}H NMR spectrum of the ring-open isomer **4.1** in benzene-d_6 contains a two-proton signal at 8.22 ppm (peak 'a') that is attributed to the phenyl-ring protons directly adjacent to the boron atom (proton H^a). When a dried and deoxygenated solution of **4.1** is exposed to 312 nm light for 10 minutes, a new signal at 8.13 ppm (peak 'b') appears. This signal is attributed to the same proton on the ring-closed isomer **4.2** (proton H^b). When a solution of **4.1** is irradiated for 10 minutes in normal benzene-d_6 (not degassed and dried), two new sets of signals appear in addition to those of the ring-closed isomer **4.2**. Peak 'c' at 8.27 ppm perfectly overlap with the signal of the phenyl-ring protons directly adjacent to the boron atom of pure phenyl boronic acid solutions (proton H_c) and peak 'd' at 7.73 ppm perfectly overlaps with the signal of pure diketone **4.12**.

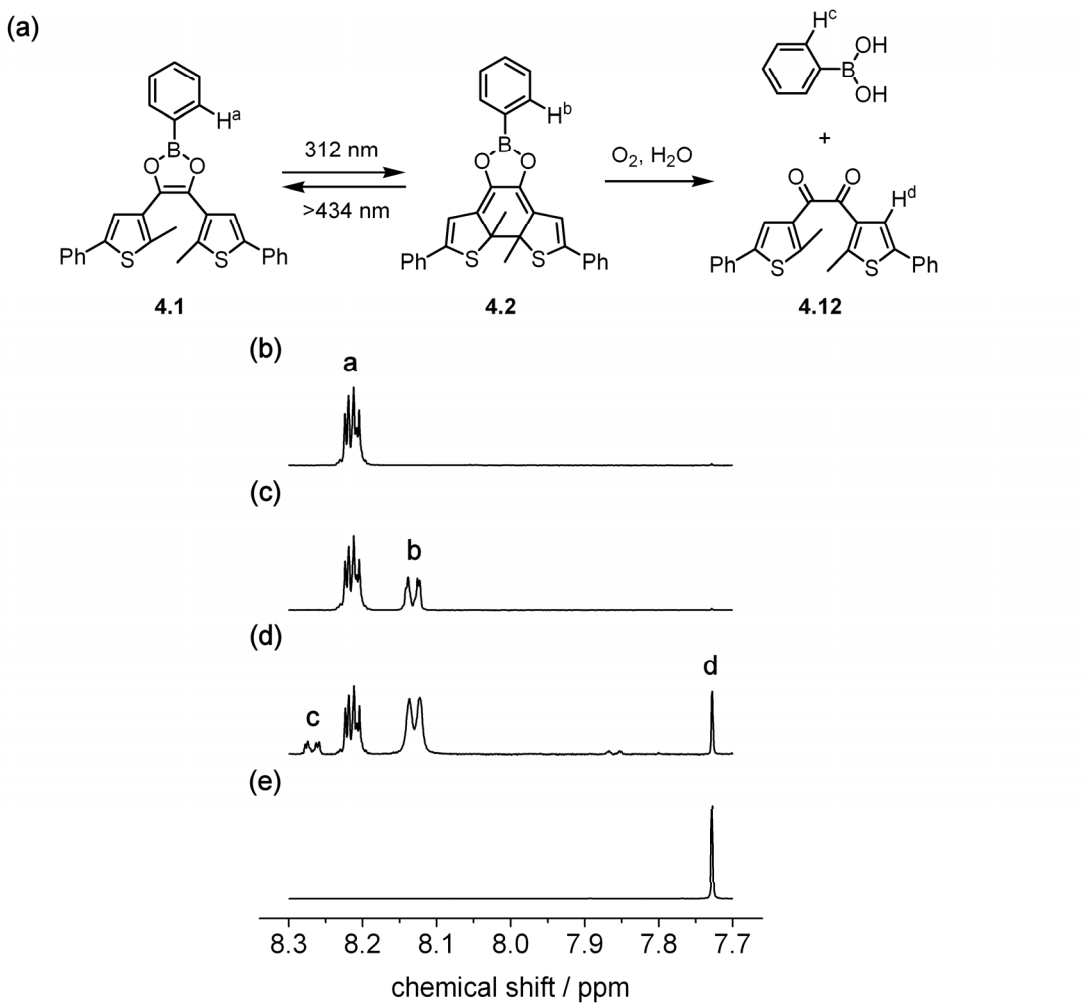

Figure 4.3.5 (a) Reversible photocyclization of the ring-open isomer **4.1** generating the ring-closed isomer **4.2** and possible degradation products. (b-e) ^{1}H NMR spectra (500 MHz) of a benzene-d_6 solution (5.0×10^{-3} M) of the ring-open isomer **4.1** (b) before irradiation and after irradiation with 312 nm light for 10 min in (c) dried and deoxygenated solvent and in (d) solvent not dried and deoxygenated. (e) Spectrum of pure **4.12** prepared by oxidation of the hydroxyketone **4.3**.

4.3.5 A general introduction to the determination of Lewis acidity

The relative Lewis acidity of a compound can be evaluated by measuring its respective binding affinity to a Lewis base. Throughout the next sections, the Lewis acidic moiety will be referred to as the host (H), the Lewis base as the guest (G) and their Lewis complex as the complex (C). For the formation of a 1:1 binding complex between one host and one guest, Equation 4.3.1 describes the equilibrium.

Equation 4.3.1 Complex (C) formation between a host (H) and a guest (G) at equilibrium.

The binding constant (K), also known as the equilibrium constant or the association constant, is a stability constant for the formation of the complex. It is based on the concentration of the host, the concentration of the guest, and the concentration of the complex ([H], [G], and [C] respectively) at equilibrium as expressed by Equation 4.3.2. Thus, determining the concentration of each species at equilibrium is essential to evaluate the binding constant of a host-guest complex.[180]

$$K = \frac{[C]}{[H] \times [G]}$$

Equation 4.3.2 Equilibrium constant (K) determination from the concentration of host ([H]), guest ([G]), and complex ([C]) at equilibrium.

Binding studies by NMR spectroscopy

Nuclear magnetic resonance (NMR) spectroscopy is an effective technique to determine the concentration of species in solution and is widely used for the evaluation of binding constants.[180] Nuclei involved in complex formation are generally partitioned

between two magnetically non-equivalent sites. Hence, a free host and a free guest should have different observables (e.g. chemical shifts) than their bound forms. The nature of the NMR signal depends on the complexation rate (k) and the decomplexation rate (k') as shown in Equation 4.3.3.

$$H + G \underset{k'}{\overset{k}{\rightleftharpoons}} C$$

Equation 4.3.3 Complex formation showing rates of reaction, k and k'.

Depending on the rate of exchange relative to the NMR timescale, the nature of the signal is divided in three categories: slow exchanges, fast exchanges, and coalescence. When the host-guest complexation equilibrium has a similar exchange rate compared to the NMR time scale, the NMR peaks broaden and/or disappear. This lineshape broadening results from the energy-time uncertainty principle.[180] When the equilibrium exchange occurs on the same timeframe as the NMR measurement, the energy of the transition cannot be precisely measured and the peak is broad (Figure 4.3.6d). In this case, the system is said to be at coalescence and it is impossible to determine the relative concentration of each species. For example, a typical resonance frequency difference between a bound and a free form is on the order of 100 Hz (0.2 ppm on a 500 MHz NMR spectrometer), which corresponds to a lifetime of 0.01 s. To be able to measure a signal, the lifetime of the bound species needs to be much longer than 0.01 s (slow exchange) or much shorter (fast exchange).

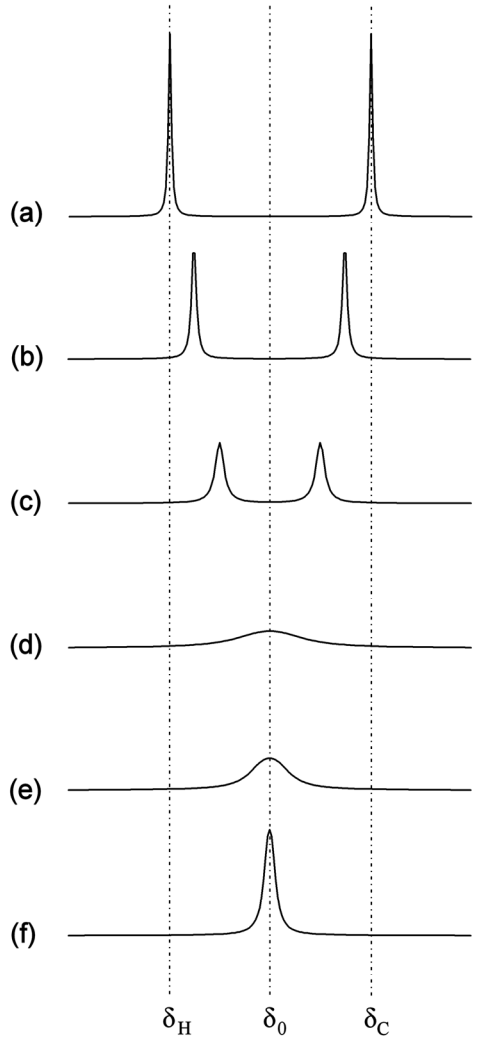

Figure 4.3.6 NMR signals of a hypothetical binding system formed from a host and a guest forming a complex. (a) Slow exchange limit. (b-c) Moderately slow exchange. (d) Coalescence. (e) Moderately fast exchange. (f) Fast exchange limit.

In slow exchanges, the host and the guest spend enough time in both of their states (free and bound) to be independently detected during the NMR experiment (Figure 4.3.6a); integration of the individual signals gives the relative occurrences of each state of the host and guest molecules. In fast exchanges, the complexation and decomplexation rate is too fast to obtain a signal for both states of the molecules; a single absorption band

is observed corresponding to the average of the signal of both species weighed by their concentration (Figure 4.3.6f).

Complexations with fast exchange rates

Organoboranes are known to form exclusively 1:1 binding complexes with pyridine.[145,147,148] Hence, the complex formation between a trivalent boron containing molecule as the host (H) and pyridine as the guest (G) can be described by Equation 4.3.1.

The binding constant (K), defined by Equation 4.3.2, can also be written in function of the initial concentration of host and guest, $[H]_t$ and $[G]_t$ (Equation 4.3.4), which are experimentally set. Solving Equation 4.3.4 for the concentration of complex ([C]) gives Equation 4.3.5.

$$K = \frac{[C]}{([H]_t - [C])([G]_t - [C])}$$

Equation 4.3.4 Equation relating the equilibrium constant (K) with the concentration of a complex ([C]) and the initial concentration of host ($[H]_i$) and guest ($[G]_i$).

$$[C] = \frac{\left([H]_t + [G]_t + \frac{1}{K}\right) \pm \sqrt{\left([H]_t + [G]_t + \frac{1}{K}\right)^2 - 4[H]_t[G]_t}}{2}$$

Equation 4.3.5 Equation 4.3.4 solved for the complex concentration at equilibrium.

The next step is to relate the concentration of complexed host to the NMR measurements. In the fast exchange limit, the exchange rate between the free and bound forms is much faster than the frequency difference between the two. Under these

conditions, a single averaged peak is observed for corresponding nuclei in the free and bound species. The observed chemical shift (δ) appears as the weighted average chemical shift of the free host (δ_h) and the complexed host (δ_c) as expressed by Equation 4.3.6, where P_h and P_c and the fractional populations of the free host and complexed host respectively.

$$\delta = P_h\delta_h + P_c\delta_c$$

Equation 4.3.6 The observed chemical shift (δ) appears as the weighted average chemical shift of the free host (δ_h) and the complexed host (δ_c), where P_h and P_c and the fractional populations of the free host and complexed host respectively.

The peak shifts progressively as the relative concentration of the two species changes. The fractional population of bound host P_c is equal to $[C] / [H]_t$ or 1 - P_h. Substitution of the respective fractional population of each species gives in Equation 4.3.6 and Equation 4.3.7, which can be written as a function of the complex concentration [C] as shown in Equation 4.3.8.

$$\delta = (1 - \frac{[C]}{[H]_t})\,\delta_h + \frac{[C]}{[H]_t}\,\delta_c$$

Equation 4.3.7 Substitution of the fractional population of free and bond host in Equation 4.3.6.

$$[C] = [H]_t \frac{(\delta - \delta_h)}{(\delta_c - \delta_h)}$$

Equation 4.3.8 Rearrangement of equation Equation 4.3.7.

Combining Equation 4.3.8 and Equation 4.3.5 relates a 1:1 binding constant to the NMR chemical shift in a fast exchange regime as shown in Equation 4.3.9 and Equation 4.3.10, after rearrangement.

$$[H]_t \frac{(\delta - \delta_h)}{(\delta_c - \delta_h)} = \frac{\left([H]_t + [G]_t + \frac{1}{K}\right) \pm \sqrt{\left([H]_t + [G]_t + \frac{1}{K}\right)^2 - 4[H]_t[G]_t}}{2}$$

Equation 4.3.9 Combining Equation 4.3.8 and Equation 4.3.5 relates a 1:1 binding constant to the NMR chemical shift in a fast exchange regime.

$$(\delta - \delta_h) = \left(\frac{(\delta_c - \delta_h)}{2}\right)\left[(1 + n + Q) \pm \sqrt{(1 + n + Q)^2 - 4Q}\right]$$

$$\text{where } Q = \frac{[G]_t}{[H]_t} \; ; \; n = \frac{1}{K[H]_t}$$

Equation 4.3.10 Rearrangement of Equation 4.3.9.

A titration curve, showing the chemical shift of the signal as a function of the guest concentration, can then be prepared. A two parameter fit of the titration curve with Equation 4.3.10 using a software such as Origin allows the determination of both the chemical shift of the complex (δ_c) and the association constant (K).[181]

4.3.6 Binding studies between the photoisomers of the boron-containing DTE derivative and pyridine

The relative Lewis acidity of the ring-open (**4.1**) and ring-closed photoisomers (**4.2**) can be evaluated by measuring their respective binding affinities to pyridine, a Lewis base. Figure 4.3.7 shows the changes in the peaks in the ^{1}H NMR spectra

corresponding to protons H_a as a benzene-d_6 solution of the ring-open photoisomer **4.1** (1.3×10^{-2} M) is treated with successive additions of a solution of pyridine in benzene-d_6 (1.0×10^{-1} M). There are minimal recordable spectral changes even after 10 equivalents of pyridine are added to the solution. Experimental details are presented in Section 4.5.6.

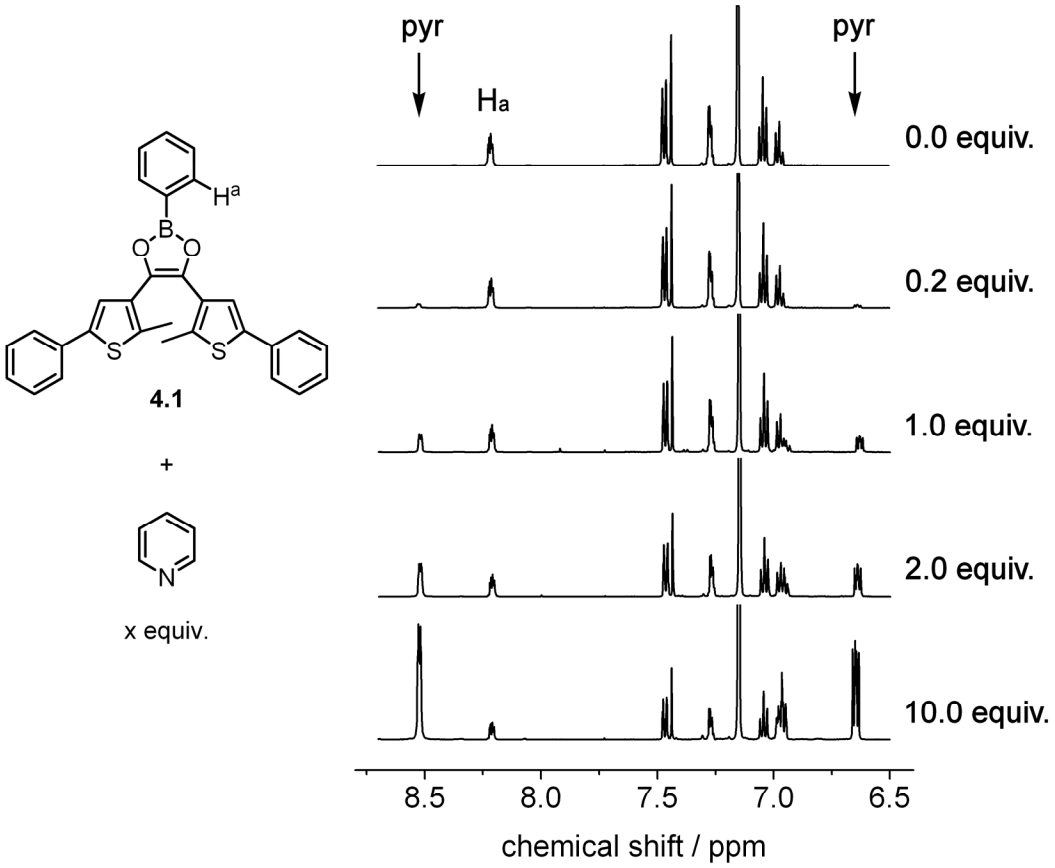

Figure 4.3.7 ^{1}H NMR titration of the ring-open isomer **4.1** with up to 10 equivalents of pyridine. The arrows indicate two of the pyridine signals. The signal attributed to proton H_a shows minimal shifting.

A similar ^{1}H NMR titration experiment was carried out to evaluate the binding affinity of the ring-closed isomer **4.2** to pyridine. In this case, a benzene-d_6 solution of the ring-open form **4.1** (5.3×10^{-3} M) was irradiated for 10 minutes with 312 nm light to afford 51% of the ring-closed photoisomer **4.2** (2.7×10^{-3} M) and the resulting solution

was treated with successive additions of a pyridine solution in benzene-d_6 (3.7×10^{-2} M). Figure 4.3.8 shows the changes in the signal in the ^{1}H NMR spectra corresponding to protons H_b of the ring-closed form **4.2** (peak 'b') as pyridine is added. The signal attributed to the ring-open form **4.1** (peak 'a') is unaffected by the presence of pyridine, whereas peak 'b' shifts upfield by more than 0.2 ppm. Figure 4.3.8 also shows the appearance of a new signal (peak 'c') attributed to the oxidation product of **4.2**, the diketone **4.12** described in section 4.2.5 and Figure 4.3.5. The decomposition of compound **4.2** during the course of the titration studies leads to changes in its concentration beyond the dilution caused by the addition of the pyridine solution. This phenomenon could be prevented by adding the pyridine solution in an oxygen-free atmosphere, which was not done due to the complications it entails.

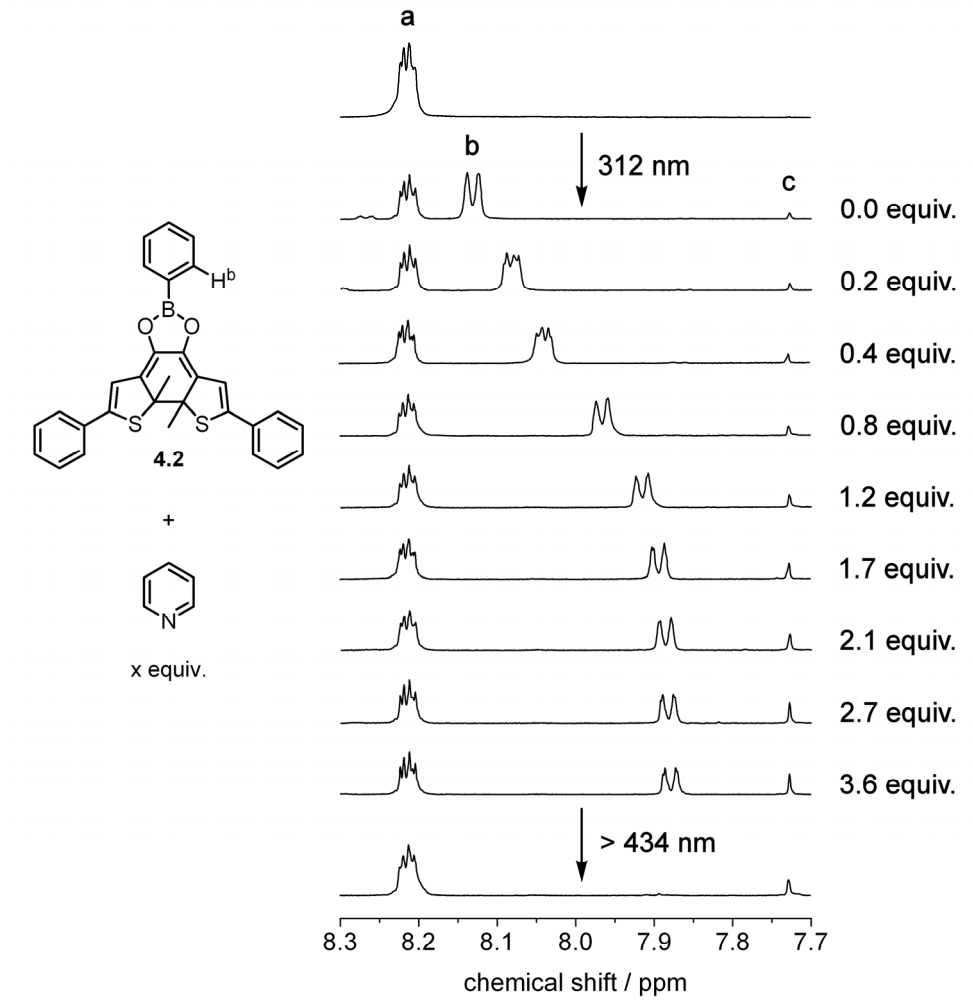

Figure 4.3.8 ^{1}H NMR titration of the ring-closed isomer **4.2** with up to 3.6 equivalents of pyridine. Peak 'b' is attributed to proton H_b of **4.2** and peak 'a' corresponds to the same proton on **4.1**. Peak 'c' is attributed to the oxidation product of **4.2**.

The observed signals are relatively sharp and the addition of pyridine to **4.2** causes them to shift, indicating that the binding between **4.2** and pyridine occurs in the ^{1}H NMR fast exchange limit. Under these conditions, the changes in chemical shift for **4.2** can be fit to the 1:1 binding model described in Section 4.3.5 and represented by Equation 4.3.10, giving an association constant of (7.0 ± 0.4) x 10^3 M^{-1} (full details are provided in Section 4.5.6), which is expected for dioxaborole derivatives.[171] Figure 4.3.9

shows the changes in chemical shift as a function of the equivalents of pyridine added to solutions of the ring-open (**4.1**) and ring-closed (**4.2**) photoisomers. Because of the small changes in chemical shift (0.003 ppm after 10 equivalents of pyridine added) in the case of **4.1**, an association constant could not be reliably estimated for this isomer. It can be assumed to be very small. Computational predictions performed by Dr. K. K. Baldridge at the M06-2X/DZ(2d,p) level of theory for the addition of pyridine to the ring-open and ring-closed isomers supports these results, with ΔE_{rxn} = 0.6 and 6.32 kcal/mol, respectively.

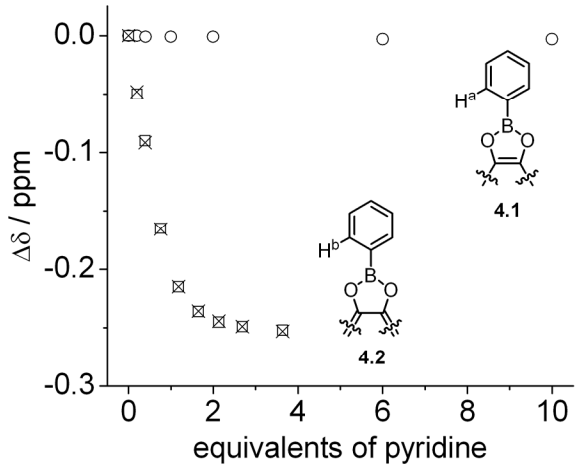

Figure 4.3.9 Change in the chemical shift of proton H_a in **4.1** (○) and H_b in **4.2** (□) as benzene-d_6 solutions (described earlier) are treated with pyridine. The calculated chemical shifts are also shown for **4.2** (×).

In order to demonstrate that the ring-open isomer **4.1** binds with pyridine even though a very weakly bound complex is formed, a ^{11}B NMR experiment was performed. As shown in Figure 4.3.10, the ^{11}B NMR spectrum of a solution of the boron-containing compound **4.1** in benzene-d_6 (1.6 x 10^{-1} M) contains only one broad signal at 31.4 ppm

relative to BF_3OEt_2, a result in agreement with a planar tricoordinated boron centre attached to two oxygen atoms and one carbon centre.[149]

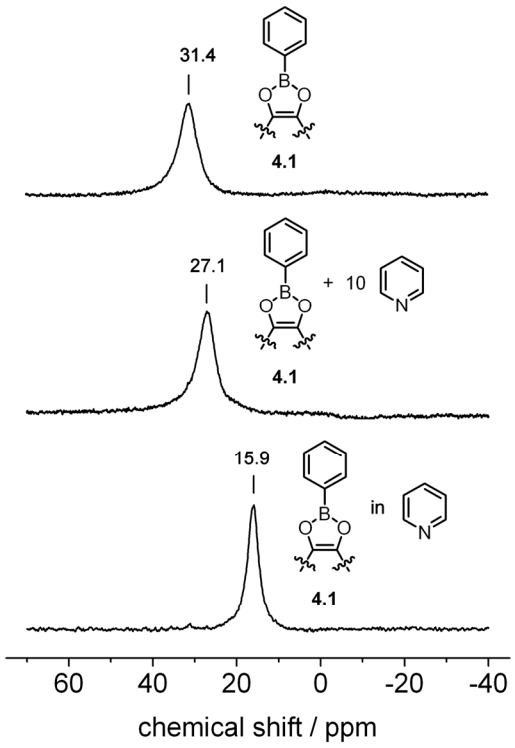

Figure 4.3.10 ^{11}B NMR spectra (192 MHz) of a benzene-d_6 solution of **4.1** (1.6 x 10^{-1} M) before (top) and after the addition of 10 equivalents of pyridine (middle) and of **4.1** in pyridine (bottom).

The addition of 10 equivalents of pyridine causes the boron signal to shift upfield to 27.1 ppm. Moreover, when a spectrum is recorded in pyridine, the boron signal for **4.1** shifts to 15.9 ppm. This change is consistent with a trigonal planar boron compound becoming tetrahedral upon binding with a guest.[149] For comparison, the ^{11}B NMR chemical shift of the catecholborane photoswitch described in Section 4.1.3, which has a boron environment similar to **4.1**, shifts from 30.8 ppm in benzene to 11.2 ppm in pyridine.[171]

Compound **4.1** seems to interact only weakly with pyridine even at fairly high concentration (1.6×10^{-1} M) since even after the addition of 10 equivalents of pyridine a shift of only 4.3 ppm is observed, whereas in pyridine the boron signal shifts by 15.5 ppm. In comparison, using a much more dilute solution of the ring-closed isomer **4.2** (2.7×10^{-3} M), a plateau is reached after the addition of 3 equivalents of pyridine, indicating that most molecules are bound, as shown in Figure 4.3.9.

When a mixture of compound **4.1**, compound **4.2** and approximately 1.1 molar equivalents of pyridine (relative to **4.2**) in benzene-d_6 is irradiated with visible light (wavelengths greater than 434 nm), the peaks in the ^{1}H NMR spectrum corresponding to hydrogen H_a in the complex **4.2**•pyridine shift from 7.91 ppm back to 8.22 ppm (Figure 4.3.11a), which corresponds to the ring-open isomer, illustrating the release of the pyridine from the complex. As shown in Figure 4.3.11b, alternatively irradiating the same solution with UV and visible light toggles the system between **4.2**•pyridine and compound **4.1** + pyridine. These results indicate that compound **4.1** retains its photochromic activity in presence of pyridine and shows selective, light-induced Lewis acid-base reactivity.

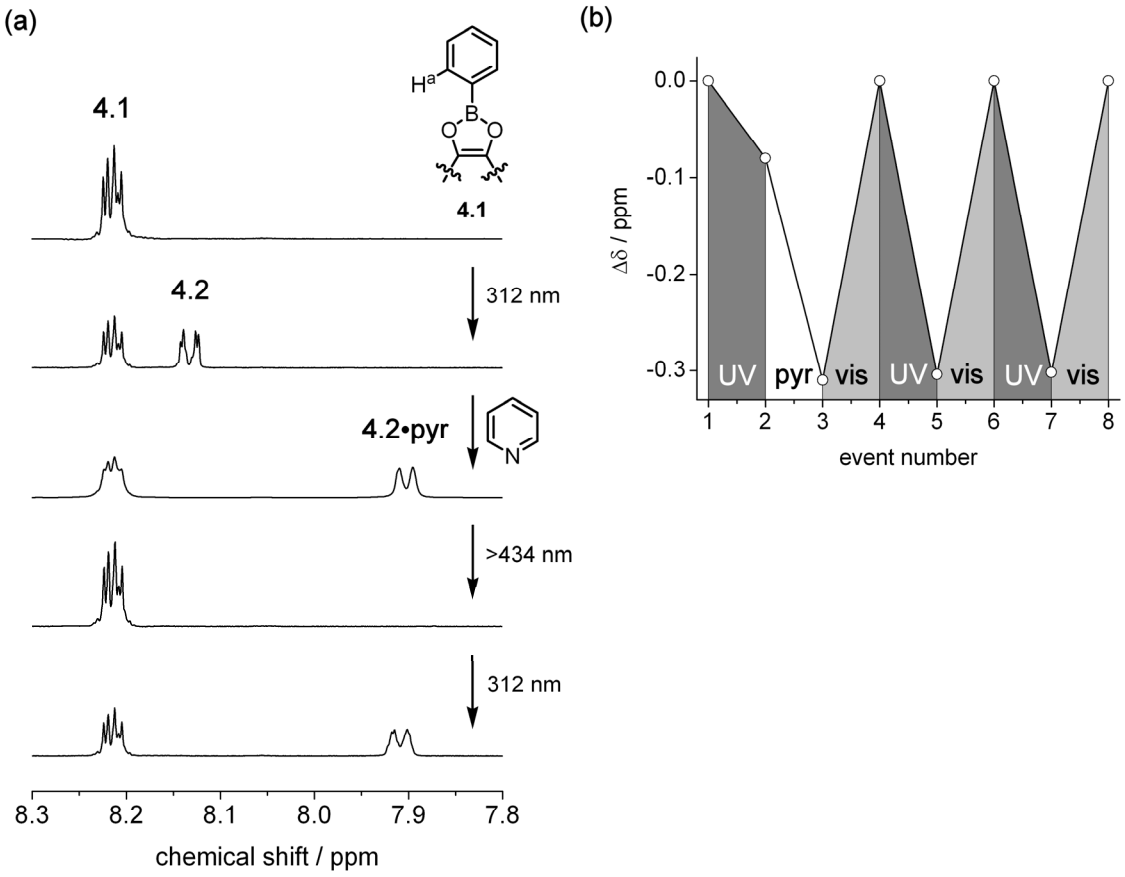

Figure 4.3.11 (a) ^{1}H NMR spectra (500 MHz) of a benzene-d_6 solution of **4.1** (9.7 x 10^{-3} M) before and after irradiation with 312 nm light for 10 min, after the addition of 1.1 equivalents of pyridine (1.1 x 10^{-2} M), after 7 min exposure to visible light (>434 nm), and after another 10 min exposure to 312 nm light. (b) Representation of the changes in chemical shift when the same solution is irradiated with UV light, treated with pyridine, and irradiated with alternating visible and UV light. UV (312 nm) irradiation periods are 10 min generating 40-45% of **4.2**. Visible (>434 nm) irradiation periods are 5-7 min to regenerate 100% of the ring-open isomer.

4.3.7 Gated photochromism of the boron-containing DTE derivative

Although the boron-containing molecular switch retains its photochromic activity in the presence of pyridine, the absorption maxima of the ring-closed isomer **4.2** in benzene is blue-shifted by 10 nm (from 535 nm to 525 nm) by the addition of 4.8 equivalents of pyridine as shown in Figure 4.3.12a. This phenomenon can be explained by the fact that the p-orbital of the boron is occupied when bound to pyridine, thus removing the contribution of this p-orbital from the observed transition.

Pyridine also affects the rate at which the photochemistry takes place. The rate constant for the ring-opening reaction in the presence and absence of pyridine was evaluated to be (0.029 ± 0.006) s^{-1} and (0.13 ± 0.02) s^{-1}, respectively (Figure 4.3.12b), showing that the ring-opening process is approximately 4 times slower in the presence of the Lewis base. Experimental details are presented in Section 4.5.7.

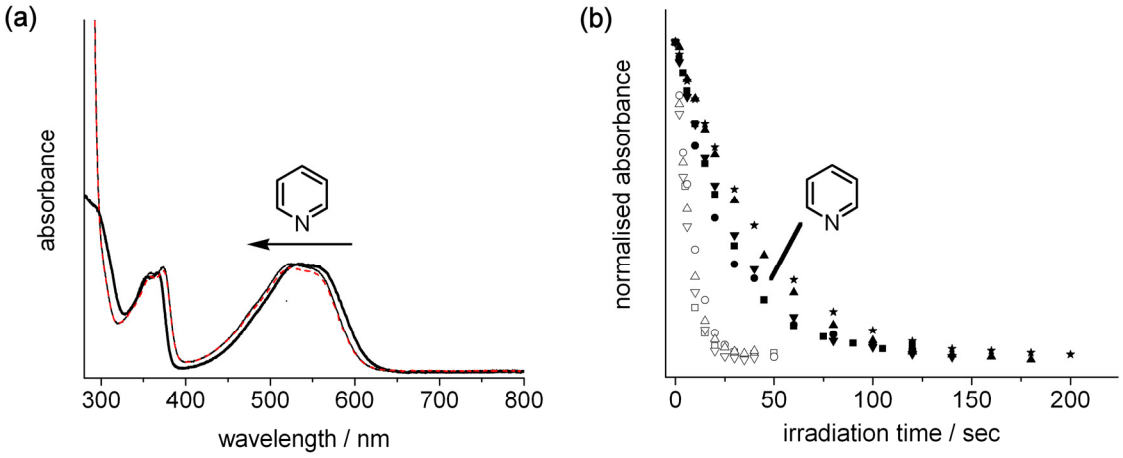

Figure 4.3.12 (a) UV-vis absorption spectra of a benzene solution (2.5 x 10^{-5} M) of **4.1** and **4.2** at PSS obtained after 14 s irradiation with 312 nm light before (bold line) and after (solid line) the addition of 5 equivalents of pyridine. The solution was then irradiated with >434 nm light for 120 s and 312 nm light for 22 s to reach the PSS (red dashed line). In this case the PSS is evaluated to be 80 % instead of 81% without pyridine. (b) Changes in the UV-vis absorption spectra of benzene solution (3.2 × 10^{-5} M) of **4.1** and **4.2** at PSS as they are irradiated with >434 nm light in the presence (solid symbols) and absence (empty symbols) of pyridine.

This rate difference could be due to a lowering of the quantum yield of the photoreaction or to slower kinetics, and could be attributed to the fact that regenerating the aromatic character in the dioxaborole contributes to the driving force for the ring-opening reaction. When isomer **4.2** is bound to pyridine, the boron centre adopts a tetrahedral geometry minimising the extent to which regenerating the aromatic stabilisation can contribute (the dioxaborole group must become planar to enhance aromaticity). In the absence of pyridine, **4.2** can adopt a planar geometry. Similar kinetics and hypsochromic shifts are observed when pyridine is used as the solvent, supporting the conclusion that the photochemistry is not significantly hindered in the **4.2**•pyridine complex.

Addition of 4.8 equivalents of pyridine to a benzene solution of the ring-open isomer **4.1** does not cause any observable shift in the absorbance band attributed to this isomer as shown in Figure 4.3.13a; the only effect of this addition is an increase in the intensity of absorbance below 300 nm due to pyridine itself. In the presence of pyridine, the photochemical ring-closure rate is diminished as shown in Figure 4.3.13b. In pure pyridine, the ring-closure rate is further diminished as it takes up to 230 seconds to reach the photostationary state compare to 12 seconds in benzene at the same concentration (2.5×10^{-5} M).

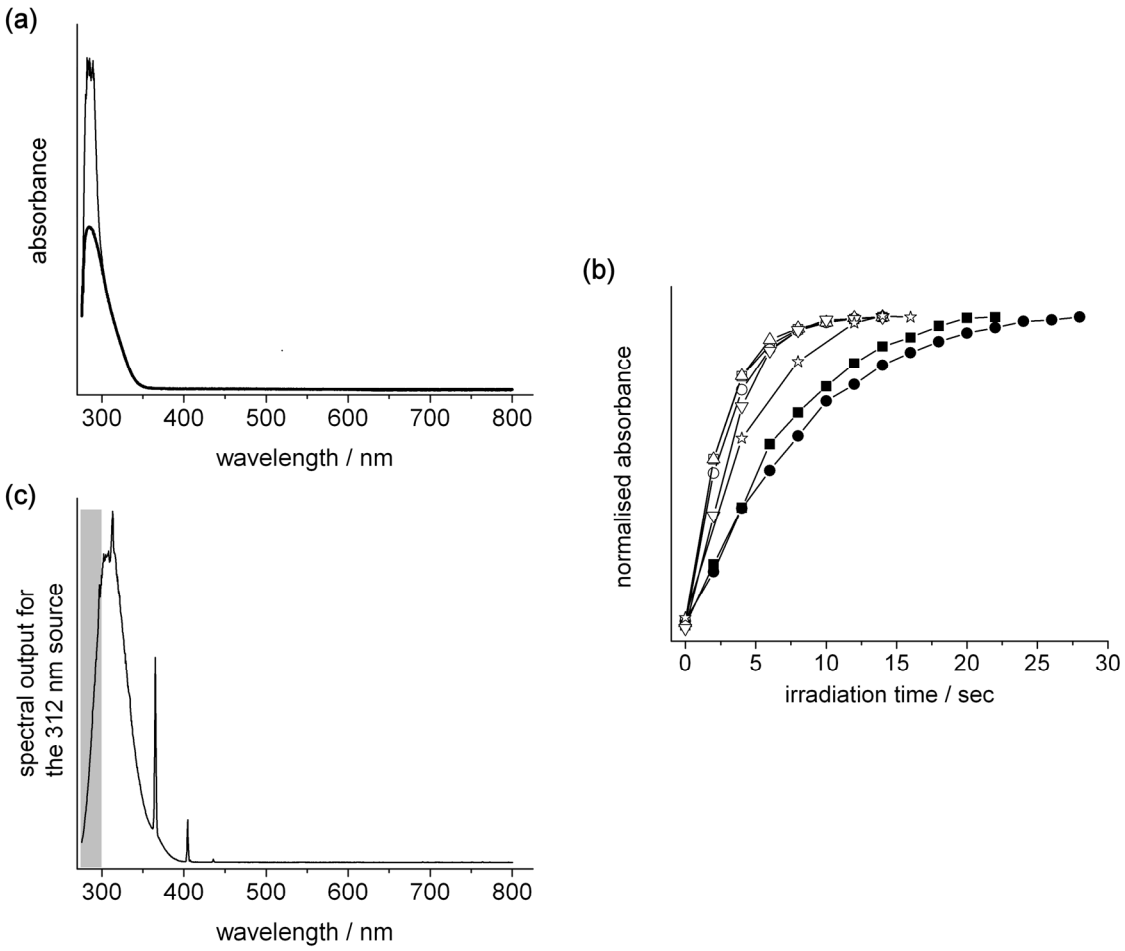

Figure 4.3.13 (a) UV-vis absorption spectra of a benzene solution (3.3 x 10^{-5} M) of **4.1** before (bold line) and after the addition of 4.6 equivalents of pyridine (solid line). (b) Changes in the UV-vis absorption spectra of benzene solutions (3.2 × 10^{-5} M) of **4.1** upon irradiation with 312 nm light in the presence (solid symbols) and absence (empty symbols) of pyridine. Connections are added as a guide for the eyes. (c) Spectral output of the 312 nm light source used for the ring-closure of **4.1**. The gray area highlights the region where both pyridine and **4.1** absorb.

As discussed previously, ^{1}H NMR studies revealed very little interaction between pyridine and the ring-open compound **4.1**, such an interaction can thus not explain the slower ring-closure. The effect of pyridine on the ring-closure rate of **4.1** could be explained by the fact that pyridine absorbs light before it can reach the photoswitchable molecule. As shown in Figure 4.3.13c, the 312 nm light source used for these studies emits a non-negligible amount of light at wavelengths smaller than 300 nm, a range in

which both compounds, **4.1** and pyridine, absorb light. Hence, some of the photons are absorbed by pyridine before they can reach **4.1**, decreasing its ring-closure rate.

4.4 Conclusion and perspectives

In summary, this chapter has demonstrated that the Lewis acidity of a boron atom integrated into a photochromic DTE backbone can be modulated using light of the appropriate wavelength. Changes in Lewis acidity were reported by taking advantage of the photoinduced rearrangement of the π-bond in the central 5-membered ring of the DTE system which is also part of a 1,3,2-dioxaborole unit.

Compound **4.1** was shown to be photochromic since 312 nm light induces ring-closure of the 1,3,5-hexatriene moiety forming the photoisomer **4.2** with a relatively good PSS of 81% in benzene, and visible light of wavelengths greater than 434 nm induces full recovery of **4.1**. Titration experiments with pyridine uncovered the poor affinity of **4.1** to this Lewis base and demonstrated the increased affinity of the ring-closed photoisomer. This ability to regulate the Lewis acidity could enable the control of chemical processes requiring a Lewis acid as an activator, reagent, or catalyst.

Gated photochromism experiments showed that the presence of pyridine has little effects on the photochromic properties of the boron-containing DTE derivative. These results suggest that the Lewis acidity of the molecule could be turned on and off in the presence of a substrate in a chemical process without limitations arising from strong gating effects.

The main limitation of the presented boron-containing DTE derivative is its instability towards oxidation, especially in the ring-closed form. It can thus be used only in dry and oxygen-free atmospheres.

Another limitation comes from the dioxaborole unit itself. The Lewis acidity of this architecture is limited by the presence of the two oxygen atoms attached to the boron centre; the oxygen atoms interact with the vacant p-orbital of the boron through π-overlap. However, the molecular design developed could enable functionalisation of the molecule with strongly electron-withdrawing groups that could enhance the Lewis acidity of the ring-closed isomer. For example, the top phenyl ring could be replaced with a pentafluorophenyl ring as shown in Figure 4.4.1. The phenyl groups on the DTE backbone could also be substituted with strongly electron-withdrawing moieties.

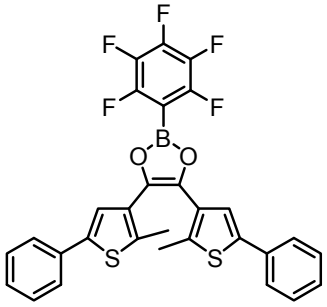

Figure 4.4.1 Boron-containing DTE derivative functionalised with a pentafluorophenyl ring, which could show improved Lewis acidity.

The change in Lewis acidity between the ring-open (**4.1**) and the ring-closed (**4.2**) photoisomers of the boron-containing DTE derivative could offer a means to control chemical processes that are catalysed by Lewis acids and to modulate the behaviour of functional materials containing them. Future work could involve testing compound **4.1**, or a more Lewis acidic analogue, as a phototunable catalyst in a suitable reaction.

4.5 Experimental

4.5.1 Materials

All solvents used for synthesis were dried and degassed by passing them through steel columns containing activated alumina under nitrogen using an MBraun solvent purification system. Solvents for NMR analysis were purchased from Cambridge Isotope Laboratories and used as received, except benzene-d_6 which was dried and degassed. The benzene used for UV-vis absorption spectroscopy measurements and NMR analysis was dried over calcium hydride for 6 hours, distilled onto freshly activated 4Å molecular sieves and degassed by 4 freeze-pump-thaw cycles before being stored in a glove box. Column chromatography was performed using silica gel 60 (230-400 mesh) purchased from Silicycle Inc. and solvents purchased from Aldrich. Phenylboronic acid was purchased from Acros Organics and used as received. All other reagents were purchased from Aldrich. The pyridine used for titration studies was distilled and stored on freshly activated 4A molecular sieves. 3-Bromo-2-methyl-5-phenylthiophene (**4.10**) was prepared from 2-methyl-thiophene (**4.4**) according to literature procedures.[72]

4.5.2 Instrumentation

^{1}H NMR and ^{13}C NMR characterisations were performed on a Varian INOVA 500 working at 499.767 MHz and 125.666 MHz respectively. Chemical shifts (δ) are reported in part per million relative to tetramethylsilane using the residual solvent peak as a reference standard. ^{11}B NMR characterisations were performed on a Bruker AdvanceII 600 working at 192.546 MHz. Chemical shifts (δ) are reported in part per million relative to BF_3OEt_2. Coupling constants (J) are reported in Hertz. UV-vis absorption spectroscopy measurements were performed using an Ocean Optics USB 2000 Plug-and-Play

Spectrometer with a USB-ISS-UV/Vis Integrated Sampling System inside an MBraun UNILab glove box. Microanalysis (C, H, N) were performed at Simon Fraser University by Mr. Mei-Keng Yang on a Carlo Erba EA 1110 CHN Elemental Analyser. Low resolution mass spectrometry measurements were performed at Simon University by Mr. Simon Wong using a Varian 4000 GC/MS/MS with electron impact operating at 10 mA as the ionisation source (EI) or with chemical ionisation (CI) using methanol.

4.5.3 Photochemistry

All ring-closing reactions were carried out using the light source from a lamp used for visualising TLC plates at 312 nm (Spectroline E series, 470 W/cm^2). The ring opening reactions were carried out using the light of a 300-W halogen photooptic source passed through a 434 nm cut-off filter to eliminate higher energy light.

4.5.4 Synthesis

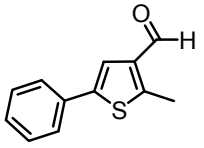

4.11

Synthesis of 2-methyl-5-phenylthiophene-3-carboxaldehyde (4.11)

A mixture of dry THF (50 mL) and magnesium ribbon (excess) at reflux was treated drop-wise and under a nitrogen atmosphere with a solution of 3-bromo-2-methyl-5-phenylthiophene (**4.10**) (2.00 g, 7.90 mmol) in dry THF (20 mL) using a syringe. After 2 h at reflux, the reaction was treated with anhydrous DMF (3 mL, excess). The heating source was removed and the reaction was allowed to cool to ambient temperature and then water (50 mL) was added. The aqueous layer was removed and extracted with

EtOAc (3 x 50 mL). The combined organic extracts were washed with water (1 x 50 mL) and then brine (1 x 50 mL), dried with $MgSO_4$, filtered and evaporated under reduced pressure. Column chromatography (1:4 EtOAc/hexanes) afforded aldehyde **4.11** as a yellow solid (1.07 g, 5.29 mmol, 70 %).

M.p.: 80-81 °C; ^{1}H NMR (chloroform-d, 500 MHz): δ 10.01 (s,1H), 7.55 (s, 1H), 7.54 (d, J = 7.4 Hz, 2H), 7.38 (t, J = 7.4 Hz, 2H), 7.30 (t, J = 7.4 Hz, 1H), 2.78 (s, 3H); ^{13}C NMR (chloroform-d, 125 MHz) δ 184.4, 151.2, 141.1, 137.9, 133.0, 128.9, 127.9, 125.6, 121.9, 13.5; Anal. Calcd. for $C_{12}H_{10}OS$: C, 71.25; H, 4.98; Found: C, 71.03; H, 4.93; LRMS (EI) m/z = 202 [M^+]; (CI) m/z = 203 [M^++1].

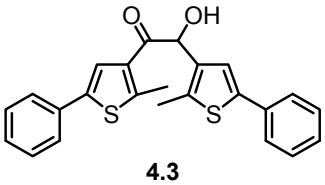

4.3

Synthesis of 1,2-*bis*(2'-methyl-5'-phenylthien-3'-yl)-2-hydroxy-1-ethanone (4.3)

A solution of 2-methyl-5-phenylthiophene-3-carboxaldehyde (**4.11**) (2.00 g, 9.89 mmol) in anhydrous EtOH (20 mL) was heated close to its boiling point and nitrogen gas was bubbled into it for 1 h. 3-Benzyl-5-(2-hydroxyethyl)-4-methylthiazolium chloride (20 mg, 0.074 mmol) and *N*,*N*-diisopropylamine (0.1 mL, 0.7 x 10^{-3} mmol) were added to the reaction vessel and the resulting solution was heated at reflux and stirred under nitrogen atmosphere for 3 h. The heating source was removed, the solution was allowed to cool to 40 °C and the precipitate formed was filtered. The filtrate was treated with nitrogen using the same procedure as described previously and then with the same amounts of diisopropylamine and thiazolium salt. After another 3 h of stirring under

nitrogen at reflux, the solution was allowed to cool to 40 °C and the precipitate was filtered. This procedure was repeated one more time. Column chromatography (1:4 EtOAc/hexanes) of the combined precipitates afforded **4.3** as a white powder (777 mg, 1.92 mmol, 40%).

M.p.: 189-191 °C; ^{1}H NMR (benzene-d_6, 500 MHz): δ 7.3 (2 overlapping d, 4H), 7.19 (s, 1H), 7.09 (s, 1H), 7.03-6.92 (4 overlapping t, 6H), 5.55 (d, J = 5.5 Hz, 1H), 4.66 (d, J = 5.5 Hz, 1H), 2.56 (s, 3H), 2.23 (s, 3H); ^{13}C NMR (chloroform-*d*, 125 MHz): δ 194.1, 152.0, 141.6, 140.2, 137.0, 135.8, 133.8, 133.1, 132.5, 129.0, 128.8, 127.9, 127.4, 125.6, 125.5, 122.5, 122.2, 71.2, 16.5, 13.4; Anal. Calcd for $C_{24}H_{20}O_2S_2$: C 71.25, H 4.98; Found: C, 71.57; H, 5.17; LRMS (EI) m/z = 403 [M^+-1]; (CI) m/z = 403 [M^+-1], 389 [M^+-15].

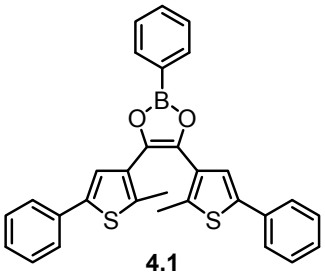

4.1

Synthesis of 4,5-*bis*(2'-methyl-5'-phenylthien-3'-yl)-2-phenyl-1,3,2-dioxaborole (4.1)

A solution of 1,2-*bis*(2'-methyl-5'-phenylthien-3'-yl)-2-hydroxy-1-ethanone **4.3** (163 mg, 0.40 mmol) and phenylboronic acid (48 mg, 0.39 mmol) in benzene (10 mL) was heated to reflux in a round-bottom flask fitted with a take-off adapter to removed the water-containing azeotrope. After 3 h, the heating source was removed, the solution was allowed to cool to ambient temperature and the solvent was removed under reduced

pressure to afford an off-white solid. Recrystallisation from hot hexane afforded compound **4.1** (164 mg, 0.34 mmol, 85 % yield) as a white solid.

M.p.: 166-168 °C; ^{1}H NMR (benzene-d_6, 500 MHz): δ 8.21 (m, 2H), 7.46 (d, J = 7.2 Hz, 4H), 7.43 (s, 2H), 7.27 (m, 3H), 7.05 (t, J = 7.2 Hz, 4H), 6.97 (t, J = 7.2 Hz, 2H), 2.18 (s, 6H); ^{13}C NMR (benzene-d_6, 125 MHz): δ 141.4, 137.8, 137.2, 134.8, 134.4, 132.0, 129.2, 128.7, 128.6, 128.3, 127.7, 125.8, 123.8, 14.6; ^{11}B NMR (benzene-d_6, 190 MHz): δ 31.4; ^{11}B NMR (pyridine, 190 MHz): δ 15.9; Anal. Calcd for $C_{30}H_{23}BO_2S_2$: C, 73.47; H, 4.73; Found: C 73.43, H 4.97; LRMS (EI) m/z = 490 [M^+]; (CI) m/z = 491 [M^++1].

4.5.5 Photoswitching studies

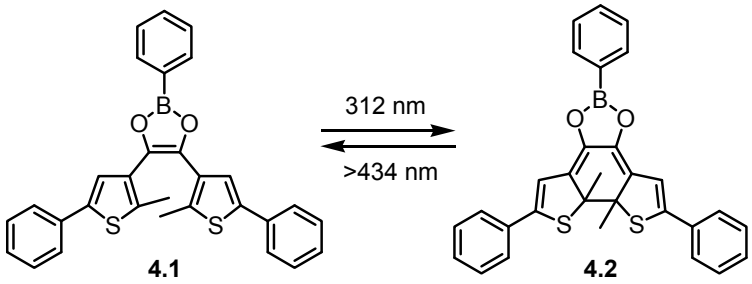

Using UV-vis absorption spectroscopy

A solution of dioxaborole **4.1** (3.3 x 10^{-5} M) in dry and degassed benzene was prepared in a glove box and placed in a 1 cm quartz cuvette for UV-vis absorption spectroscopy. A spectrum of the ring-open form was acquired using an Ocean Optics spectrometer directly in the glove box. The sample was irradiated for a cumulative time of 14 seconds in 2 seconds intervals using a 312 nm light source. An absorption spectrum was recorded after each irradiation. Irradiation of the sample with light of wavelengths

larger than 434 nm for 50 seconds induced the ring-opening reaction. The results are shown in Figure 4.3.3a.

Photochemical cycling

A solution of dioxaborole **4.1** (2.5 x 10^{-5} M) in dry and degassed benzene was prepared in a glove box and placed in a 1 cm quartz cuvette for UV-vis absorption spectroscopy. A spectrum of the ring-open form **4.1** was acquired using an Ocean Optics spectrometer directly in the glove box. The sample was irradiated for 16 seconds using a 312 nm light source. A spectrum of the ring-closed isomer **4.2** was acquired. The sample was then irradiated for 30 seconds using a visible light source (greater than 434 nm). A spectrum of the ring-open isomer **4.1** was acquired. This cycle was repeated a total of ten times. The results are shown in Figure 4.3.3b.

Using ^{1}H NMR spectroscopy

A solution of dioxaborole **4.1** (5.0 x 10^{-3} M) in dry and degassed benzene-d_6 was prepared in a boro-silicate glass NMR tube equipped with a Teflon screw cap and kept under a nitrogen atmosphere. The ^{1}H NMR spectrum of the ring-open form was acquired. The sample was then irradiated using a 312 nm light source until the photostationary state was reached after 65 minutes of irradiation, yielding a solution containing 81% of the ring-closed isomer. Irradiation with light in the visible region of the spectrum (wavelengths greater than 434 nm) for 5 minutes afforded a solution of the pure ring-open isomer. The results are shown in Figure 4.3.4.

Characterisation of the ring-closed isomer by NMR spectroscopy

^{1}H NMR (benzene-d_6, 500 MHz): δ 8.13 (d, J = 6.7 Hz, 2H), 7.39 (bd, J = 7.2 Hz, 4H), 7.24-7.18 (m, 3H), 7.06-6.97 (bm, 6H), 6.68 (bs, 2H), 2.37 (bs, 6H); ^{13}C NMR

(benzene-d_6, 125 MHz) δ 147.5, 140.4, 135.4, 134.5, 133.1, 126.6, 126.2, 112.4, 66.2, 27.7. The signals for the carbons at the *meta* and *para* positions of the three phenyl groups were not observed and were assumed to be underlying the solvent signal.

Degradation studies of 4.1 when exposed to UV light

A solution of dioxaborole **4.1** (5.0×10^{-3} M) in benzene-d_6 (from a bottle that had been opened for a long time) was prepared in a boro-silicate glass NMR tube and kept under a normal atmosphere. The ^{1}H NMR spectrum of the ring-open form **4.1** was acquired. The sample was then irradiated using a 312 nm light source for 10 minutes. Spectra were then acquired periodically over 20 hours. The signals attributed to the ring-closed isomer **4.2** progressively decreased as a new set of signal attributed to diketone **4.12** appeared. Diketone **4.12** was provided by Dr. M. D. Spantulescu. The results are shown in Figure 4.3.5.

^{1}H NMR (benzene-d_6, 500 MHz): δ 7.73 (s, 2H), 7.27 (d, J = 7.7 Hz, 4H), 7.99 (m, 6H), 2.56 (s, 6H); ^{1}H NMR (chloroform-*d*, 500 MHz): δ 7.55 (d, 4H), 7.52 (s, 2H), 7.38 (t, 4H), 7.30 (t, 2H), 2.85 (s, 6H); ^{13}C NMR (chloroform-*d*, 125 MHz) δ 189.12, 153.05, 141.08, 133.27, 133.02, 129.25, 128.30, 126.06, 124.76, 16.60.

4.5.6 ^{1}H NMR titrations

^{1}H NMR titration of ring-open isomer 4.1 with pyridine

A solution of compound **4.1** (2.5 mg, 10.2 mM) in dry and degassed benzene-d_6 (0.50 mL) was prepared in a standard boro-silicate NMR tube. Successive aliquots of a pyridine stock solution in dry and degassed benzene-d_6 (102 mM) were added to the solution of **4.1**. Seven measurements were made in the range of 0.2 to 10.0 equivalents of pyridine. The duration of the experiments was limited to 30 minutes, because slow deborylation catalysed by the base was observed. Even after the addition of 10 equivalents of pyridine to compound **4.1**, a shift of the ^{1}H NMR signals of only 0.003 ppm was observed, which is within the uncertainty of the spectrometer. Hence, we concluded that the equilibrium constant (K) for the binding of the ring-open form of the boron-containing molecular switch **4.1** with pyridine cannot be evaluated by ^{1}H NMR spectroscopy due to a negligible binding affinity of pyridine for the boron switch at these concentrations. The results are shown in Figure 4.3.7.

^{1}H NMR titration of ring-closed isomer 4.2 with pyridine

A solution of compound **4.1** (1.3 mg, 5.3 mM) in dry and degassed benzene-d_6 (0.50 mL) was prepared in a standard boro-silicate NMR tube and was irradiated for 10 minutes using a 312 nm light source to afford 51% of the ring-closed isomer **4.2** (2.7 mM). Successive aliquots of a pyridine stock solution (37 mM) in dry and degassed benzene-d_6 were added to the solution. Eight measurements were made in the range of 0.10 to 2.20 equivalents of pyridine. The duration of the experiments was limited to 30 minutes because of the slow deborylation catalysed by the added base. The value of the binding constant (K) was approximated from the shifts in the ^{1}H NMR signals of the

ortho protons on the phenyl unit directly attached to the boron atom. The binding of the ring-open isomer was neglected since no shift of the ^{1}H NMR signals of that species was observed in the range of concentration studied. The results are shown in Figure 4.3.8.

Determination of binding constant (4.2•pyridine)

The equilibrium constant for the complex formation between the ring-closed photoisomer **4.2** and pyridine was obtained mathematically by performing a nonlinear two parameter fit using Equation 4.3.10 and assuming a 1:1 binding model.[181] A Levenberg-Marquardt least squares routine included in the Non Linear Curve Fitting tool of Origin 6.10.52 was used to fit Equation 4.3.10 directly to experimental data (Q, [**4.2**], δ), setting δ_c and K as variable parameters.

$$(\delta - \delta_h) = \left(\frac{(\delta_c - \delta_h)}{2}\right)\left[(1 + n + Q) \pm \sqrt{(1 + n + Q)^2 - 4Q}\right]$$

Equation 4.3.10

Where:
δ = observed chemical shift
δ_c = chemical shift of the bound **4.2**
δ_h = chemical shift of the free **4.2**
[**4.2**] = total concentration of the ring-closed isomer **4.2**
[pyridine] = total concentration of pyridine
K = equilibrium constant
n = 1 / (K x [**4.2**])
Q = [pyridine] / [**4.2**]

Method A

The initial estimation of the equilibrium constant (K) was made using the experimental data shown in Table 4.5.1.

Table 4.5.1 Data used for Method A.

$vol_{pyridine}$ (uL)	[pyridine] (mM)	[**4.2**] (mM)	Q	chemical shift (ppm)
0	0.00	2.70	0.00	8.138
5	0.37	2.68	0.14	8.088
10	0.73	2.65	0.28	8.048
20	1.43	2.60	0.55	7.973
30	2.11	2.55	0.83	7.923
40	2.76	2.50	1.10	7.902
50	3.39	2.46	1.38	7.893
60	3.99	2.41	1.65	7.889
80	5.14	2.33	2.20	7.886

$vol_{pyridine}$ = total volume of pyridine solution added
[pyridine] = total concentration of pyridine
[**4.2**] = total concentration of **4.2**
Q = [pyridine] / [**4.2**]

initial volume of the host solution = 500 μL
initial concentration of ring-open isomer **4.1** = 5.30 mM
ratio of ring-closed to ring-open isomer after irradiation (**4.2** / **4.1**) = 0.51
initial concentration of **4.2** = 2.70 mM
concentration of the pyridine stock solution: 37.24 mM

As shown in Figure 4.5.1, a poor fit was obtained with this data set resulting in an equilibrium constant (K) of (3 ± 6) x 10^4 M^{-1}.

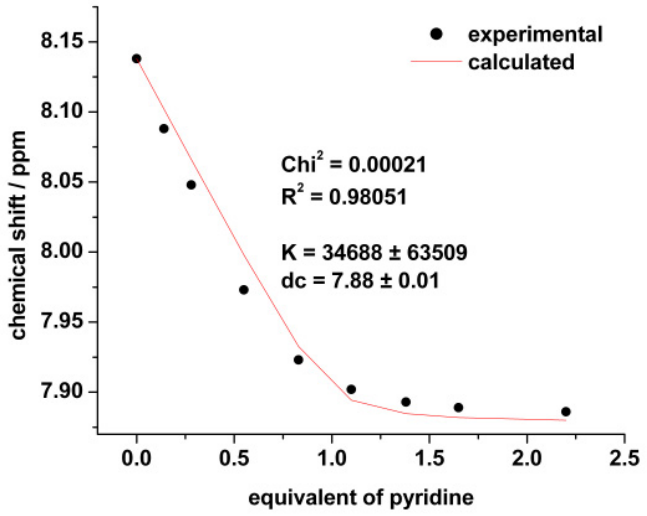

Figure 4.5.1 Change in chemical shift for aromatic proton H^b in compound **4.2** using the data listed in Table 4.5.1. The line shows the resulting fit using Equation 4.3.10. The optimal K and δ_c are indicated as well as the reduced chi^2 and the R^2 parameters.

Method B

A more careful examination of the NMR data showed that over time, the concentration of the ring-closed isomer **4.2** decreases slowly as deborylation occurs. Assuming that the deborylation product does not bind to pyridine and that the concentration of pyridine is known, the concentration of **4.2** was approximated by the integration of the NMR signals of **4.2** and pyridine. The corrected concentrations of the solution of **4.2** are shown in Table 4.5.2.

Table 4.5.2 Data used for Method B.

Q (determined by integration)	[pyridine] (mM)	[**4.2**] (mM)	chemical shift (ppm)
0.00	0.00	2.70	8.138
0.20	0.37	1.84	8.088
0.39	0.73	1.87	8.048
0.76	1.43	1.89	7.973
1.18	2.11	1.79	7.923
1.65	2.76	1.67	7.902
2.13	3.39	1.59	7.893
2.69	3.99	1.48	7.889
3.64	5.14	1.41	7.886

Method B resulted in an improved fit as seen in Figure 4.5.2. In this latter case, an equilibrium constant of (7.0 ± 0.4) x 10^3 M^{-1} was calculated

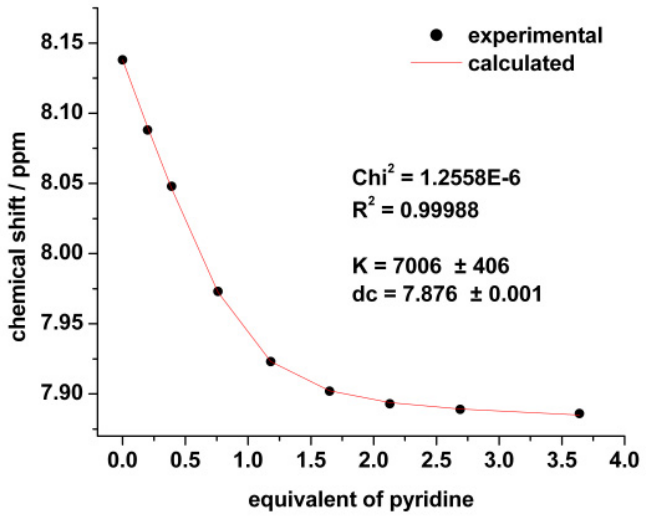

Figure 4.5.2 Change in chemical shift for aromatic proton in compound **4.2** using the data listed in Table 4.5.2. The line shows the resulting fit using Equation 4.3.10. The optimal K and δ_c are indicated as well as the reduced chi^2 and the R^2 parameters.

4.5.7 Gated photochromism

Ring-opening reaction of 4.2 to 4.1 in the absence of pyridine

A solution of dioxaborole **4.1** (3.3 x 10^{-5} M) in dry and degassed benzene was prepared in a glove box and placed in quartz cuvette for UV-vis absorption spectroscopy having a 1 cm path length. A spectrum of the ring-open form **4.1** was acquired using an Ocean Optics spectrometer directly in the glove box. The sample was irradiated in 2 seconds intervals until the photostationary state was reached using a 312 nm light source. An absorption spectrum was recorded after each irradiation. The sample was then irradiated using visible light (wavelengths greater than 434 nm) for various intervals until the presence of the ring-closed isomer **4.2** could not be detected by UV-vis spectroscopy. The results are shown in Figure 4.3.12.

Ring-opening reaction of 4.2 to 4.1 in the presence of pyridine (method 1 – pyridine added prior to UV irradiation)

A solution of dioxaborole **4.1** (3.3 x 10^{-5} M) in dry and degassed benzene was prepared in a glove box and 2 mL of the solution was transferred to a quartz cuvette for UV-vis absorption spectroscopy having a 1 cm path length. A spectrum of the ring-open form **4.1** was acquired using an Ocean Optics spectrometer directly in the glove box. Pyridine (25 μL) was then added to the cuvette (1.6 x 10^{-4} M). The sample was irradiated using a 312 nm light source in 2 seconds intervals until the photostationary state was reached. An absorption spectrum was recorded after each irradiation. The sample was then irradiated using visible light (greater than 434 nm) for various intervals until the presence of the ring-closed isomer **4.2** could not be detected by UV-vis spectroscopy. The results are shown in Figure 4.3.12.

Ring-opening reaction of 4.2 to 4.1 in the presence of pyridine (method 2 – pyridine added after UV irradiation)

A second sample was prepared as described above, however, in this case, pyridine was not added until the sample was irradiated using a 312 nm light source in 2 seconds intervals until the photostationary state was reached. After pyridine (25 μL) was added to the cuvette (1.6×10^{-4} M), it was irradiated using visible light (wavelengths greater than 434 nm) for various intervals until the presence of the ring-closed isomer could not be detected by UV-vis spectroscopy. The results are shown in Figure 4.3.12.

Determination of the rate constant for the ring-opening reactions with and without pyridine

Figure 4.5.3 shows the changes in the absorption (at 535 nm) for solutions of the photostationary state of **4.1** and **4.2** as they are irradiated with visible light. The rate constants for the ring-opening reactions were obtained by performing nonlinear fits using a first order exponential model with the Non Linear Curve Fitting tool of Origin 6.10.52. The resulting rate constants in presence and absence of pyridine for individual experiments are listed in Table 4.5.3. The errors in the rate constant averages were evaluated using a confidence level of 95% with the confidence function on Microsoft Excel 2003.

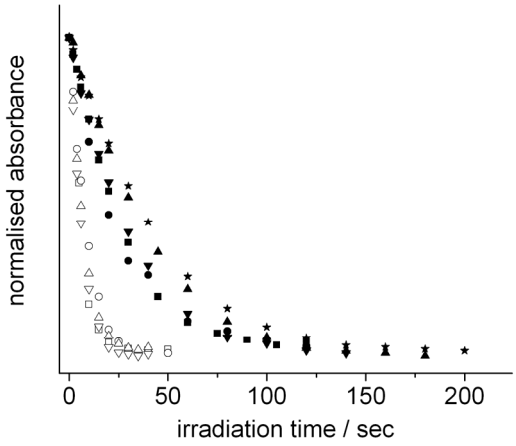

Figure 4.5.3 Change in the absorbance at 535 nm for solutions of compound **4.2** (with (5 runs, empty symbols) and without (4 runs, dark symbols) pyridine added) as they are irradiated with visible light (greater than 434 nm).

Table 4.5.3 Rate constants for the ring-opening reactions with and without pyridine.

without pyridine		with pyridine	
run	Rate constant (s^{-1})	run	Rate constant (s^{-1})
1	0.15 ± 0.01	1 (method 1)	0.0241 ± 0.0007
2	0.107 ± 0.003	2 (method 1)	0.037 ± 0.001
3	0.127 ± 0.003	3 (method 2)	0.0331 ± 0.0008
4	0.146 ± 0.003	4 (method 2)	0.0311 ± 0.0004
		5 (method 2)	0.0217 ± 0.0004
Average	**0.13 ± 0.01**	Average	**0.029 ± 0.006**
Std dev.	0.019	Std dev.	0.0064

4.5.8 Computational methods (at the AM1 level of theory)

Computational structures and properties of the molecules described in this chapter were carried out using the HyperChem Release 7.1 software that was kindly given to the author, free of charge, as a HyperCube Scholar Award in 2003. Structures were obtained using the semi-empirical AM1 method using a Polak-Ribiere (conjugated gradient) algorithm for geometrical optimisation. After optimisation, the properties were obtained

directly from the HyperChem software. The Mulliken charges of the boron centres were obtained by displaying the charge label from the menu (Display>Labels…>Charge). The 3D mapped isosurface electrostatic potential was also obtained from the menu (Compute>Plot Molecular Graphs…). Their Gouraud shaded surface rendering was obtained with a total charge density contour value of 0.01 and a grid mesh size set to fine; the mapped function range was set from -0.1 to 0.1 and all other parameters were left as default. The LUMOs were obtained from the menu (Compute>Orbitals…) as 3D isosurfaces. Their Gouraud shaded surface rendering was obtained with an orbital contour value of 0.01 and a grid mesh size set to fine; all other parameters were used as default.

4.5.9 Computational methods reported by Dr. Kim K. Baldridge

Computation structures and properties of molecules reported by Dr. Kim K. Baldridge were carried out using the GAMESS[182] software. Structures were obtained using both MP2[183] and HDFT (Becke's 3 parameter functional[184] with nonlocal correlation provided by Lee-Yang-Parr[185,186] with both local and nonlocal terms, B3LYP, and the M06-2X functional[187]). The ccpVDZ,[188] DZ(2d,p) and DZ+(2d,p)[189] basis sets were employed. Full geometry optimisations were performed and characterised via Hessian analysis, and ZPE corrections extracted for energetic predictions. From the fully optimised structures, single point MP2 energies and single point time-dependent absorption computations[190] for evaluation of spectral properties were performed. Molecular orbital contour plots were generated and depicted using QMView[191] and electrostatic plots were generated using Molekel.[192]

Chapter 5: Conclusion

Molecular systems with integrated chemical reactivity and photochromic functions are powerful assets for the development of novel "smart" materials. Rationally designed photoswitches can be used to regulate chemical reactivity using light, and such systems could significantly impact both synthesis and drug delivery by increasing reaction efficiency and decreasing undesired side-reactions or side effects. Chemical reactivity can also be employed to regulate the photochromic behaviour of photoswitches, providing a locking mechanism and enabling chemical detection through facile monitoring.

The dithienylethene-based molecular switches are particularly well-suited to the development of photoresponsive systems with integrated chemical reactivity functions since they have well-behaved photochromic properties and increased thermal stability of both isomers compared to other systems. Dithienylethene derivatives exhibit significant differences between their ring-open and ring-closed forms, which can influence their reactivity. Upon exposure to an appropriate light source, the isomerisation reaction causes changes to (1) the geometry (sterics), (2) the electronic communication along the backbone, and (3) the π-bond arrangement of the molecules. Harnessing these differences allows the photoregulation of chemical reactivity. Alternatively, the modification of their spatial and electronic configuration, the presence or absence of a competing mechanism, or the creation or destruction of their photoresponsive architecture through chemical reactions or interactions can permit the regulation of their photochromic properties. In

this thesis, both sides of the relationship between photochromism and chemical reactivity were integrated into molecular systems based on the dithienylethene architecture.

The concept of reactivity-gated photochromism was introduced in *Chapter 2*. The presented dienes are not photoswitchable as they lack the required hexatriene functionality. However, the butadiene portions of the compounds spontaneously undergo thermal Diels-Alder reactions with electron-deficient alkenes and result in the formation of cycloadducts. The rearrangement of the π-bonds creates the dithienylethene architecture and renders the dienes photoactive. Light of the appropriate wavelengths can then be used to convert the products back and forth between their ring-open and ring-closed photoisomers. In addition to allowing photochromic detection of dienophiles, this strategy offers new sites and mechanisms to further functionalise photoresponsive molecular switches based on the dithienylethene scaffold, and provides synthetic access to unprecedented and innovative systems.

In *Chapter 3*, it was demonstrated that by combining the two approaches to the integration of chemical reactivity and light, (reactivity-gated photochromism and photogated reactivity), one can create molecular systems with novel and appealing properties. The presented fulvene derivatives are not photoswitchable unless they undergo Diels-Alder cycloadditions with dienophiles to generate adducts that contain the photoresponsive dithienylethene substructure. When solutions of the fulvene derivatives are treated with a dienophile auxiliary, reversible reactions are immediately observed and equilibria between the fulvenes and the cycloadducts are reached within 20 minutes. The reverse cycloaddition reactions can be prevented by locking the structures in their ring-closed, “armed” forms upon exposure of the solutions to UV irradiation to produce

compounds that are thermally stable and can be isolated. As long as they are kept in the dark, the ring-closed isomers can be stored with no observable degradation. Irradiation of the solutions with light of the appropriate wavelength in the visible range triggers the ring-opening reaction and subsequent release of the dienophile.

This is a prime example of photogated reactivity whereby light triggers a structural change in the molecule and imparts chemical reactivity unique to each form of the compound, and represents a novel approach towards the development of photorelease technologies. Moreover, the fact that the light used to activate the release reaction is in the visible range leads to the dual advantages of limiting biological damage and increasing penetration depth. Additionally, because differently functionalised ring-closed Diels-Alder adducts absorb visible light of different wavelengths, selective and sequential release was achieved by tuning the light source to trigger the ring-opening reaction of only one of the ring-closed compound in the presence of another.

The concept of using the dithienylethene architecture to trigger a fragmentation reaction does not only have important implications for the development of controlled release applications whereby designer reagents or therapeutic agents can be delivered on-demand, but it could also lead to the development of novel materials with unique properties. For example, polymers with phototunable thermal properties could be prepared or the self-assembly of nanostructures could be modulated by light.

In *Chapter 3*, the photoinduced rearrangement of the π-bonds in the central ring of dithienylethene was shown to be highly effective in controlling how molecules behave in chemical reactions. The same approach was exploited in *Chapter 4* to modulate the Lewis acidity of two photoisomers of a boron-containing dithienylethene derivative. The

preparation of a dithienylethene derivative containing a boron atom in its central 5-membered ring was described and the photochromic behaviour of the molecule was presented. Upon exposure to light of the appropriate wavelengths, the isomerisation of the dithienylethene backbone causes a bond rearrangement of the 1,3,2-dioxaborole unit, directly affecting the electron density of the boron centre and changing the Lewis acidity of the atom. This ability to regulate the Lewis acidity could enable the control of chemical processes requiring a Lewis acid as an activator, reagent, or catalyst.

In summary, this thesis presented novel strategies to integrate chemical reactivity and photochromism based on dithienylethene molecular switches. The creation of the dithienylethene architecture by a mild and spontaneous reaction with an external chemical species was shown to be a very efficient way to "gate" the photochromism of a system. Alternatively, the integration of a reactive functional group into the dithienylethene backbone such that it can only exist in one form of the photoswitch was proven to be a very effective way to modulate chemical reactivity using light. Overall, the integration of chemical reactivity with dithienylethene derivatives opens promising avenues for the development of functional materials enabling chemical detection, photorelease applications, regulation of chemical processes, and fabrication of light responsive structures.

Chapter 6: Appendices

6.1 NMR characterisation of new compounds from *Chapter 2*

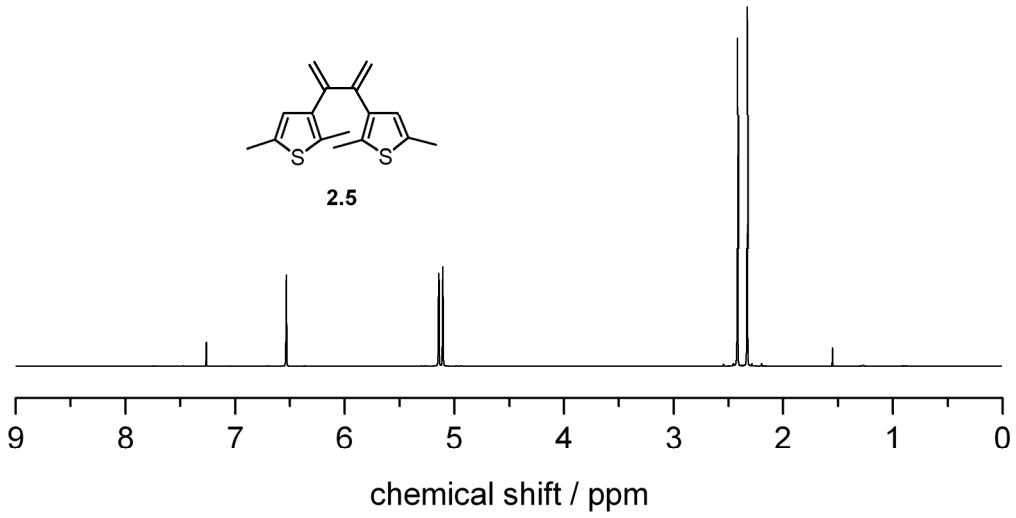

Figure 6.1.1 ^{1}H NMR (400 MHz) spectrum of compound **2.5** in chloroform-*d*.

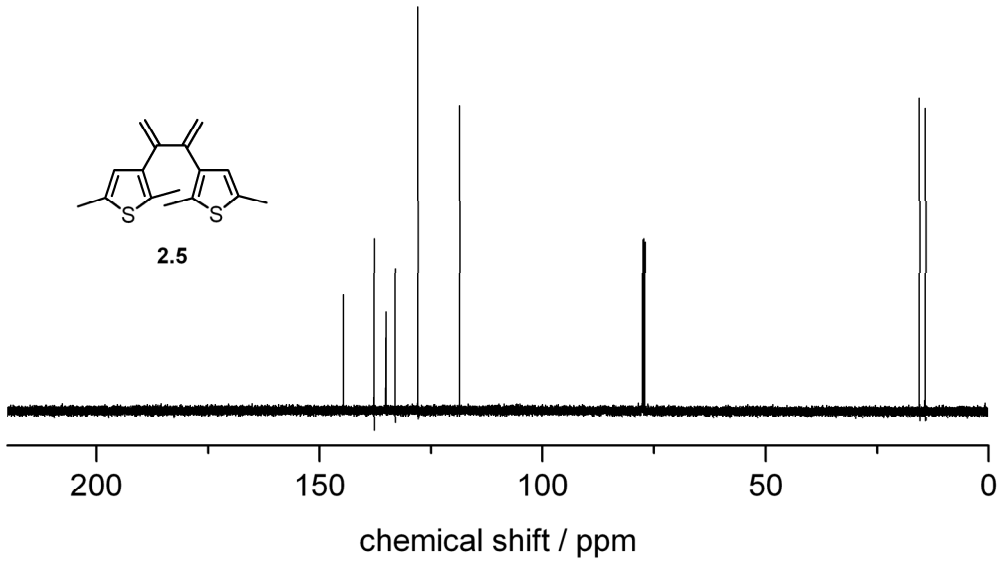

Figure 6.1.2 ^{13}C NMR (125 MHz) spectrum of compound **2.5** in chloroform-*d*.

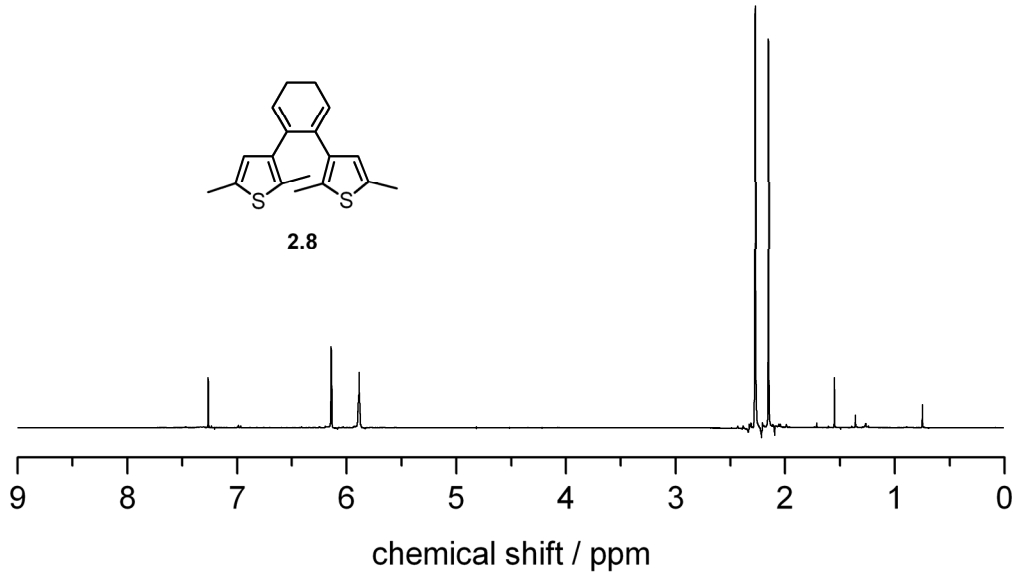

Figure 6.1.3 ^{1}H NMR (400 MHz) spectrum of compound **2.8** in chloroform-*d*.

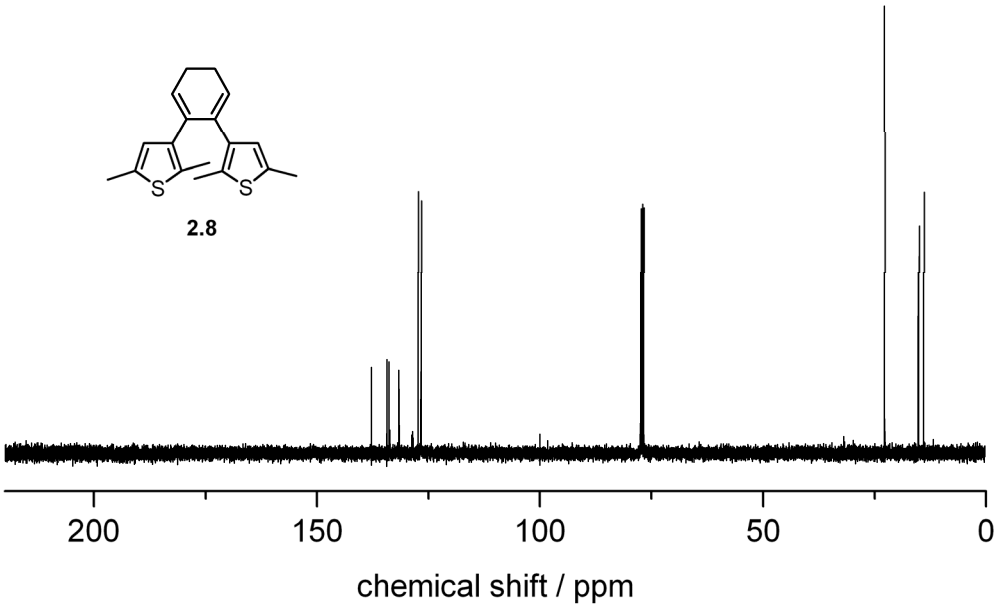

Figure 6.1.4 ^{13}C NMR (100 MHz) spectrum of compound **2.8** in chloroform-*d*.

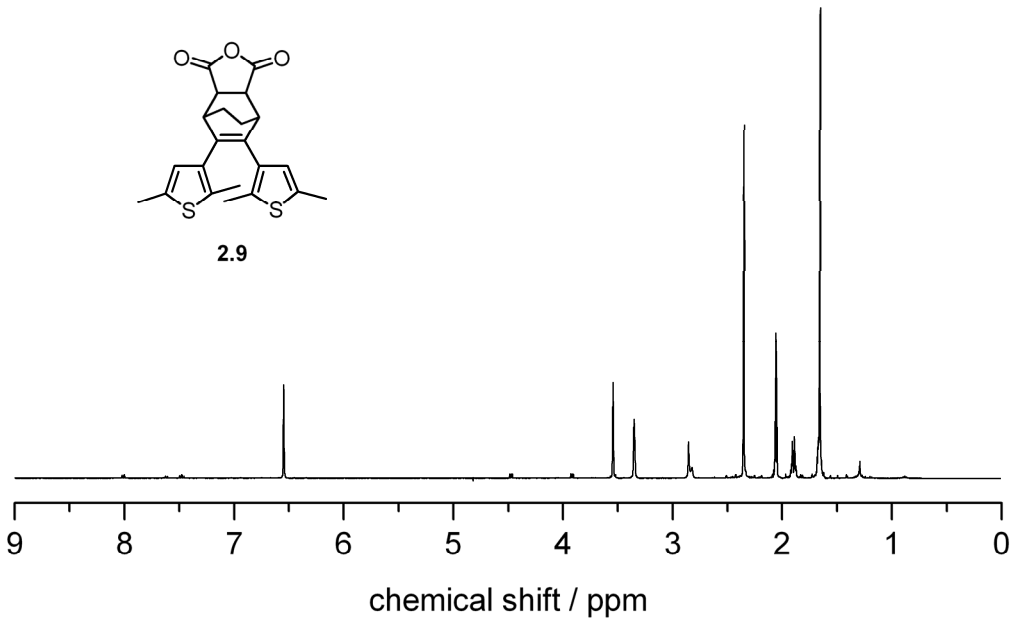

Figure 6.1.5 ^{1}H NMR (400 MHz) spectrum of compound **2.9** in acetone-d_6.

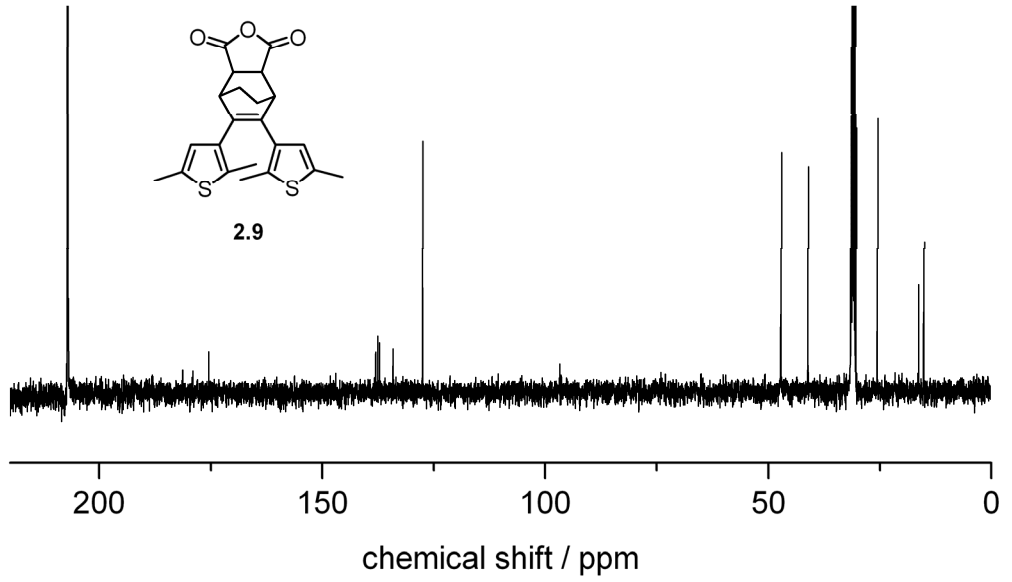

Figure 6.1.6 ^{13}C NMR (100 MHz) spectrum of compound **2.9** in acetone-*d*.

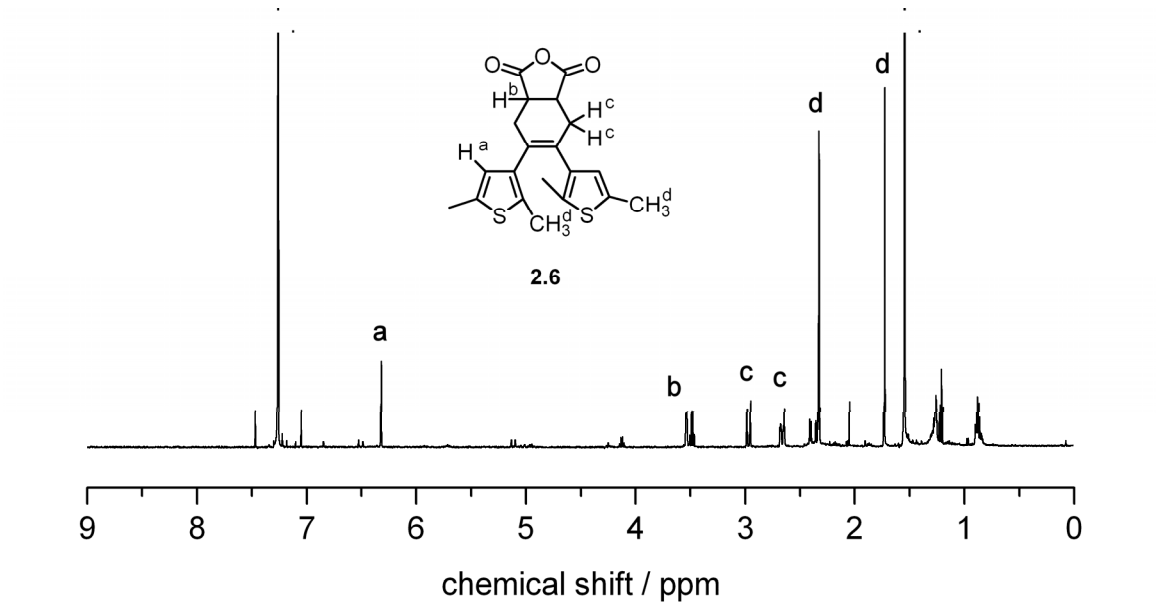

Figure 6.1.7 Crude ^{1}H NMR (400 MHz) spectrum of compound **2.6** in chloroform-*d*.

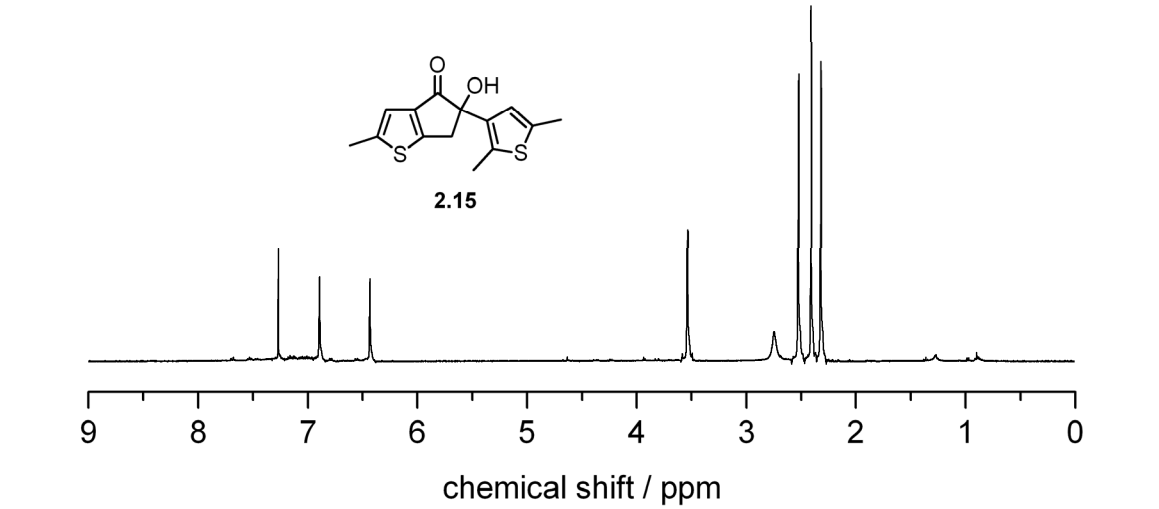

Figure 6.1.8 ^{1}H NMR (400 MHz) spectrum in chloroform-*d* of the main product of the cyclopentadienone reaction and its proposed structure as shown by compound **2.15**.

6.2 NMR Characterisation of previously known compounds from *Chapter 2*

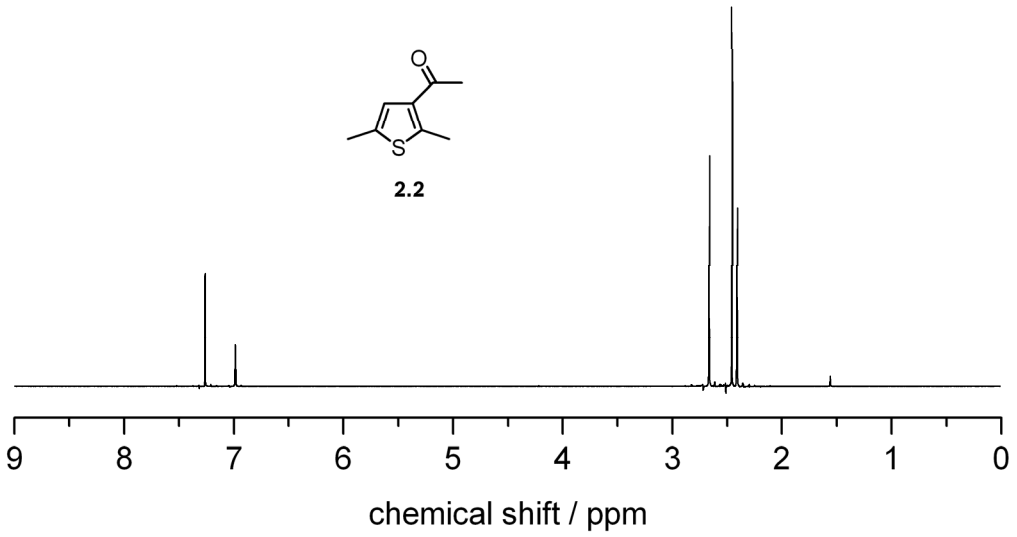

Figure 6.2.1 ^{1}H NMR (400 MHz) spectrum of compound **2.2** in chloroform-*d*.

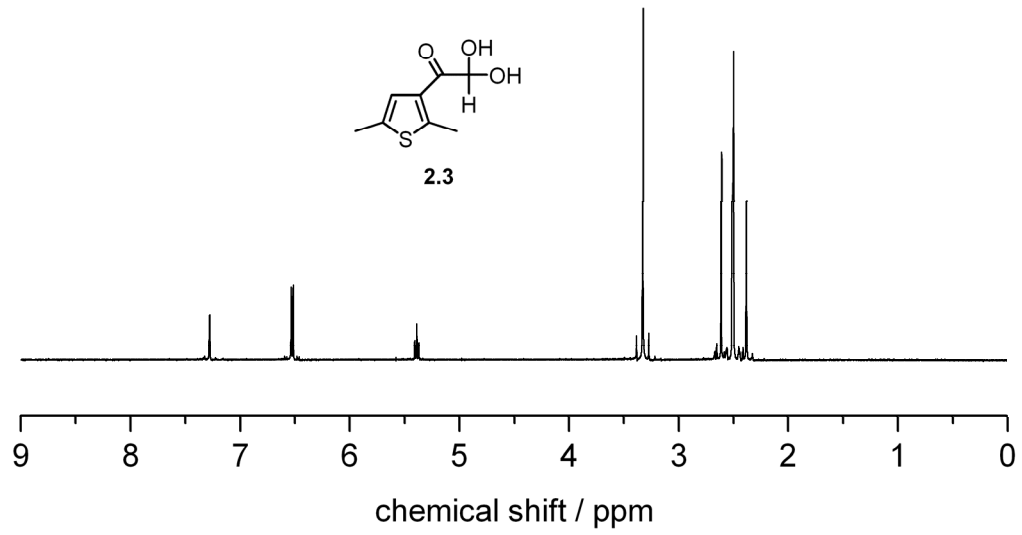

Figure 6.2.2 ^{1}H NMR (400 MHz) spectrum of compound **2.3** in DMSO-d_6.

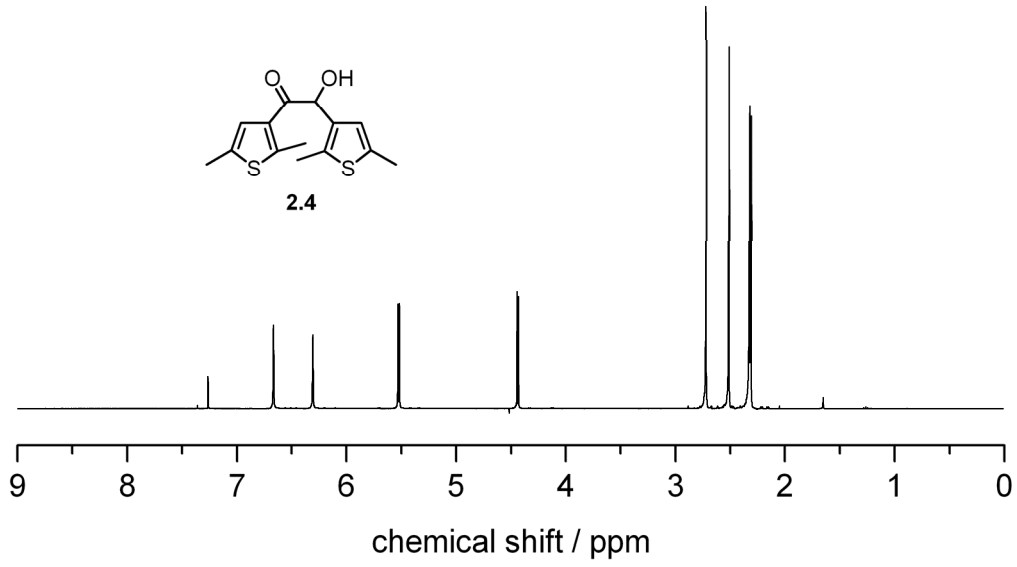

Figure 6.2.3 ^{1}H NMR (400 MHz) spectrum of compound **2.4** in chloroform-*d*.

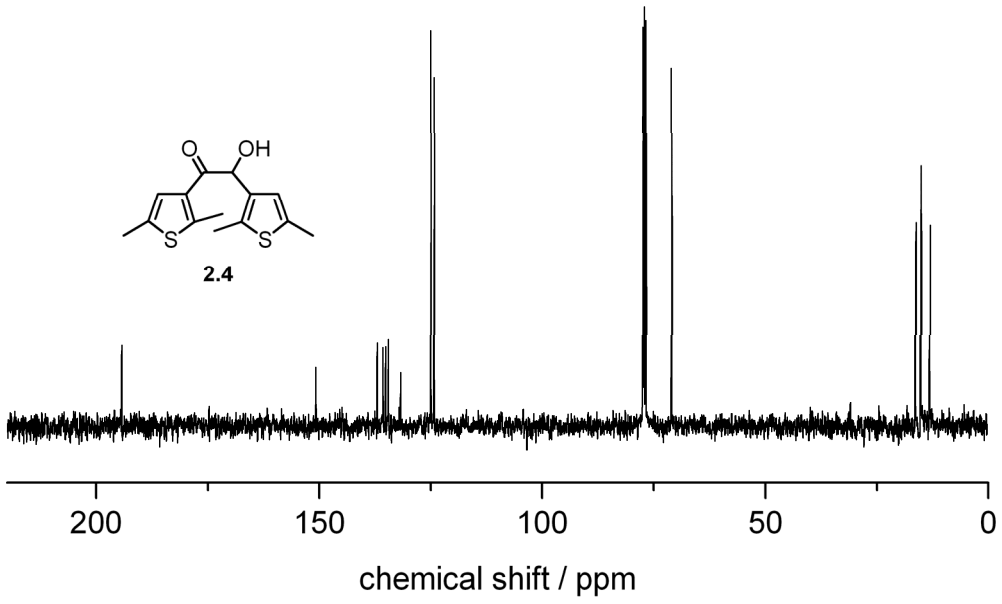

Figure 6.2.4 ^{13}C NMR (125 MHz) spectrum of compound **2.4** in chloroform-*d*.

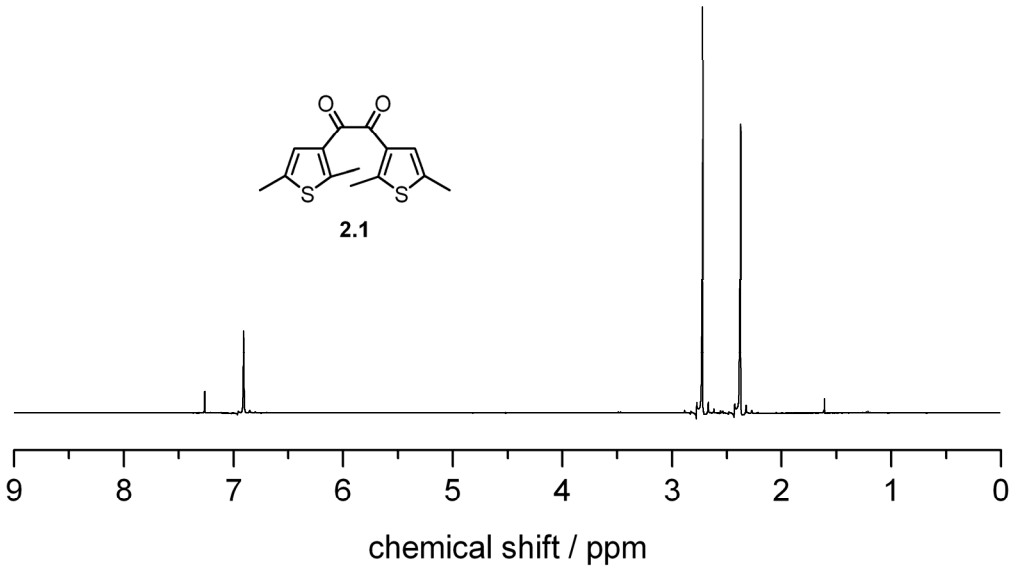

Figure 6.2.5 ^{1}H NMR (400 MHz) spectrum of compound **2.1** in chloroform-*d*.

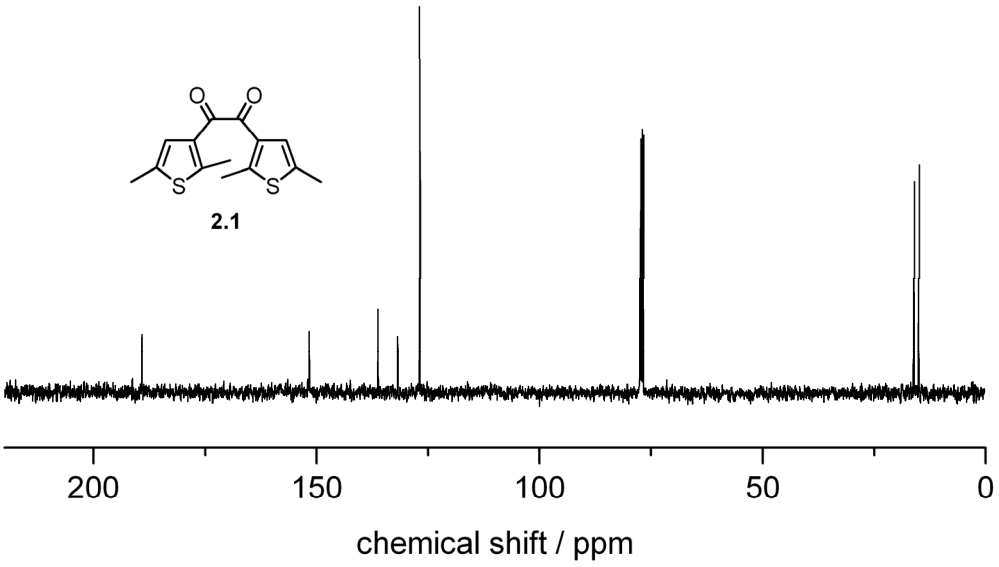

Figure 6.2.6 ^{13}C NMR (125 MHz) spectrum of compound **2.1** in chloroform-*d*.

6.3 NMR characterisation of new compounds from *Chapter 3*

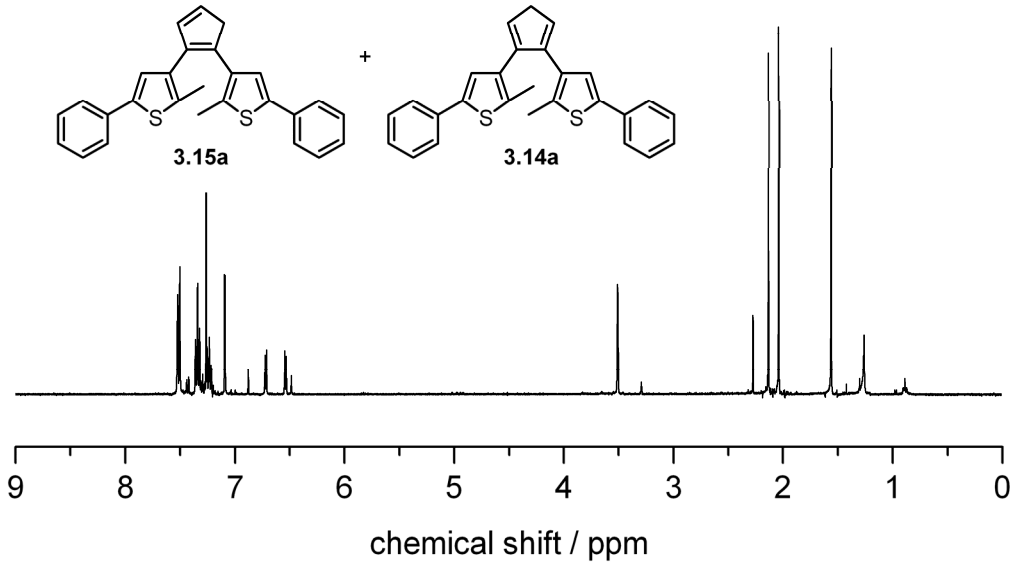

Figure 6.3.1 ^{1}H NMR (400 MHz) spectrum of compounds **3.14a** and **3.15a** in chloroform-*d*.

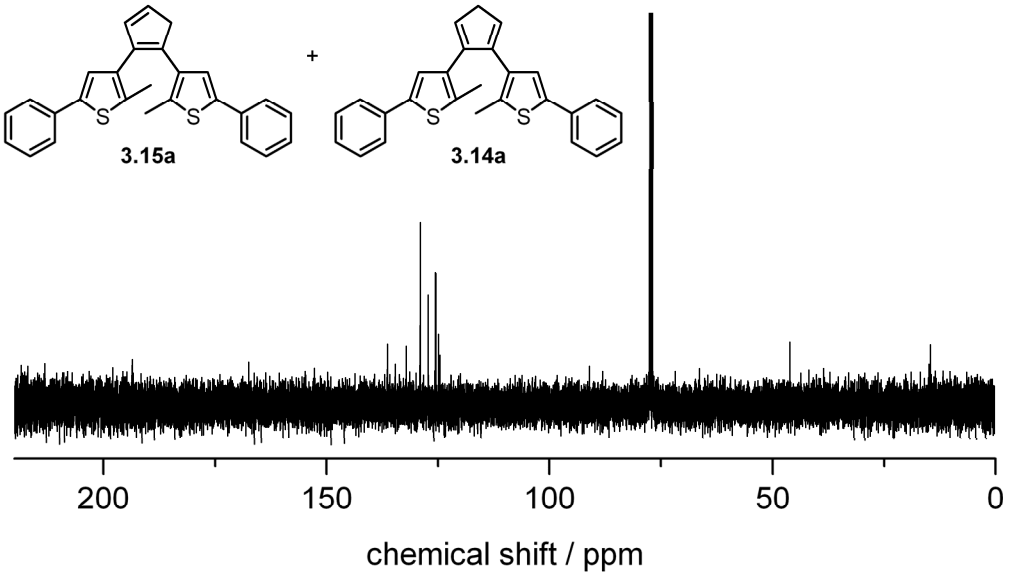

Figure 6.3.2 ^{13}C NMR (100 MHz) spectrum of compounds **3.14a** and **3.15a** in chloroform-*d*.

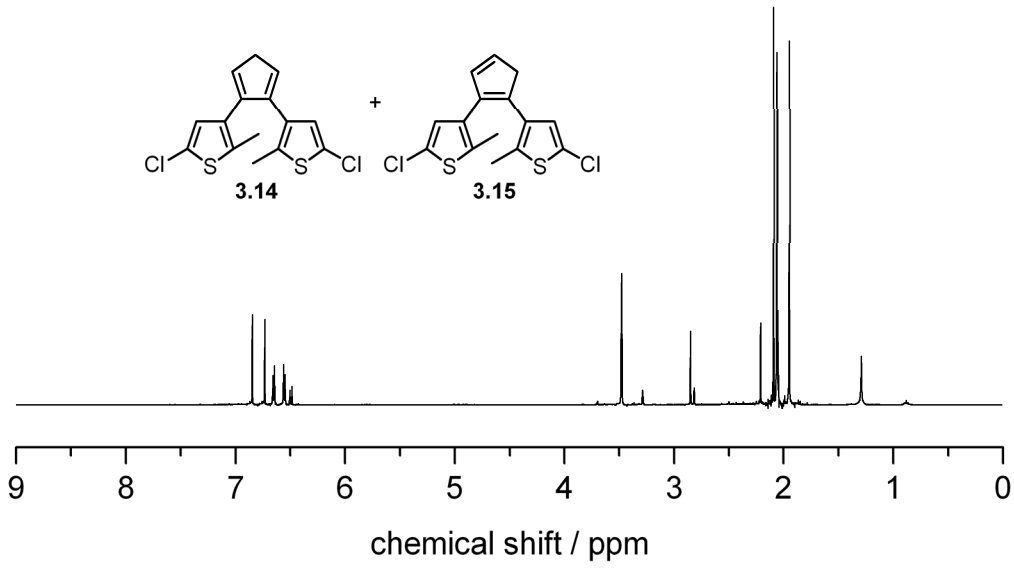

Figure 6.3.3 ^{1}H NMR (500 MHz) spectrum of compounds **3.14** and **3.15** in acetone-d_6.

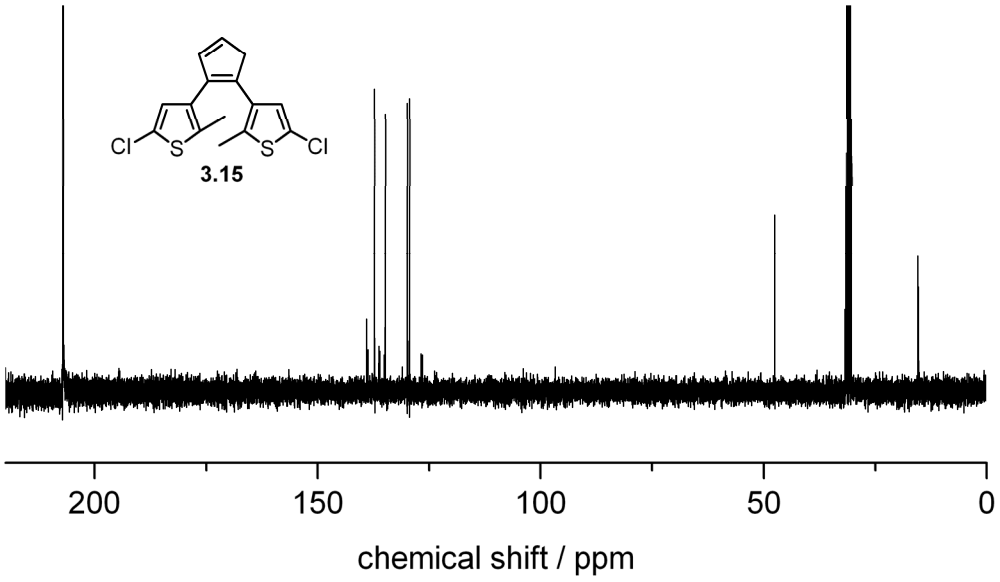

Figure 6.3.4 ^{13}C NMR (100 MHz) spectrum of compounds **3.15** in acetone-d_6.

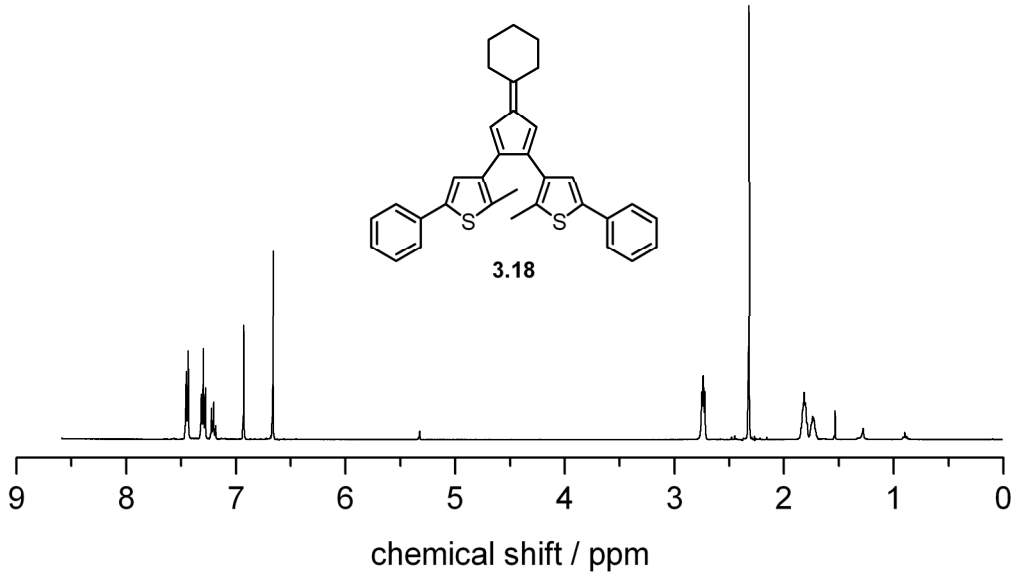

Figure 6.3.5 ^{1}H NMR (400 MHz) spectrum of compounds **3.18** in dichloromethane-d_2.

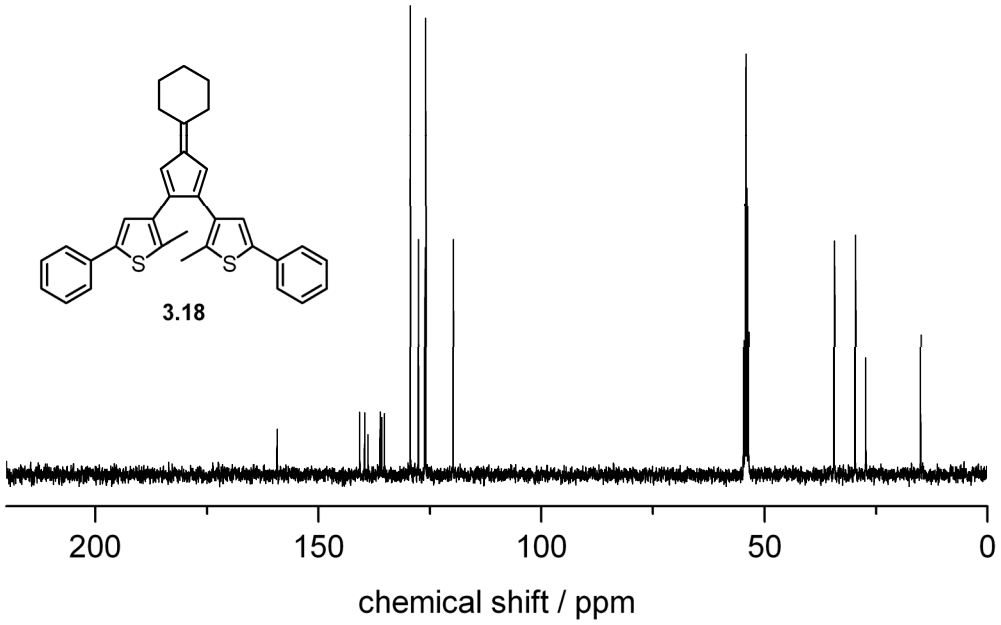

Figure 6.3.6 ^{13}C NMR (100 MHz) spectrum of compounds **3.18** in dichloromethane-d_2.

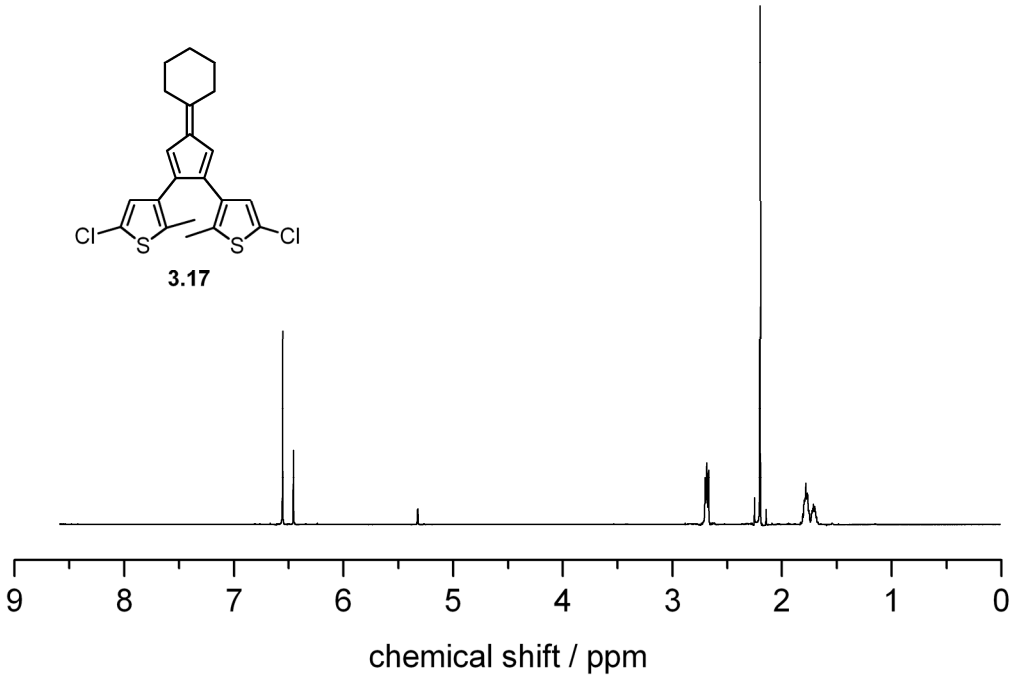

Figure 6.3.7 ^{1}H NMR (500 MHz) spectrum of compound **3.17** in dichloromethane-d_2.

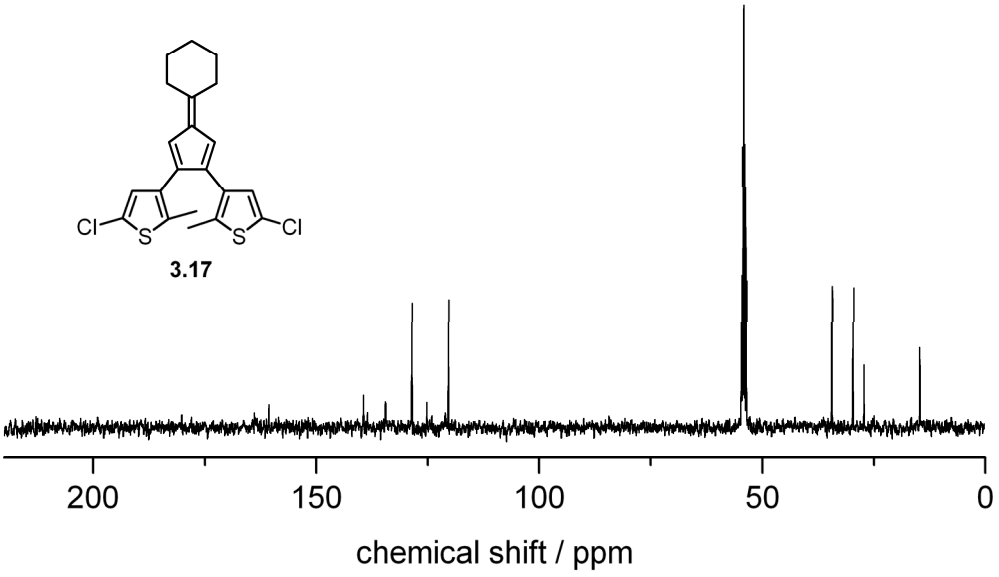

Figure 6.3.8 ^{13}C NMR (100 MHz) spectrum of compound **3.17** in dichloromethane-d_2.

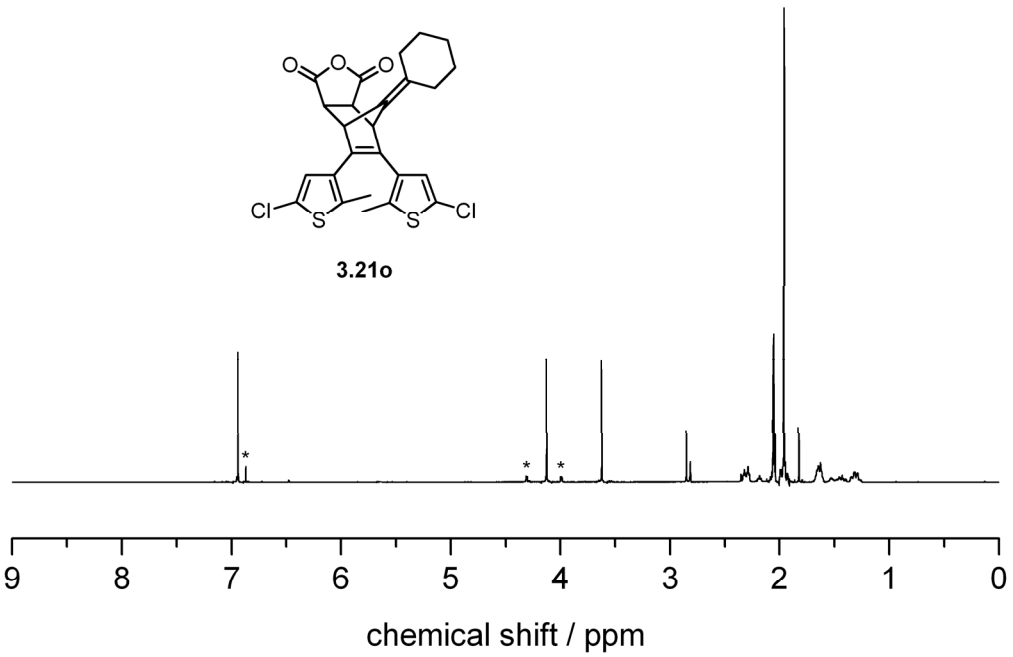

Figure 6.3.9 ^{1}H NMR (500 MHz) spectrum of compound **3.21o** in acetone-d_6. The peaks marked with an asterisks (*) are assigned to the *exo* isomer.

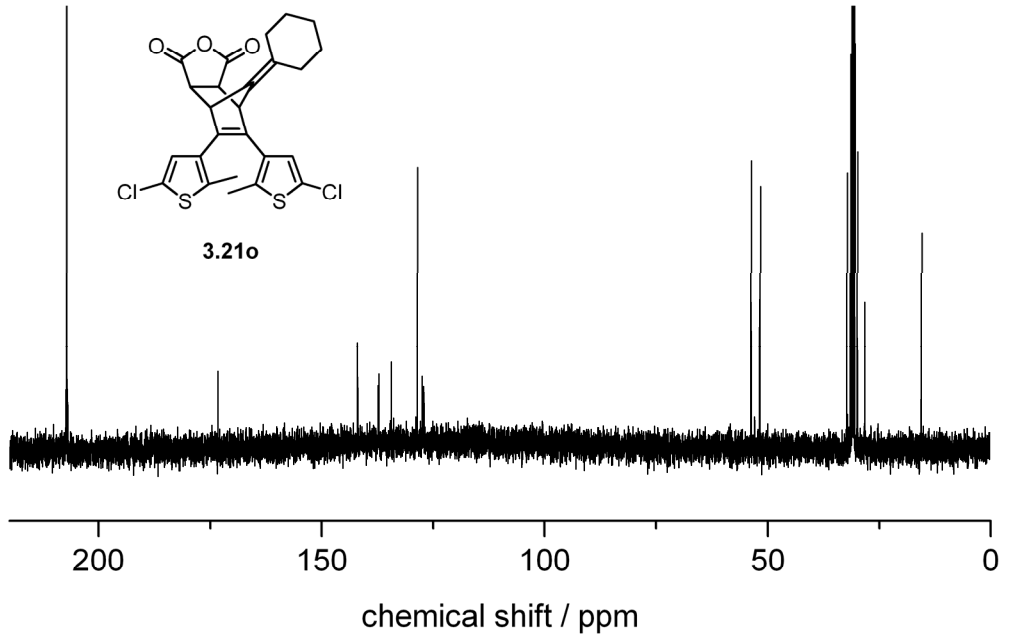

Figure 6.3.10 ^{13}C NMR (125 MHz) spectrum of compound **3.21o** in acetone-d_6.

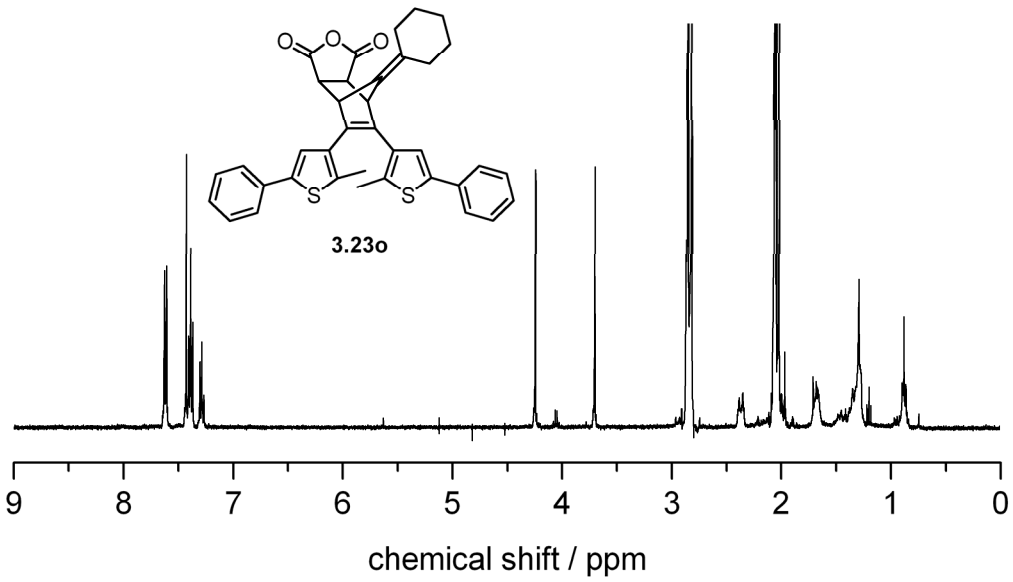

Figure 6.3.11 ^{1}H NMR (500 MHz) spectrum of compound **3.23o** in acetone-d_6.

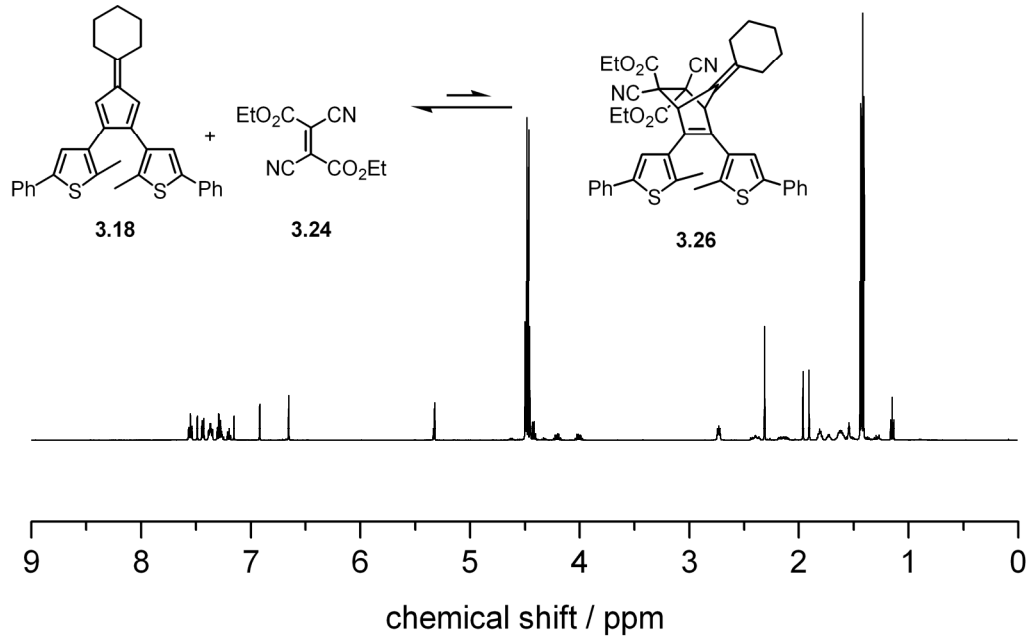

Figure 6.3.12 ^{1}H NMR (500 MHz) spectrum of compound **3.26** at equilibrium with **3.18** and **3.24** in dichloromethane-d_2.

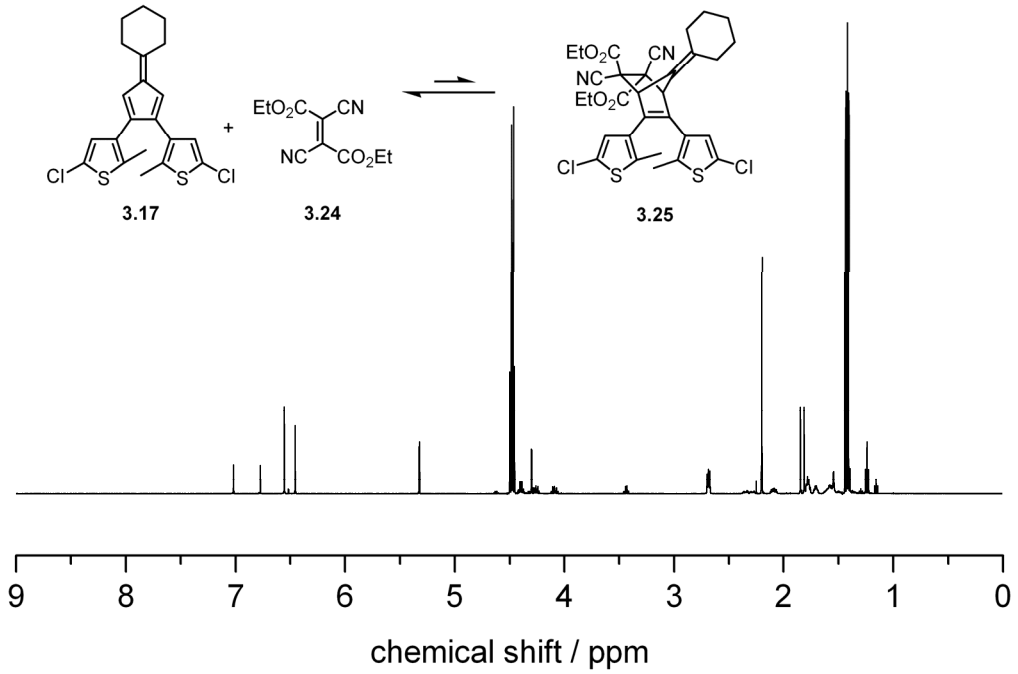

Figure 6.3.13 ^{1}H NMR (400 MHz) spectrum of compound **3.25** at equilibrium with **3.17** and **3.24** in dichloromethane-d_2.

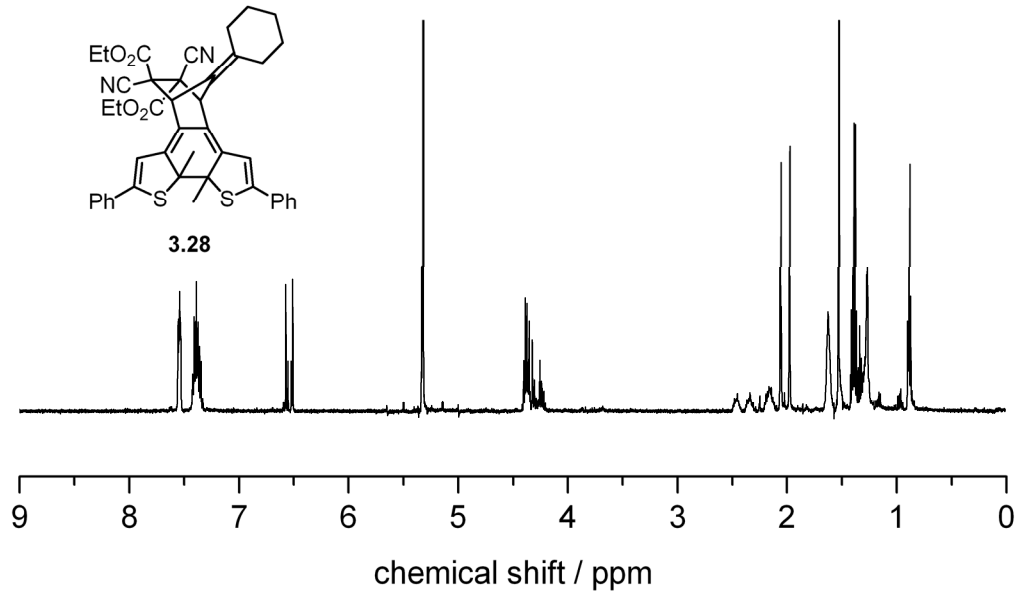

Figure 6.3.14 ^{1}H NMR (500 MHz) spectrum of compound **3.28** in dichloromethane-d_2.

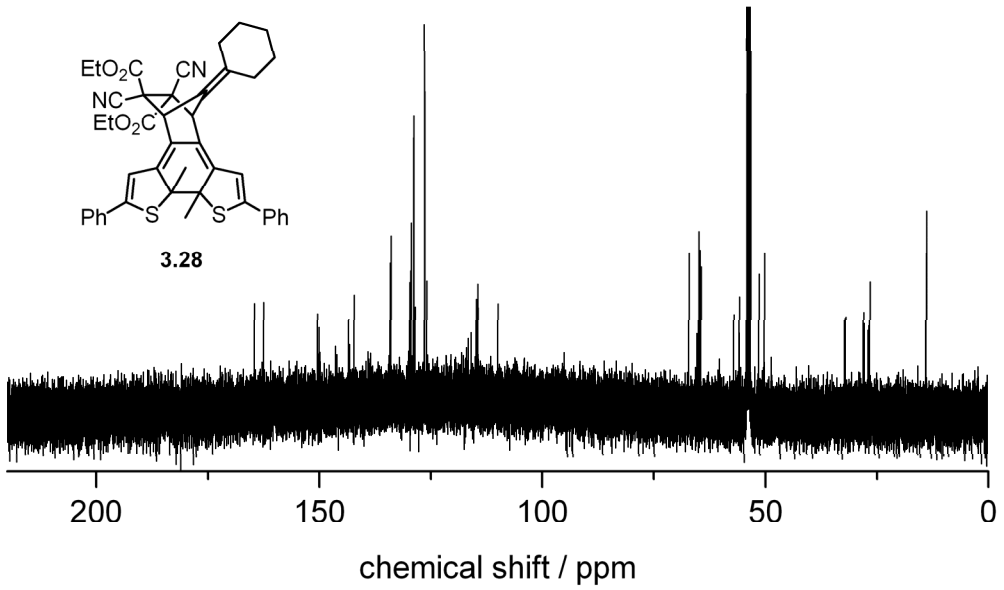

Figure 6.3.15 ^{13}C NMR (125 MHz) spectrum of compound **3.28** in dichloromethane-d_2.

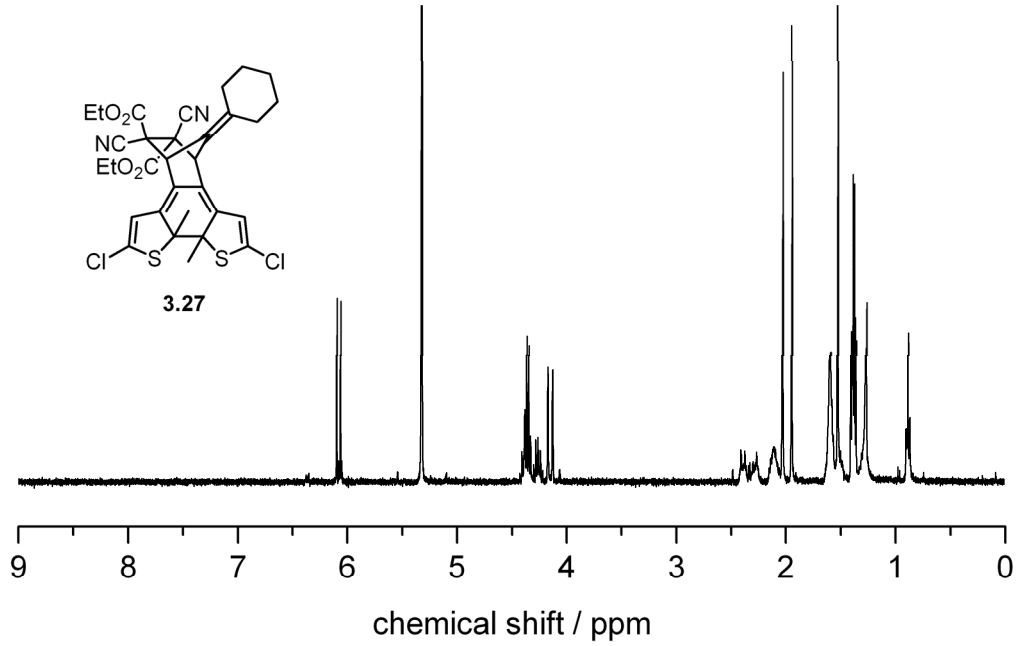

Figure 6.3.16 ^{1}H NMR (400 MHz) spectrum of compound **3.27** in dichloromethane-d_2.

6.4 Characterisation of previously known compounds from *Chapter 3*

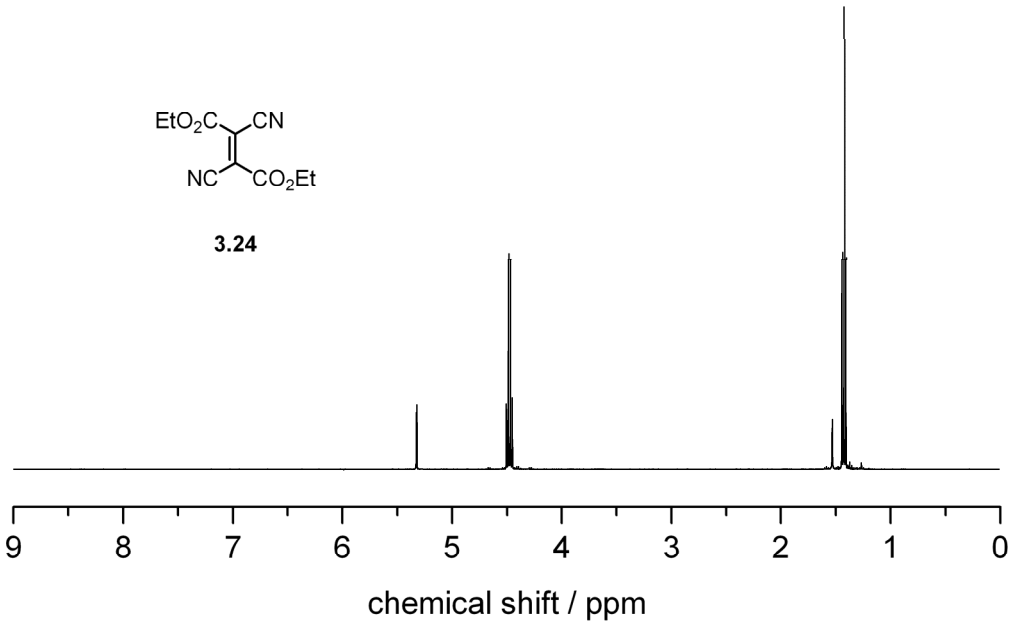

Figure 6.4.1 ^{1}H NMR (500 MHz) spectrum of compound **3.24** in dichloromethane-d_2.

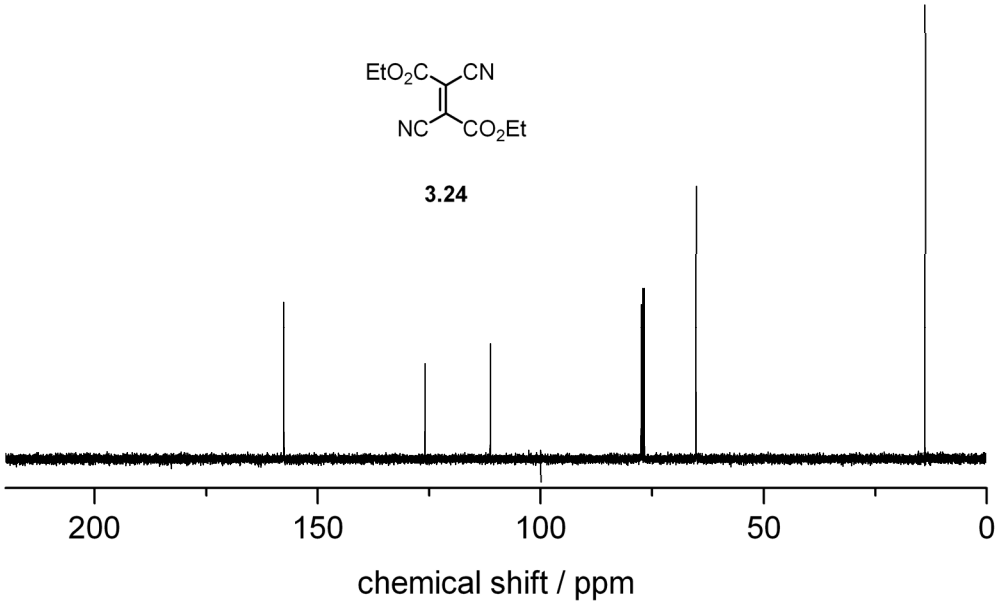

Figure 6.4.2 ^{13}C NMR (125 MHz) spectrum of compound **3.24** in chloroform-*d*.

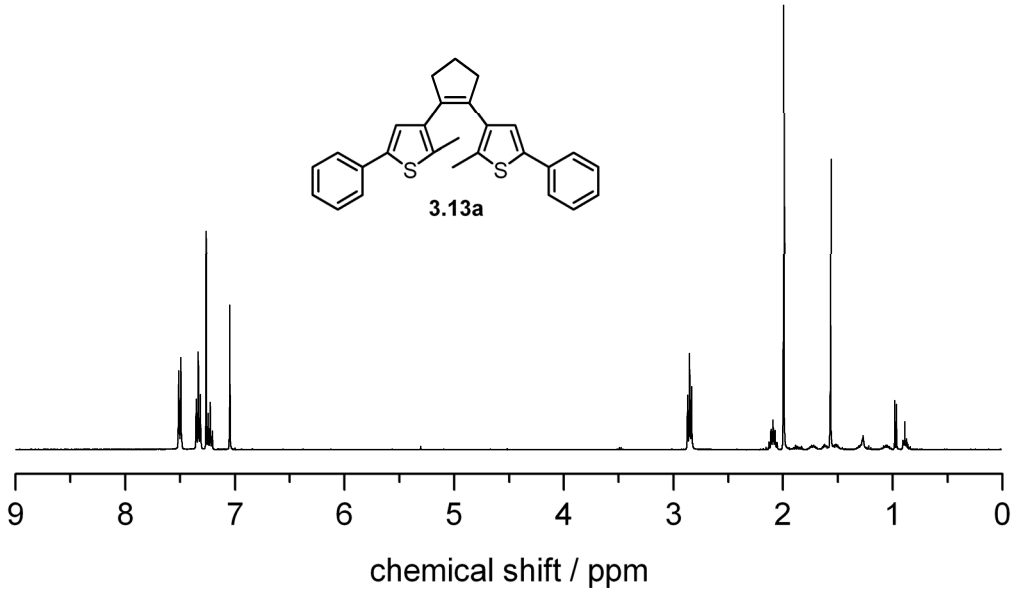

Figure 6.4.3 ^{1}H NMR (500 MHz) spectrum of compound **3.13a** in chloroform-*d*.

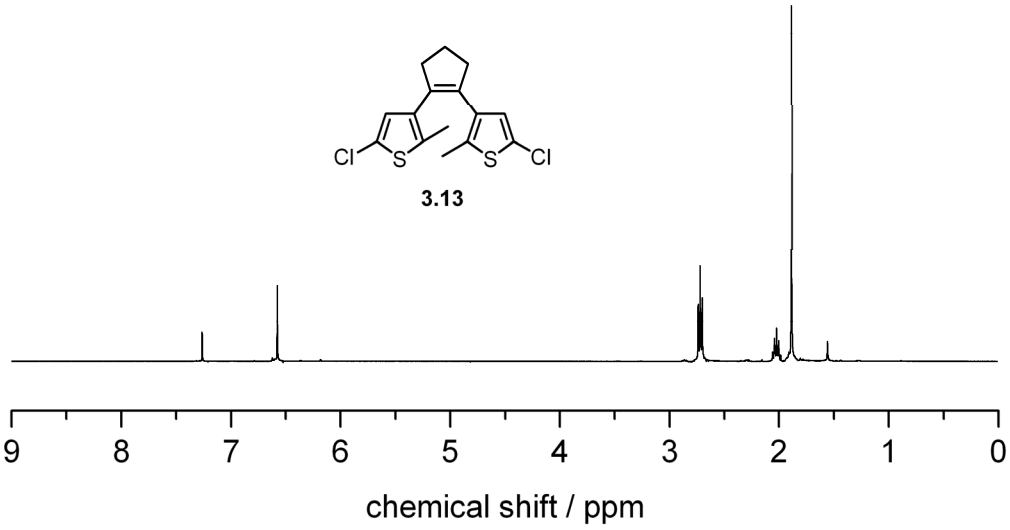

Figure 6.4.4 ^{1}H NMR (500 MHz) spectrum of compound **3.13** in chloroform-*d*.

6.5 NMR characterisation of new compounds from *Chapter 4*

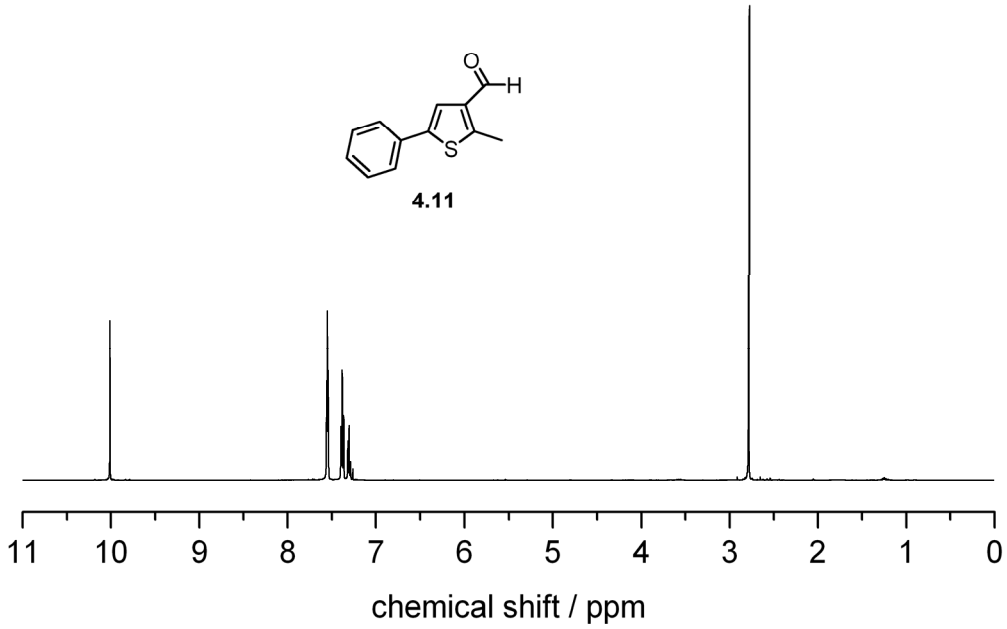

Figure 6.5.1 ^{1}H NMR (500 MHz) spectrum of compound **4.11** in chloroform-*d*.

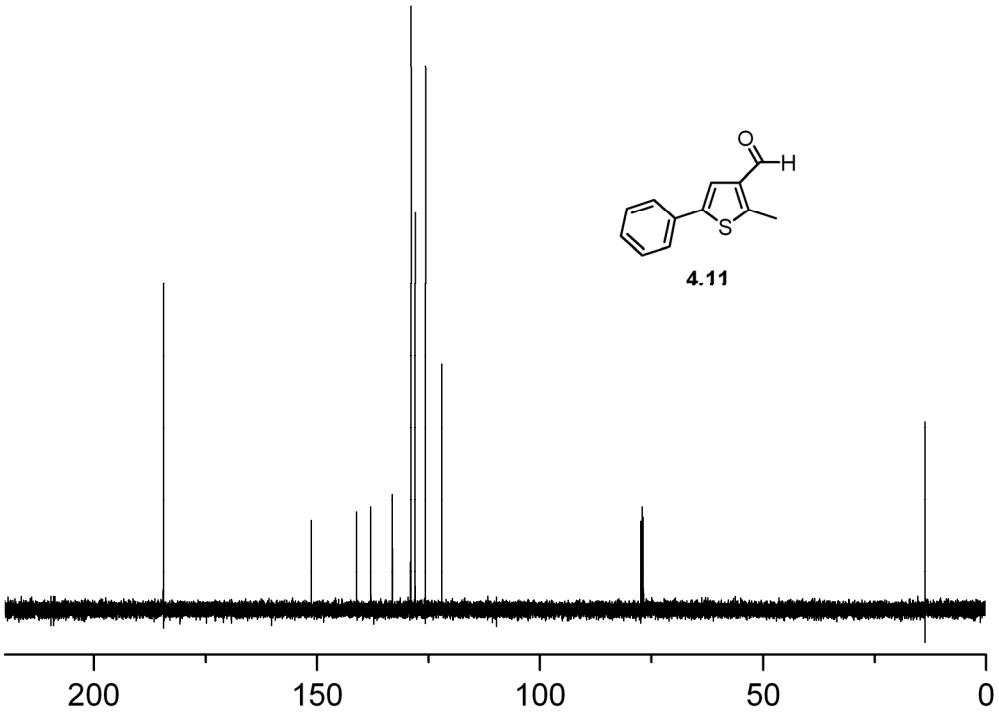

Figure 6.5.2 ^{13}C NMR (125 MHz) spectrum of compound **4.11** in chloroform-*d*.

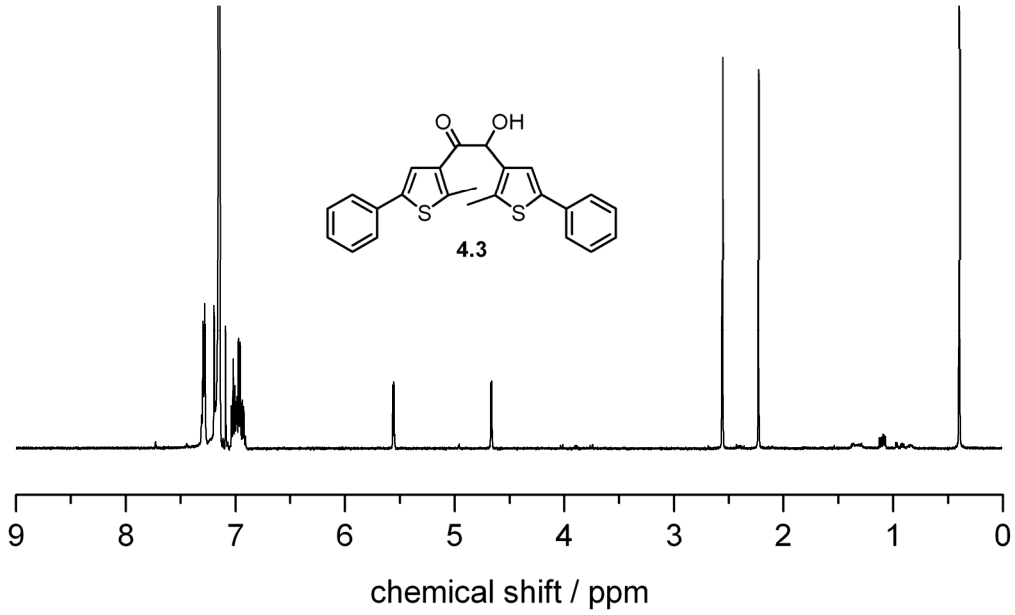

Figure 6.5.3 ^{1}H NMR (500 MHz) spectrum of compound **4.3** in benzene-d_6.

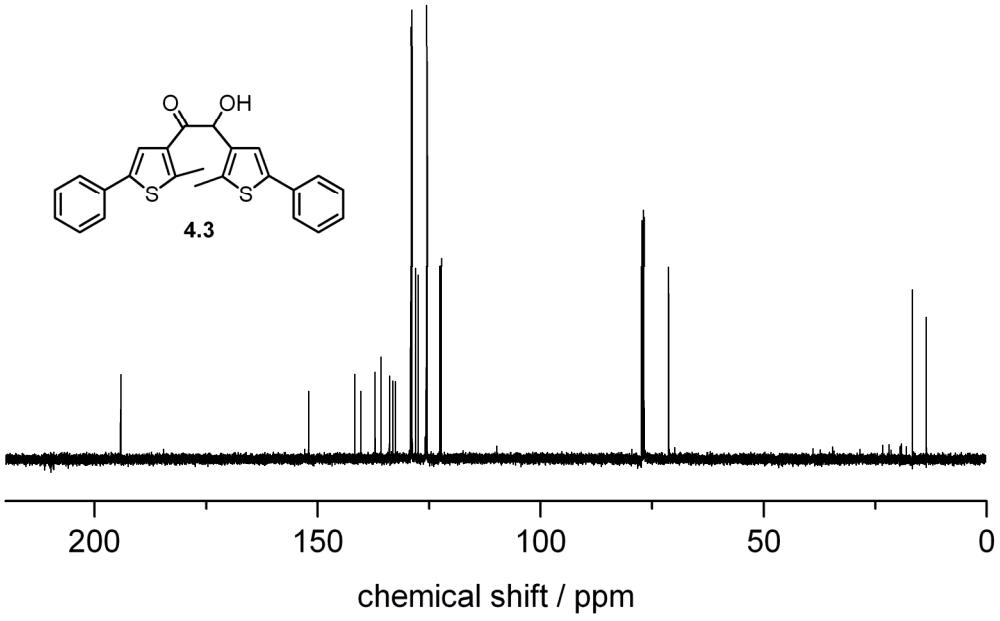

Figure 6.5.4 ^{13}C NMR (125 MHz) spectrum of compound **4.3** in chloroform-*d*.

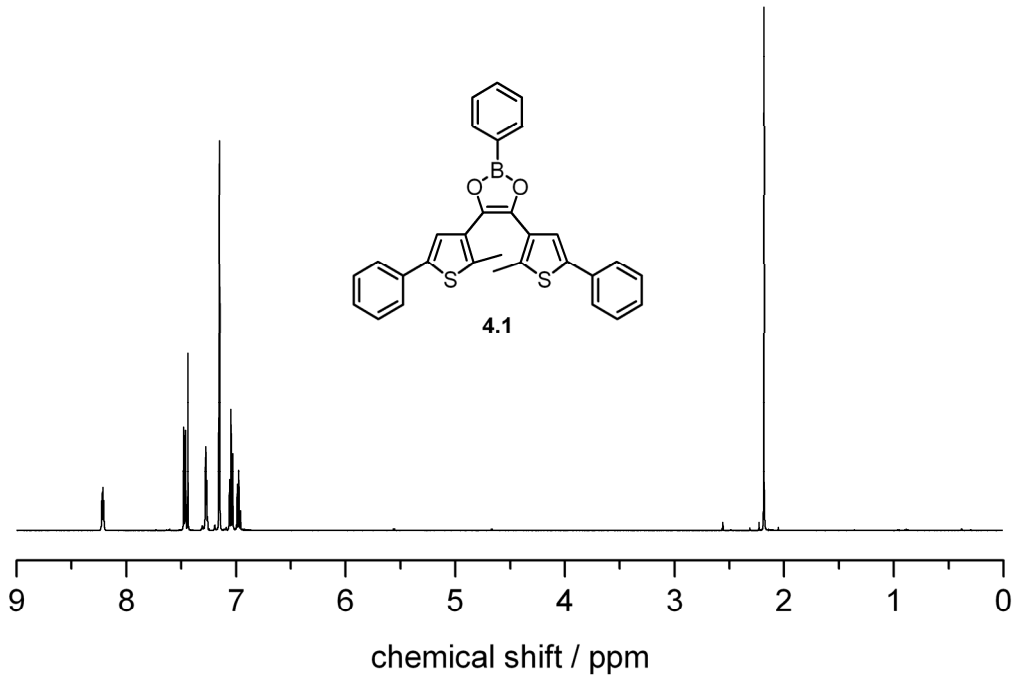

Figure 6.5.5 ^{1}H NMR (500 MHz) spectrum of compound **4.1** in benzene-d_6.

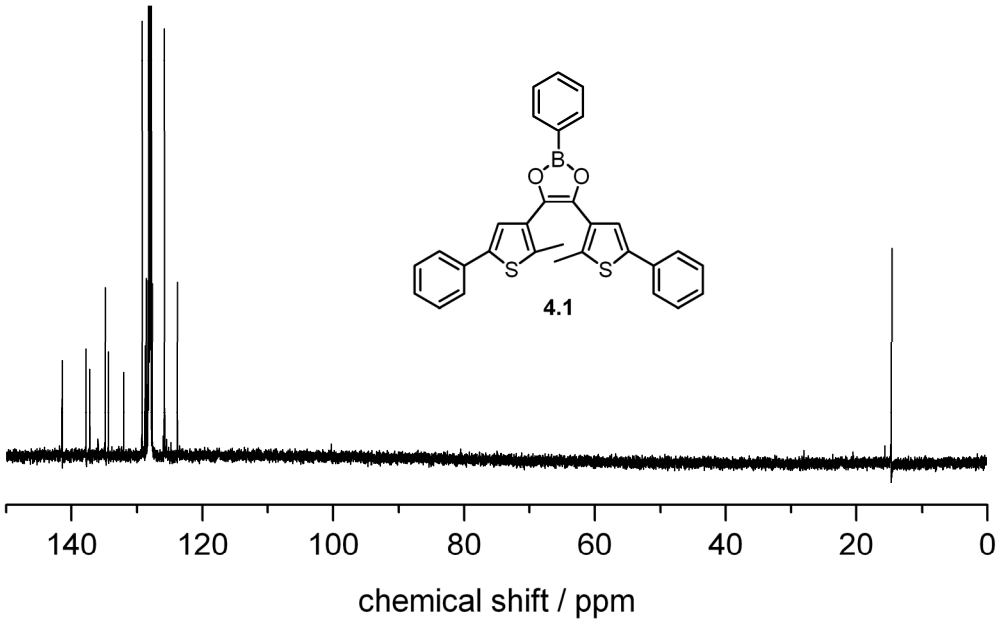

Figure 6.5.6 ^{13}C NMR (100 MHz) spectrum of compound **4.1** in benzene-d_6.

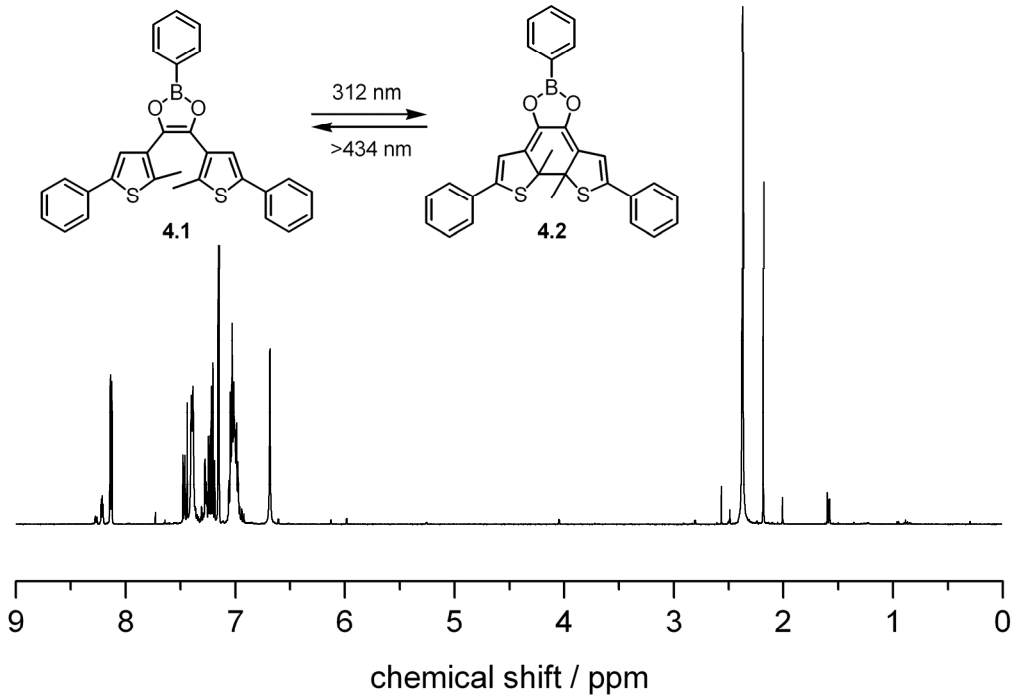

Figure 6.5.7 ^{1}H NMR (500 MHz) spectrum of compound **4.1** and **4.2** at PSS in benzene-d_6.

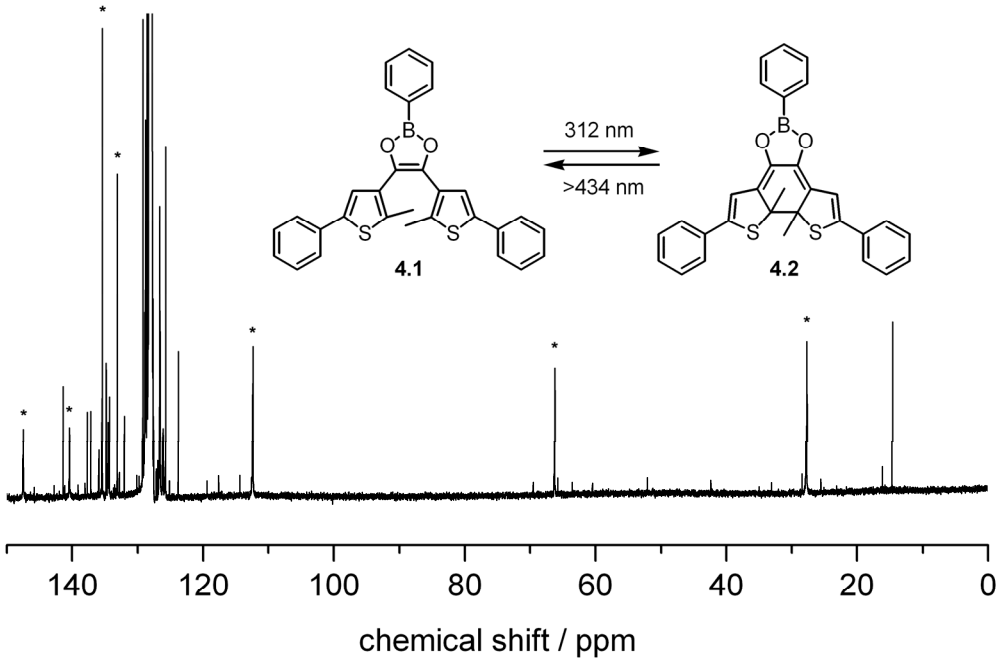

Figure 6.5.8 ^{13}C NMR (150 MHz) spectrum of compound **4.1** and **4.2** at PSS in benzene-d_6. The peaks marked with an asterisks (*) are assigned to the ring-closed isomer **4.2**.

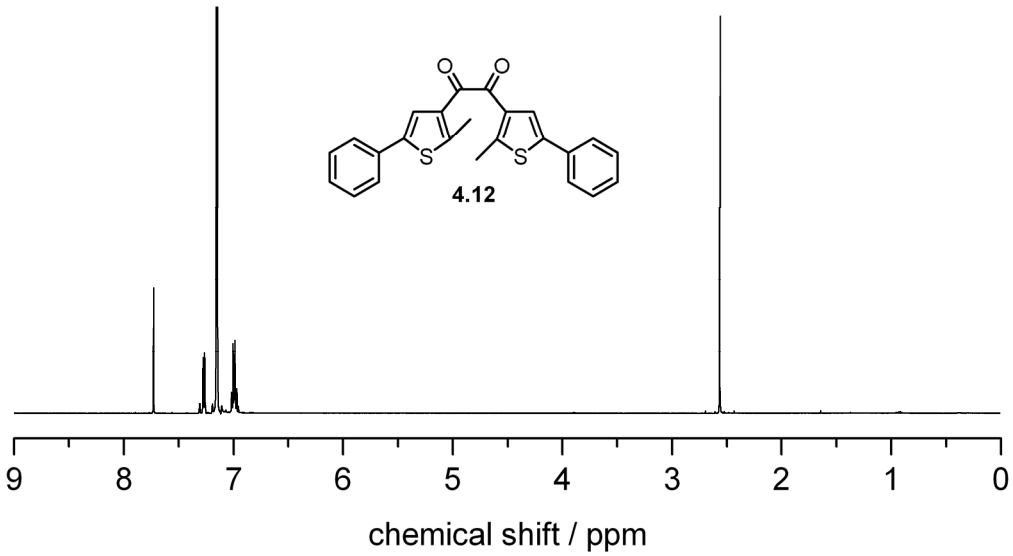

Figure 6.5.9 ^{1}H NMR (500 MHz) spectrum of compound **4.12** in benzene-d_6.

Bibliography

1. A. Gilbert, J. Baggott, *Essentials of molecular photochemistry*, CRC Press, Boca Raton, 1991, p.538.

2. R. B. Woodward, R. Hoffmann, *The conservation of orbital symmetry*, Verlag Chemie, Weinheim, 1970, p.177.

3. P. Suppan, *Chemistry and light*, The Royal Society of Chemistry, Cambridge, 1994, p.295.

4. *Current trends in polymer photochemistry* (Eds.: N. S. Allen, M. Edge, I. R. Bellobono, E. Selli), Ellis Horwood, New York, 1995, p.382.

5. A. P. Castano, P. Mroz, M. R. Hamblin, "Photodynamic therapy and anti-tumour immunity", *Nature Reviews Cancer* **2006**, *6*, 535-545.

6. H. J. Montgomery, B. Perdicakis, D. Fishlock, G. A. Lajoie, E. Jervis, J. G. Guillemette, "Photo-control of nitric oxide synthase activity using a caged isoform specific inhibitor", *Biorg. Med. Chem.* **2002**, *10*, 1919-1927.

7. Y. Zhang, F. Erdmann, R. Baumgrass, M. Schutkowski, G. Fisher, "Unexpected side chain effects at residue 8 of cyclosporin A derivatives allow photoswitching of immunosuppression", *J. Biol. Chem.* **2005**, *280*(6), 4842-4850.

8. A. P. Pelliccioli, J. Wirz, "Photoremovable protecting groups: reaction mechanisms and applications", *Photochemical and Photobiological Sciences* **2002**, *1*, 441-458.

9. S. P. A. Fodor, J. L. Read, M. C. Pirrung, L. Stryer, A. T. Lu, D. Solas, "Light-directed, spatially addressable parallel chemical synthesis", *Science* **1991**, *251*, 767-773.

10. A. P. de Silva, H. Q. N. Gunaratne, T. Gunnlaugsson, A. J. M. Huxley, C. P. McCoy, J. T. Rademacher, T. E. Rice, "Signaling recognition events with fluorescent sensors and switches", *Chem. Rev.* **1997**, *97*(5), 1515-1566.

11. D. T. McQuade, A. E. Pullen, T. M. Swager, "Conjugated polymer-based chemical sensors", *Chem. Rev.* **2000**, *100*(7), 2537-2574.

12. S. W. Thomas III, G. D. Joly, T. M. Swager, "Chemical sensors based on amplifying fluorescent conjugated polymers", *Chem. Rev.* **2007**, *107*(4), 1339-1386.

13. H. Bouas-Laurent, H. Dürr, "Organic photochromism", *Pure Appl. Chem.* **2001**, *73*(4), 639-665.

14. *Molecular switches* (Ed.: B. L. Feringa), Wiley-VCH, Weinheim, 2001, p.454.

15. *Photochromism: molecules and systems* (Eds.: H. Dürr, H. Bouas-Laurent), Elsevier, Amsterdam, 2003, p.1044.

16. *Organic photochromic and thermochromic compounds, Vol. 1* (Eds.: J. C. Crano, R. J. Guglielmetti), Plenum Press, New York, 1999, p.378.

17. M. Irie, in *Organic photochromic and thermochromic compounds, Vol. 1* (Ed.: O. P. a. T. Compounds), Plenum Press, New York, 1999, pp. 207-222.

18. M. Irie, in *Molecular switches* (Ed.: B. L. Feringa), Wiley-VCH, Weinheim, 2001, pp. 37-62.

19. K. Matsuda, M. Irie, "Recent development of 6 pi-electrocyclic photochromic systems", *Chem. Lett.* **2006**, *35*(11), 1204-1209.

20. H. Tian, S. Wang, "Photochromic bisthienylethene as multi-function switches", *Chem. Commun.* **2007**, 781-792.

21. H. Tian, S. Yang, "Recent progresses on diarylethene based photochromic switches", *Chem. Soc. Rev.* **2004**, *33*, 85-97.

22. M. Irie, "Diarylethenes for Memories and Switches", *Chem. Rev.* **2000**, *100*(5), 1685-1716.

23. S. Nakamura, M. Irie, "Thermally irreversible photochromic systems. A theoretical study." *J. Org. Chem.* **1988**, *53*(26), 6136-6138.

24. K. Higashiguchi, K. Matsuda, S. Kobatake, T. Yamada, T. Kawai, M. Irie, "Fatigue mechanism of photochromic 1,2-bis(2,5-dimethyl-3-thienyl)perfluorocyclopentene", *Bull. Chem. Soc. Jpn.* **2000**, *73*(10), 2389-2394.

25. M. Irie, T. Lifka, K. Uchida, S. Kobatake, Y. Shindo, "Fatigue resistant properties of photochromic dithienylethenes: by-product formation", *Chem. Commun.* **1999**, 747-750.

26. H. Taniguchi, A. Shinpo, T. Okazaki, F. Matsui, M. Irie, "Photodegradation mechanism of photochromic diarylethene derivatives", *Nippon Kagaku Kaishi* **1992**, *10*, 1138-1140.

27. K. Higashiguchi, K. Matsuda, T. Yamada, T. Kawai, M. Irie, "Fatigue mechanism of photochromic 1,2-bis(3-thienyl)perfluorocyclopentene", *Chem. Lett.* **2000**, *29*(12), 1358-1359.

28. Y.-C. Jeong, D. G. Park, E. Kim, K.-H. Ahn, S. I. Yang, "Fatigue-resistant photochromic dithienylethenes by controlling the oxidation state", *Chem. Commun.* **2006**, 1881-1883.

29. H. D. Samachetty, N. R. Branda, "Integrating molecular switching and chemical reactivity using photoresponsive hexatrienes", *Pure Appl. Chem.* **2006**, *78*(12), 2351-2359.

30. M. Takeshita, K. Uchida, M. Irie, "Novel saccharide tweezers with diarylethene photoswitch", *Chem. Commun.* **1996**, 1807-1808.

31. M. Takeshita, M. Irie, "Photoresponsive cesium ion tweezers with a photochromic dithienylethene", *Tetrahedron Lett.* **1998**, *39*(7), 613-616.

32. M. Takeshita, M. Irie, "Photoresponsive tweezers for alkali metal ions. Photochromic diarylethenes having two crown ether moieties", *J. Org. Chem.* **1998**, *63*(19), 6643-6649.

33. S. H. Kawai, "Photochromic bis(monoaza-crown ether)s. Alkali-metal cation complexing properties of novel diarylethenes." *Tetrahedron Lett.* **1998**, *39*(25), 4445-4448.

34. M. Takeshita, C. F. Soong, M. Irie, "Alkali metal ion effect on the photochromism of 1,2-bis(2,4-dimethylthien-3-yl)-perfluorocyclopentene having benzo-15-crown-5 moieties", *Tetrahedron Lett.* **1998**, *39*(42), 7717-7720.

35. A. Mulder, A. Joković, F. W. B. v. Leeuwen, H. Kooijman, A. L. Spek, J. Huskens, D. N. Reinhoudt, "Photocontrolled release and uptake of a porphyrin guest by dithienylethene-tethered β-cyclodextrin host dimers", *Chem. Eur. J.* **2004**, *10*, 1114-1123.

36. D. Sud, T. B. Norsten, N. R. Branda, "Photoswitching of stereoselectivity in catalysis using a copper dithienylethene complex", *Angew. Chem. Int. Ed.* **2005**, *44*(13), 2019-2021.

37. S. H. Kawai, S. L. Gilat, J.-M. Lehn, "Photochemical pKa-modulation and gated photochromic properties of a novel diarylethene switch", *Eur. J. Org. Chem.* **1999**, (9), 2359-2366.

38. Y. Odo, K. Matsuda, M. Irie, "pKa switching induced by the change in the pi-conjugated system based on photochromism", *Chem. Eur. J.* **2006**, *12*(16), 4283-4288.

39. J.-P. Malval, I. Gosse, J.-P. Morand, R. Lapouyade, "Photoswitching of cation complexation with a monoaza-crown dithienylethene photochrome", *J. Am. Chem. Soc.* **2002**, *124*(6), 904-905.

40. R. A. Vaidya, L. J. Mathias, "Polymeric supernucleophilic pyridine catalysts: homogeneous esterolysis of p-nitrophenyl esters", *J. Am. Chem. Soc.* **1986**, *108*(18), 5514-5520.

41. E. F. V. Scriven, "4-Dialkylaminopyridines: super acylation and alkylation catalysts", *Chem. Soc. Rev.* **1983**, *12*(2), 129-161.

42. H. D. Samachetty, N. R. Branda, "Photomodulation of Lewis basicity in a pyridine-functionalized 1,2-dithienylcyclopentene", *Chem. Commun.* **2005**, 2840-2842.

43. H. D. Samachetty, V. Lemieux, N. R. Branda, "Modulating chemical reactivity using a photoresponsive molecular switch", *Tetrahedron* **2008**, *64*(36), 8292-8300.

44. K. Uchida, E. Tsuchida, Y. Aoi, S. Nakamura, M. Irie, "Substitution effect on the coloration quantum yield of a photochromic bisbenzothienylethene", *Chem. Lett.* **1999**, *28*(1), 63-64.

45. T. Yamaguchi, M. Irie, "Photochromism of bis(2-alkyl-1-benzothiophen-3-yl)perfluorocyclopentene derivatives", *J. Photochem. Photobiol., A* **2006**, *178*(2-3), 162-169.

46. L. Dinescu, Z. Y. Wang, "Synthesis and photochromic properties of helically locked 1,2-dithienylethenes", *Chem. Commun.* **1999**, 2497-2498.

47. M. M. Krayushkin, S. N. Ivanov, B. V. Lichitskii, A. A. Dubinov, L. G. Vorontsova, Z. A. Starikov, A. Y. Martynkin, "Photochromic dihetarylethenes: XX. Synthesis and photochromic Properties of dithienylethenes with a fixed conformation", *Russ. J. Org. Chem.* **2004**, *40*(1), 79-84.

48. M. Takeshita, C. N. Choi, M. Irie, "Enhancement of the photocyclization quantum yield of 2,2-dimethyl-3,3-(perfluorocyclopentene-1,2-diyl)bis(benzo[b]-thiophene-6-sulfonate) by inclusion in a cyclodextrin cavity", *Chem. Commun.* **1997**, 2265-2266.

49. M. Takeshita, N. Kato, S. Kawauchi, T. Imase, J. Watanabe, M. Irie, "Photochromism of dithienylethenes included in cyclodextrins", *J. Org. Chem.* **1998**, *63*(25), 9306-9313.

50. M. Takeshita, M. Yamada, N. Kato, M. Irie, "Photochromism of dithienylethene-bis(trimethylammonium) iodide in cyclodextrin cavities", *J. Chem. Soc., Perkin Trans. 2* **2000**, (4), 619-622.

51. M. Irie, O. Miyatake, K. Uchida, "Blocked photochromism of diarylethenes", *J. Am. Chem. Soc.* **1992**, *114*(22), 8715-8716.

52. M. Irie, O. Miyatake, K. Uchida, T. Eriguchi, "Photochromic diarylethenes with intralocking arms", *J. Am. Chem. Soc.* **1994**, *116*(22), 9894-9900.

53. M. Irie, O. Miyatake, R. Sumiya, M. Hanazawa, Y. Horikawa, K. Uchida, "Photochromism of diarylethenes with intralocking arms", *Mol. Cryst. Liq. Cryst. Sci. Technol., Sect. A* **1994**, *246*(1), 155-158.

54. M. Walko, B. L. Feringa, "Synthesis and properties of dipyridylcyclopentenes", *Molecular Crystals and Liquid Crystals* **2005**, *431*(1), 549-553.

55. B. Qin, R. Yao, X. Zhao, H. Tian, "Enhanced photochromism of 1,2-dithienylcyclopentene complexes with metal ion", *Org. Biomol. Chem.* **2003**, *1*, 2187-2191.

56. S. H. Kawai, S. L. Gilat, J.-M. Lehn, "A dual-mode optical – electrical molecular switching device", *J. Chem. Soc., Chem. Commun.* **1994**, 1011-1013.

57. S. H. Kawai, S. L. Gilat, R. Ponsinet, J.-M. Lehn, "A dual-mode molecular switching device: Bisphenolic diarylethenes with integrated photochromic and electrochromic properties", *Chem. Eur. J.* **1995**, *1*(5), 285-293.

58. K. Yumoto, M. Irie, K. Matsuda, "Control of the photoreactivity of diarylethene derivatives by quaternarization of the pyridylethynyl group", *Org. Lett.* **2008**, *10*(10), 2051-2054.

59. M. Irie, T. Eriguchi, T. Takada, K. Uchida, "Photochromism of diarylethenes having thiophene oligomers as the aryl groups", *Tetrahedron* **1997**, *53*(36), 12263-12271.

60. M. Ohsumi, T. Fukaminato, M. Irie, "Chemical control of the photochromic reactivity of diarylethene derivatives", *Chem. Commun.* **2005**, (31), 3921-3923.

61. J. Kühni, P. Belser, "Gated photochromism of 1,2-diarylethenes", *Org. Lett.* **2007**, *9*(10), 1915-1918.

62. Z. Chen, S. Zhao, Z. Li, Z. Zhang, F. Zhang, "Acid/alkali gated photochromism of two diarylperfluorocyclopentenes", *Sci. China, Ser. B* **2007**, *50*(5), 581-586.

63. K. Uchida, T. Matsuoka, S. Kobatake, T. Yamaguchi, M. Irie, "Substituent effect on the photochromic reactivity of bis(2-thienyl)perfluorocyclopentenes", *Tetrahedron* **2001**, *57*(21), 4559-4565.

64. Z. Zhou, S. Xiao, J. Xu, Z. Liu, M. Shi, F. Li, T. Yi, C. Huang, "Modulation of the photochromic property in an organoboron-based diarylethene by a fluoride ion", *Org. Lett.* **2006**, *8*(18), 3911-3914.

65. Z. Zhou, H. Yang, M. Shi, S. Xiao, F. Li, T. Yi, C. Huang, "Photochromic organoboron-based dithienylcyclopentene modulated by fluoride and mercuric(II) ions", *ChemPhysChem* **2007**, *8*(9), 1289-1292.

66. X.-D. Liu, Z.-H. Chen, G.-F. Fan, F.-S. Zhang, "Lewis acid modulation in a amido-functional diarylethene and its hypsochromism effect", *Chin. J. Chem.* **2006**, *24*(10), 1462-1464.

67. S. Xiao, T. Yi, Y. Zhou, Q. Zhao, F. Li, C. Huang, "Multi-state molecular switches based on dithienylperfluorocyclopentene and imidazo [4,5-f] [1,10] phenanthroline", *Tetrahedron* **2006**, *62*(43), 10072-10078.

68. P. H.-M. Lee, C.-C. Ko, N. Zhu, V. W.-W. Yam, "Metal coordination-assisted near-infrared photochromic behavior: A large perturbation on absorption wavelength properties of N,N-donor ligands containing diarylethene derivatives by coordination to the rhenium(I) metal center", *J. Am. Chem. Soc.* **2007**, *129*(19), 6058-6059.

69. V. W.-W. Yam, C.-C. Ko, N. Zhu, "Photochromic and luminescence switching properties of a versatile diarylethene-containing 1,10-phenanthroline ligand and its rhenium(I) complex", *J. Am. Chem. Soc.* **2004**, *126*(40), 12734-12735.

70. C.-C. Ko, W.-M. Kwok, V. W.-W. Yam, D. L. Phillips, "Triplet MLCT photosensitization of the ring-closing reaction of diarylethenes by design and synthesis of a photochromic rhenium(I) complex of a diarylethene-containing 1,10-phenanthroline ligand", *Chem. Eur. J.* **2006**, *12*(22), 5840-5848.

71. S. Kobatake, Y. Terakawa, "Acid-induced photochromic system switching of diarylethene derivatives between P- and T-types", *Chem. Commun.* **2007**, 1698-1700.

72. D. Sud, T. J. Wigglesworth, N. R. Branda, "Creating a reactive enediyne by using visible light: Photocontrol of the Bergman cyclization", *Angew. Chem. Int. Ed.* **2007**, *46*(42), 8017-8019.

73. F. Fringuelli, A. Taticchi, *The Diels Alder reaction: selected practical methods* Wiley, New York, 2002, p.340.

74. A. E. Konovalov, V. D. Kiselev, "Diels-Alder reaction. Effect of internal and external factors on the reactivity of diene-dienophile systems", *Russ. Chem. Bull.* **2003**, *52*(2), 293-311.

75. B. Rickborn, in *Organic reactions, Vol. 52* (Ed.: L. A. Paquette), John Wiley & Sons, Inc., 1998, pp. 1-393.

76. H. Kwart, K. King, "The reverse Diels-Alder or retrodiene reaction", *Chem. Rev.* **1968**, *68*(4), 415-447.

77. P. Reutenauer, "Réactions de Diels-Alder et chimie dynamique constitutionnelle", Ph.D. Thesis, Université Louis Pasteur de Strasbourg (Strasbourg), **2006**.

78. K. Uchida, G. Masuda, Y. Aoi, K. Nakayama, M. Irie, "Synthesis of tetrathiafulvalene derivatives with photochromic diarylethene moieties", *Chem. Lett.* **1999**, (10), 1071-1072.

79. S. N. Ivanov, B. V. Lichitskii, A. A. Dudinov, A. Y. Martynkin, M. M. Krayushkin, "Synthesis of substituted 1,2,4-triazines based on 1,2-bis(2,5-dimethyl-3-thienyl)ethanedione", *Chem. Heterocycl. Compd.* **2001**, *37*(1), 85-90.

80. O. L. Chapman, C. L. McIntosh, "Cyclopentadienone", *J. Chem. Soc. D* **1971**, 770-771.

81. C. F. H. Allen, J. A. VanAllan, "Dimerization of cyclopentadienones", *J. Am. Chem. Soc.* **1950**, *72*(11), 5165-5167.

82. S. Ito, M. Wehmeier, J. D. Brand, C. Kübel, R. Epsch, J. P. Rabe, K. Müllen, "Synthesis and self-assembly of functionalized hexa-peri-hexabenzocoronenes", *Chem. Eur. J.* **2000**, *6*(23), 4327-4342.

83. A. Peters, N. R. Branda, "Electrochromism in photochromic dithienylcyclopentenes", *J. Am. Chem. Soc.* **2003**, *125*(12), 3404-3405.

84. A. P. Glaze, S. A. Harris, H. G. Heller, W. Johncock, S. N. Oliver, P. J. Strydom, J. Whittall, "Photochromic heterocyclic fulgides. Part 4. The thermal and photochemical reactions of (E)-isopropylidene-[-(2- and -(3-thienyl)ethylidene]succinic anhydrides and related compounds", *J. Chem. Soc., Perkin Trans. 1* **1985**, 957-961.

85. A. Tambuté, A. Collet, "Dédoublement et détermination de la configuration absolue des énantiomères de l'acide (thiényl-3)-2 cyclohexyl-2 hydroxy-2 acétique. Application à la synthèse d'esters anticholinergiques du quinuclidinol-3." *Bull. Soc. Chim. Fr.* **1984**, (1-2), 77-82.

86. R. Faust, F. Mitzel, "NIR chromophores from small acetylenic building blocks: a Diels–Alder approach to octaalkynylphthalocyanines", *J. Chem. Soc., Perkin Trans. 1* **2000**, 3746-3751.

87. P. Calcagno, B. M. Kariuki, S. J. Kitchin, J. M. A. Robinson, D. Philp, K. D. M. Harris, "Understanding the structural properties of a homologous series of bis-diphenylphosphine oxides", *Chem. Eur. J.* **2000**, *6*(13), 2338-2349.

88. *Dynamic studies in biology: phototriggers, photoswitches and caged biomolecules* (Eds.: M. Goeldner, R. Givens), Wiley-VCH, Weinheim, 2005.

89. C. P. McCoy, C. Rooney, C. R. Edwards, D. S. Jones, S. P. Gorman, "Light-triggered molecule-scale drug dosing devices", *J. Am. Chem. Soc.* **2007**, *129*(31), 9572-9573.

90. C. G. Bochet, "Photolabile protecting groups and linkers", *J. Chem. Soc., Perkin Trans. 1* **2002**, 125-142.

91. J. H. Kaplan, B. Forbush III, J. F. Hoffman, "Rapid photolytic release of adenosine 5'-triphosphate from a protected analogue: Utilization by the Na:K pump of human red blood cell ghosts", *Biochemistry* **1978**, *17*(10), 1929--1935.

92. C. Sundararajan, D. E. Falvey, "Photolytic release of carboxylic acids using linked donor-acceptor molecules: Direct versus mediated photoinduced electron transfer to N-alkyl-4-picolinium esters", *Org. Lett.* **2005**, *7*(13), 2631-2634.

93. C. Sundararajan, D. E. Falvey, "Photorelease of carboxylic acids, amino acids, and phosphates from N-alkylpicolinium esters using photosensitization by high wavelength laser dyes", *J. Am. Chem. Soc.* **2005**, *127*(22), 8000-8001.

94. K. Lee, D. E. Falvey, "Photochemically removable protecting groups based on covalently linked electron donor-acceptor systems", *J. Am. Chem. Soc.* **2000**, *122*(39), 9361-9366.

95. J. B. Borak, S. Lopez-Sola, D. E. Falvey, "Photorelease of carboxylic acids mediated by visible-light-absorbing gold-nanoparticles", *Org. Lett.* **2008**, *10*(3), 457-460.

96. C. G. Bochet, "Orthogonal photolysis of protecting groups", *Angew. Chem. Int. Ed.* **2001**, *40*(11), 2071-2073.

97. A. Blanc, C. G. Bochet, "Wavelength-controlled orthogonal photolysis of protecting groups", *J. Org. Chem.* **2002**, *67*(16), 5567-5577.

98. M. Morimoto, S. Kobatake, M. Irie, "Multicolor photochromism of two- and three-component diarylethene crystals", *J. Am. Chem. Soc.* **2003**, *125*(36), 11080-11087.

99. A. Fernandez-Acebes, J.-M. Lehn, "Combinatorial color generation with mixtures of dithienyl photochromes", *Adv. Mater.* **1999**, *11*(11), 910-913.

100. K. Higashiguchi, K. Matsuda, N. Tanifuji, M. Irie, "Full-color photochromism of a fused dithienylethene trimer", *J. Am. Chem. Soc.* **2005**, *127*(25), 8922-8923.

101. T. J. Wigglesworth, N. R. Branda, "A family of multiaddressable, multicolored photoresponsive copolymers prepared by ring-opening metathesis polymerization", *Chem. Mater.* **2005**, *17*(22), 5473-5480.

102. J. R. R. Majjigapu, A. N. Kurchan, R. Kottani, T. P. Gustafson, A. G. Kutateladze, "Release and report: A new photolabile caging system with a two-photon fluorescence reporting function", *J. Am. Chem. Soc.* **2005**, *127*(36), 12458-12459.

103. Y. Inokuma, T. Matsunari, N. Ono, H. Uno, A. Osuka, "A doubly N-fused benzohexaphyrin and its rearrangement to a fluorescent macrocycle upon DDQ oxidation", *Angew. Chem. Int. Ed.* **2005**, *44*(12), 1856-1860.

104. C.-K. Choi, I. Tomita, T. Endo, "Synthesis of novel pi-conjugated π-conjugated polymer having an enyne unit by palladium-catalyzed three-component coupling polymerization and subsequent retro-diels-alder reaction", *Macromolecules* **2000**, *33*(5), 1487-1488.

105. A. Ichihara, "Retro-Diels-Alder strategy in natural product synthesis", *Synthesis* **1987**, (3), 207-222.

106. M.-C. Lasne, J.-L. Ripoll, "New synthesic developments of the [4π + 2π] cycloreversion", *Synthesis* **1985**, 121-143.

107. J. Zhu, A. J. Kell, M. S. Workentin, "A retro-Diels-Alder reaction to uncover maleimide-modified surfaces on monolayer-protected nanoparticles for reversible covalent assembly", *Org. Lett.* **2006**, *8*(22), 4993-4996.

108. S. D. Bergman, F. Wudl, "Mendable polymers", *J. Mater. Chem.* **2008**, *18*, 41-62.

109. R. N. Warrener, D. Margetic, G. Sun, "The N,O-bridged sesquinorbornadienes: a testing ground for establishing the superiority of N-Z pyrrole over furan as dienofuge in retro-Diels-Alder reactions", *Tetrahedron Lett.* **2001**, *42*(25), 4263-4265.

110. G. Stájer, F. Miklós, I. Kanizsai, F. Csende, R. Sillanpää, P. Sohár, "Application of furan as a diene: preparation of condensed 1,3-oxazines by retro-Diels-Alder reactions", *Eur. J. Org. Chem.* **2004**, 3701-3706.

111. N. Bensel, N. Bahr, M. T. Reymond, C. Schenkels, J.-L. Reymond, "Catalytic antibodies by fluorescence screening", *Helv. Chim. Acta* **1999**, *82*(1), 44-52.

112. M. Hugot, N. Bensel, M. Vogel, M. T. Reymond, B. Stadler, J.-L. Reymond, U. Baumann, "A structural basis for the activity of retro-Diels–Alder catalytic antibodies: Evidence for a catalytic aromatic residue", *PNAS* **2002**, *99*(15), 9674-9678

113. M. E. Bunnage, K. C. Nicolaou, "The oxide anion accelerated retro-Diels-Alder reaction", *Chem. Eur. J.* **1997**, *3*(2), 187-192.

114. O. Papies, W. Grimme, "Acceleration of the (4+2)-cycloreversion by the alkoxide substituent", *Tetrahedron Lett.* **1980**, *21*(29), 2799-2802.

115. W. Neukam, W. Grimme, "Anionic (4+2)-cycloreversions leading to the cyanocyclopentadienide ion", *Tetrahedron Lett.* **1978**, *19*(25), 2201-2204.

116. T. M. Balthazor, B. Gaede, D. E. Korte, H.-S. Shieh, "Reaction of 1,1,1-trichloro-3-nitro-2-propene with furans: A reexamination", *J. Org. Chem.* **1984**, *49*(23), 4547-4549.

117. P. D. Bartlett, C. Wu, "Reactions of tetracyanoethylene (TCNE) with the three isodicyclopentadiene isomers", *J. Org. Chem.* **1984**, *49*(11), 1880-1890.

118. I. Lamparth, C. Maichle-Mössmer, A. Hirsch, "Reversible template-directed activation of equatorial double bonds of the fullerene framework: Regioselective direct synthesis, crystal structure, and aromatic properties of T_h-$C_{66}(COOEt)_{12}$", *Angew. Chem. Int. Ed.* **1995**, *34*(15), 1607-1609.

119. G.-W. Wang, M. Saunders, R. J. Cross, "Reversible Diels-Alder addition to fullerenes: A study of equilibria using ^{3}He NMR spectroscopy", *J. Am. Chem. Soc.* **2001**, *123*(2), 256-259.

120. M. H. Howard, V. Alexander, W. J. Marshall, D. C. Roe, Y.-J. Zheng, "Reaction of 2,2-bis(trifluoromethyl)-1,1-dicyanoethylene with 6,6-dimethylfulvene: cycloadditions and a rearrangement", *J. Org. Chem.* **2003**, *68*(1), 120-129.

121. P. J. Boul, P. Reutenauer, J.-M. Lehn, "Reversible Diels-Alder Reactions for the generation of dynamic combinatorial libraries", *Org. Lett.* **2005**, *7*(1), 15-18.

122. J. H. Day, "The fulvenes", *Chem. Rev.* **1953**, *53*(2), 167-189.

123. O. Diels, K. Alder, "Syntheses in the hydroaromatic series. IV. Addition of maleic anhydride to arylated dienes, trienes and fulvenes", *Berichte der Deutschen Chemischen Gesellschaft [Abteilung] B: Abhandlungen* **1929**, *62B*, 2081-2087.

124. E. P. Kohler, J. Kable, "The Diels-Alder reaction in the fulvene series", *J. Am. Chem. Soc.* **1935**, *57*(5), 917-918.

125. K. Alder, G. Stein, "Untersuchungen über den Verlauf der Diensynthese", *Angew. Chem.* **1937**, *50*(28), 510-519.

126. R. B. Woodward, H. Baer, "Studies on diene-addition reactions. II. The reaction of 6,6-pentamethylenefulvene with maleic anhydride", *J. Am. Chem. Soc.* **1944**, *66*(4), 645-649.

127. J. A. Berson, "Kinetics, thermodynamics, and the problem of selectivity: the maturation of an idea", *Angew. Chem. Int. Ed.* **2006**, *45*(29), 4724-4729.

128. B. Halton, "The fulvalenes", *Eur. J. Org. Chem.* **2005**, 3391-3414.

129. M. Jones, *Organic Chemistry*, W. W. Norton & Company, New York, 1997, p.1394.

130. L. N. Lucas, J. J. D. d. Jong, J. H. v. Esch, R. M. Kellogg, B. L. Feringa, "Syntheses of dithienylcyclopentene optical molecular switches", *Eur. J. Org. Chem.* **2003**, 155-166.

131. L. N. Lucas, J. v. Esch, R. M. Kellogg, B. L. Feringa, "A new class of photochromic 1,2-diarylethenes; synthesis and switching properties of bis(3-thienyl)cyclopentenes", *Chem. Commun.* **1998**, 2313-2314.

132. K. Chajara, H. Ottosson, "An improved pathway to 6,6-disubstituted fulvenes", *Tetrahedron Lett.* **2004**, *45*(36), 6741-6744.

133. K. J. Stone, R. D. Little, "An exceptionally simple and efficient method for the preparation of a wide variety of fulvenes", *J. Org. Chem.* **1984**, *49*(11), 1849-1853.

134. *Biomedical nanostructures* (Ed.: K. E. Gonsalves), Wiley-Interscience, Hoboken, N.J., 2008, p.507.

135. C. J. Ireland, K. Jones, J. S. Pizey, S. Johnson, "Tetra-substituted ethylenes", *Synth. Commun.* **1976**, *6*(3), 185-191.

136. Unpublised results

137. R. Wenger, "Pharmacology of cyclosporin", *Pharmacological Reviews* **1989**, *41*(3), 239-247.

138. J. A. Smulik, S. T. Diver, F. Pan, J. O. Liu, "Synthesis of Cyclosporin A-derived affinity reagents by olefin metathesis", *Org. Lett.* **2002**, *4*(12), 2051-2054.

139. E. Plettner, A. Mohle, M. T. Mwangi, J. Griscti, B. O. Patrick, R. Nair, R. J. Batchelor, F. Einstein, "2-Chlorobicyclo[2.2.1]hept-5-ene-2-carboxamide and 2-chlorobicyclo[2.2.1]heptane-2-carboxamide as precursors of bicyclo[2.2.1]hept-5-en-2-one and bicyclo[2.2.1]heptan-2-one: resolution, absolute configuration and hydrogen-bonding properties", *Tetrahedron: Asymmetry* **2005**, *16*(16), 2754-2763.

140. X. Chen, M. A. Dam, K. Ono, A. Mal, H. Shen, S. R. Nutt, K. Sheran, F. Wudl, "A thermally re-mendable cross-linked polymeric material", *Science* **2002**, *295*(5560), 1698-1702.

141. K. Ishihara, H. Yamamoto, "Arylboron compounds as acid catalysts in organic synthetic transformations", *Eur. J. Org. Chem.* **1999**, (3), 527-538.

142. E. Y. X. Chen, T. J. Marks, "Cocatalysts for metal-catalyzed olefin polymerization: Activators, activation processes, and structure-activity relationships", *Chem. Rev.* **2000**, *100*(4), 1391-1434.

143. G. L. Jialanella, T. Ristoski, "Stabilized organoborane polymerization initiators and polymerizable compositions", U.S. Patent 7,247,596, July 24, 2007.

144. S. Yamaguchi, A. Wakamiya, "Boron as a key component for new π-electron materials", *Pure Appl. Chem.* **2006**, *78*(7), 1413-1424.

145. C. E. Housecroft, *Boranes and metallaboranes, structure, bonding and reactivity, 2nd Ed.*, Ellis Horwood, Hertfordshire, Great Britain, 1994, p.156.

146. *The chemistry of boron and its compounds* (Ed.: E. L. Muetterties), John Wiley & Sons, New York, United States of America, 1967.

147. T. Onak, *Organoborane Chemistry*, Academic Press, New York, 1975, p.146-163.

148. W. E. Piers, in *Adv. Organomet. Chem., Vol. 52* (Eds.: R. West, A. F. Hill), Elsevier, San Diego, United States of America, 2005, pp. 1-76.

149. R. G. Kidd, in *NMR of Newly Accessible Nuclei, Vol. 2* (Ed.: P. Laszlo), Academic Press, New York, United States of America, 1983, pp. 49-77.

150. C. D. Entwistle, T. B. Marder, "Boron chemistry lights the way: optical properties of molecular and polymeric systems", *Angew. Chem. Int. Ed.* **2002**, *41*(16), 2927-2931.

151. C. D. Entwistle, T. B. Marder, "Applications of three-coordinate organoboron compounds and polymers in optoelectronics", *Chem. Mater.* **2004**, *16*(23), 4574-4585.

152. S. Yamaguchi, S. Akiyama, K. Tamao, "A new approach to photophysical properties control of main group element π-electron compounds based on the coordination number change", *J. Organomet. Chem.* **2002**, *652*(1-2), 3-9.

153. S. Yamaguchi, T. Shirasaka, S. Akiyama, K. Tamao, "Dibenzoborole-containing π-electron systems: remarkable fluorescence change based on the “on/off” control of the p_π-π* conjugation", *J. Am. Chem. Soc.* **2002**, *124*(30), 8816-8817.

154. K. Ma, M. Scheibitz, S. Scholz, M. Wagner, "Applications of boron–nitrogen and boron–phosphorus adducts in organometallic chemistry", *J. Organomet. Chem.* **2002**, *652*(1-2), 11-19.

155. *Lewis acids in organic synthesis* (Ed.: E. H. Yamamoto), Wiley/VCH, New York, 2000, p.945.

156. F. Jäkle, "Lewis acidic organoboron polymers", *Coord. Chem. Rev.* **2006**, *250*(9-10), 1107-1121.

157. A. Sundararaman, M. Victor, R. Varughese, F. Jäkle, "A family of main-chain polymeric Lewis acids: synthesis and fluorescent sensing properties of boron-modified polythiophenes", *J. Am. Chem. Soc.* **2005**, *127*(40), 13748-13749.

158. S. Itsuno, in *Lewis acids in Organic Synthesis, Vol. 2* (Ed.: H. Yamamoto), Wiley/VCH, Weinheim, 2000, p. 945.

159. B. A. Deore, I. S. Yu, P. M. Aguiar, C. Recksiedler, S. Kroeker, M. S. Freund, "Highly cross-linked, self-doped polyaniline exhibiting unprecedented hardness", *Chem. Mater.* **2005**, *17*(15), 3803-3805.

160. Y. Qin, G. L. Cheng, O. Achara, K. Parab, F. Jakle, "A new route to organoboron polymers via highly selective polymer modification reactions", *Macromolecules* **2004**, *37*(19), 7123-7131.

161. P. A. Chase, P. E. Romero, W. E. Piers, M. Parvez, B. O. Patrick, "Fluorinated 9-borafluorenes vs. conventional perfluoroayl borane - Comparative Lewis acidity", *Can. J. Chem.* **2005**, *83*, 2098-2105.

162. M. V. Metz, D. J. Schwartz, C. L. Stern, P. N. Nickias, T. J. Marks, "Organo-Lewis acid cocatalysts in single-site olefin polymerization - A highly acidic perfluorodiboraanthracene", *Angew. Chem. Int. Ed.* **2000**, *39*(7), 1312-1316.

163. T. K. Wood, W. E. Piers, B. A. Keay, M. Parvez, "1-Borabarrelene derivatives via Diels-Alder additions to borabenzenes", *Org. Lett.* **2006**, *8*(13), 2875-2878.

164. M. Yasuda, S. Yoshioka, S. Yamasaki, T. Somyo, K. Chiba, A. Baba, "Cage-shaped borate esters with enhanced Lewis acidity and catalytic activity", *Org. Lett.* **2006**, *8*(4), 761-764.

165. T. Agou, J. Kobayashi, T. Kawashima, "Tuning the optical properties and Lewis acidity of dibenzopnictogenaborins by modification on bridging main group elements", *Inorg. Chem.* **2006**, *45*(22), 9137-9144.

166. C.-W. Chiu, F. P. Gabbaï, "Fluoride ion capture from water with a cationic borane", *J. Am. Chem. Soc.* **2006**, *128*(44), 14248-14249.

167. K. Venkatasubaiah, I. Howik, R. H. Herber, F. Jäkle, "Lewis acidity enhancement of organoboranes via oxidation of appended ferrocene moieties", *Chem. Commun.* **2007**, 2154-2156.

168. T. D. James, K. R. A. S. Sandanayake, R. Iguchi, S. Shinka, "Novel saccharide-photoinduced electron transfer sensors based on the interaction of boronic acid and amine", *J. Am. Chem. Soc.* **1995**, *117*(35), 8982-8987.

169. S. L. Wiskur, J. J. Lavigne, H. Ait-Haddou, V. Lynch, Y. H. Chiu, J. W. Canary, E. V. Anslyn, "pK_a values and geometries of secondary and tertiary amines complexed to boronic acids - Implications for sensor design", *Org. Lett.* **2001**, *3*(9), 1311-1314.

170. A. V. Fedorov, A. A. Ermoshkin, A. Mejiritski, D. C. Neckers, "New method to reduce oxygen surface inhibition by photorelease of boranes from borane/amine complexes", *Macromolecules* **2007**, *40*(10), 3554-3560.

171. N. Kano, J. Yoshino, T. Kawashima, "Photoswitching of the Lewis acidity of a catecholborane bearing an azo group based on the change in coordination number of boron", *Org. Lett.* **2005**, *7*(18), 3909-3911.

172. J. Yoshino, N. Kano, T. Kawashima, "Synthesis of organoboron compounds bearing an azo group and substituent effects on their structures and photoisomerization", *Tetrahedron* **2008**, *64*(33), 7774-7781.

173. N. Xie, D. X. Zeng, Y. Chen, "3,4-Bis(5-iodo-2-methylthien-3-yl)-2,5-dihydrothiophene: A powerful synthon for the preparation of photochromic dithienylethene derivatives", *Synlett* **2006**, (5), 737-740.

174. P. M. Maitlis, "Heterocyclic organic boron compounds", *Chem. Rev.* **1962**, *62*(3), 223-245.

175. R. L. Letsinger, S. B. Hamilton, "Organoboron compounds. XII. Heterocyclic compounds from benzeneboronic acid", *J. Org. Chem.* **1960**, *25*(4), 592-595.

176. G. Smolinski, "Heterocyclic organoboron compounds. Some derivatives of 1,3,2-dioxaborole", *J. Org. Chem.* **1961**, *26*(12), 4915-4917.

177. J. G. de Vries, S. A. Hubbard, "Conversion of benzoin into 9-10-phenanthrenequinone by photocyclization", *J. Chem. Soc., Chem. Commun.* **1988**, 1172-1173.

178. Unpublished results.

179. J. P. Girault, P. Scribe, G. Dana, "Electrophilic substitutions on pentagonal heterocycles. 2. Role of steric factors in acylation reactions of 2-phenyl-5-methylthiophene", *Tetrahedron* **1973**, *29*(2), 413-418.

180. K. A. Connors, *Binding contants - The measurement of molecular complex stability*, John Wiley & Sons, New York, 1987, p.411.

181. K. Hirose, "A practical guide for the determination of binding constants", *Journal of Inclusion Phenomena and Macrocyclic Chemistry* **2001**, *39*(3-4), 193-209.

182. M. W. Schmidt, K. K. Baldridge, J. A. Boatz, S. T. Elbert, M. S. Gordon, J. H. Jensen, S. Koseki, N. Matsunaga, K. A. Nguyen, S. Su, T. L. Windus, S. T. Elbert, "General atomic and molecular electronic structure system", *J. Comput. Chem.* **1993**, *14*(11), 1347-1363.

183. C. Moller, M. S. Plesset, "Note on an approximation treatment for many-electron systems", *Physical Review* **1934**, *46*, 618-622.

184. A. D. Becke, "Density-functional thermochemistry. III. The role of exact exchange", *J. Chem. Phys.* **1993**, *98*(7), 5648-5652.

185. C. Lee, W. Yang, R. G. Parr, "Development of the Colle-Salvetti correlation-energy formula into a functional of the electron density", *Phys. Rev. B: Condens. Matter* **1988**, *37*(2), 785-789.

186. B. Miehlich, A. Savin, H. Stoll, H. Preuss, "Results obtained with the correlation energy density functionals of becke and Lee, Yang and Parr", *Chem. Phys. Lett.* **1989**, *157*(3), 200-206.

187. Y. Zhao, D. G. Truhlar, "The M06 suite of density functionals for main group thermochemistry, thermochemical kinetics, noncovalent interactions, excited states, and transition elements: two new functionals and systematic testing of four M06-class functionals and 12 other functionals", *Theor. Chem. Acc.* **2008**, *120*(1-3), 215-241.

188. T. H. Dunning, "Gaussian basis sets for use in correlated molecular calculations. I. The atoms boron through neon and hydrogen", *J. Chem. Phys.* **1989**, *90*(2), 1007-1023.

189. T. H. Dunning, P. J. Hay, in *In Modern theoretical Chemistry, Vol. 3* (Ed.: H. F. Schaefer), Plenum Press, New York, 1976, pp. 1-27.

190. M. E. Casida, C. Jamorski, K. C. Casida, D. R. Salahub, "Molecular excitation energies to high-lying bound states from time-dependent density-functional response theory: Characterization and correction of the time-dependent local density approximation ionization threshold", *J. Chem. Phys.* **1998**, *108*(11), 4439-4449.

191. K. K. Baldridge, J. P. Greenberg, "QMView: A computational 3-D visualization tool at the interface between molecules and man", *J. Mol. Graphics Modell.* **1995**, *13*, 63-66.

192. S. Portmann, H.-P. Luthi, "Molekel: an interactive molecular graphics tool", *Chimia* **2000**, *54*(12), 766-770.